Open–File Report 2004–1078

Field Trip Guidebook – Metallogeny of the Great Basin Project, August 17–22, 2003

Great Basin Paleozoic Carbonate Platform: Facies, Facies Transitions, Depositional Models, Platform Architecture, Sequence Stratigraphy, And Predictive Mineral Host Models

By Harry E. Cook[1] and James J. Corboy[1]

U.S. Department of the Interior
U.S. Geological Survey

[1]U.S. Geological Survey
345 Middlefield Road
Menlo Park, CA 94025 U.S.A.

GREAT BASIN PALEOZOIC CARBONATE PLATFORM: FACIES, FACIES TRANSITIONS, DEPOSITIONAL MODELS, PLATFORM ARCHITECTURE, SEQUENCE STRATIGRAPHY, AND PREDICTIVE MINERAL HOST MODELS

H.E.COOK AND J.J. CORBOY
U.S. Geol. Survey
Menlo Park, CA 94025 USA

Booming Tonopah (Elliot, 1966)

TABLE OF CONTENTS

ITINERARY

Day 0, Sunday, August 17

~1400-1700 hours:	Arrival of field trip participants at the Best Western Motor Inn, 527 East Topaz Blvd., Delta, Utah, 84624, Tel. 435-864-3882, Fax 435-864-4834.
~1700-1800 hours:	Pool side Best Western if possible: Field trip discussion: safety and caravan logistics, distribution of guidebook material; geological objectives; discussion of basic carbonate principles, standard facies belts and facies analysis, carbonate sequence stratigraphy, static and dynamic stratigraphic and depositional facies models, history of the depositional facies profile used on the field trip, and potential host (reservoir) facies for minerals and petroleum.
~1800-2000 hours:	Supper. *Recommend all vehicles gassed up, fluids and tires checked, etc. prior to Monday morning.

Day 1, Monday, August 18

0700 hours:	Leave Best Western Motor Inn parking lot and caravan to Confusion Range, Utah.
Stop 1-1:	Kings Canyon, Confusion Range, Utah. Orientation and examination of Silurian Laketown Dolomite (middle shelf) and overlying Devonian Sevy Dolomite (tidal flats). Stopping time about 1.5 hours.
Stop 1-2:	Little Mile-and-a-half Canyon, Confusion Range, Utah. Upper Devonian Guilmette Limestone (middle shelf) and Pilot Shale (basin) contact. Stopping time about 0.5 hours.
Stop 1-3:	Little Mile-and-a-half Canyon, Confusion Range, Utah. Upper Devonian-Lower Mississippian Pilot Shale (basin-to-upper slope) and Lower Mississippian Joana Limestone (platform margin). Stopping time about 3.5 hours.
1530 hours:	Leave parking area and drive to Ely, Nevada. Stay at the Motel 6, 770 Ave 0, Ely, Nevada, 89301, Tel. 775-289-6671.

Day 2, Tuesday, August 19

0700 hours: Leave Motel 6 and drive to Eureka, Nevada.

Stop 2-1:	Overview of Devils Gate area near Whistler Mountain, Nevada. Stopping time about 0.5 hours.
Stop 2-2:	Devils Gate, Nevada. Upper Devonian Devils Gate Limestone (middle shelf to slope), Upper Devonian-Lower Mississippian Pilot Shale (basin), and Chainman Shale (basin). Stopping time about 5 hours.
1630 hours:	Leave parking area and return to Best Western Eureka Inn, 251 North Main Street, Eureka, Nevada, 89316, Tel. 775-237-5247, Fax 775-237-5155.

Day 3, Wednesday, August 20

0700 hours: Leave Best Western Eureka Inn and drive to Roberts Mountains, Nevada.

Stop 3-1: Garden Pass, Sulphur Springs Range. Ordovician Vinini Formation (basin). Stopping time about 0.5 hours.

Stop 3-2: Willow Creek Canyon, Roberts Mountains, Nevada. Silurian-Lower Devonian Roberts Mountains Formation (slope-to-platform margin) and Lone Mountain Dolomite (platform margin and tidal flat). Stopping time about 5 hours.

1630 hours: Leave parking area and return to Best Western Eureka Inn in Eureka, Nevada.

Day 4, Thursday, August 21

0700 hours: Leave Best Western Eureka Inn and drive to Monitor Range, Nevada.

Stop 4-1: Copenhagen Canyon, Monitor Range, Nevada. Lower Devonian Rabbit Hill Limestone (slope). Stopping time about 3.0 hours.

1500 hours: Leave parking area and drive to Tonopah, Nevada.

Stop 4-2: Overview stop on eastside of Toquima Range in Monitor Valley near Ikes Canyon, Nevada. Discuss the origin of the Lower Devonian Tor Limestone. Is it totally allochthonous and comprised of megabreccia debris flow and turbidite deposits or is it an in-situ shoal-water reef/bank? Is the "Toiyabe Ridge" a valid concept? Stopping time about 1.0 hours.

? hours: Monitor Valley, Nevada. Brief stop at Diana's Punch Bowl and the almost-ghost town of Belmont. Continue driving to Tonopah. Stay at the Best Western Hi-Desert Inn, 320 Main Street, Tonopah, Nevada, 89049, Tel # 775-482-3511, Fax # 775-482-3000.

Day 5, Friday, August 22

0700 hours: Leave the Best Western and drive to the Hot Creek Range, Nevada.

Stop 5-1, 5-2, 5-3 Warms Springs, Hot Creek Range, Nevada (one of these three stops TBD). Upper Devonian Denay Limestone (basin), Pilot Shale (basin), Woodruff Formation (basin), and Lower Mississippian Webb Formation (basin), Tripon Pass Limestone (basin), and Eleana Formation (basin). Stopping time about 2 hours.

Stop 5-4: Tybo Canyon, Hot Creek Range, Nevada. Upper Cambrian and Lower Ordovician Swarbuck Limestone (outer basin), Dunderberg Shale (inner basin), and Hales Limestone (slope). Stopping time about 2 hours.

Stop 5-5: Eastern end of Hot Creek Canyon, Hot Creek Range, Nevada. Overview of Cambrian–Devonian stratigraphy and structure. Stopping time about 0.5 hours.

Stop 5-6: Western end of Hot Creek Canyon, Hot Creek Range, Nevada. Lower Devonian Kobeh (platform margin/platform interior), Bartine (basin-slope) and Coils Creek (basin-slope) members of the McColley Canyon Limestone and Middle Devonian Denay Limestone (slope-upper slope), Bay State Dolomite (platform margin), and Chainman Shale (basin). Stopping time about 2.0 hours.

Stop 5-7 (optional): Western end of Hot Creek Canyon, Hot Creek Range, Nevada. Briefly examine and discuss Tertiary ignimbrite reservoir rocks if there is an interest.

1700 hours: Leave parking area and return to Best Western, Tonopah, Nevada.

Day 6, Saturday, August 23

0830-1030 hours: **(optional)** Pool side of Best Western Motel. Informal group discussion of the field trip stops and our metallogeny project goals.

1030 hours: End of Field trip.

Sleep corral (Browne, 1961)

PALEOZOIC OF THE GREAT BASIN

Introductory Perspectives

A basic premise implicit on this field trip is that the better we understand the origin of rocks and the processes under which they formed the better able we will be to make well founded stratigraphic predictions.

The Great Basin (Figure 1) provides an excellent opportunity to study facies, facies transitions and depositional sequences in one of the world's most stratigraphically complete and best exposed examples of a Paleozoic passive carbonate platform (Cook, 1988). The purpose of this field trip is to recognize and gain an understanding of both shallow water and deep-water carbonate settings and their facies. To this end emphasis is placed on understanding depositional environments, facies, diagenetic patterns, and the stratigraphic analysis of vertical facies successions as embodied in sequence stratigraphic principles. Better geologic interpretations of these elements in carbonate sedimentology and facies analysis are usually critical in both petroleum and mineral exploration for sediment-hosted minerals. Facies analyses are receiving wider importance in mineral exploration as world-class mineral deposits in Nevada and elsewhere are probably controlled by primary depositional facies patterns (for example, Raines and others, 1991; Cook, 1993; Lydon, 1996; Armstrong and others, 1998; Emsbo, 1999, 2000; Hofstra and others, 1999; Hofstra and Cline, 2000). Based on these and other papers, many of the sediment-hosted gold deposits of Nevada appear to have developed at or near platform margin/basin margin sites (Figures 2 and 3).

One of the steps in petroleum or mineral exploration lies in predicting the location of porous and permeable zones likely to be commercial host facies. Depositional facies and facies patterns often control depositional porosity trends and strongly influence post-depositional diagenetic porosity patterns in carbonates. Thus, it follows that the correct recognition of environments and knowledge of carbonate depositional sequences in these environments can provide important advantages in designing exploration and production strategies.

Objectives of Field Trip

1. Examine several chronostratigraphic sequences up to 200 miles wide (including Cenozoic extension), from western Utah to central Nevada, that illustrate carbonate facies transitions through tidal flat, middle platform, bank and reef margin, and deeper marine slope, debris apron and fan, and basin-plain environments.
2. Relate depositional and diagenetic facies and carbonate depositional sequences to distally-steepened carbonate ramp, carbonate ramp, rimmed platform, slope and base-of-slope debris aprons, and carbonate fan models.
3. Discuss potential host/reservoir facies and traps for sediment-hosted gold and petroleum in both shallow water platform margin and deeper-water carbonate sequences.
4. Discuss how static and dynamic carbonate models and carbonate sequences can be used for making observations, for making stratigraphic and facies interpretations, and for making predictions of the locations and architecture of potential mineral and petroleum host/reservoir facies.

Depositional, Stratigraphic, and Tectonic Setting

A summary of the geologic history of the Great Basin is in Cook, 1988. Figures 2 and 3 are draft depositional facies profiles that have been extensively updated and revised from earlier ones in Cook (1988). These profiles show the relationships between age, relative sea-level cycles, carbonate sequences, formations, examples of sediment-hosted gold deposit stratigraphic occurrences and field stop localities for pre-Antler orogeny (Figure 2) and post-Antler orogeny (Figure 3) stratigraphy.

Figure 4 shows the broad aspects of the chronostratigraphic slices we will be examining as they relate to age and major tectonic events. As seen on figure 2 the overall emerging framework is one of a passive carbonate continental margin whose shoal-water platform margins evolved through time by aggradation (upbuilding), seaward progradation, and landward retrogradation or retreating.

This carbonate platform evolved through several stages of platform margin architecture from distally-steepened ramps with submarine fans (Late Cambrian-Early Ordovician) to low-angle homoclinal ramps (Late Ordovician) to

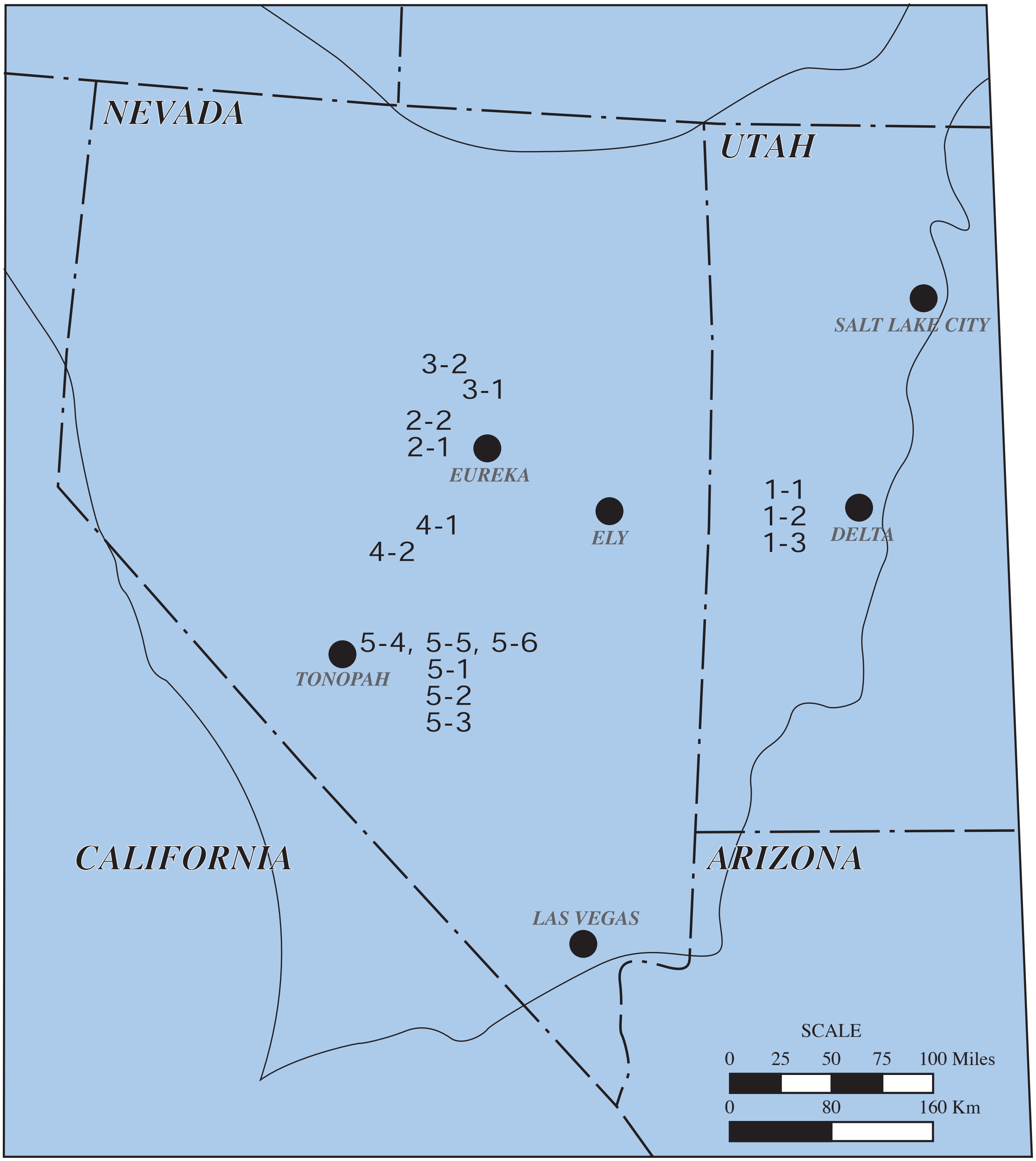

Figure 1. Outline of Great Basin and itinerary of MGB field trip with approximate locations of field trip stops. Day 1, Stop 1 (1-1).

rimmed platforms with slope debris aprons that formed on low angle slopes (Silurian-Early Devonian) to rimmed margins with base-of-slope debris aprons that formed on steeper angle slopes (Early Devonian-Late Devonian). Throughout its history the platform underwent subsidence and relative sea-level rises and falls that had significant effects on the geometric patterns (sequence stratigraphy) of its carbonate facies in both shallow water and deeper water depositional environments.

During the Late Devonian through Early Mississippian (Figure 3) the Antler orogeny profoundly reshaped the structural and depositional framework of the long-standing early Paleozoic platform-slope-basin plain couplet (for example, Poole, 1974; Perry and Abbott, 1997). It is generally considered that deep water basin plain sediments in the western Great Basin were uplifted and thrust eastward (Roberts Mountains thrust), on the order of 100 to 150 km, over the carbonate platform margin facies in central Nevada during the Late Devonian-Early Mississippian. During the Antler Orogeny, the former continental slope and a wide portion of the adjacent platform were warped downward drowning Upper Devonian and Lower Mississippian shallow water carbonates. This downward warping of the continental margin created a foreland basin (Poole, 1974; Giles and Dickinson, 1995; Sandberg and others, 2003). Large volumes of siliciclastics were eroded from the newly developed Antler orogenic highlands and were shed eastward into the foreland basin as well as westward. These Mississippian foreland basin siliciclastics probably served as source rocks for some of the petroleum accumulations hosted in Paleozoic carbonate reservoirs and Tertiary ignimbrite reservoirs (Poole and Claypool, 1984; Poole and others, 1983; McLean, 1995). For a review of foreland basins, see Dorobek and Ross, (1995). A contrasting interpretation of the tectonic style of the Antler Orogeny and the timing of the Antler Orogeny versus the Roberts Mountains thrust are discussed by Ketner (1998).

This foreland basin persisted until gradually Upper Mississippian and Pennsylvanian carbonates were able to prograde seaward over the basinal deposits. Thus, once again shallow water carbonate continental margin deposits occupied paleogeographic positions that were occupied prior to the Antler orogeny (Figure 3).

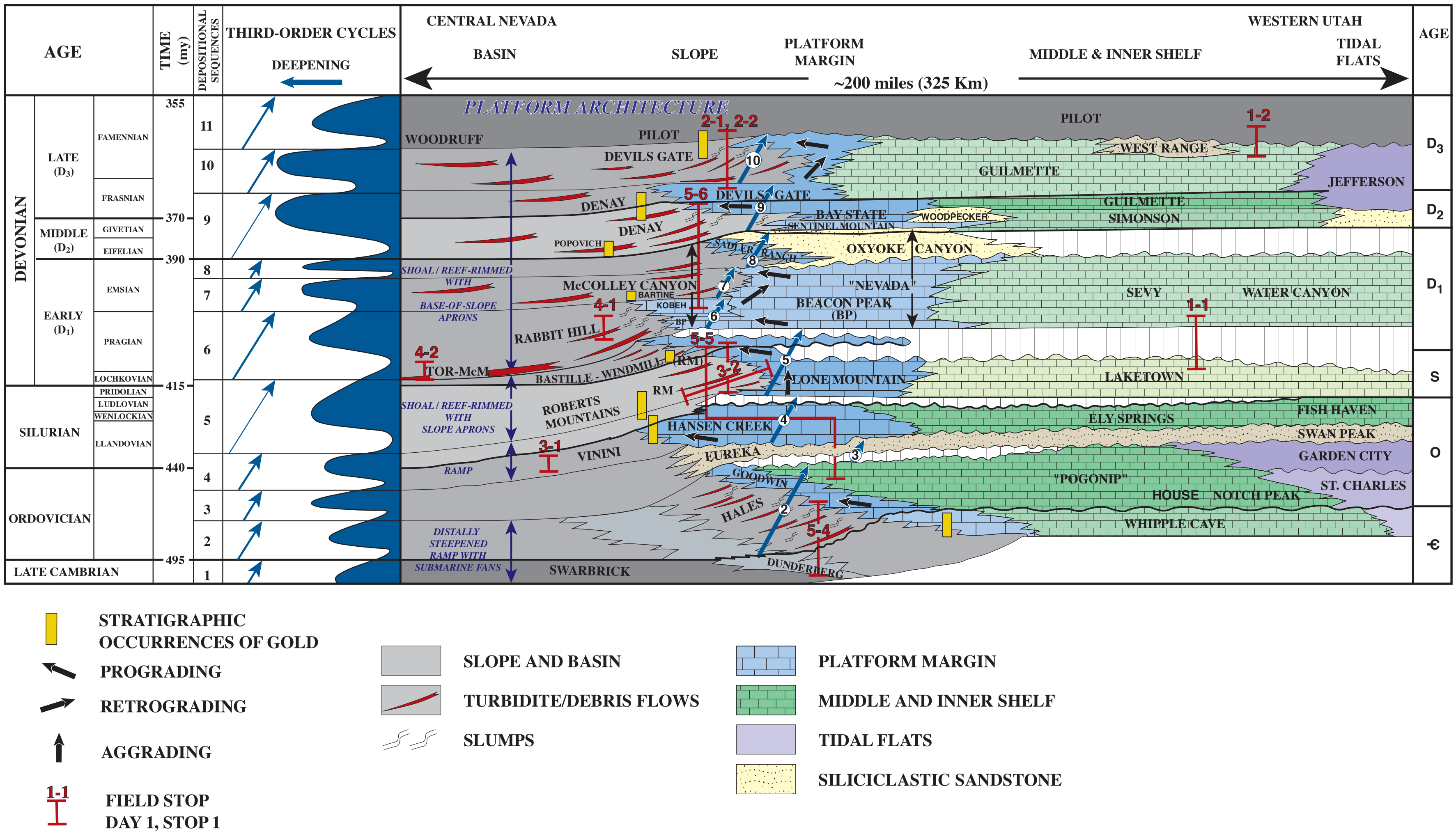

Figure 2. Generalized pre-Antler Orogeny depositional facies profile from western Utah to central Nevada showing formational terminology, location of field stops, stratigraphic occurrences of gold, relative rise/fall of sea level, carbonate platform architecture, and ten complete depositional sequences from Upper Cambrian through the Devonian. Total stratigraphic thickness at the platform margin is about 12,000 to 15,000 feet (3,500 to 5,000 meters). The relative thickness of each depositional sequence has been altered for diagrammatic purposes. Modified from Cook and others (1983) and based on data from Winterer and Murphy (1960), Cook (1966), Murphy and Gronberg (1970), Matti and McKee (1977), Poole and others (1977), Kendall and others (1983), Johnson and Bird (1991), Murphy and Anderson (1991), Raines and others (1991), Kerans and Tinker (1997), Haq and Eysinga (1998), and Sandberg and others (2003).

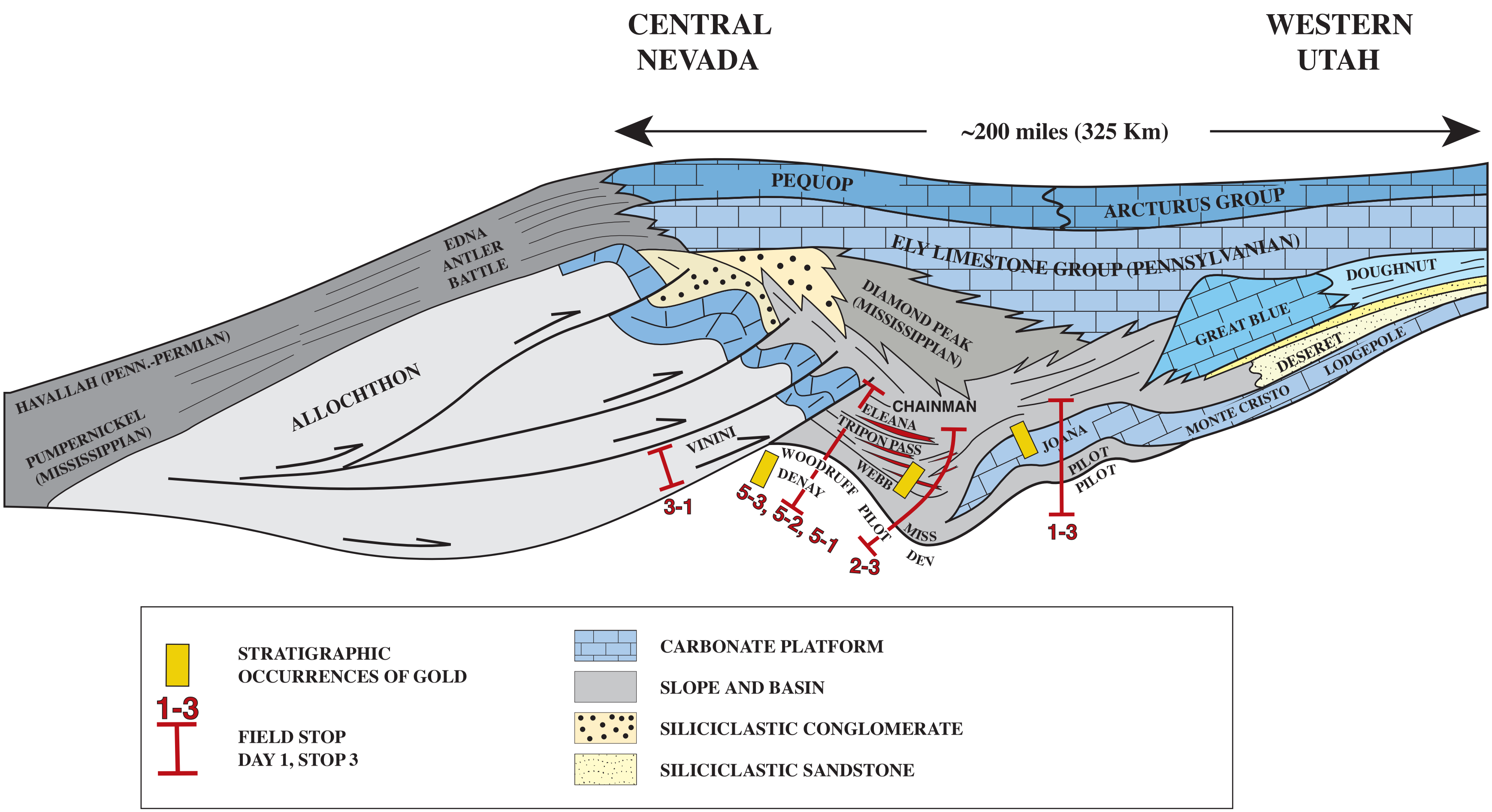

Figure 3. Generalized post-Antler Orogeny structural and depositional facies profile from western Utah to areas west of the Antler orogenic belt showing formational terminology from Mississippian through the Permian. Modified from Cook (1988).

Figures 4-13 illustrate some stratigraphic-tectonic models and geologic framework elements in the Great Basin and other parts of North America.

BASIC CARBONATE PRINCIPLES

The following is a summary from Cook and others (1983) on basic carbonate principles. People interested in pursuing this topic can find excellent discussions in Wilson (1975), Scholle and others (1983, and in several SEPM Special Publications. Basic principles of carbonate sedimentology and stratigraphy can be thought of as guidelines by which a carbonate geologist attempts to decipher the database at hand and to generate ideas, predictive models and exploration approaches for mineral and petroleum. This database may consist of only a hand full of cuttings or it may include a diverse array of logs, seismic reflection profiles, gravity and magnetic data, cores, and beautifully exposed mountains of carbonate rocks. The intangible database is, of course, the experience, perspective, and imagination of the person interpreting these data.

Carbonates Versus Siliciclastics

Most carbonate sediment is the product of shallow, warm, clear marine waters at low latitudes (Figure 14). A fundamental difference between siliciclastic systems and carbonate systems is that carbonate sediments are not delivered to a depositional site, as is the case for siliciclastics (Figure 15), but rather carbonates are produced ("born") in the marine depositional site by organic and inorganic processes (Figure 16). Thus, the carbonate facies that one examines in the field "was born and died" approximately where it is found – whether this be on tidal flats, middle platforms, platform margin setting, etc. The notable exception to this basic principal are submarine sediment-gravity flow deposits (e.g., carbonate debris flow deposits and turbidity current deposits) that usually originate in shoal-water carbonate platform margins and basin margins and can transported seaward down slopes and into basins 10's to 100s of km.

Depositional Environments

There are six basic depositional environments in carbonate systems (Figure 17): 1) Inner Platform ("tidal flats") with supratidal marshes in humid environments or sabkhas in arid environments; intertidal flats; supratidal levees; ponds on tidal flats; beach ridges; 2) Middle Platform with patch reefs and biostromes, platform lagoonal facies with abundant biota and intense burrowing in many locations, and some shoal-water carbonate sands; 3) Platform Margin with ooid and bioclastic shoals and organic banks and reefs; tidal flats can occur near platform margins separating the subtidal bank/reef margin from the middle platform, 4) Slope with debris flow and turbidite deposits, slides and slumps, and laminated to slightly bioturbated in-situ lime muds; 5) Inner Basin with laminated lime muds and shales and turbidites; and 6) Outer Basin where pelagic chalks accumulated in Mesozoic–Recent.

Carbonate Components and Skeletal Compositions

All carbonate rocks are composed of only four main components: these are 1) fossils or fossil fragments, 2) ooids and/or other coated grains, 3) carbonate mud as micrite, as pelloids, and as intraclasts, and 4) carbonate cement. These four components are made up of only four basic carbonate minerals – 1) aragonite, 2) magnesium calcite, 3) calcite, and 4) dolomite (Figure 18). The skeletal compositions of the major taxa are shown in Figure 19.

Textural Considerations

Because most carbonate grains accumulate where they are produced, the textures of many carbonate sediments are highly dependent upon the nature of the contributing organic or inorganic producers rather than on external processes as in siliciclastic systems. Thus, carbonate sediment can originate with carbonate particles of a wide variety of shapes or sizes. If these constituents undergo relatively little net transport, as is commonly the case, special care must be taken in interpreting this texture. An example that well exemplifies this point is that in some middle platform low energy settings large pebble-sized, articulated crinoid columns can be admixed with abundant lime mud. The message here is that the presence or absence of original lime mud is considered a better guide to water energy than grain size or shape.

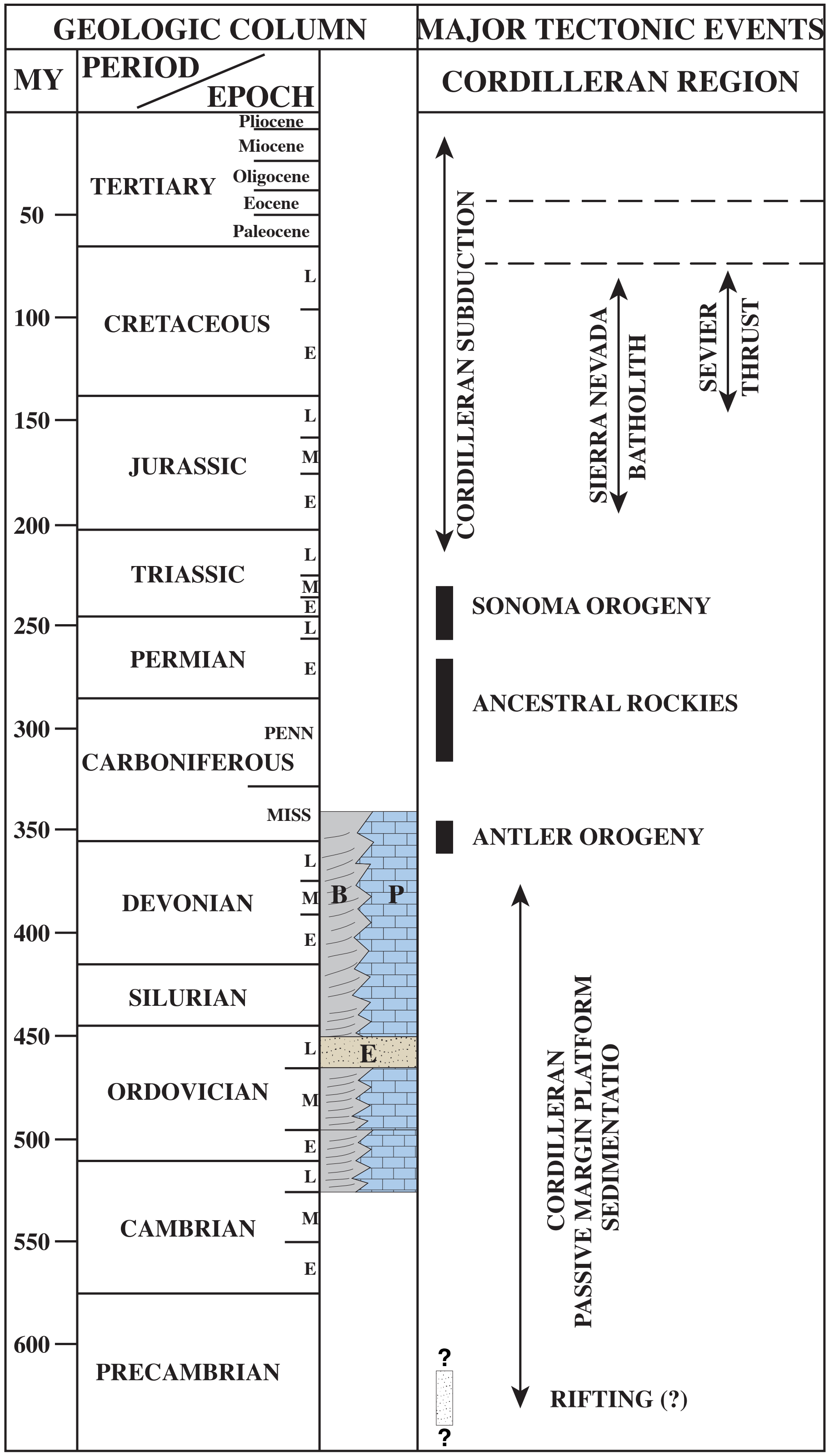

Figure 4. Chronostratigraphic horizons that will be seen during the field trip (colored) and major tectonic events of the Cordilleran region (Modified from Dickinson and others, 1983). (P) = carbonate platform; (B) = slope and basin; (E) = Eureka Quartzite.

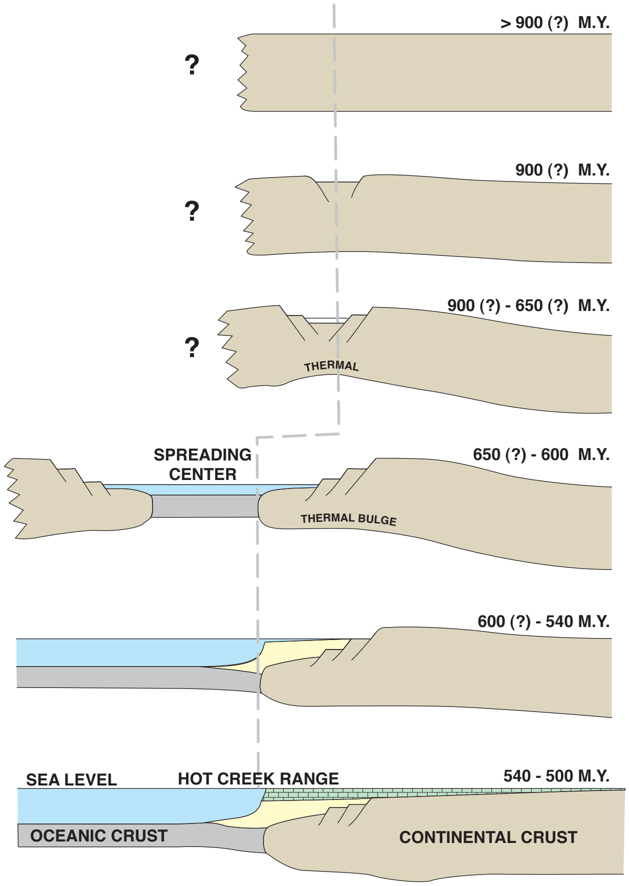

Figure 5. Model of late Precambrian and Cambrian development of the western United States (Modified from Stewart and Suczek, 1977; Cook and Egbert, 1981b).

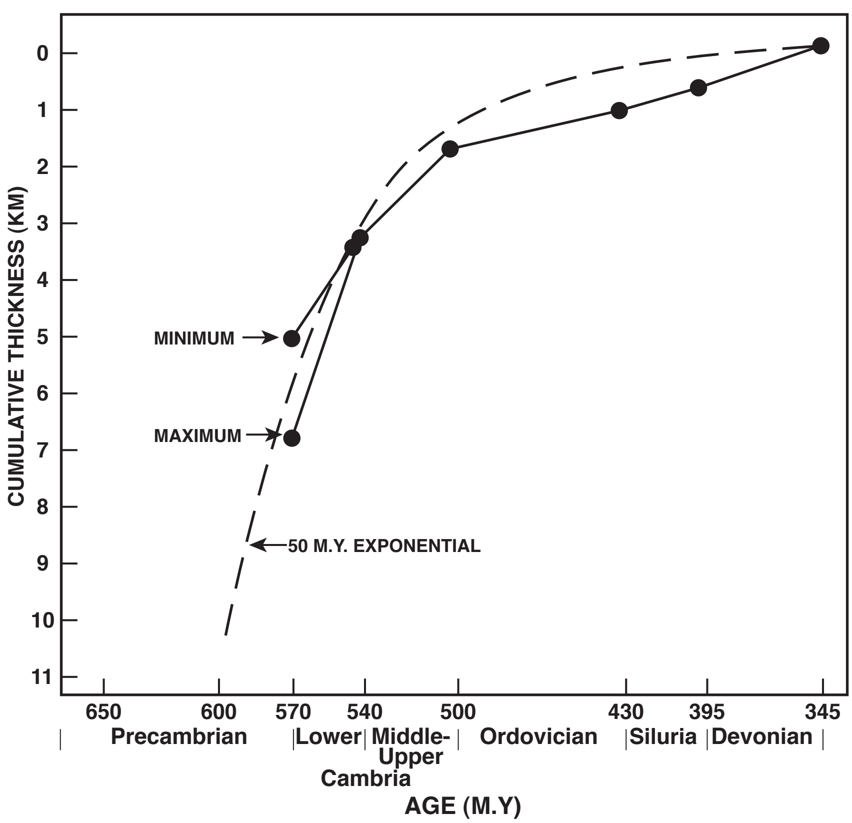

Figure 6. Cumulative thickness with time curve of upper Precambrian and lower Paleozoic rocks in the western Basin and Range Province (Modified from Stewart and Suczek, 1977).

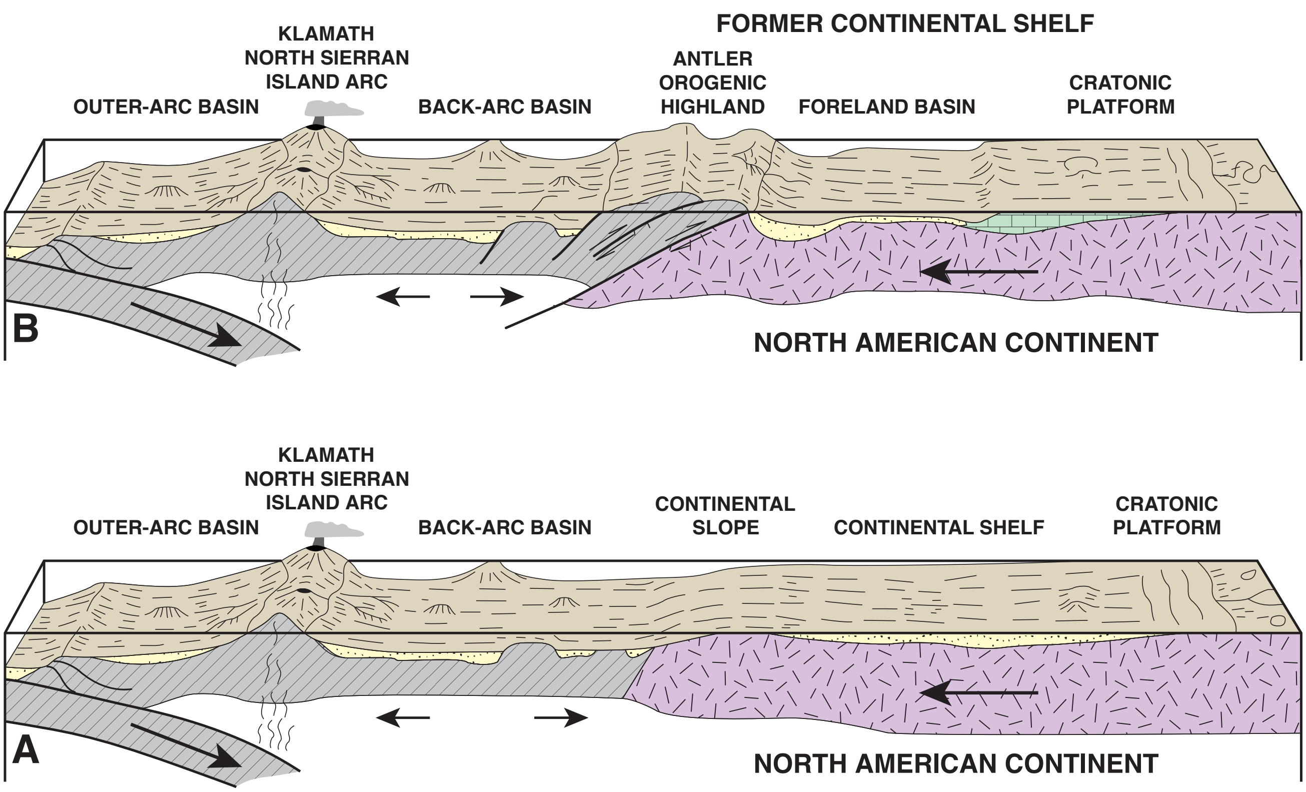

Figure 7. (A) Hypothetical diagram showing the relationship between the Devonian island-arc system and the North American continent based on an east-dipping subduction model. (B) Model of the late Devonian and Mississippian Antler orogeny by back-arc compression associated with an east-dipping subduction zone (Modified from Poole and others, 1977; Poole and Sandberg, 1977).

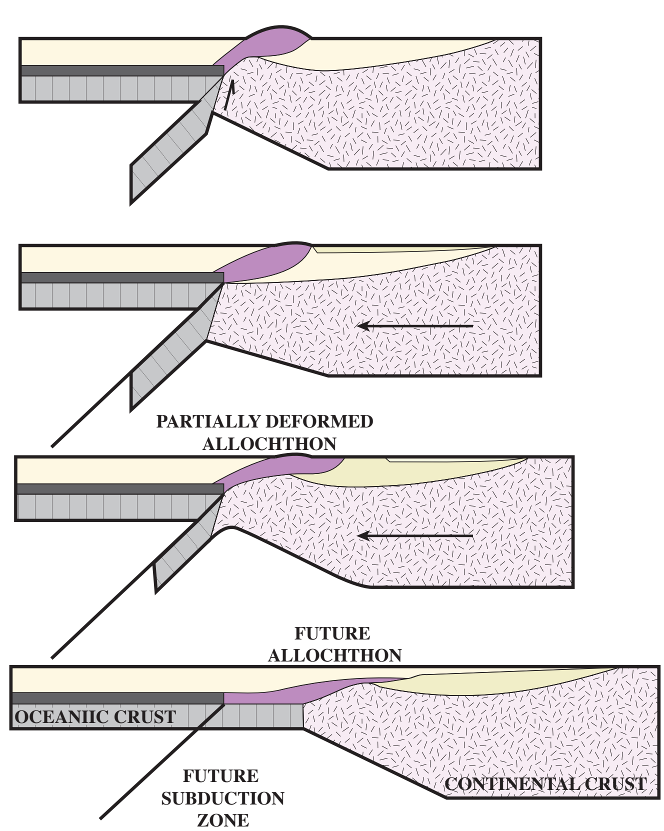

Figure 8. Model for the origin of the Antler orogeny by incipient subduction associated with westward-dipping subduction of the North America continent (Modified from Johnson and Pendergast, 1981).

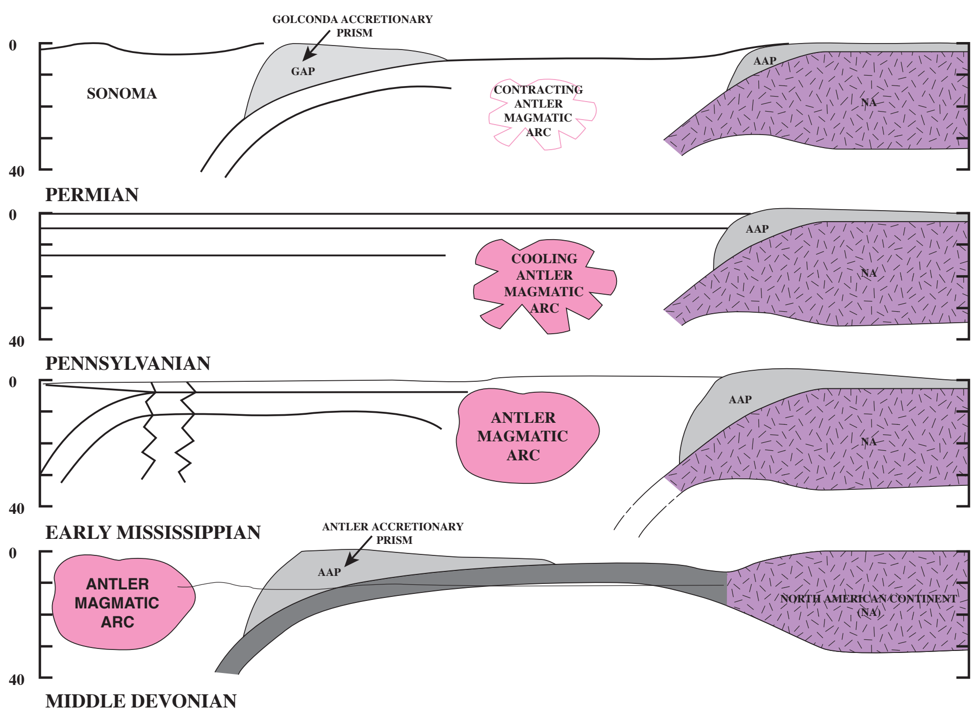

Figure 9. Model for the origin of the Antler orogeny by arc-continent collision associated with westward-dipping subduction of the North American continent (Modified from Speed and Sleep, 1982).

Figure 10. Regional extent of the Antler orogenic belt as mapped by Poole (1974) and Poole and Sandberg (1977).

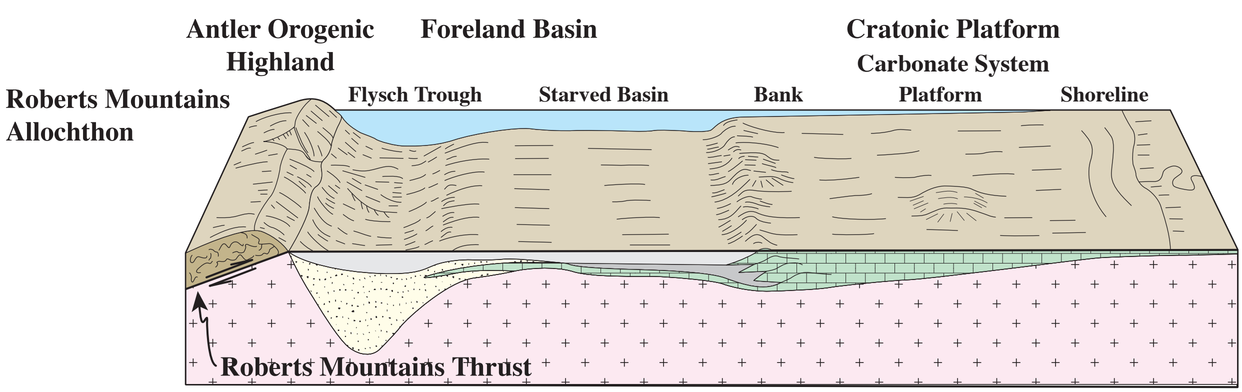

Figure 11. Depositional settings of foreland basin and cratonic platform during early Mississippian (Modified from Poole and Sandberg (1977).

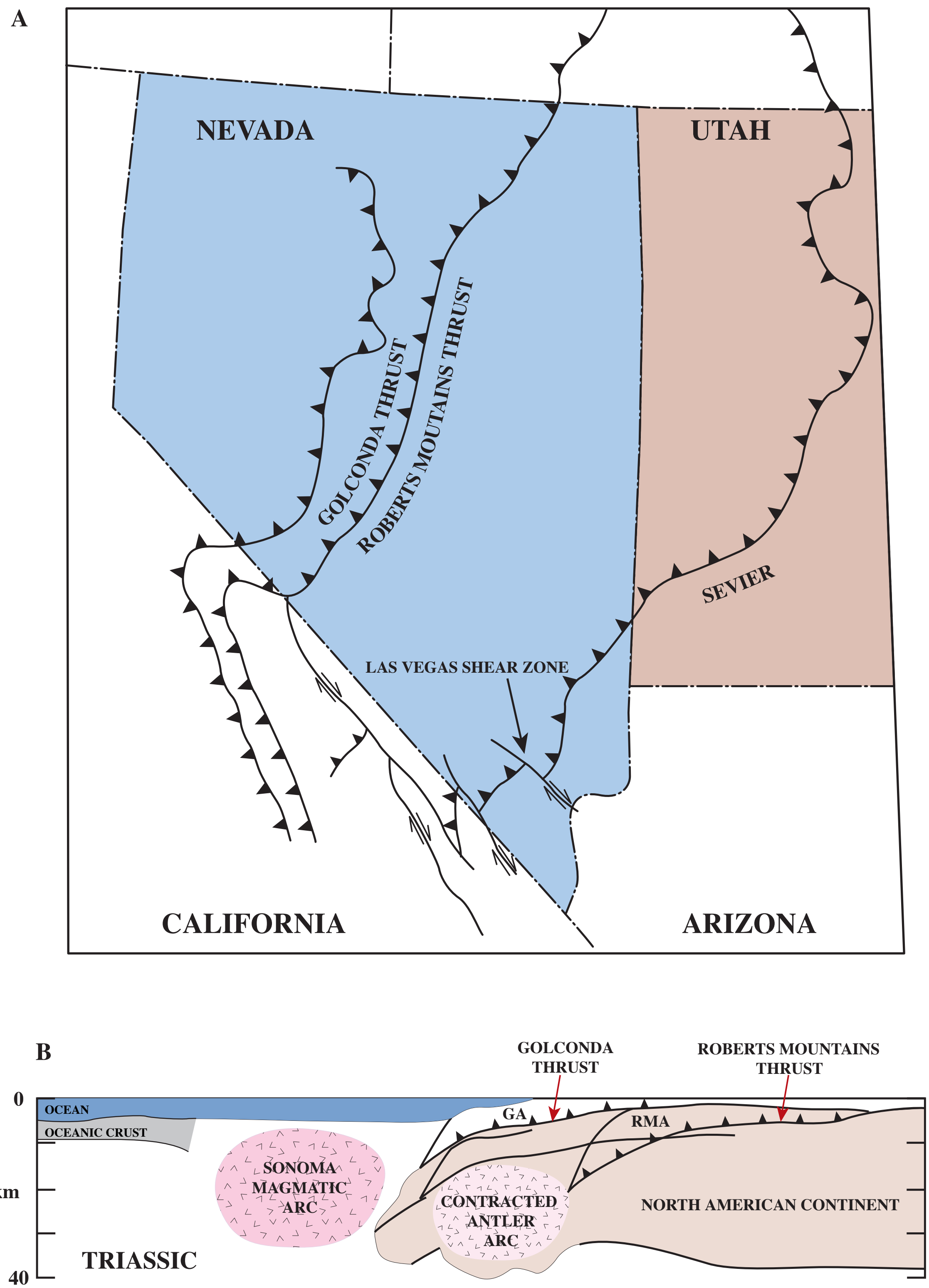

Figure 12. (A) Map showing locations of Permo-Triassic Golconda thrust, Devonian-Mississippian Roberts Mountains thrust, and Mesozoic Sevier thrust. (B) Model for the origin of the Sonoman orogeny by arc-continent collision associated with westward-dipping subduction of the North American continent (GA=Golconda Allochthon; RMA = Roberts Mountains Allochthon; Modified from Speed and Sleep, 1982).

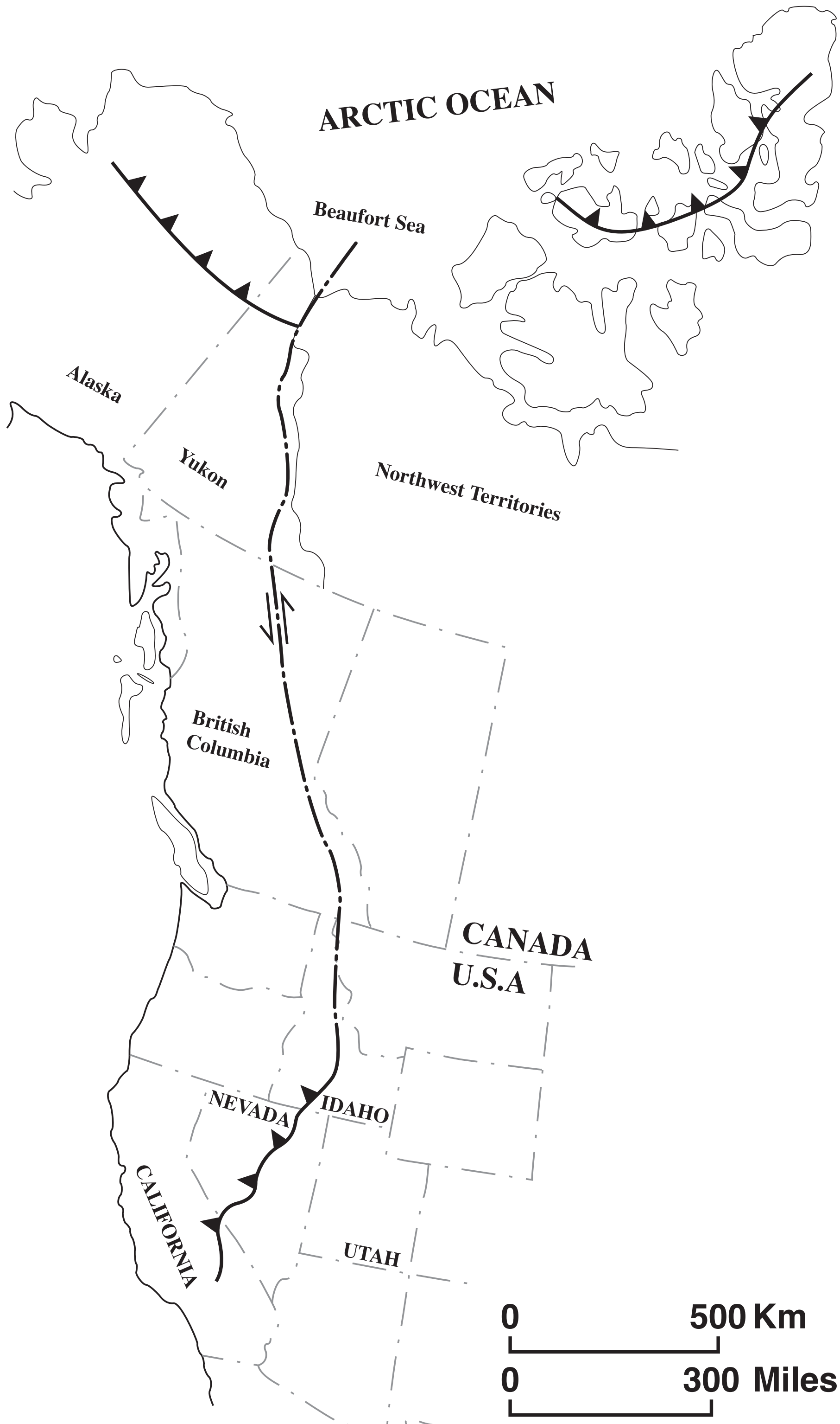

Figure 13. Map showing inferred connection between Devonian-Mississippian Ellesmerian and Antler orogenic belts by a large scale sinistral fault (Modified from Eisbacher, 1983).

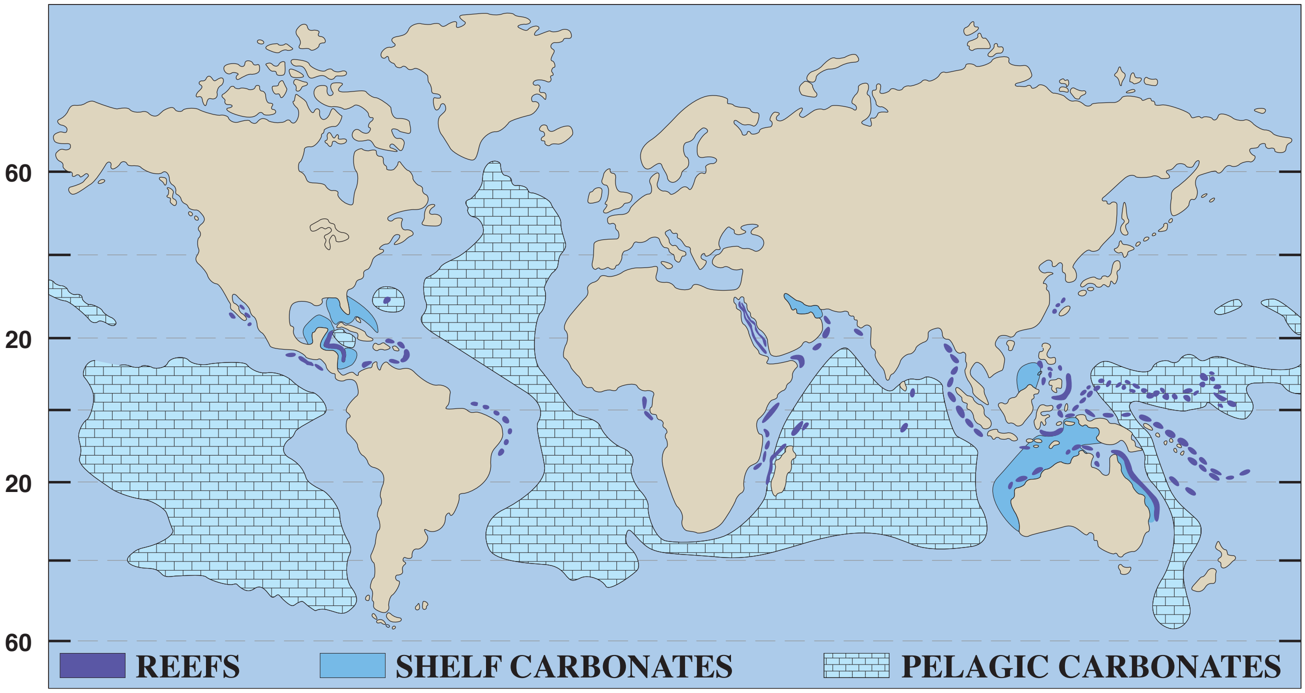

Figure 14. Distribution of modern shoal water carbonates and deeper water pelagic carbonates (Modified from Wilson, 1975).

Figure 15. Russian River in northern California at flood stage illustrating that siliciclastics can have a provenance far from their ultimate depositional site (Photo courtesy of M. E. Field)

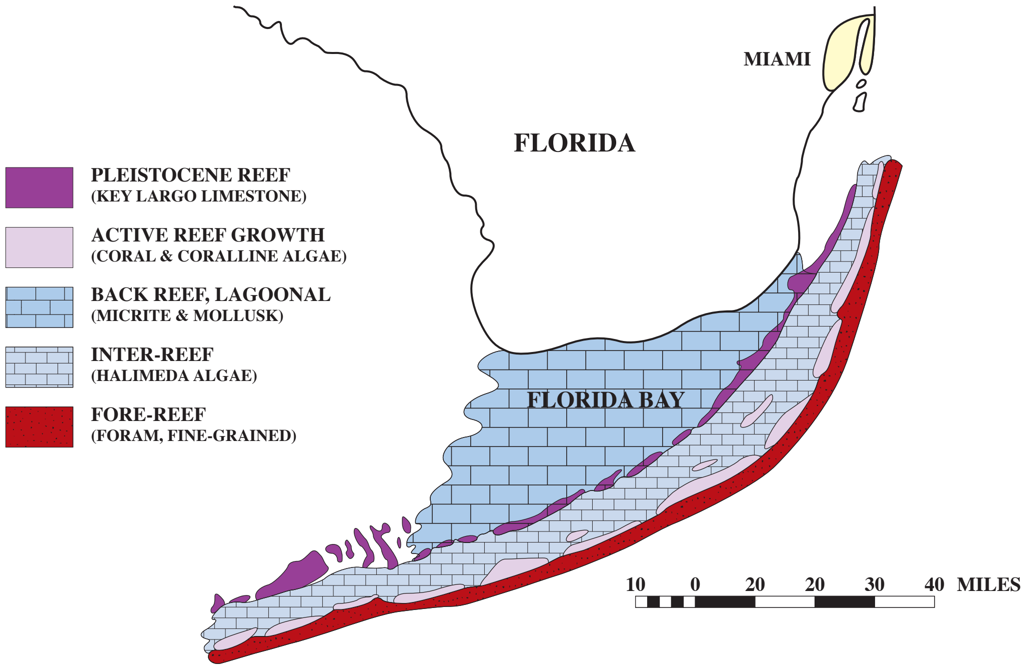

Figure 16. Florida Bay modern carbonate depositional environments. Carbonate constituents are "born" where they are ultimately found in the ancient record.

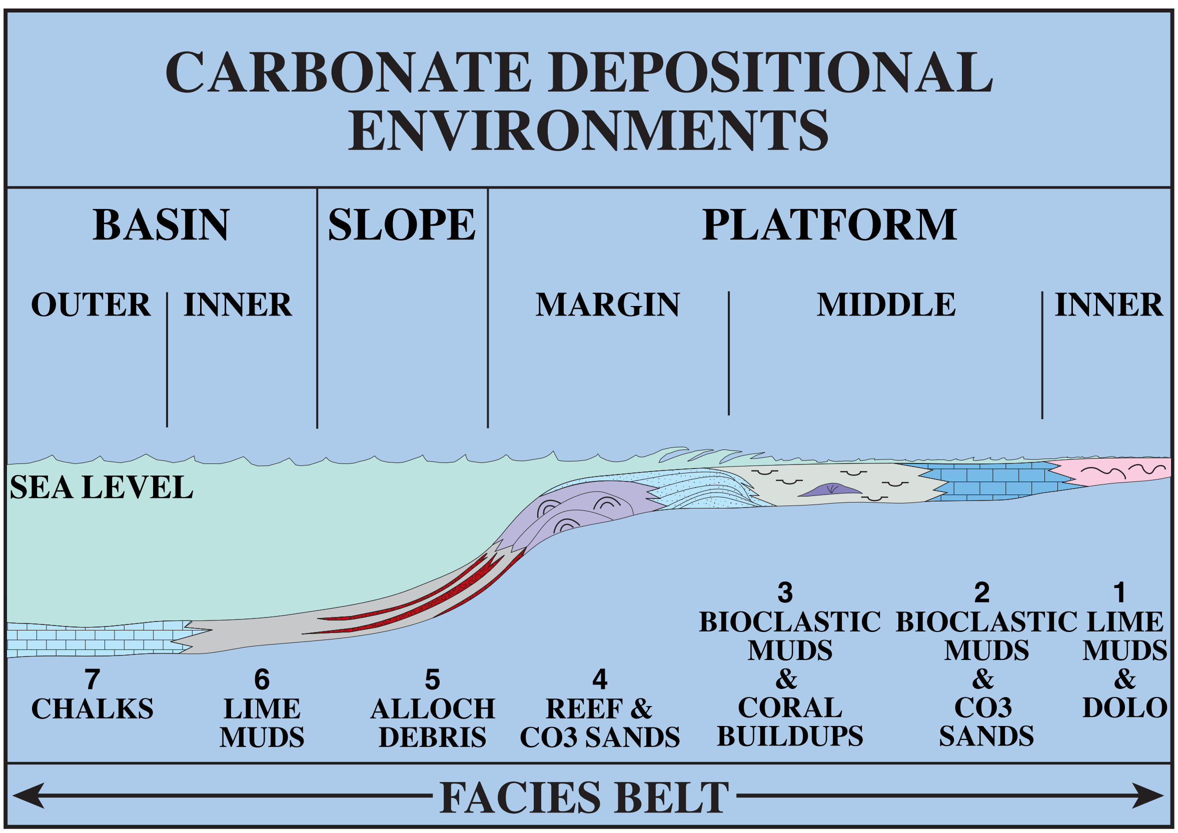

Figure 17. Carbonate facies and depositional environments.

With the above and other concepts in mind Dunham (1962) designed a simple yet elegant classification of carbonate rocks. His classification is simple to use, descriptive, yet his descriptive modifiers have powerful genetic overtones (Figure 20). In this classification the focus is on the presence or absence of lime mud, and whether or not the sediment is grain-supported. Because carbonate mud can be generated in-situ in both quiet and high energy environments the presence of lime mud in a carbonate rock tells us something about the energy level or currents of removal at that site. Likewise rather than simply stating that a carbonate rock contains a certain percentage of grains the concept of grain support fabrics implies emphatically that the rock is full of its particular assortment of grains. Also, because the shapes of carbonate grains can vary from spherical oolites to platy algal fragments like cornflakes an oolite grainstone contains a higher percentage of grains than does a Halide algal grainstone or a phylloid algal grainstone – the common genetic denominators, however, are that both rocks are grain supported and contain as many grains as the shape of the constutuents will geometrically allow (Figure 21).

Rates of Sedimentation

An important point that must be included in any examination and interpretation of carbonate strata is the paradox that carbonate geologists have noted for years. Wilson (1975, p. 15, 16, 18) stated it well by noting that carbonate sedimentation can be extremely rapid with growth rates of Holocene shallow-water carbonates and reefs being at least one order of magnitude higher than net accumulation rates of ancient carbonates. Wilson (1975, p. 16) goes on to say that "when conditions remain favorable, carbonate production can keep up with almost any amount of tectonic subsidence or eustatic sea level rise" (Figure 22, 23). As Schlager said, "there should be no drowning at all" (1981, p. 198). Also see Figure 1-8 in the Read (1995) handout.

Schlager (1981) suggests that "causes of platform drowning include 1) reduction of benthic growth due to environmental stress, such as (a) global salinity drops due to fresh water injections or excessive evaporative deposition or (b) regional deterioration during drift to higher latitudes; or 2) rapid pulses of relative sea level, such as regional downfaulting or global rises due to desiccation of small ocean basins, submarine volcanic outpourings, or glacio-eustacy".

Diagenetic Considerations

Carbonate sediments have a high susceptibility to change, that is, they have a high diagenetic potential (Figure 24). In its simplest from, the diagenetic potential of a carbonate sediment or rock is a measure of its geochemical-textural-constituent maturity. Diagenetic processes in carbonates include, but are not limited to, gravitational compaction, geochemical compaction, mineral stability transformations such as the transformation of aragonite and magnesium calcite to calcite, solution (dissolution), pressure solution, cementation, organic rotting, bioerosion, crystal rearrangement (neomorphism), dolomitization, fracturing, and karsting. The eogenetic diagenetic environments include vadose, phreatic, mixed and marine phreatic settings (Figure 25).

In both petroleum and mineral exploration, major emphasis is placed on better understanding diagenetic environments and the geologic processes in these environments that lead to porosity and permeability modifications. The mark of a potential carbonate reservoir/host for minerals and petroleum is one in which the pore-reducing processes (e.g., cementation, and compaction) were either non-existent or arrested at some stage, and/or porosity enhancing factors (e.g., dissolution, dolomitization, fracturing, and karsting) came into existence or were dominant.

Choquette and Pray (1970) present an excellent and still definitive paper on the classification of porosity in sedimentary carbonates (Figure 26).

FOUR COMPONENTS

1. FOSSILS
2. OOIDS AND OTHER COATED GRAINS
3. CARBONATE MUD, PELOIDS, INTRACLASTS
4. CEMENT

FOUR MINERALS

	COMPONENTS 1	2	3	4
A. ARAGONITE	X	X	X	X
B. MG-CALCITE	X	X		X
C. CALCITE	X		X	X
D. DOLOMITE				X

Figure 18. Carbonate components and their mineralogy.

TAXON	ARAGONITE	CALCITE, % Mg (0 5 10 15 20 25 30 35 40)	BOTH ARAGONITE AND CALCITE
Calcareous Algae:			
Red		X———X	
Green	X		
Coccoliths		X	
Foraminifera:			
Benthonic	O	X———X – –X	
Planktonic		X—X	
Sponges:	O	X—X	
Coelenterates:			
Stromatoporoids (A)	X	X ?	
Milleporoids	X		
Rugosa (A)		X···	
Tabulate (A)		X ?	
Scleractinian	X		
Alcyonarian	O	X—X	
Bryozoans:	O	X—X	O
Brachiopods:		X—X	
Mollusks:			
Chitons	X		
Pelecypods	X	X—X	X
Gastropods	X	X—X	X
Pteropods	X		
Cephalopods (most)	X		
Belemnoids & Aptychi (A)		X	
Annelids (Serpulids):	X	X—X	X
Arthropods:			
Decapods		X—X	
Ostracods		X—X	
Barnacles		X—X	
Trilobites (A)		X	
Echinoderms:		X	

X = Common O = Rare A = Not based on modern forms

Figure 19. Skeletal composition of the major taxa (Modified from Scholle, 1978).

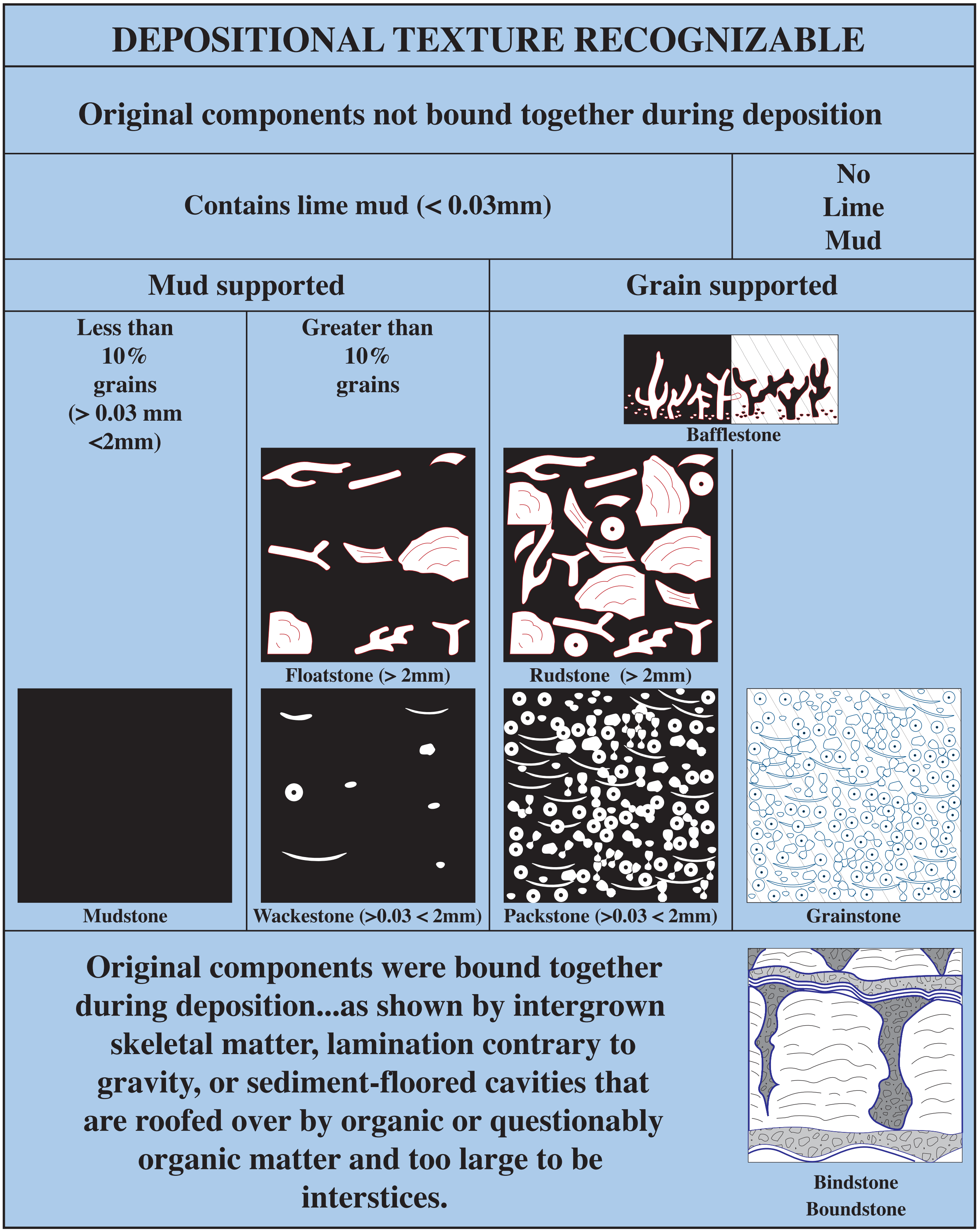

Figure 20. Classification of limestones modified from Dunham (1962) and James (1983).

- COMPONENTS ORIGINATE WITH WIDE VARIETY OF SHAPES AND SIZES AND ARE DEPOSITED WHERE THEY FORM
  - EXCEPTIONS = MASS TRANSPORT

- TEXTURE: NATURE OF THE COMPONENTS AND NOT EXTERNAL PROCESSES AS IN SILICICLASTIC SYSTEMS.

- PERCENT OF LIME MUD GUIDE TO ENERGY LEVEL.

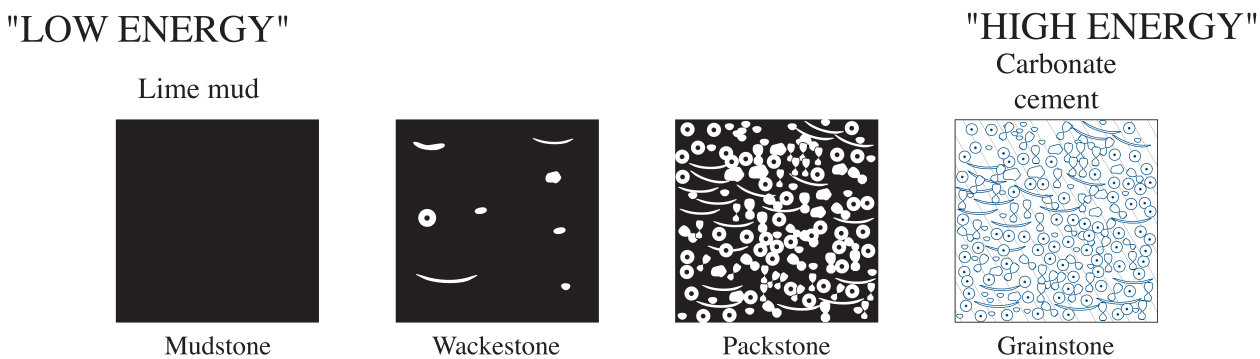

Figure 21. Rock texture.

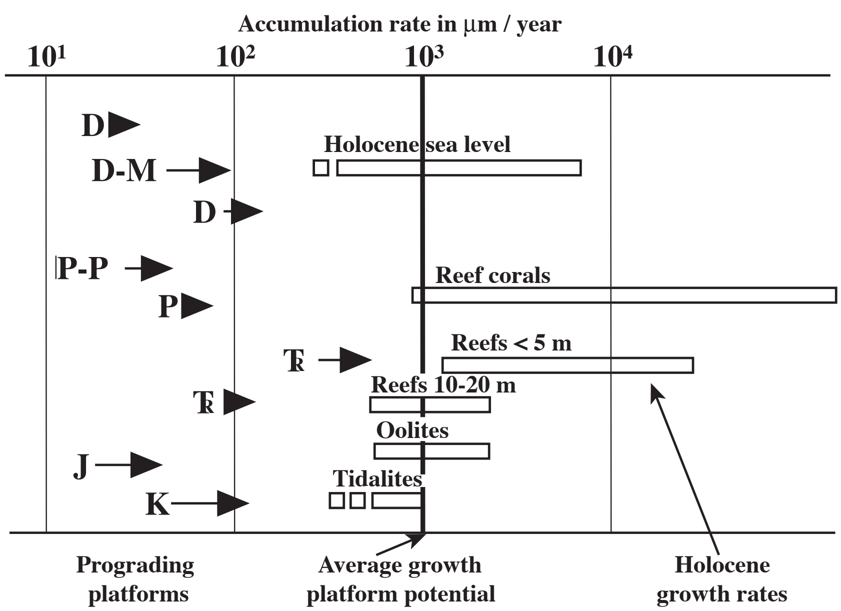

Figure 22. Average growth potential of carbonate platforms estimated from growth rates and accumulation rates during Holocene transgression (open bars) and from accumulation rates of prograding platforms in the geologic record (triangles). Average growth potential is probably in the 1,000 µm / year range (Modified from Schlager, 1981).

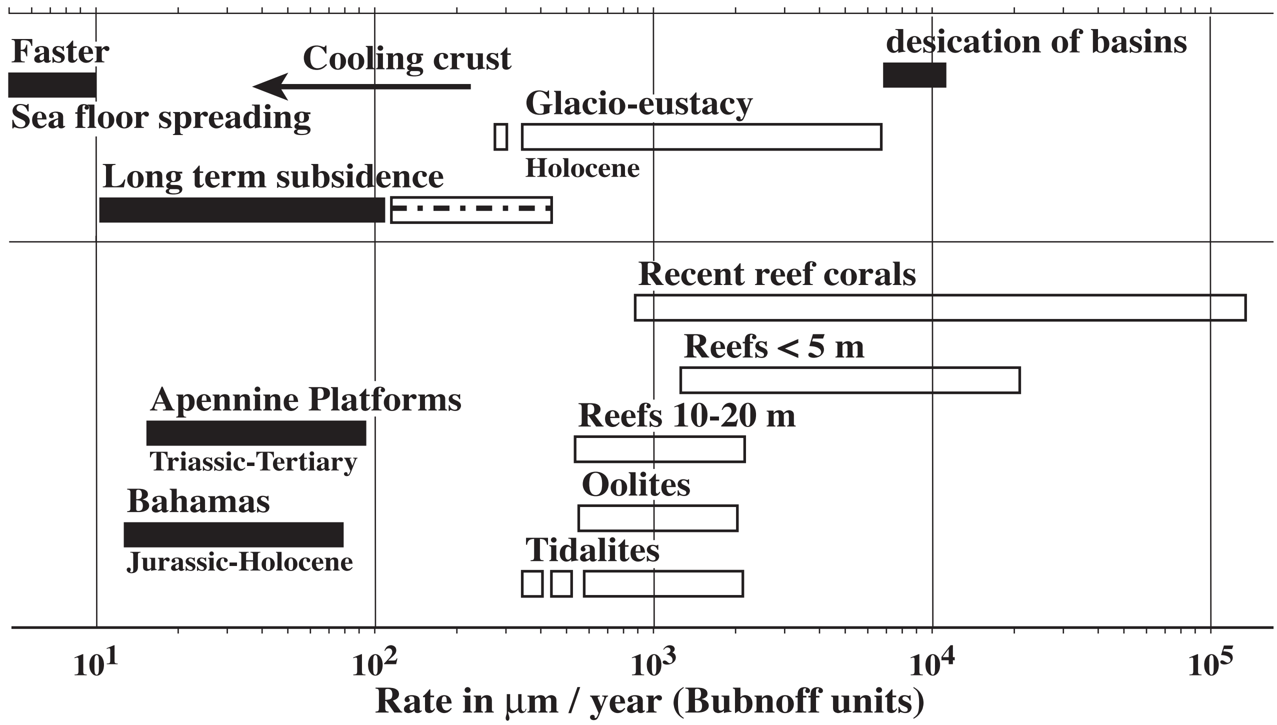

Figure 23. The paradox of carbonate platform drowning is illustrated by a comparison of rates of relevant processes Rates of relative rise of sea level produced by various processes in upper part of graph, rates of growth, and sediment accumulation in lower part. Holocene rates (open bars), distant geologic past rates (black bars). Holocene accumulation matches or exceeds glacio-eustatic Holocene rise of sea level, all Holocene rates are one to several orders of magnitude faster than those of the geologic record (Modified from Schlager, 1981).

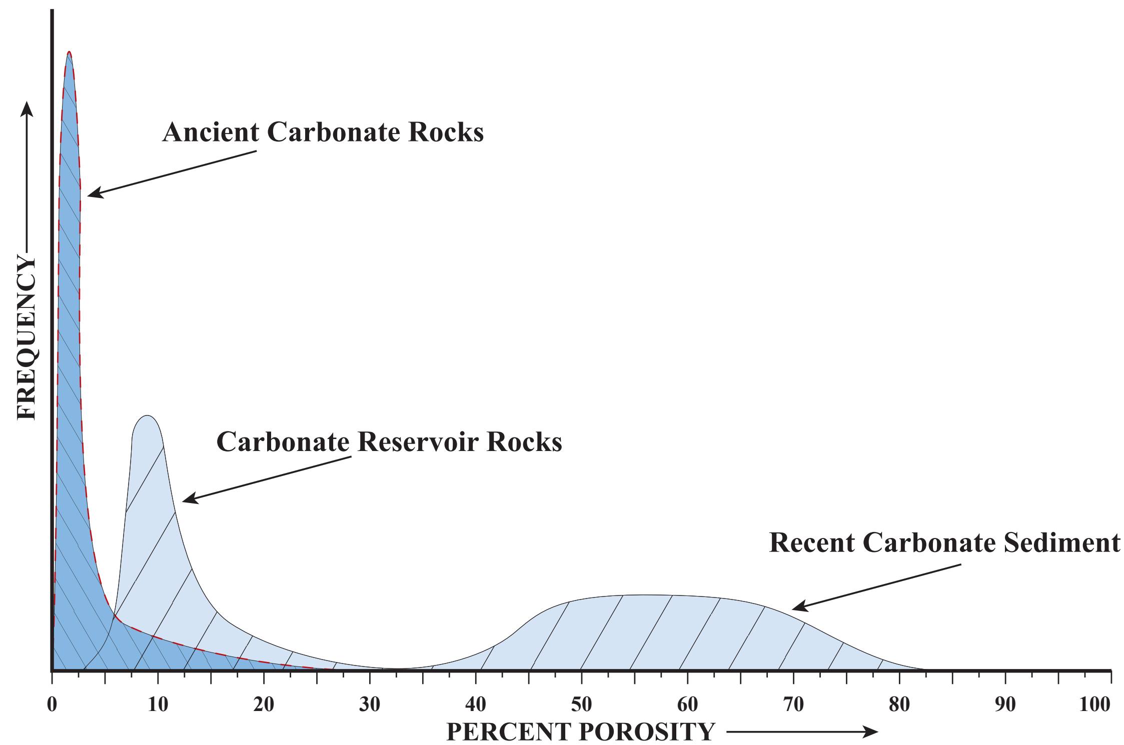

Figure 24. Porosity in carbonates (Modified from Pray, pers.comm., 1966).

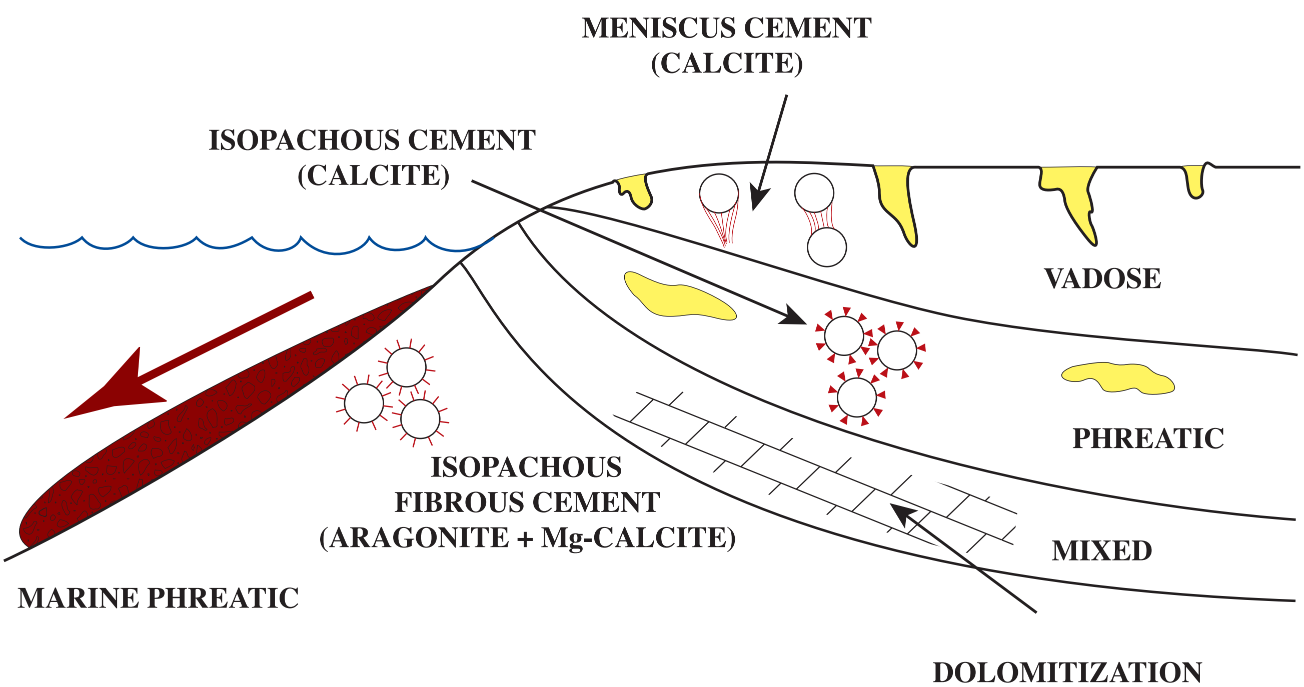

Figure 25. Eogenetic diagenetic environments. Eogenetic zone extends from the surface of newly deposited carbonate to depths where processes genetically related to surface become ineffective.

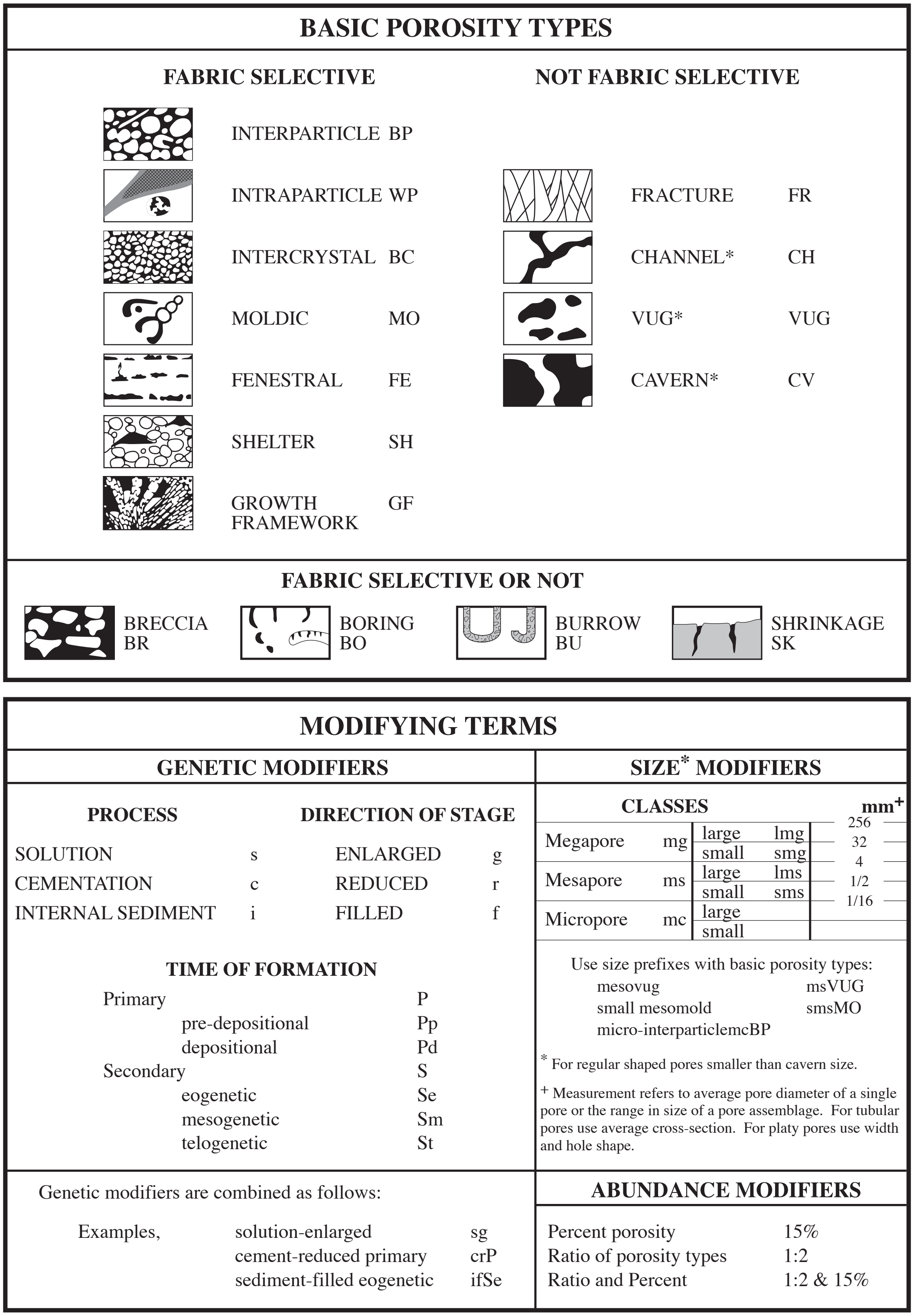

Figure 26. Porosity classification (Choquette and Pray, 1970).

STATIC CARBONATE DEPOSITIONAL MODELS

Depositional models can be an aid in understanding and correctly interpreting lateral and vertical facies transitions and for assigning facies and facies associations to certain depositional environments (Cook and others, 1983). Although there are only a relatively small number of basic depositional environments in carbonate systems as shown in Figure 17 (also see the facies belts of Wilson, 1975; Scholle and others, 1983) there are sub-environments within each environment and numerous variables that can lend considerable variation to the sediments themselves. Some of the larger scale variables include the nature of the paleobathymetric profile of the sediment-water interface (paloetopography), tectonic setting, evolutionary patterns of organisms through time, climatic variations, the magnitude and frequency of sea level fluctuations, subsidence rates, sedimentation rates, and siliciclastic influx. Smaller scale influences include a myriad of inorganic and organic depositional and diagenetic processes.

In using depositional models for making environmental, facies, and sequence stratigraphic interpretations, one must remember that models are basically summary statements and as such one should expect to see details at the scale of an outcrop that reflect local variability. In spite of the many factors that affect facies and facies patterns it is these very factors that commonly exert predictable controls on the location, geometry, and overall characteristics of depositional facies. Thus, the major facies sequences that characterize different depositional environments, from boulder-bearing deep water fan and apron deposits to supratidal muds, rarely were developed at random within a carbonate system – there is a reason for the distribution patterns of depositional facies. Depositional models can be an aid in guiding us to know what to look for, to a degree of predictability. A distinct danger of depositional models is to become too attached to a particular model – at this point one loses objectivity. Models should continually undergo modification and updating, as more data is gathered.

Some examples of attempts to classify shallow water carbonate facies, define basic facies belts, and to position these facies belts in specific depositional environmental models, and depositional sequences and systems tracts are those of Wilson (1975), Mazzullo (1982), Read (1982), numerous authors in Scholle and others (1983), Wilgus and others (1988); Crevello and others (1989); Handford and Loucks (1993), Read and others (1995); Kerans and Tinker (1997); Harris and others (1999); and Zempolich and Cook (2002). Models for deeper water slope and carbonate apron and fan systems have been developed by Cook and others (1972), Cook and Taylor (1975, 1977), McIlreath and James (1978), Cook (1979), Cook and Egbert (1981a, b), Cook and Mullins, 1983, Mullins and Cook (1986), Cook and others (1983) and in several SEPM Special Publications and AAPG Memoirs.

Figure 27 is a compilation of selected stratigraphic horizons that produce petroleum and sediment-hosted minerals from carbonate platform and basin margin facies. Horizontal bars plot the depositional environment of the fields' reservoir/host facies. Many of the environmental facies that will be examined in the Great Basin are similar to proven producing petroleum reservoir and mineral-host facies outside of the field trip area.

Homoclinal Ramp Model (Figure 28)

As discussed by Read (1982) platforms with profiles of the ramp model (Ahr, 1973) have gently sloping (1 to a few degrees/meter) substrates that progress into offshore, deeper-water environments without a marked break in slope. On ramps, wave-base impinges close to the shoreline, resulting in the localization of high-energy potential reservoir facies that trend parallel and proximal to the shoreline. These high-energy facies may consist of peloid-ooid grainstones or bioclastic grainstones. Shoreward shoal lagoon lime mudstones, wackestones, and tidal flat sediments occur. Seaward of the shoals deeper water ramp argillaceous lime wackestones and mudstones occur and contain normal open-marine biota. These facies pass gradually into deeper-water pelagic muds and/or periplatform muds. Only minor evidence of mass transport processes occurs in the deeper-water ramp facies. With perhaps the exception of inner platform high-energy shoals, broad, gradational and irregular facies belts seem to characterize ramps.

The Persian Gulf is an example of a modern ramp (Wilson and Jordan, 1983, Figure 32), whereas the Jurassic Smackover of the U. S. Gulf Coast is considered to be an excellent example of an ancient continental margin ramp (Ahr, 1973; Read, 1982). In the Great Basin the Ordovician Hansen Creek Formation may represent shoal water homoclinal ramp facies (Dunham, 1977).

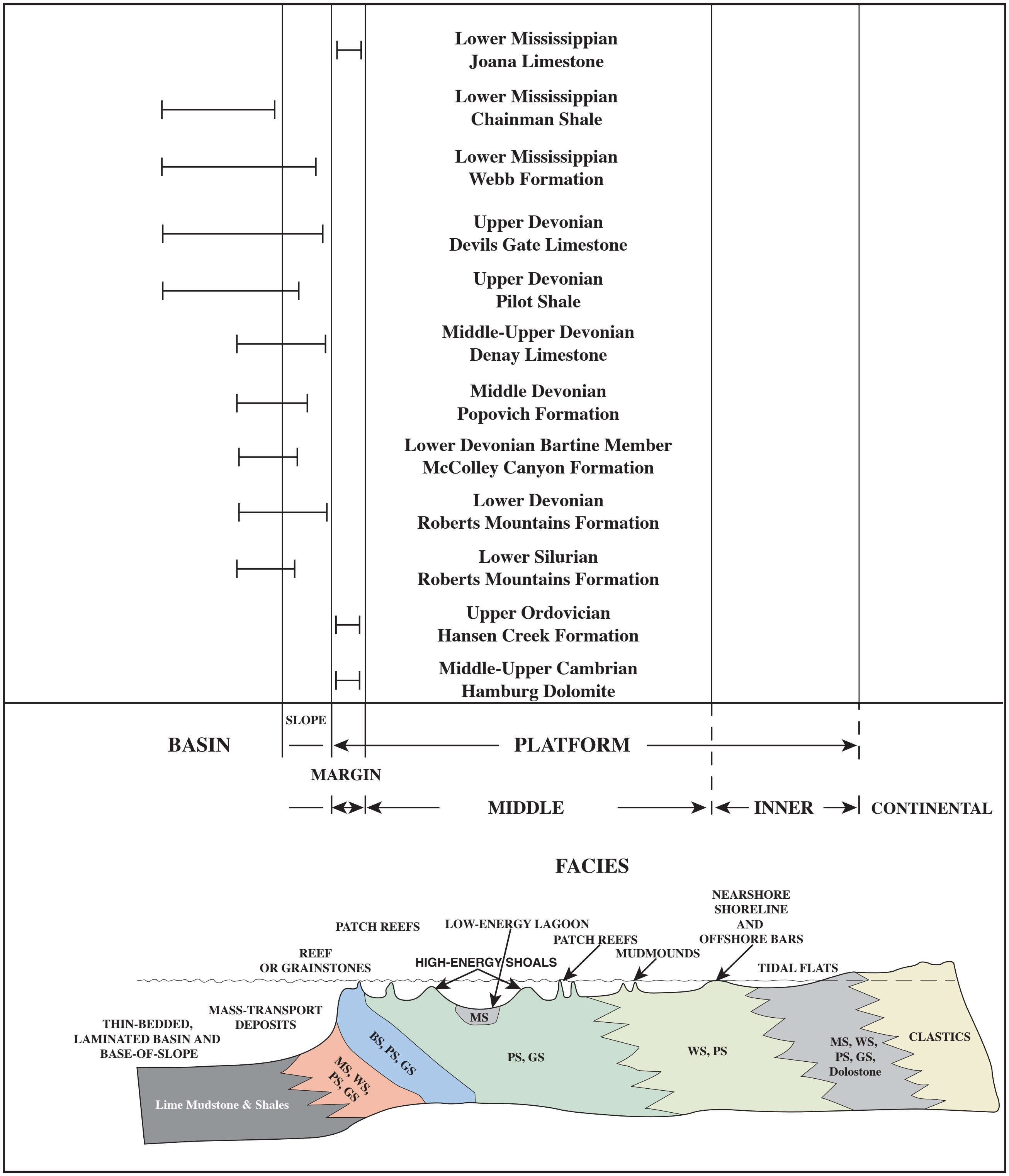

Figure 27. Carbonate platform profile showing examples of Carlin-type gold host facies in platform margin, slope, and basin environments (Platform model modified from Wilson and Jordan, 1983; References for host facies cited in field stop texts).

Distally Steepend Ramp Model (Figure 29)

These ramps have many of the same facies of homoclinal ramps. The main difference, however, is that at some location on the seaward part of the ramp a major break in slope occurs. This break in slope, however, is in relatively deep water and thus shoal water carbonates do not form at the platform edge. The platform/slope break is characterized by submarine slides and slumps, and a wide variety of sediment gravity flow deposits that can be organized into apron and fan facies.

Examples of distally steepened ramp facies occur in the Upper Cambrian-Lower Ordovician sequences in the Great Basin (Cook and Taylor, 1977; Taylor and Cook, 1976; Cook, 1979; Cook and others, 1983). The Yucatan area may be a modern example (Read, 1982).

Rimmed Platform Model (Figure 30)

Rimmed platforms (Ginsburg and James, 1974; Read, 1982) are platforms whose outer platform margin is in shallow agitated water depths and is characterized by a relatively steep increase in declivity (few degrees to 60° or more) marking the boundary between the outer platform and slope. Platforms with rimmed profiles often have well-developed high-energy linear facies belts, trending parallel to the platform edge.

There is potentially more petroleum reservoir facies in the rimmed model than in the ramp models. Potential reservoir facies include 1) deep water carbonate submarine fans and aprons (Cook and others, 1972; Enos, 1977. 1983; Cook, 1983; Cook and Mullins, 1983; Enos and Moore, 1983; Mullins and Cook, 1986; Cook and others, 1983; Hobson and others, 1985); 2) platform margin reefs and tidal bars (Wilson and Jordan, 1983); 3) middle platform grainstone facies (Powers, 1962; Wilson and Jordan, 1983); 4) inner platform offshore bar and beach facies, and tidal flat facies (Enos, 1983; Inden and Moore, 1983; Shinn, 1983).

Modern examples of the rimmed model include the Belize platform margin and the Great Bahaman Banks (Wilson and Jordan, 1983). Numerous examples in the ancient record exist (Scholle and others, 1983). A few studied examples cited by Wilson and Jordan (1983) include the Permian Hueco Limestone of southeast New Mexico and west Texas, the Cretaceous Edwards Formation of Texas, and the Jurassic D zone in the Persian Gulf area, the Permian Guadeloupe mountains in west Texas (Kerans and Tinker 1997). The Devonian carbonate province of Alberta, Canada has abundant examples of giant oil fields, especially in isolated rimmed platforms (Klovan, 1964; Cook and others, 1972; Harris, 1983). A billion-barrel oil field occurs in deep-water carbonate aprons in the Cretaceous of Mexico (Enos, 1977, 1985; Enos and Moore, 1983; Roehl and Choquette, 1985). Smaller lesser known fields in the Permian of west Texas occur in carbonate submarine fan and apron facies (Cook and others, 1972; Cook, 1983; Cook and Mullins, 1983; Cook and others, 1983; Hobson and others, 1985, Moore, 2001). Devonian-Mississippian super giant oil fields occur in the North Caspian Basin of Kazakhstan (Cook and others, 2002b; Zempolich and Cook, 2002)

In the Great Basin Silurian through Devonian carbonates are interpreted to have formed on broad rimmed platforms (Figure 2). Some of the Lower Mississippian carbonates may have formed on rimmed platforms or on isolated platforms surrounded by basin facies (Figure 3).

Carbonate Slope Apron and Base-of-Slope Apron Models (Figures 31 and 32)

During the late 1960’s and early 1970’s the first well documented depositional models for basin margin carbonate and siliciclastic sediment gravity flow sequences were being formulated. Pray and others (1967, 1968) and Cook and others (1972) developed the carbonate debris sheet model (Figure 33) while at the same time Walker (1966), Jacka (1968), and Mutti and Ricci-Lucchi (1972) were establishing the siliciclastic submarine fan model. Two fundamental differences exist between these models. In carbonate basin margins the redeposited facies are dominantly the result of numerous unchanneled sheet-flow events that originate parallel to platform margins – i.e. along a “line-source”. Fan facies, in contrast, originated from major “point-sources” and are characterized by channelized flow in their inner and mid-fan regions and sheet-flow in the outer parts of the fan. A further difference emphasized by these two models is that carbonate debris flows can form a major facies type whereas debris flows occur less frequently in the fan model. Turbidity-current processes dominate fan facies.

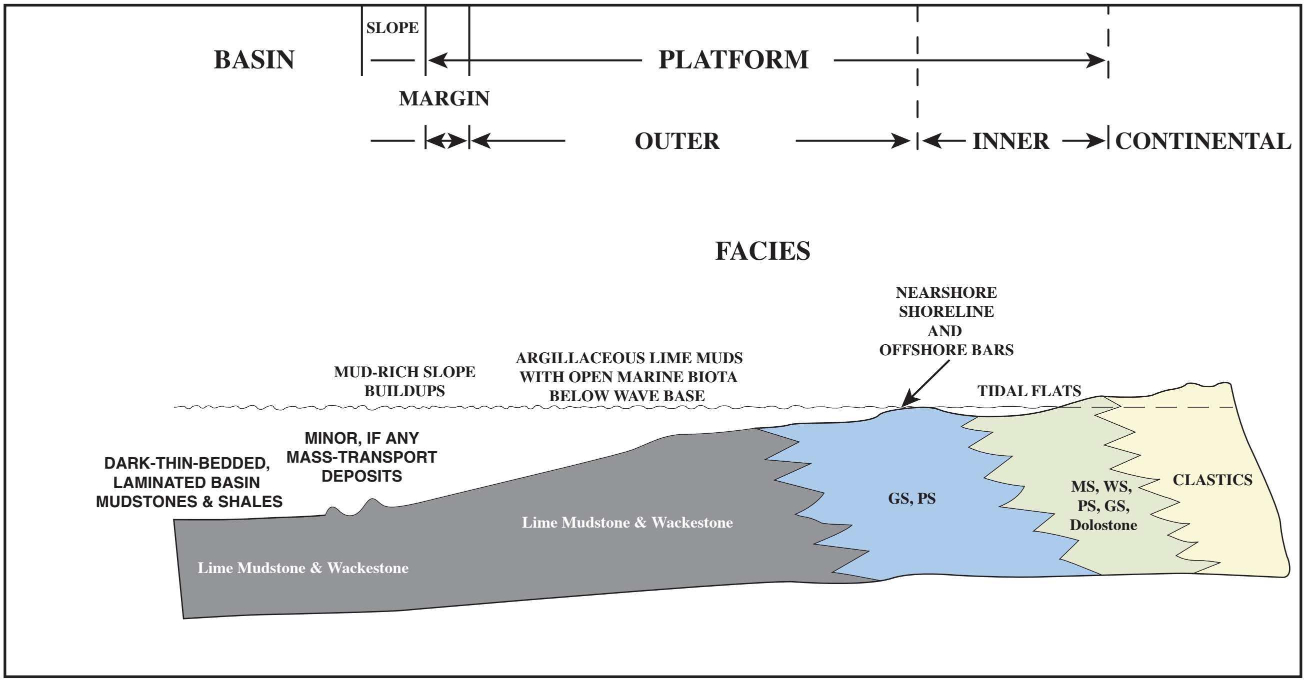

Figure 28. Profile of homoclinal ramp model (Modified from Wilson and Jordan, 1983).

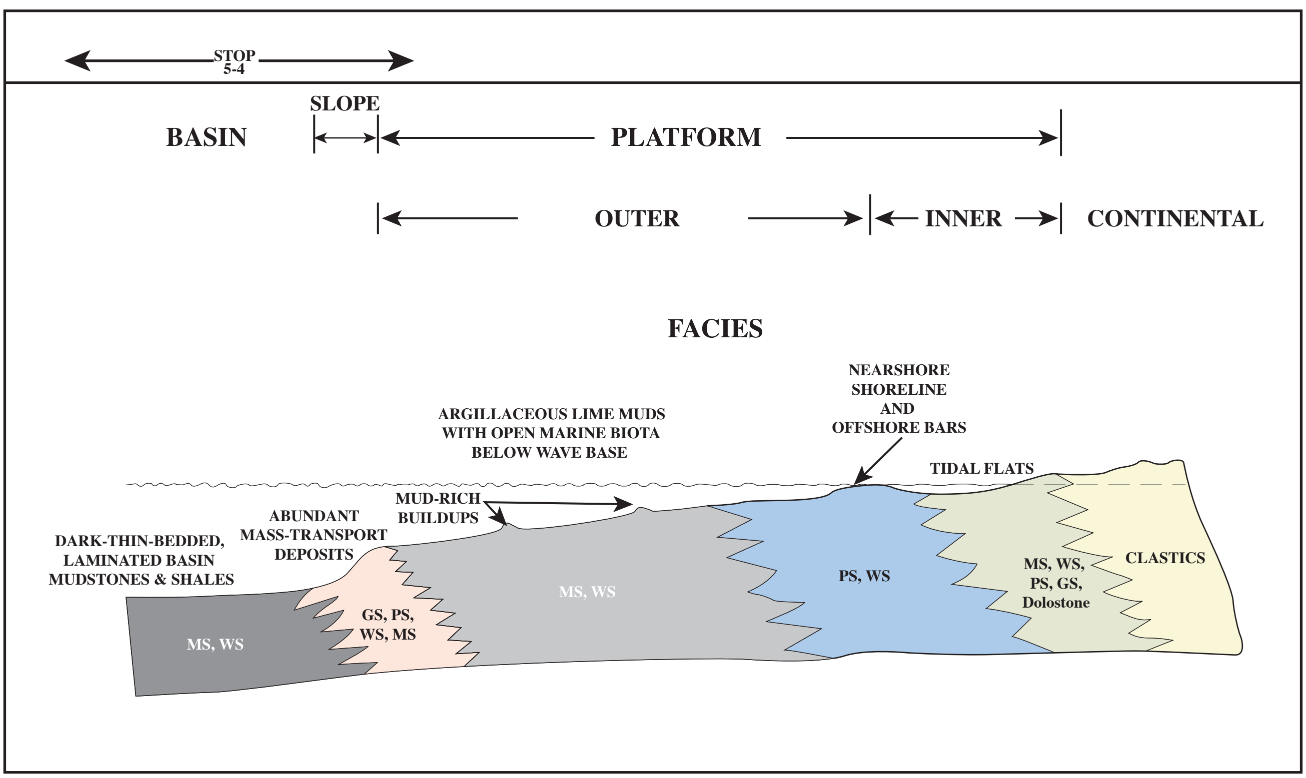

Figure 29. Profile of distally steepend ramp model. Top of figure shows depositional environments of field stops (Modified from Wilson and Jordan, 1983).

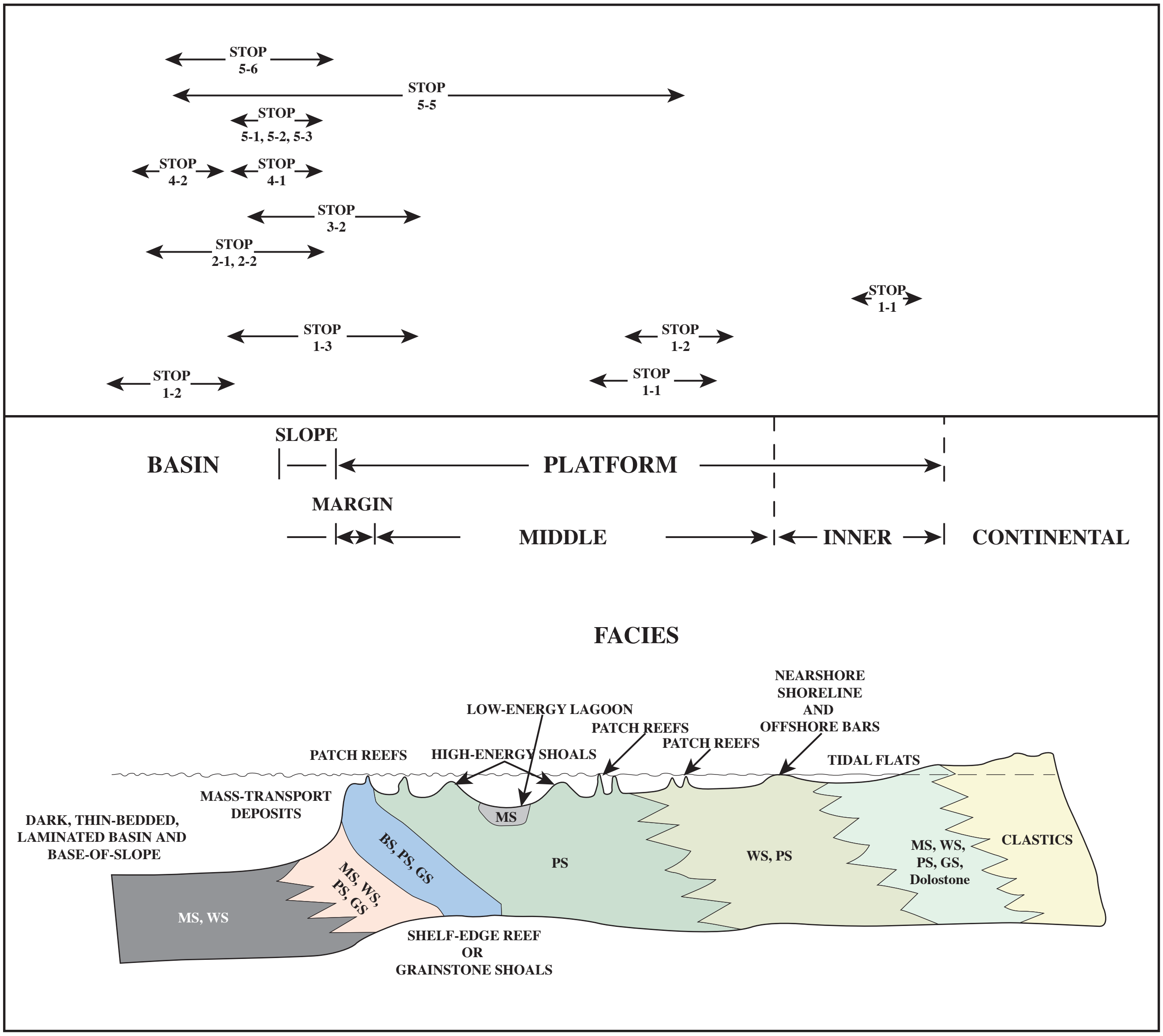

Figure 30. Profile of a rimmed cabonate shelf model. Top of figure shows depositional environments of field stops (Modified from Wilson and Jordan, 1983).

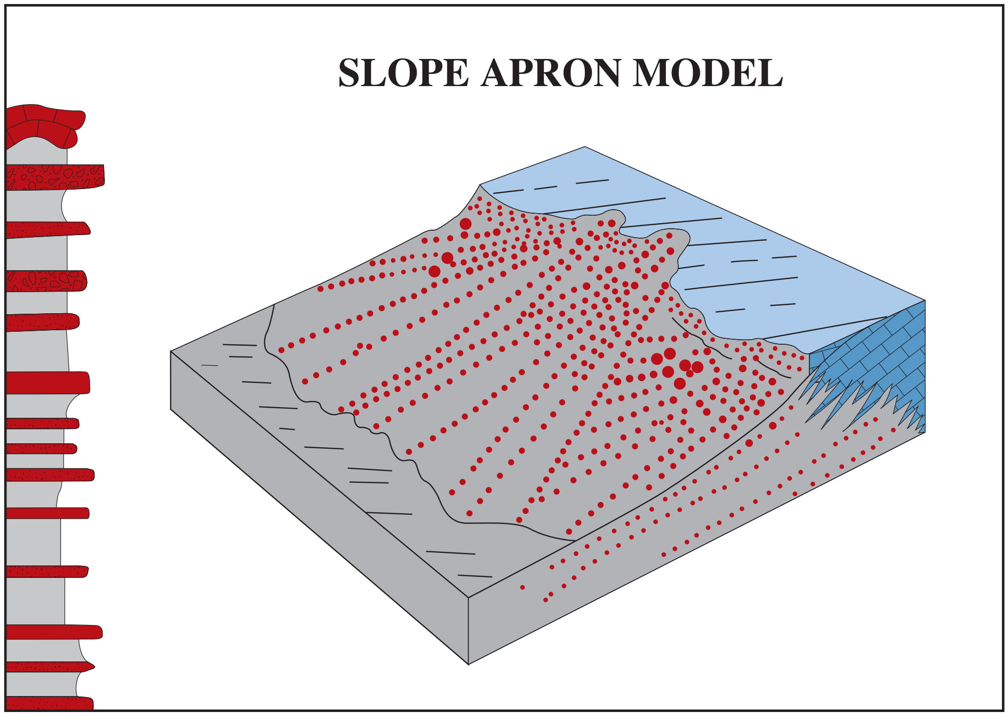

Figure 31. Carbonate debris slope apron model showing shoal water derived debris originating along line source. Debris is transported as broad sheet flows on low angle slopes with debris extending virtually to the platform margin (Modified from Cook and others, 1983).

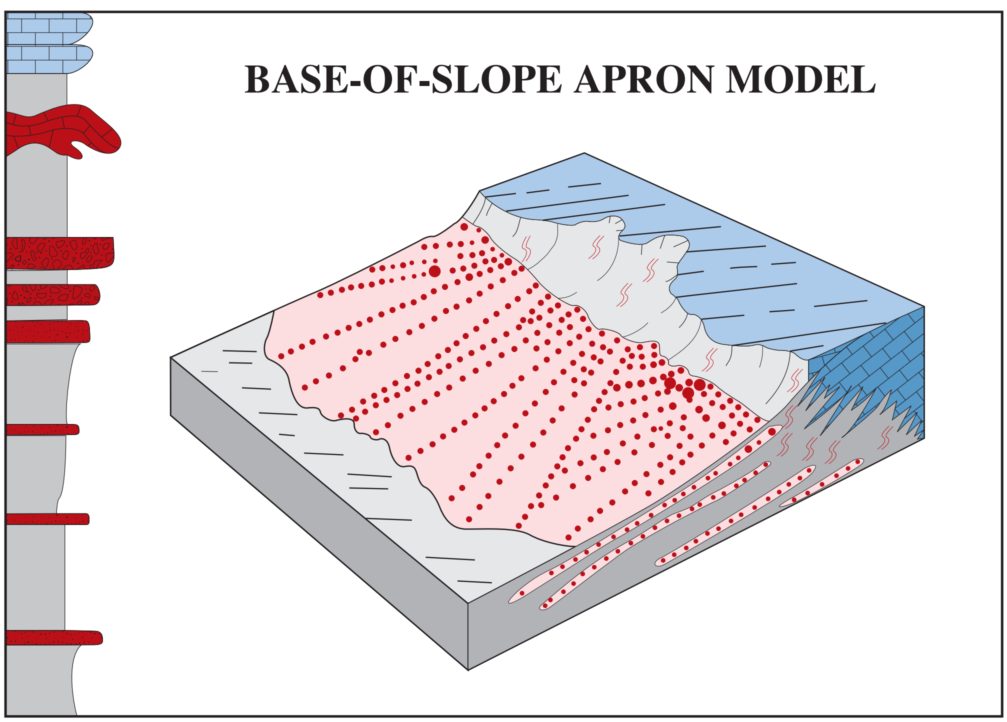

Figure 32. Carbonate base-of-slope apron model showing shoal water derived debris originating along line source. Mass-flow deposits originating at platform margin largely by-pass the slope with the bulk of debris deposited at the base-of-slope (Modified from Cook, 1982).

The siliciclastic submarine fan model is now well established in the geologic literature and is widely used for paleoenvironmental interpretations of coarse-grained deep-sea facies, as well as a predictive model in the exploration for hydrocarbons from deep-water reservoirs. Although the submarine fan model has enjoyed considerable success in its application to siliciclastic deposits, it is clear from the study of both modern and ancient carbonate mass-transported sequences that the siliciclastic submarine fan model cannot be applied to most deep carbonate basin margin deposits (Cook and Mullins, 1983; Mullins and Cook, 1986). Absence of submarine canyons in most carbonate systems is a major factor in the lack of fan morphologic facies. Instead of orderly sequences of fan facies associations, ancient carbonate mass transported deposits commonly consist of seemingly randomly distributed debris more closely resembling the debris sheet model of Cook and others (1972). In fact, well-documented examples of ancient carbonate submarine fans with recognizable fan facies association are quite rare (for example, Cook and Egbert, 1981a, 1981b; Cook, 1982; Ruiz-Ortiz, 1983). Despite this, numerous papers in the literature have indiscriminately used the terms “fan” or “submarine fan” in their discussion of carbonate mass flow facies sequences without presenting evidence that documents the existence of distinct fan facies associations (Cook and Mullins, 1983).

The carbonate slope apron and base-of-slope apron models (Figures 31 and 32) use the debris sheet model (Figure 33) as a foundation in that they retain the fundamental summary aspects of the sheet model (Cook and others, 1972; Cook and others, 1983; Mullins and Cook, 1986). The apron models, however, go much farther by utilizing data from modern environments, re-defining debris facies terminology and facies associations, and by comparing carbonate apron facies to siliciclastic fan facies. The apron models offer an alternative to the siliciclastic fan model for the interpretation of gravity displaced limestone sequences that occur in slope, base-of-slope, and basin plain settings.

Carbonate slope aprons and base-of-slope aprons develop via line-source sedimentation that results in mass-transport facies that parallel the adjacent platform edge and thin in a seaward direction, producing an overall wedge-shaped geometry. Unlike submarine fans, carbonate aprons are likely to produce linear to arcuate facies belts that parallel the adjacent platform edge. The length of the belt will mainly be a function of the nature and length of the platform margin itself. Large isolated platforms such as in the Bahamas (Cook and Mullins, 1983) or the Cretaceous of Mexico (Enos, 1977; Magoon and others, 2001) appear to have very wide aprons along the strike of the platform margin. Small isolated banks, such as the Devonian Ancient Wall an Miette of Alberta, Canada, have carbonate aprons that form relatively small concentric bands around the bank margins (Cook and others, 1972). Large intracontinental platform margins such as developed around the perimeter of the Permian Basin in southeast New Mexico and west Texas may form continuous aprons (10’s to 100’s of km wide; Cook, 1983; Mazzullo, per comm., 1983).

Petroleum reservoirs in carbonate sediment gravity-flow deposits are discussed by Cook and others (1972), Enos (1977, 1985), Cook (1983), Cook and Mullins (1983), Enos and Moore (1983), Mullins and Cook (1986), Cook and others (1983), Mazzullo (1984), Hobson and others (1985), and Magoon and others (2001).

Carbonate Submarine Fan (Figures 34 and 35)

As discussed above carbonate submarine fan facies are rare in contrast to siliciclastic fan facies (Cook, 1982, 1983). This is largely a result of carbonate sediment gravity flow deposits originating along a line-source and not having major point-source canyons as in siliciclastic settings (Cook and others, 1983; Mullins and Cook, 1986).

Cook (1983), Ruiz-Ortiz (1983), Cook and Mullins (1983), and Cook and others (1983) discuss examples of subsurface and surface carbonate fan facies.

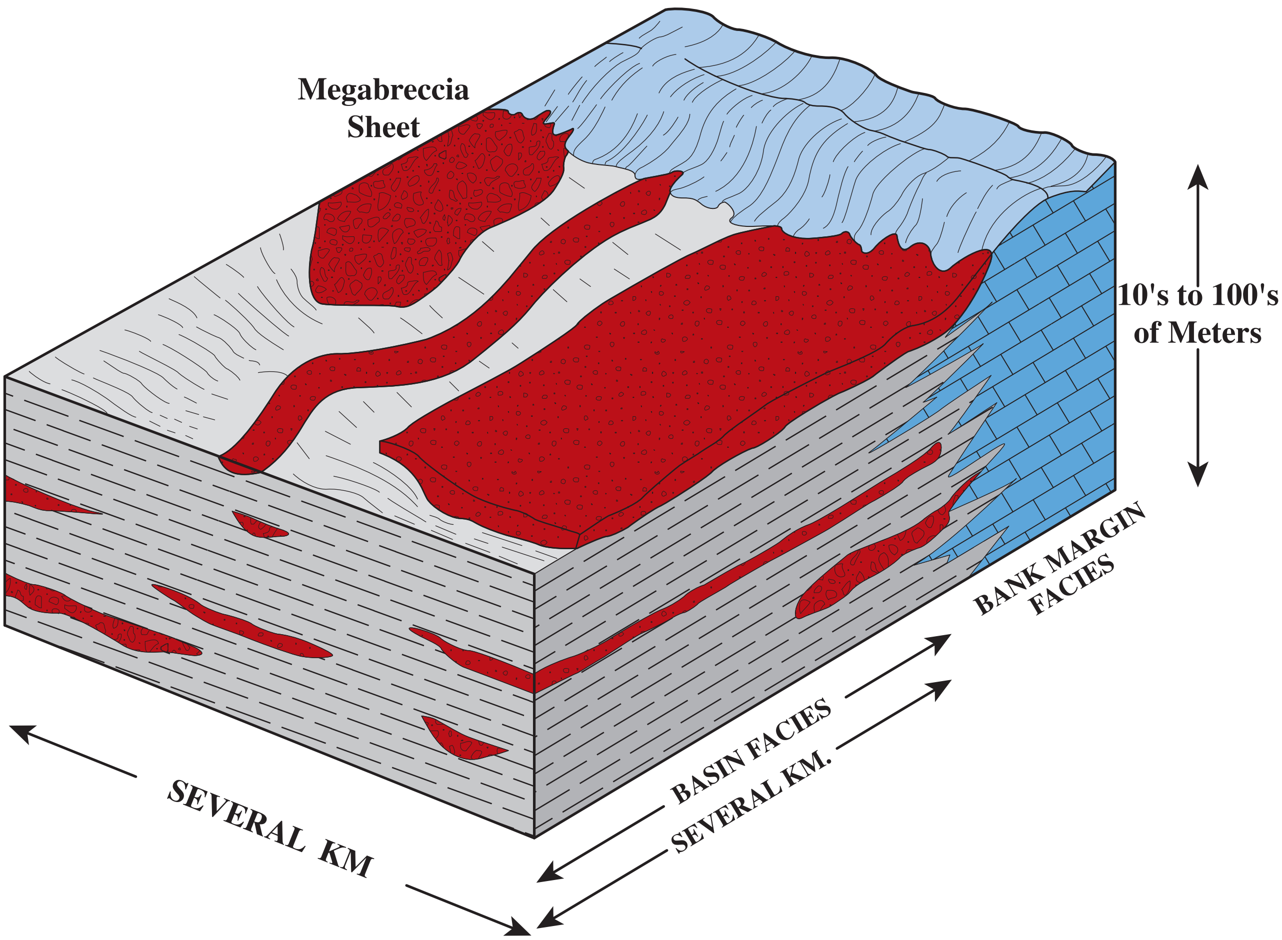

Figure 33. Generalized representation of allochthonous debris deposits showing textures , shapes and relation to platform margin and basin facies (Modified from Cook and others, 1972).

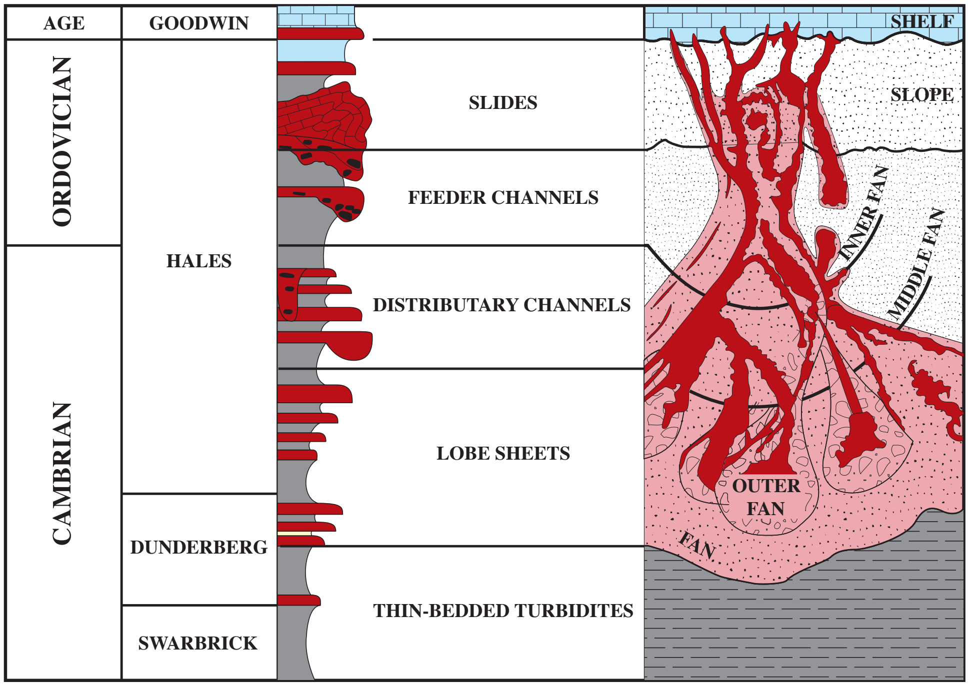

Figure 34. Carbonate submarine fan model showing that fan sediment is derived from both shoal-water shelf areas and by remolding of deeper water slides and slumps into mass-flows, large slides and channelized conglomerates that occur in slope, inner and middle fan region; calcarenites in non-channelized sheets in outer-fan sites, and thin-bedded silt-size to fine, sand-size bioclastic carbonate turbidites in fan fringe and basin plain. Slope and fan facies approximately 500 meters thick and basin plain facies approximately 1000 meters thick. Model based on studies in Cambrian and Ordovician strata in Tybo Canyon, Hot Creek Range, Nevada (Modified from Cook and Egbert, 1981b, and Cook and Mullins, 1983).

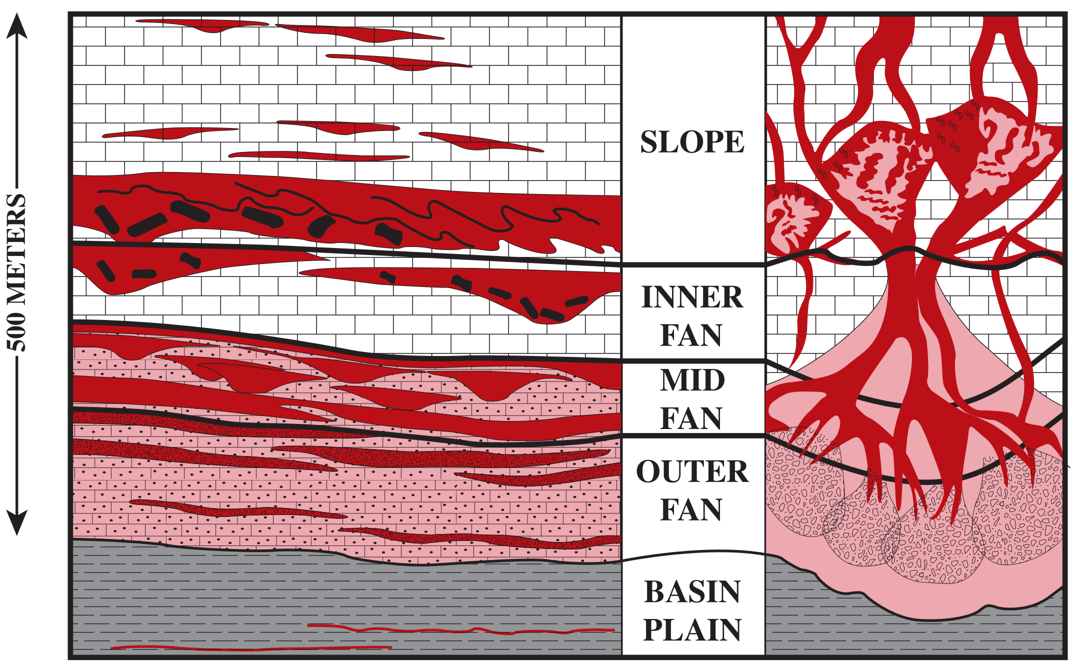

Figure 35. Carbonate submarine fan model. Schematically shows vertical and lateral facies sequences that occur in prograding continental margin section. Model based on studies in Cambrian and Ordovician carbonate submarine fan facies in Tybo Canyon, Hot Creek Range, Nevada (Modified from Cook and Egbert, 1981b and Cook and Mullins, 1983).

DYNAMIC CARBONATE SEQUENCE STRATIGRAPHY MODELS (Figure 36)

General Perspectives

Sequence stratigraphy is now considered to be a practical tool for analyzing the development and evolution of carbonate platforms (Wilgus and others, 1988, Eberli and Ginsburg, 1989; Handford and Loucks, 1993). For an in depth discussion of carbonate sequence stratigraphy see Handford and Loucks (1993), Read and others (1995), Kerans and Tinker (1997) and Wilgus and others (1998).

Over the past several decades carbonate depositional facies models, for example, Ahr (1973), Cook (1983), Read, (1985), and Wilson (1975) have been routinely used for describing, interpreting and predicting facies relationships in carbonate platforms and deeper-water basin margins. However, depositional facies models by themselves do not address or predict rigorously how carbonate platforms and their facies belts are affected by relative fluctuations in sea level. An understanding of how the "carbonate factory" responds to relative sea-level changes is of fundamental importance.

Kerans and Tinker (1997) summarizes the terminology of cycle hierarchies and orders of cyclicity and presents some useful quantitative data for better understanding tectono-eustatic and eustatic cycle orders, their duration in millions of years, relative sea level amplitudes in meters, and relative sea level rise/fall rates in cm/1,000 years (i.e., 1 cm/1,000 years = 10 m/million years = 10 Bubnoffs). Fischer and Bottjer (1991) discuss orbital forcing and sedimentary sequences. They nicely summarize the Milankovitch frequency band for the earth's orbital variations (eccentricity, obliquity, and precession) and their effects on cycles of ice growth. Read (1995) presents an excellent discussion of carbonate platform sequences, cycle stratigraphy, and reservoirs in greenhouse and icehouse worlds.

A sequence is a relatively conformable succession of genetically related strata bounded by unconformities and their correlative conformities (Mitchum, 1977). An unconformity is a surface separating older from younger strata where there is evidence of subaerial truncation, karsting, hardgrounds, and/or submarine erosion, with some degree of hiatus indicated. Sequences are composed of three parts, or systems tracts. A systems tract is a linked set of contemporaneous depositional systems (i.e., a 3-D assemblage of lithofacies; Brown and Fisher, 1977). System tracts are interpreted to form during specific time intervals of the relative change of the sea-level curve. A sequence in interpreted to be deposited during the cycle of eustatic change of sea level starting and ending in the vicinity of the inflection points on the falling limbs of the sea-level curve (Sarg, 1988).

Sequence stratigraphy integrates time and the cycles of relative-sea-level changes so we can track the migration of facies through time and space. The strength of sequence stratigraphy lies in its potential to predict facies within a chronostratigraphic framework of unconformity-bound depositional sequences (Haq and others, 1987; Handford and Loucks, 1993). Depositional sequence models are constructed to show the dynamic evolution through time and space of carbonate platforms. However, depositional sequence models should complement, rather than replace, the static models of Ahr (1973), Cook (1983), Read, (1985), Wilson (1975).

When properly used the combination of static depositional models and depositional sequence models can assist in developing predictive mineral and petroleum host/reservoir models.

Sequences and Systems Tracts

Basic carbonate depositional principles and geologic-based observations were used to construct a depositional sequence and systems tract model for a humid carbonate rimmed platform (Figure 36). Figure 37 shows how, for example, depositional sequences made up of carbonates are produced by depositional systems responding to relative lowstand, transgressive, and highstand sea-level conditions.

Lowstand (Figure 37): A lowstand systems tract develops during the later part of a relative sea level lowering. Carbonate sediment production is reduced or even terminated on platform tops and sediment production is often limited to only the platform margins and slopes. Platform margin organic buildups may undergo a forced regression and move slope. Platform margins can become gravitationally unstable and massive collapse of the platform margins can occur

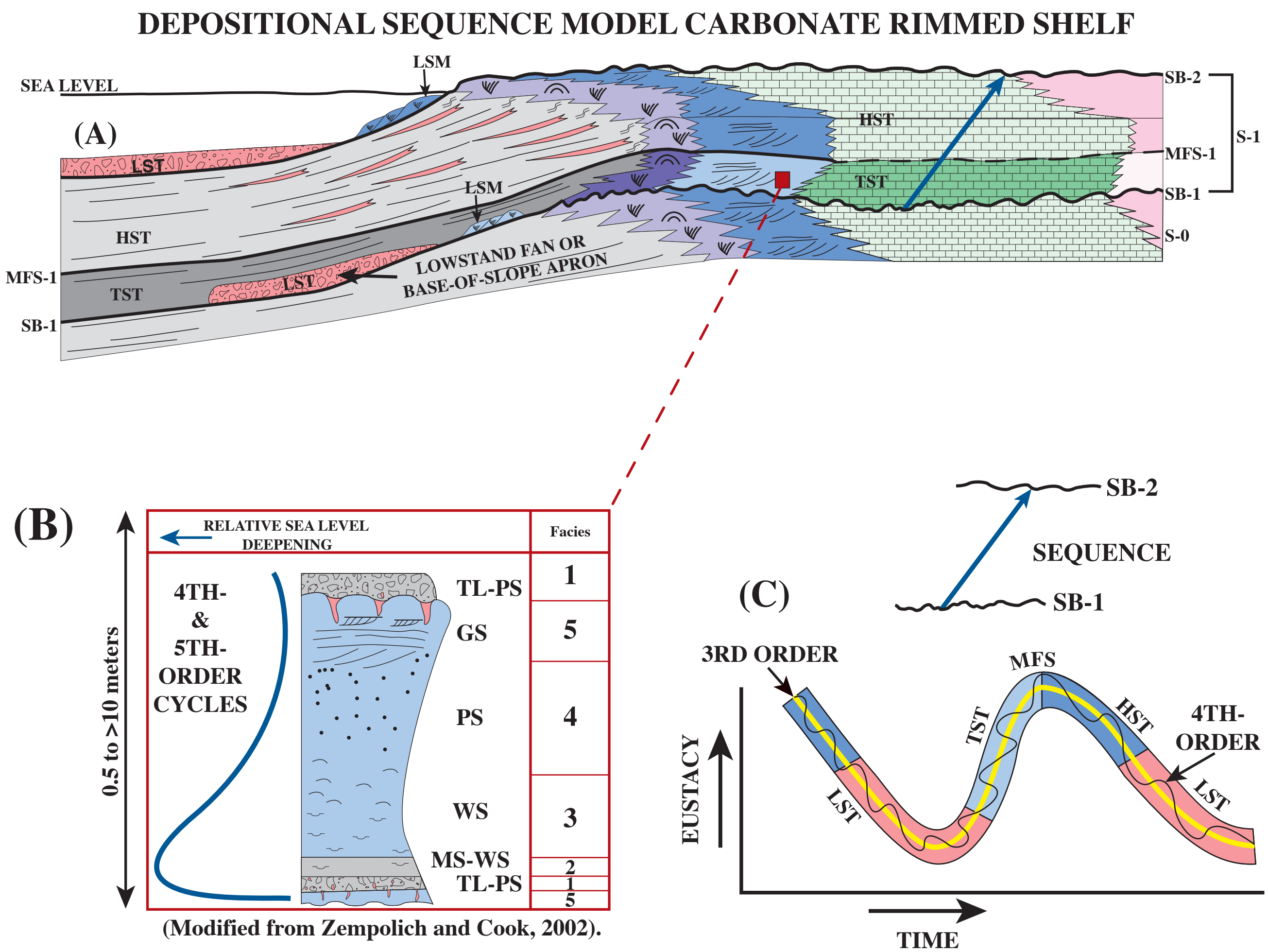

S1	SEQUENCE-1		CARBONATE SEQUENCE
SB-	SEQUENCE BOUNDARY		DEBRIS FLOWS AND TURBIDITES
MFS	MAXIMUM FLOODING SURFACE	GS	GRAINSTONE
LST	LOWSTAND SYSTEMS TRACT	PS	PACKSTONE
LSM	LOWSTAND MARGIN	WS	WACKESTONE
TST	TRANSGRESSIVE SYSTEMS TRACT	MS	MUDSTONE
HST	HIGHSTAND SYSTEMS TRACT	TL -PS	TRANSGRESSIVE LAG-PACKSTONE

Figure 36. Illustrates the basic principles of carbonate sequence stratigraphy. Lowstand systems tract forms by platform margin collapse and lowstand shedding of shoal-water derived carbonate debris during a relative sea level lowering. Platform margin may prograde downslope to form a lowstand margin. Platform interior karsting can occur during a lowstand. A transgressive systems tract develops during a rapid, relative sea level rise. This results in the platform margin backstepping and/or retrogradating. During the initial phase of the sea level lowering, following the maximum flooding surface, the highstand systems tract forms. This results in a thick, aggradational and progradational carbonate platform architecture. Sedimentation rates on the platform are high resulting in abundant carbonate sediments shedding off the platform forming slope and base-of-slope aprons (Modified from Handford and Loucks, 1993).

with the development of large amounts of lowstand debris flow and turbidite deposits forming aprons and fans (Figure 37A). These lowstand allochthonous deposits can be comprised of meter size or larger blocks (megabreccias) when parts of the platform margin collapses. These megabreccia blocks may also show signs of having been karsted prior to their detachment and transportation down slope. These submarine sediment-gravity flow deposits can make excellent host/reservoir facies for both minerals and petroleum (Mullins and Cook, 1986; Cook, 1993). Karsting in the platform interior can be important in humid environments (Cook and others, 2002b, text Figures 3, 14).

Transgression (Figure 37): A transgressive systems tract develops during a relative sea-level rise. With marine transgression carbonate sedimentation is initiated on the platform and patch reefs may locally develop atop the flooded platforms (Cook and others, 2002b, Figures 3, 12, 13). Retrogradational sequences can form and platform margins tend to retreat and/or backstep and even drown if the rate of the relative sea level is high (Figure 37B and 37C. Condensed deposits (i.e., deposits formed during very low sedimentation rates) may occur atop platforms and in the basin during maximum transgression (i.e., at the maximum flooding surface).

Highstand (Figure 37): A highstand systems tract develops during the late stages of a relative sea-level rise and during much of the relative sea level lowering. Aggradation and seaward progradation of the platform margin takes place as the platform is flooded and carbonate sedimentation rates are very fast under these conditions (Figure 37D and 37E. Abundant excess shoal-water sediments can be shed off the platform margins forming upper slope tidal bars and carbonate turbidite and debris flow slope and base-of-slope debris aprons. Highstand debris aprons are normally comprised of fewer megabreccias than lowstand debris aprons. This is especially true on the leeward margins of carbonate platforms (Mullins and Cook, 1986). These submarine sediment-gravity flow deposits can make excellent host/reservoir facies for both mineral and petroleum (Mullins and Cook, 1986; Cook, 1993).

Neither static nor dynamic depositional sequence models are meant to serve as rigid templates. Modification is often needed to accommodate each case. They can serve as working hypotheses to help geologists better understand how and why carbonate strata were deposited and fit together as they do. As a general predictor of facies, carbonate depositional sequence and systems tract models may be used in conjunction with seismic records to identify depositional systems and to locate host/reservoir, seal, trap and source prone facies.

In summary, both static and dynamic models can serve as frameworks or guides for making observations, they can provide a basis for stratigraphic and facies interpretations and they can serve as predictors.

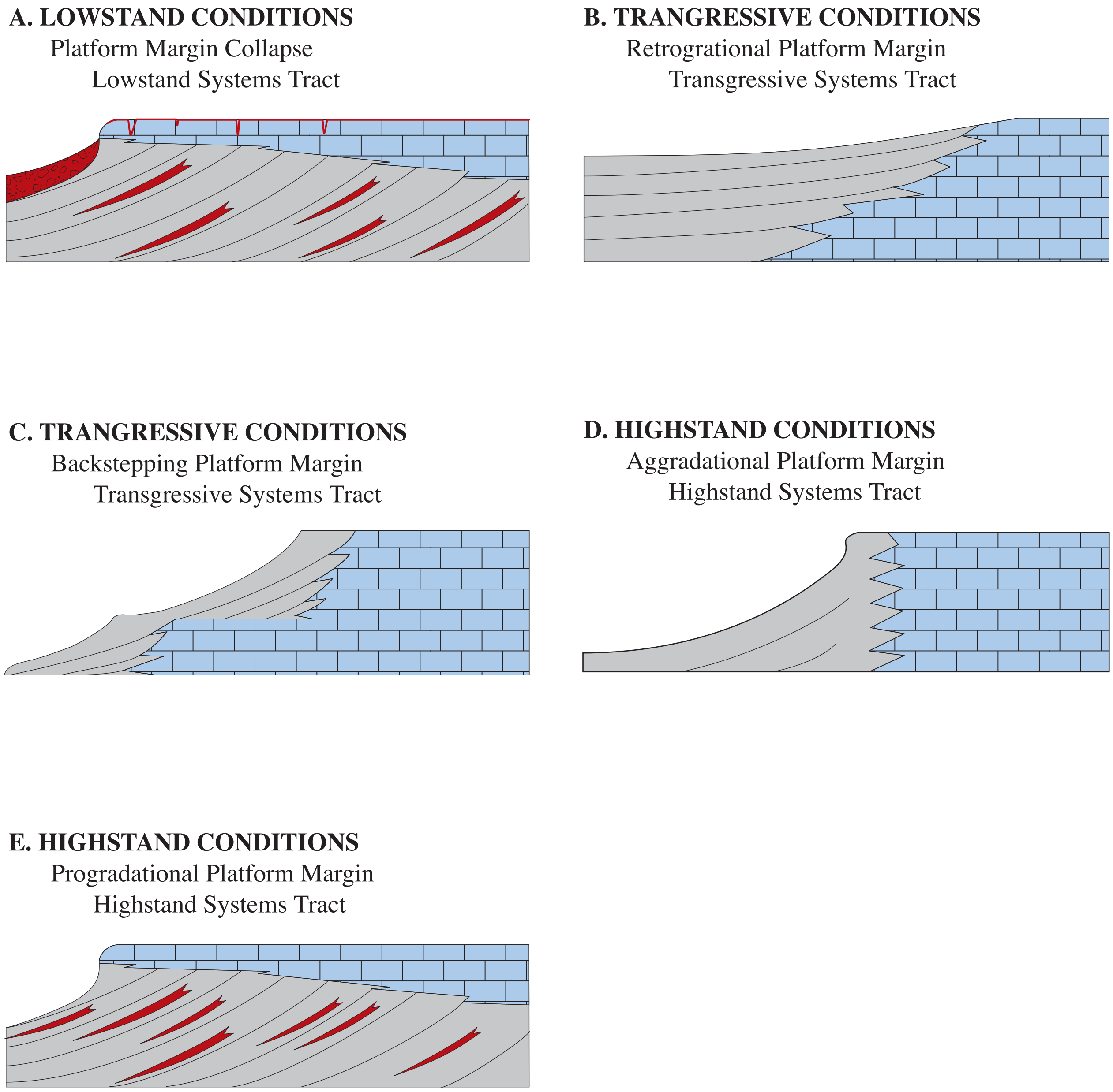

Figure 37. Morphologic evolution of carbonate outer-shelf margins to see on field trip: (A) Stop 1-1, 2-2, 4-2, 5-4, and 5-6; (B) Stops 2-2; (C) Stop 2-2 and 5-6; (D) Stops 3-2, 5-6; (E) Stops 1-3, 3-2, 5-5, 5-6 (Models modified from Playford, 1980).

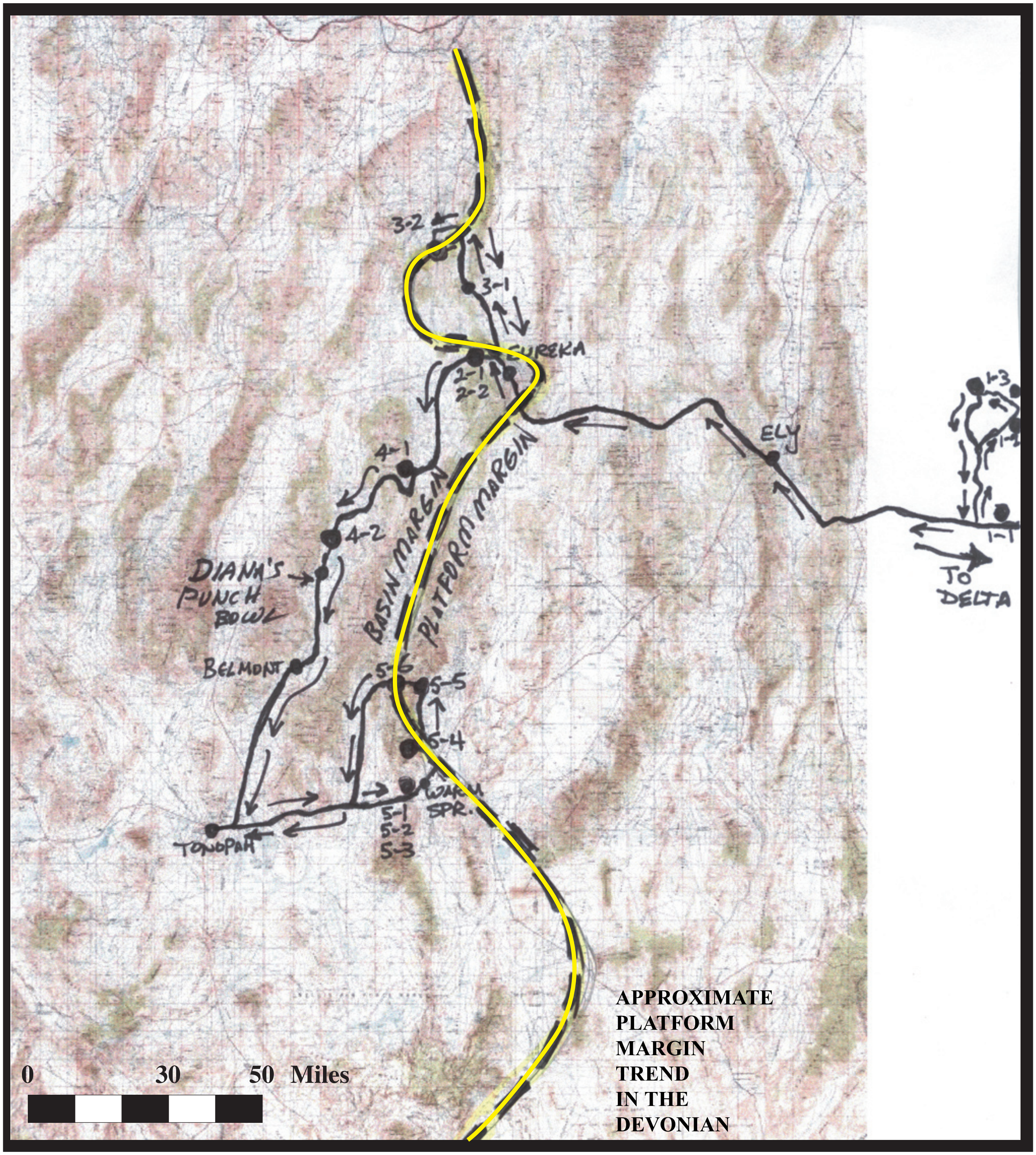

Map 1. Field trip map for the Metallogeny of the Great Basin Project Field Trip on August 17-22, 2003. Day 1, Stop 1 (1-1).

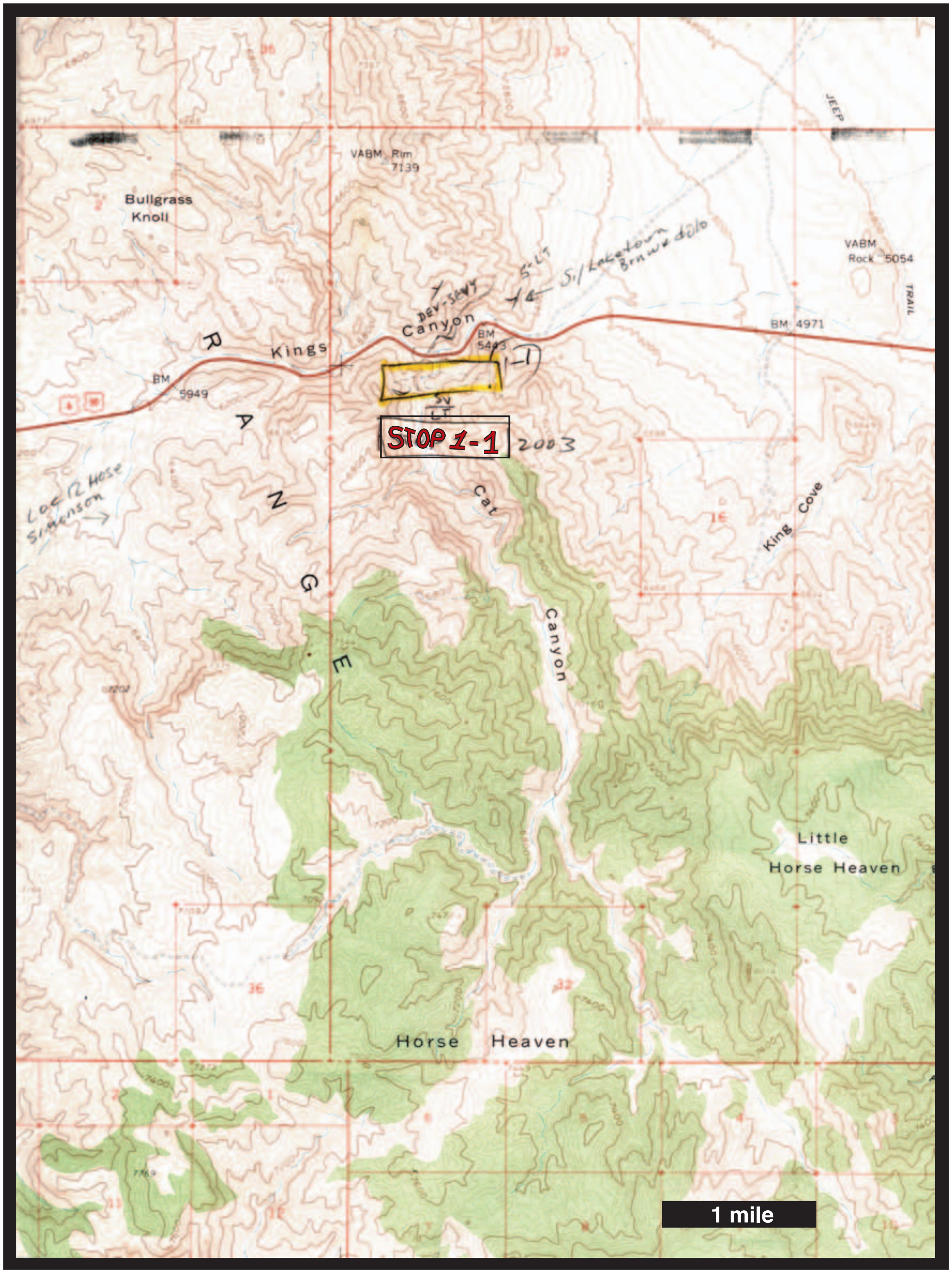

Map 2. Location of Stop 1-1 on the Conger Mountain Quadrangle, Kings Canyon, Utah.

FIELD SEMINAR STOPS

The purpose of the following text is (1) to summarize the environmental interpretations of the various types of depositional facies that existed in much of the Great Basin carbonate platform, (2) to place the facies and standard facies models into the broader framework of sequence stratigraphy and carbonate depositional sequences and systems tracts (i.e., the response of carbonate platforms to relative sea level changes through time and space), and where appropriate 3) to discuss mineral host facies and petroleum reservoir facies in the context of sequence stratigraphy.

STOP 1-1 – CONFUSION RANGE, UTAH

Age- Middle Silurian and Early Devonian

Formations- Laketown Dolomite and overlying Sevy Dolomite.

Carbonate Depositional Sequences (Figure 2)– The contact between the Laketown Dolomite and the Sevy Dolomite is interpreted to represent a sequence boundary separating Sequences #5 and #6 (Figure 2).

Depositional Environments (Figure 38) – The uppermost Laketown Dolomite is interpreted to have formed in a middle platform environment. It is characterized by highly bioturbated dolostones with relict fossils, including brachiopods, crinoids, and scattered rugose corals. Near the top of the formation are dolomitized stromatoporoid biostromes about 1 meter thick by 50 meters wide. These biostromes are comprised of bulbous and tabular stromatoporoids, and the dendroid stromatoporoids Amphipora and/or Stachyodes. The biostromes appear to laterally thin into dolomitized bioclastic wackestones.

The overlying Sevy Dolomite represents a dramatic change in depositional setting. It formed in intertidal and supratidal setting and exhibits wavy-laminated, microcrystalline dolostone and fenestral fabrics.

In both the Laketown and Sevy, several interpreted solution horizons occur. These horizons are interpreted to be the result of relative sea level fluctuations during Late Silurian and Early Devonian (Figure 2) (Cook and others, 1983; Figure 5-32) that exposed the shallow platform and tidal flat environments to meteoric vadose, phreatic, and/ or subaerial diagenesis.

Chief Features to be Observed –

Laketown Dolomite:

1. Biostromes of tabular and bulbous stromatoporoids, and dendroid stromatoporoids (Amphipora and/or Stachyodes).

Laketown and Sevy Dolomite:

1. Karst (?) breccias (relative lowering of sea level with vadose and /or subaerial leaching).

Sevy Dolomite:

1. Light gray laminated dolostones and vuggy fenestral fabrics (intertidal and supratidal with possible solution enlargement of fenestrate voids).

Economic Considerations – Biostromes (patch reefs) may form anywhere on wide platforms and as such can be difficult to locate in the subsurface. Middle platform patch reefs, however, are common petroleum exploration targets in the Permian Basin. An example of this type of reservoir is the Amacker Tippett (Wolfcampian, Permian), West Texas. Wilson (1975), and Wilson and Jordan (1985) review other patch reef fields in middle platform settings, especially in the Pennsylvanian and Permian.

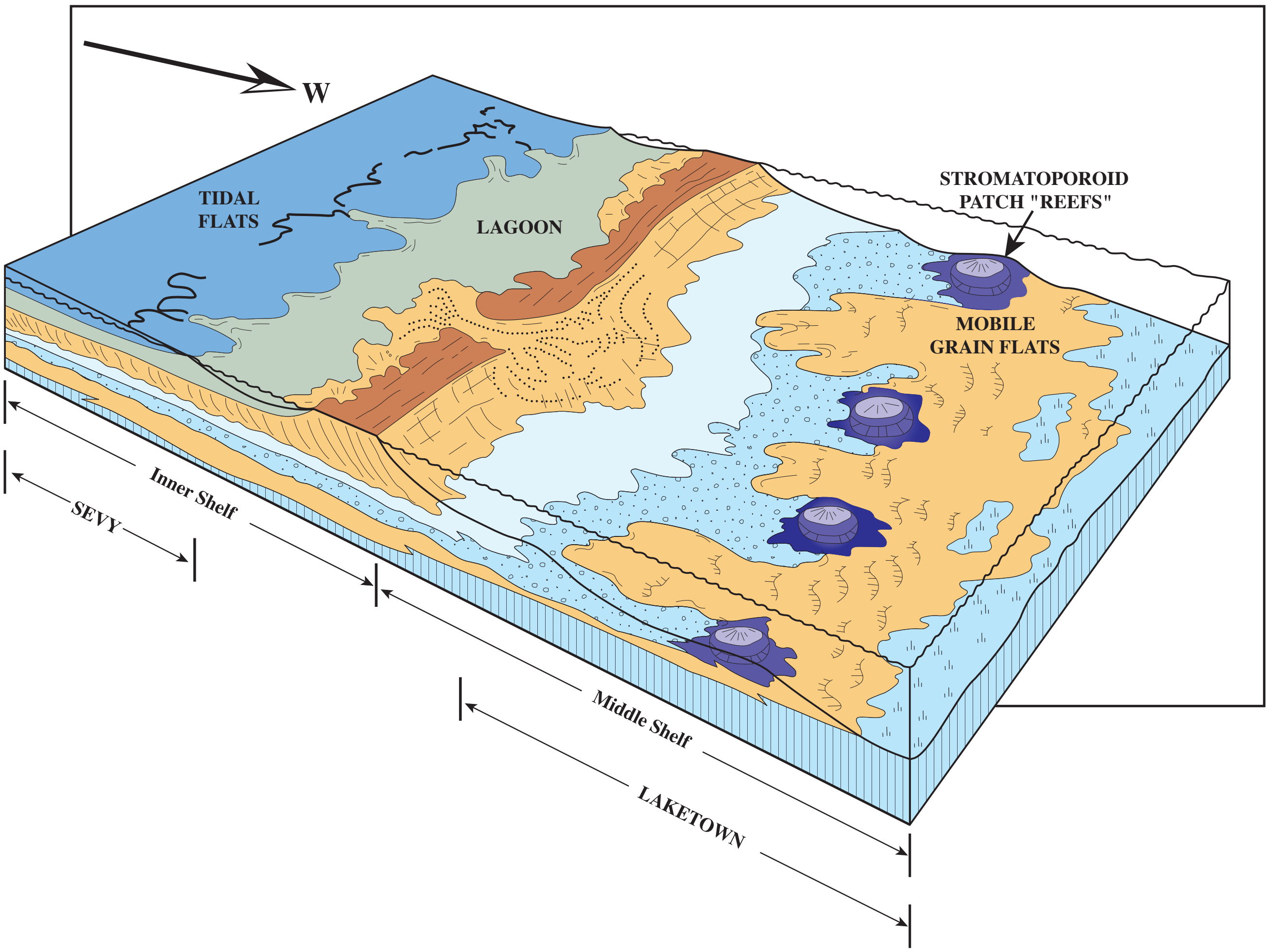

Figure 38. Depositional environments for upper Laketown and lower Sevy at Stop 1-1 (Modifed from Wilson and Jordan, 1983).

Relation to Future Stops – At Stop 3-2, we will examine approximately the same stratigraphic interval in the Roberts Mountains in central Nevada. The section in the Roberts Mountains represents aggradation and seaward progradation of a shallow water, coral-rich platform margin. These platform margin facies interfinger with and prograde westerly over deeper water slope and basin margin facies. At Stop 3-2 we will examine and discuss depositional Sequence #5 (Figure 2). South of Roberts Mountains, at Stop 5-5 in the Hot Creek Range, we will have an overview stop to see this same stratigraphic interval and the seaward prograding relationship of the platform margin and the slope/basin margin facies during the development of depositional Sequences #2, #3, #4 and #5.

Photo 1-1a. Brown Laketown Dolomite (middle platform) and overlying light grey Sevy Dolomite (inner platform tidal flats). Looking north at Stop 1-1. Kings Canyon, Confusion Range, Utah.

Photo 1-1b. Laketown Dolomite. Stromatoporoid biostrome about 1-meter thick by 50-meters wide (enclosed in red) at Stop 1-1. Confusion Range, Kings Canyon, Utah.

Photo 1-1c. Laketown Dolomite. Stromatoporoid biostromes (enclosed in red). Stop 1-1. Kings Canyon, Confusion Range, Utah.

Photo 1-1d. Laketown Dolomite. Syringoporella (?) colonial coral in biostrome. Stop 1-1. Kings Canyon, Confusion Range, Utah.

Photo 1-1e. Uppermost Laketown Dolomite exhibiting solution and karsting at the boundary of depositional sequence #5 and #6. Stop 1-1. Kings Canyon, Confusion Range, Utah.

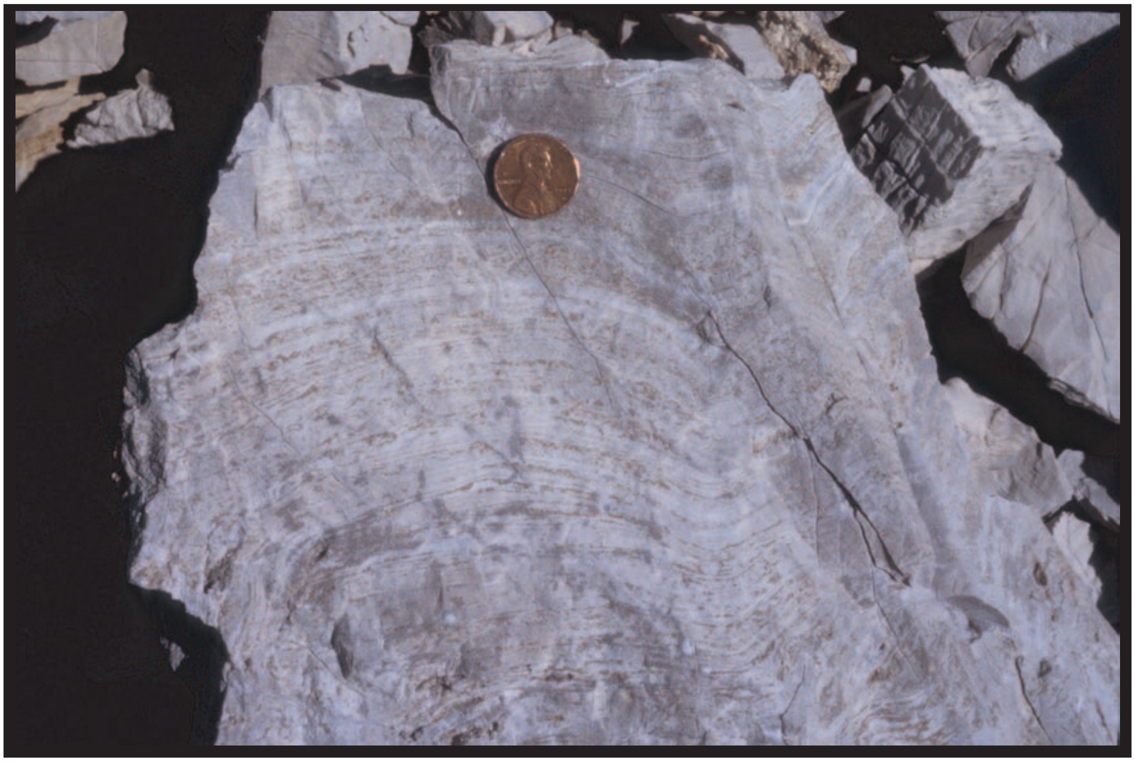

Photo 1-1f. Sevy Dolomite. Algal stromatolites in inner platform tidal flat facies. Stop 1-1. Kings Canyon, Confusion Range, Utah.

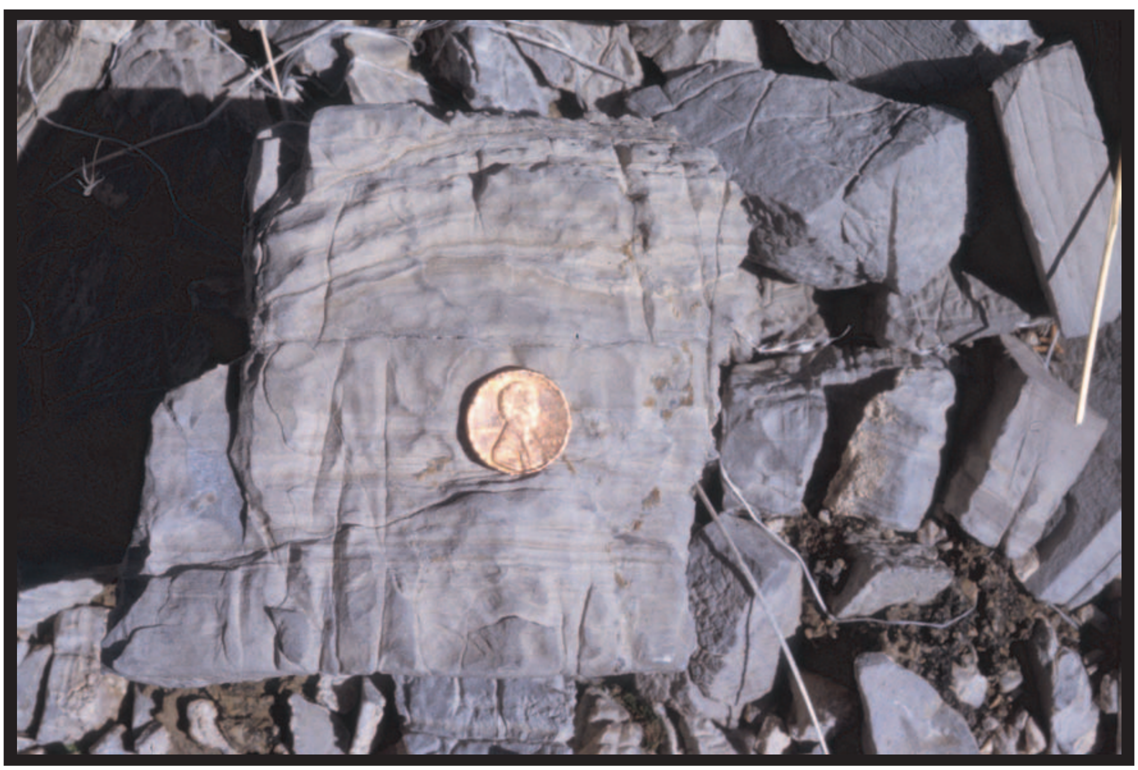

Photo 1-1g. Sevy Dolomite. Irregularly laminated inner platform tidal flat dolomites. Stop 1-1. Kings Canyon, Confusion Range, Utah.

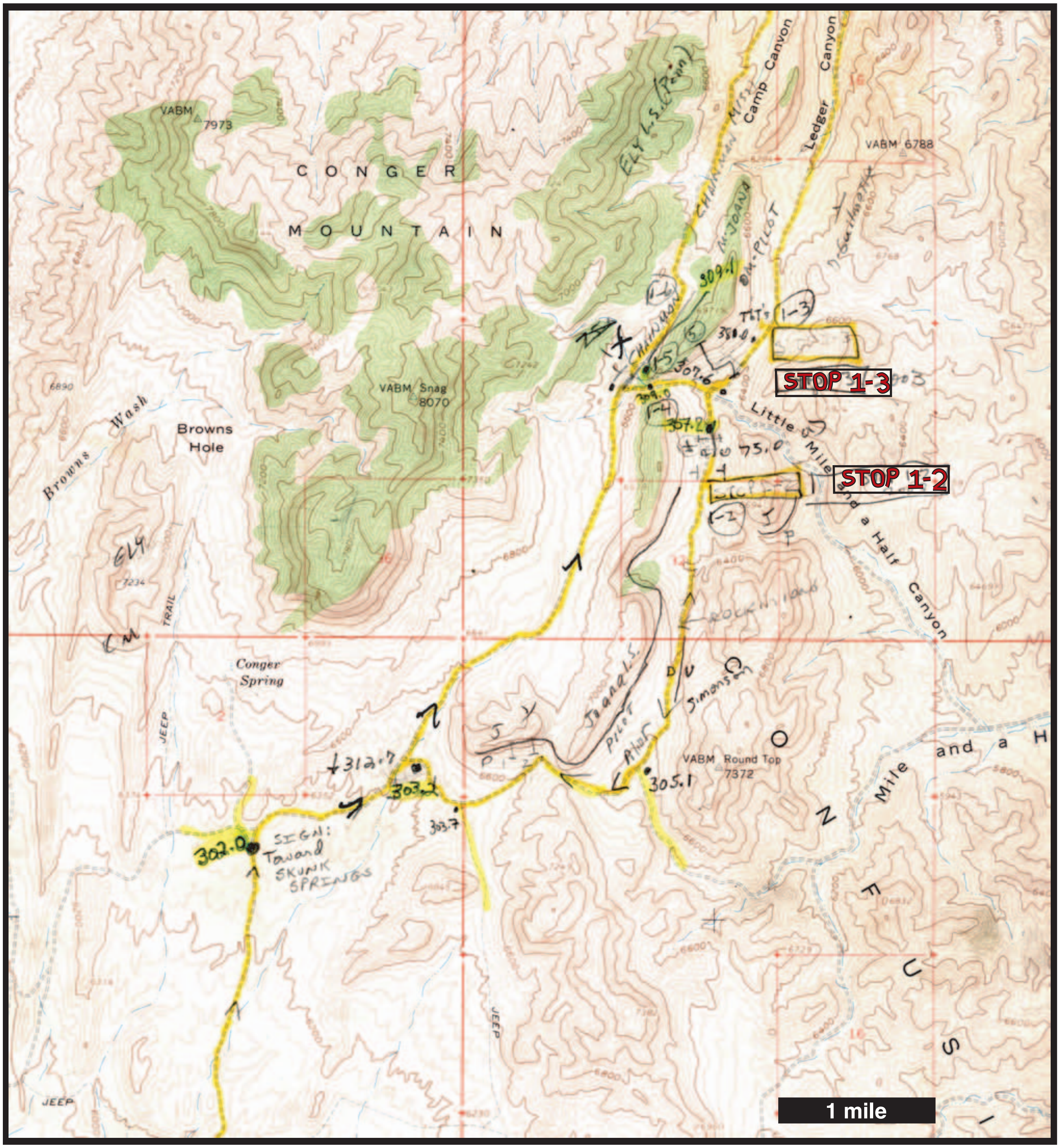

Map 3. Location of Stops 1-2 and 1-3 on the Conger Mountain Quadrangle, Little Mile and a Half Canyon, Utah.

STOP 1-2 – CONFUSION RANGE, UTAH

Age – Late Devonian.

Formation – Guilmette Limestone and overlying Pilot Shale.

Carbonate Depositional Sequences (Figure 2)– The contact between the Guilmette Limestone and the Pilot Shale is interpreted to represent a major sequence boundary separating the top of Sequence #10 and the base of Sequence #11 (Figure 2 and 3).

Depositional Environments – The uppermost Guilmette Limestone is considered to have formed in relatively quiet middle shelf settings. At this locality the rocks are dark gray, highly bioturbated wackestones with abundant open marine fossils including articulated crinoid stems, rugose corals, and brachiopods. The Guilmette Limestone is abruptly overlain by the deeper water Pilot Shale which records a relative rapid sea level rise during the initiation of the Antler Orogeny.

Chief Features to be Observed –

<u>Guilmette Limestone</u>:

1. Intensely burrowed nodular fossiliferous wackestones (quiet water, subtidal, middle shelf setting)

<u>Pilot Shale</u>:

1. Light brown calcareous quartz siltstones with faint parallel and cross laminations and silty shales (subtidal, thin-bedded turbidites and in-situ basinal shales at eastern margin of the Antler foreland basin).

Economic Considerations – The Pilot Shale at this locality has been studied in detail for its source rock characteristics by Sandberg and others (1980). According to their data both the Pilot Shale and Chainman Shale that overlies the Joana Limestone contain probable petroleum source beds in this area. Color Alteration Index values for conodonts in these shales indicate submature to mature thermal maturation of organic matter. Organic carbon percent ranges up to about 3% in both formations.

Relation to Future Stops – In the southern Egan Range of eastern Nevada, the uppermost Guilmette resembles the Guilmette at this stop. In the Egan Range the Guilmette is comprised of crinoid-rich wackestones with large articulated stems. This suggests normal marine, relatively quiet subtidal waters in a middle shelf setting.

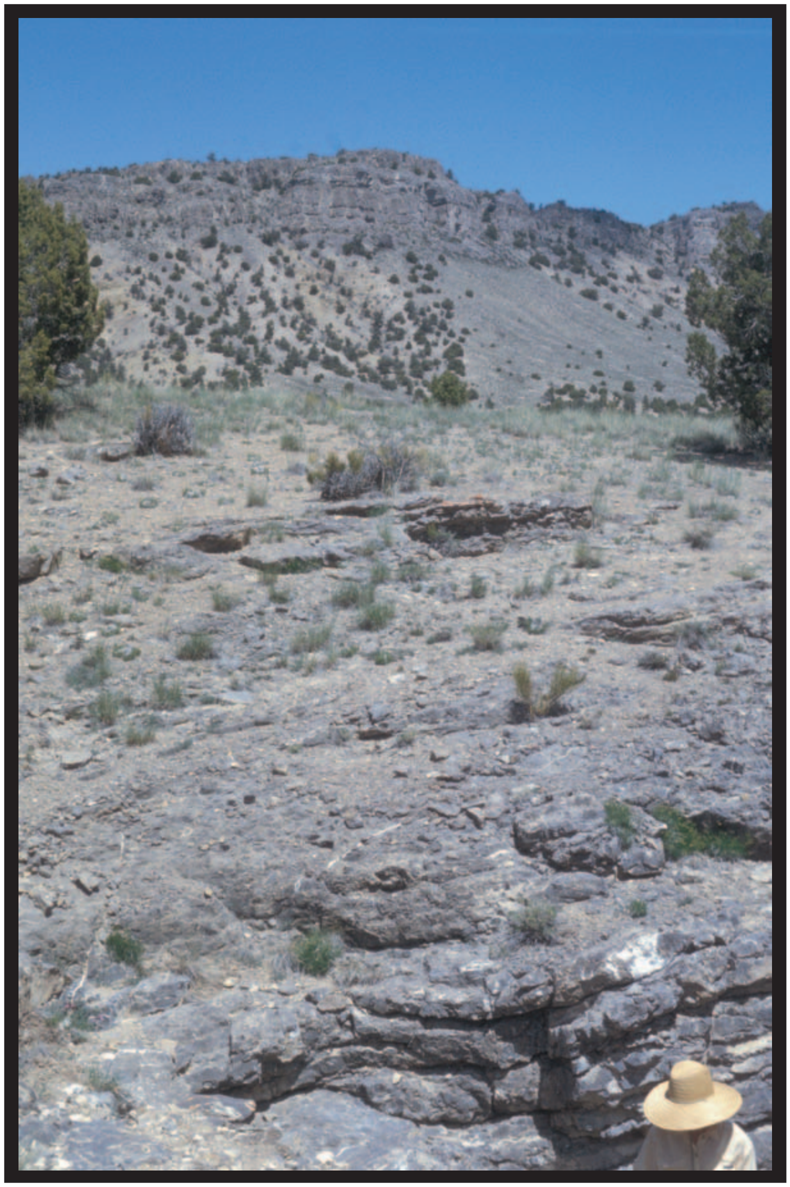

Photo 1-2a. Guilmette Limestone in foreground overlain by recessive weathering Pilot Shale and cliff-forming Joana Limestone in background. Stop 1-2. Little-Mile-and-a-Half Canyon, Confusion Range, Utah.

Photo 1-2b. Guilmette Limestone. Thin-bedded, highly bioturbated middle platform facies. Stop 1-2. Little-Mile-and-a-Half Canyon, Confusion Range, Utah.

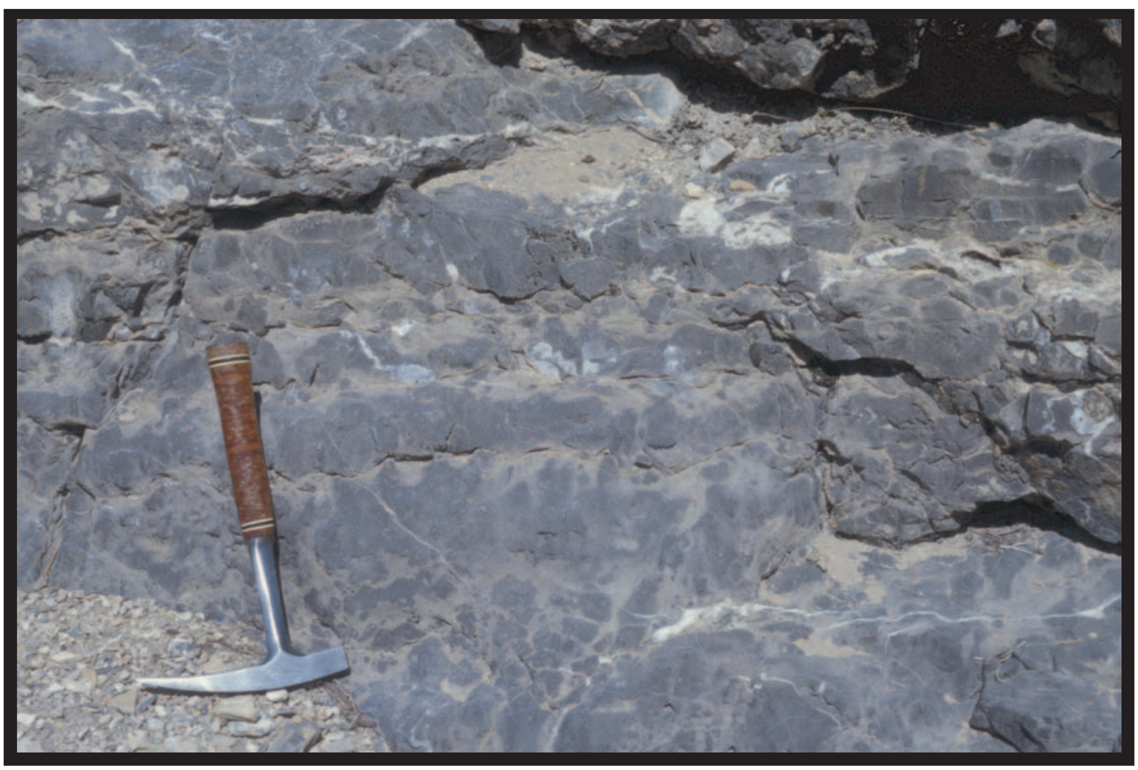

Photo 1-2c. Guilmette Limestone. Typical appearance of middle platform carbonate facies with bedding planes disrupted by burrowing. Stop 1-2. Little-Mile-and-a-Half Canyon, Confusion Range, Utah.

Photo 1-2d. Guilmette Limestone. Surface of bed showing intense burrowed fabric. Middle platform. Stop 1-2. Little-Mile-and-a-Half Canyon, Confusion Range, Utah.

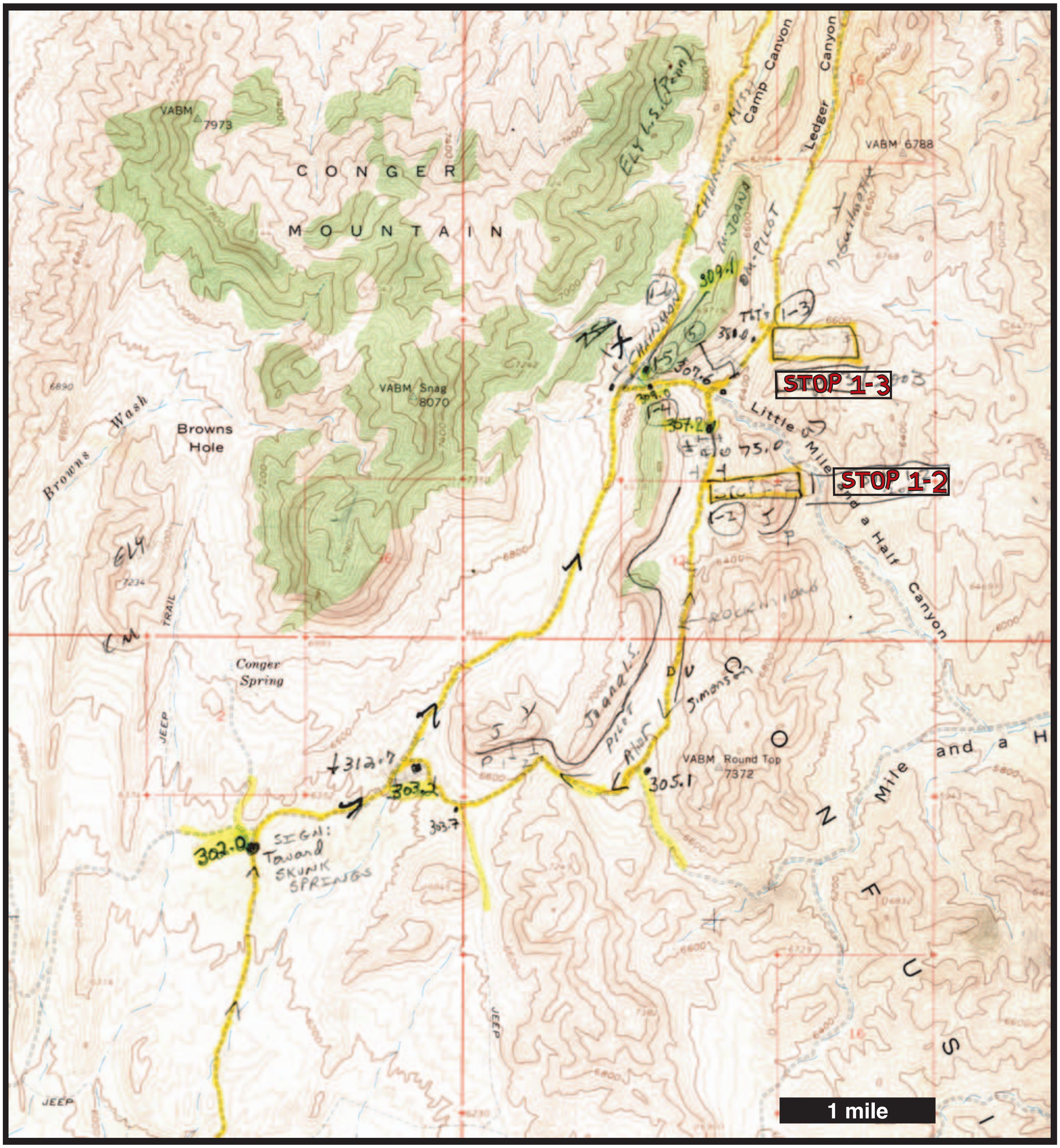

Map 4. Location of Stops 1-2 and 1-3 on the Conger Mountain Quadrangle, Little Mile and a Half Canyon, Utah.

STOP 1-3 – CONFUSION RANGE, UTAH

Age – Late Devonian and Early Mississippian**Carbonate Depositional Sequences**

Formations – Pilot Shale, Joana Limestone, and Chainman Shale.

Carbonate Depositional Sequences (Figure 2)– The overall transition from Pilot Shale to Joana Limestone records a shoaling upward sequence (Sequence #11) from basin to slope to platform margin carbonates during a major relative sea level rise and fall. The contact relationships between the Joana and the overlying Chainman are not clear. Sandberg and others (1980) imply that the contact is conformable, whereas, a few miles to the north at Granite Mountain the Joana is missing due to erosion with the Chainman Shale resting directly on the Pilot Shale. At Stop 1-3, the change from crinoid and oolitic shoals in the Joana into deeper-water Chainman Shale suggests either a rapid rise in sea level with a drowning of the Joana or an erosion contact during a relative sea-level lowstand, followed by a relative sea level rise. This contact represents a sequence boundary between Sequence #11 and #12 (note, Sequence #12 is not labeled on Figure 3).

Depositional Environments (Figure 39) – A marked change occurred during Pilot Shale time. Pilot Shale sediments were deposited in the eastern margin of the Antler foreland basin in relatively deep marine waters (Sandberg and others, 1980). Siliciclastics and carbonate turbidites and debris flow deposits in the Pilot Shale were derived mainly from the east according to Sandberg and others (1980). The Pilot Shale shoals upward from basinal sediments containing thin-bedded turbidites and interbedded organic-rich shales to carbonate debris flows deposited on basin-margin slopes and finally to shallow-water settings where siliciclastic sand bodies interfinger with platform margin crinoid shoals of the lowermost Joana Limestone.

Gutschick and others (1980) and Sandberg and others (2001) interpreted the Joana Limestone as a large north south trending elongate isolated bank (about 500 km long and 150 km wide). An alternate interpretation presented here is that the Joana Limestone, at least in the Confusion Range area, is a broad shoal water bank that was attached to the continental margin rather than being isolated and surrounded on all sides by basinal sediments. It is difficult to envision how the quartz arenite sand bodies that interfinger with the base of the Joana Limestone could have been transported from a siliciclastic provenance to an isolated carbonate bank surrounded on all sides by a deeper marine basin. Modern and ancient isolated carbonate banks effectively preclude siliciclastics from being transported to the banks' margins (e.g., Figure 40). It may be that the Joana Limestone was initiated on a siliciclastic substrate and was initially an attached carbonate platform but evolved into an isolated bank like large Devonian–Mississippian (Bashkirian) carbonate platforms in Kyrgyzstan (Cook and others, 2002a).

The facies in the Joana Limestone in the Confusion Range are relatively shoal water inorigin, especially the oolite grainstone facies that would have formed in warm agitated waters of only a few meters water depth. Crinoid carbonate sands (packstones and grainstones) are abundant throughout the Joana in the Confusion Range section and are interpreted to represent high-energy platform margin and/or upper slope grainstone bodies that formed within storm wave base conditions. Whether these carbonate bodies were tidal bar belts, marine sand belts, and/or tidal delta deposits is not known. In the southern Egan Range pellet grainstones and packstones and oolite grainstones in the Joana appear may have occupied more platform interior settings than the crinoid grainstones (Cook and Taylor, unpublished data) similar to some of the facies distribution on the Great Bahaman Bank.

Possibly Joana Limestone sedimentation was not able to keep pace with the deepening of the foreland basin during the Antler orogeny and the Chainman Shale drowned these carbonate sands. However, at this stop the Joana Limestone-Chainman Shale contact appears to be rather sharp with little or no transitional facies. Whether or not this simply represents a rapid inundation of the Joana shoals or an erosional contact is not known. As stated above, Sandberg and others (1980) infer that the contact is conformable. This raises a question of regional significance in the Great Basin concerning whether or not the distribution of the Joana Limestone outcrops reflects its original depositional extent. In areas of central Nevada where one could predict the Joana Limestone to be thin or absent is it due to original bathymetric constraints or is it due to erosion? At several localities in the Great Basin there is an interpreted unconformity at the Joana Limestone-Chainman Shale contact. The magnitude of this unconformity varies from a question mark on a wavy line (i.e., Confusion Range, Nevada) to virtually all of the Lower Mississippian (i.e., Eureka District and southern Diamond Mountains, Nevada).

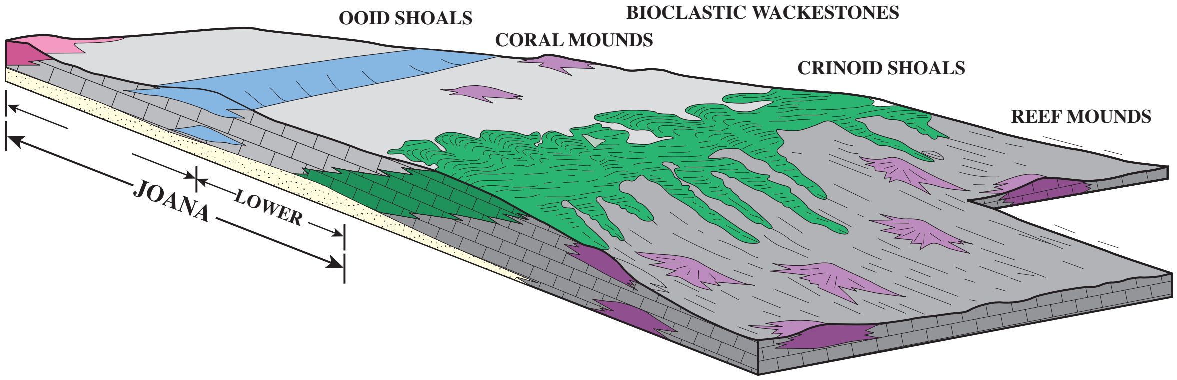

Figure 39. Rimmed shelf model for Joana facies at Stop 1-3 (Modifed from James, 1983).

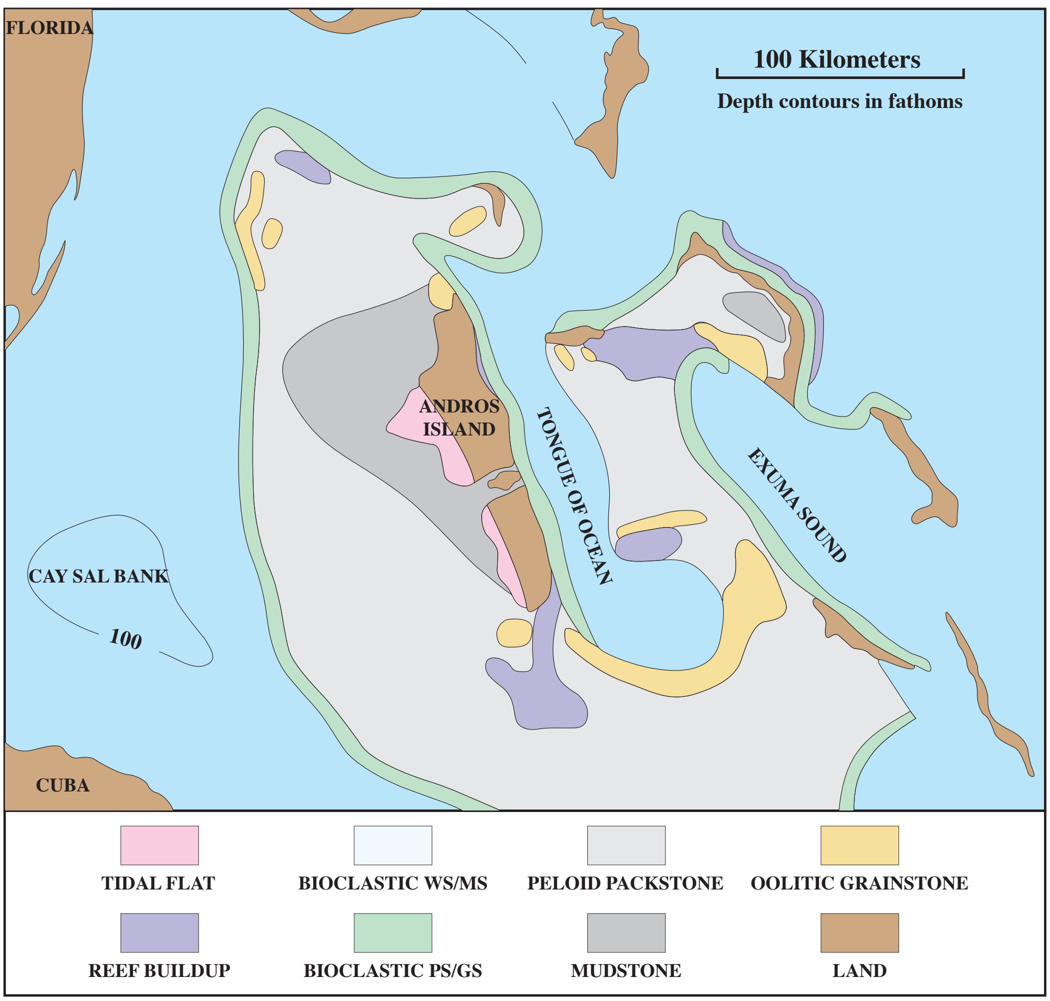

Figure 40. Great Bahama banks (Modifed from Wilson and Jordan, 1983).

In the central Egan Range of eastern Nevada near Ward Mountain the uppermost Joana Limestone is clearly a retrograding or back-stepping sequence (Cook and Taylor, unpublished data) during a relative sea level rise at the beginning of Sequence #12. There the Joana Limestone-Chainman Shale contact is gradational over a 20-meter thick interval that contains numerous carbonate turbidites (Tripon Pass Limestone?) that were derived from the Joana Limestone platform margin as it retrograded or back-stepped to the east (?). This retrogradation of the Joana platform margin at Ward Mountain may be the result of an accelerated deepening of the Antler foreland basin during the Early Mississippian.

Chief Features to be Observed –

Pilot Shale:

1. Black calcareous shale and interbedded thin-bedded turbidites (eastern margin foreland basin).
2. Channelized pebbly to conglomeratic quartzose turbidites; some cobbled-sized clasts are carbonate pellet packstones; ripples in bouma T_c division dipping N 80 W suggesting transport from the east.
3. Ten meter thick channelized argillaceous limestone debris flow deposit; lime mudstone and wackestone clasts, quartz siltstone clasts; clasts containing possible green calcareous algae (possibly derived from Joana platform margin carbonates and/or slope semi-lithified lime muds). Both Hose (1966) and Sandberg and others (1980) mention these conglomerates in their studies of the Confusion Range.
4. Thin-bedded cherts rich in radiolarians (basin margin).
5. Oncolite-rich interval a few meters thick overlying the radiolarian chert (oncolites herein interpreted to represent shoal water derived clasts that were transported into deeper water slope settings by sediment gravity flows; Sandberg and others (1980) interpret these oncolite beds to represent an in-situ “shallow-water oncolite-limestone-bank”.

Joana Limestone:

1. Pilot Shale-Joana Limestone contact is marked by an interfingering of quartz arenites and shales (Pilot Shale) and crinoid-rich bioclastic packstones and grainstones (Joana Limestone). The quartz arenites may represent part of a shallow water offshore bar system related to an eastern or laterally adjacent shoreline, whereas the Joana crinoid-rich shoals are platform margin and or upper slope shoals that were prograding over the quartz arenites.
2. Crinoid packstones and grainstones, pellet grainstones, oolite/pellet grainstones (shallow subtidal shelf edge crinoid meadows and oolite sand bodies inboard of the crinoid bank margin facies; unrestricted lagoons with scattered zones of pellet packstones).
3. Joana-Chainman contact – Crinoid wackestone and packstone shoals in contact with mud-supported siliciclastics of the Chainman (either a rapid sea level rise associated with the Antler orogeny or an erosion contact, followed by a relative sea level rise).

Economic Considerations –Oolitic grainstone bodies such as found in the Joana Limestone can form excellent reservoirs. These types of carbonate sand bodies are particularly abundant and prolific petroleum reservoirs in Mississippian, Permian, Jurassic, and Cretaceous sequences where they occur as tidal bars, tidal deltas, and broad marine sand bars on tops of banks. Tidal bars and tidal deltas can form on both the seaward slope and bankward side of shelf edges (Halley and others, 1983). The stratigraphic association of a variety of potential reservoir facies in the Joana Limestone enclosed between two possible source rock horizons such as the Pilot and Chainman Shales make this part of the Mississippian a potentially attractive exploration target. The fact that in some areas the Joana Limestone has been interpreted to be thin or missing due to Mississippian erosion has both negative and positive exploration implications. On the negative side, if the erosion trend does not follow the Joana Limestone’s original depositional trend subsurface prediction of reservoirs becomes more adventuresome. On the other hand, if this erosion occurred under subaerial conditions (i.e., during the lowstand at the end of Sequence #12) with attendant meteoric vadose and phreatic zones significant amounts of moldic, vuggy or even cavernous porosity could exist in the Joana Limestone. Enhanced solution porosity overlain by a thick sequence of organically rich Chainman Shale could offer excellent exploration potential.

Examples of petroleum reservoirs in carbonate sand bodies include the Permian Clear Fork and Abo fields, Permian Basin, west Texas (Mazzullo, 1982), Pennsylvanian Chapman Deep Atoka fields, Delaware Basin, west Texas (Mazzullo, 1981), and numerous Jurassic Smackover fields in the Gulf Coast (Halley and other, 1983).

Numerous gold discoveries in Nevada are hosted in porous calcareous silts (Ainsworth, 1984; Raines and others, 1991). Some of these calcareous silts may be turbidites in basin margin settings. If this is true, it is particularly important to determine the origin of these calcareous turbidites and to develop depositional sequence models that show the possible genetic interrelationship between the carbonate platform margin and basin margin facies. For example, sediment-hosted gold occurs in the Joana Limestone and Chainman Shale at the Nighthawk Ridge deposit southeast of Eureka (Carden, 1991) and at the Green Spring deposit (Wilson and others, 1991). If the gold-bearing host facies in the Chainman Shale represents carbonate turbidites generated from a retrograding Joana Limestone platform margin this is a significant key to any Great Basin exploration activity.

Relation to Future Stops – This same stratigraphy occurs in the Egan Range, eastern Nevada. There, the lower Joana Limestone maintains its high-energy platform margin characteristics. The same chronostratigraphic interval at Stop 2-1 (Devils Gate) is only occupied by the Pilot Shale and overlying Chainman Shale with the Joana Limestone missing.

Photo 1-3a. Pilot Shale and overlying Joana Limestone. Stop 1-3. Little-Mile-and-a-Half Canyon, Confusion Range, Utah.

Photo 1-3b. Pilot Shale. Thin-bedded, in-situ argillaceous limey shales in a basinal setting. Stop 1-3. Little-Mile-and-a-Half Canyon, Confusion Range, Utah.

Photo 1-3c. Pilot Shale. Calcareous turbidite exhibiting Bouma A (normal grading), B (parallel laminations), and C (cross-laminations) divisions. Basin or base-of-slope setting. Stop 1-3. Little-Mile-and-a-Half Canyon, Confusion Range, Utah.

Photo 1-3d. Pilot Shale. Carbonate debris flow with laminated turbidite cap facies. Slope setting. Stop 1-3. Little-Mile-and-a-Half Canyon, Confusion Range, Utah.

Photo 1-3e. Joana Limestone. Syringoporella colonial coral within the middle part of the Joana. Middle platform. Matrix surrounding coral is a wackestone. Stop 1-3. Little-Mile-and-a-Half Canyon, Confusion Range, Utah.

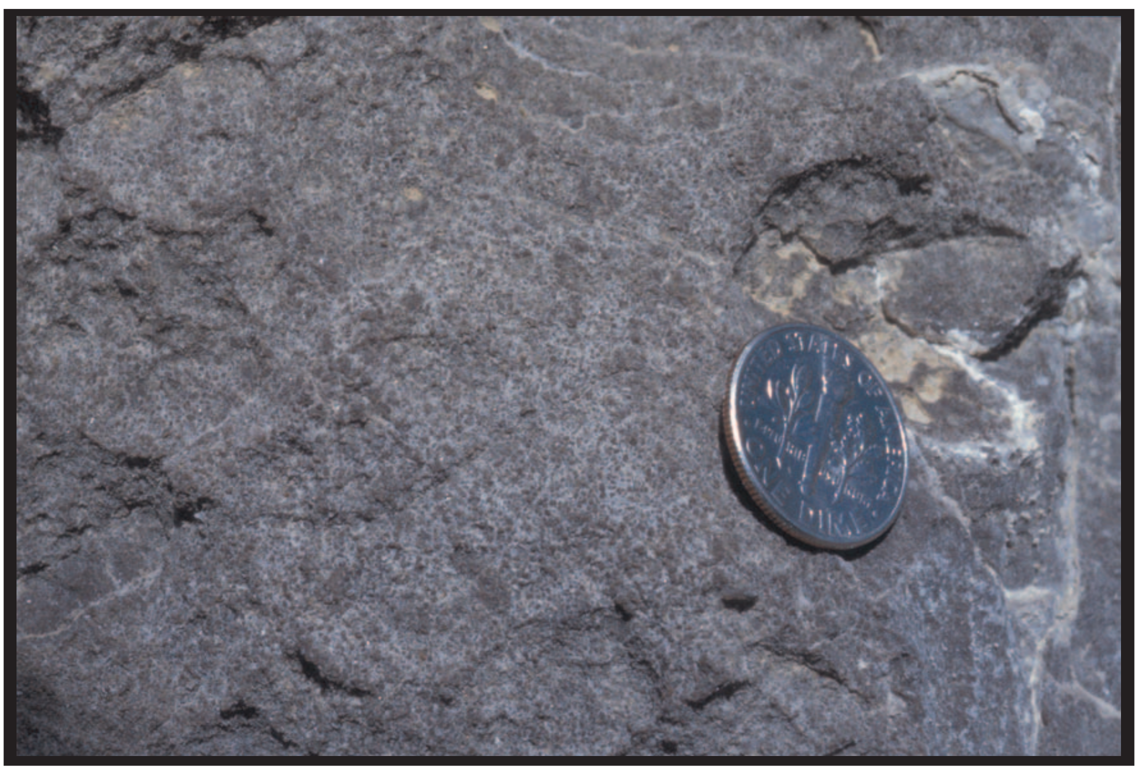

Photo 1-3f. Joana Limestone. Oolite grainstone tidal bar near the top of the Joana Limestone. Platform margin. Stop 1-3. Little-Mile-and-a-Half Canyon, Confusion Range, Utah.

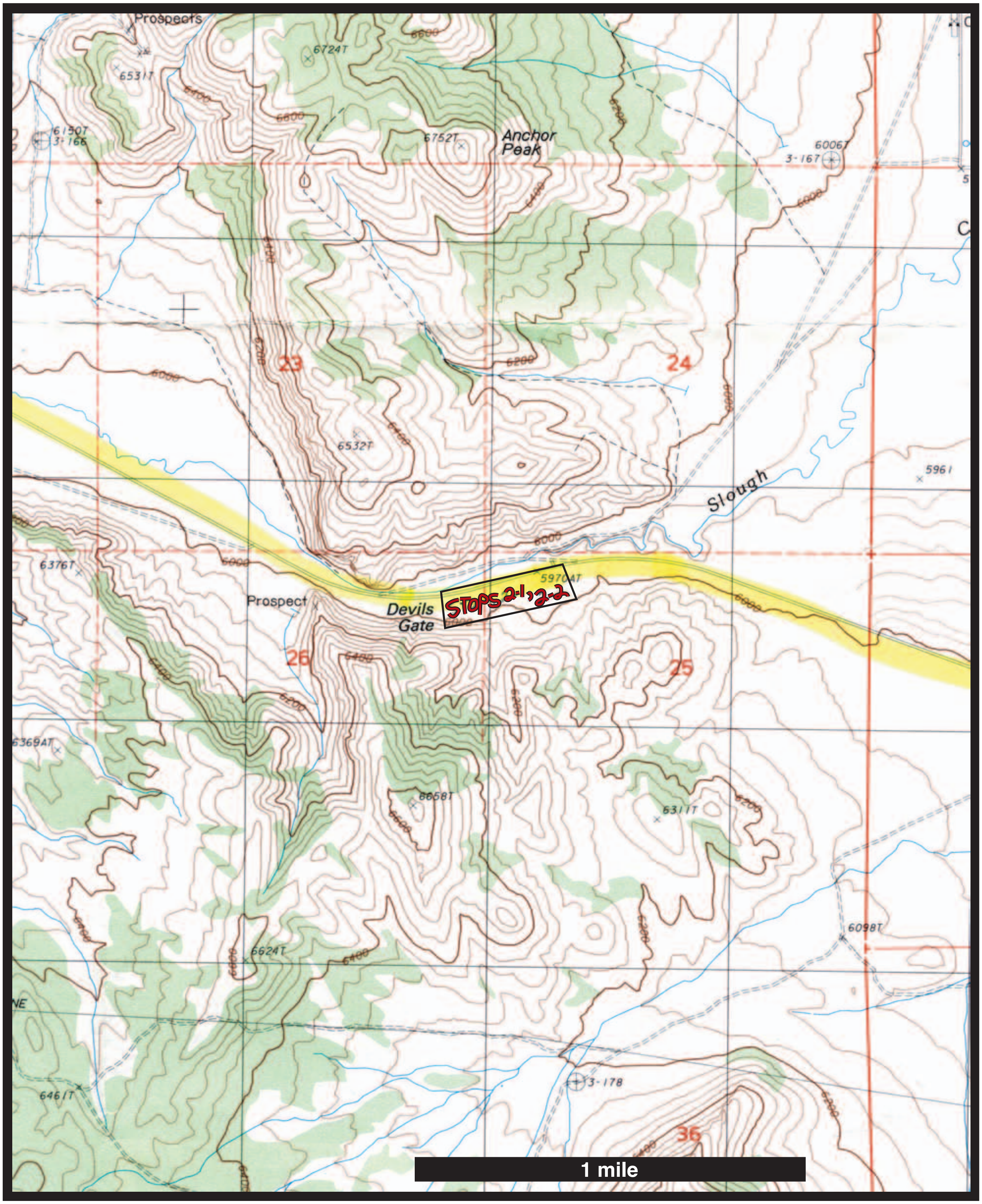

Map 5. Location of Stops 2-1 and 2-2 on the Devon Peak Quadrangle, Devils Gate, Nevada.

STOP 2-1 – OVERVIEW OF WHISTLER MOUNTAIN, NEVADA

Age – Late Devonian (Frasnian-Famennian) and Early Mississippian.

Formations – Devils Gate Limestone (Late Devonian), Pilot Shale (Late Devonian-Early Mississippian), and Chainman Shale (Early Mississippian).

Carbonate Depositional Sequences (Figure 2)– Before we examine this section in detail, this vantage spot affords a good overall view of parts of Sequence #9 and #10. At this locality (Devils Gate), the Devils Gate Limestone consists of a lower shallow water platform margin member and an upper deeper water basinal and slope member (Sandberg and others, 2003):

1) The lower member consists of thick-bedded, muddy, stromatoporoid-rich packstones deposited in a middle shelf lagoon setting.

2) The upper member consists of lime muds, calcarenite turbidites, bioclastic conglomeratic debris flows, and submarine slumps representing deposition in deeper water basin and slope environments.

Depositional Environments –These two contrasting members are herein interpreted to represent parts of two separate carbonate depositional sequences. The lower member is interpreted to represent the upper part of the highstand systems tract of Sequence #9 and the upper member is interpreted to be comprised of the transgressive and highstand systems tracts of Sequence #10 (Figure 2). The sequence boundary between Sequence #9 and #10 may be represented at or near the stratigraphic horizon identified as SR in Sandberg and others (2003, Figure 5).

STOP 2-2 – WHISTLER MOUNTAIN, NEVADA

Age – Devils Gate Limestone (Late Devonian), Pilot Shale (Late Devonian-Early Mississippian), and Chainman Shale (Early Mississippian).

Carbonate Depositional Sequences (Figure 2)– According to Poole and others (1979) and Sandberg and others, (2003), at this stop the Devils Gate Limestone exhibits a retrogradational, deepening upward event from platform margin to slope to basin environments during the Frasnian and Famennian.

We agree that the lower member of the Devils Gate Limestone represents deposition in a relatively shallow water shelf lagoon setting, whereas the upper member formed in deeper water settings. However, as discussed at Stop 2-1, we offer an alternative interpretation for the origin of this environmental change. If this change were a simple progressive retrogradational event, one could expect the stromatoporoid-Amphipora shelf lagoon facies in the lower member to be directly overlain by a high energy platform margin grainstone facies with massive stromatoporoids, followed by slides and slumps of an upper slope facies, then overlain by base-of-slope debris apron facies and finally overlain by basin-plain turbidites.

The stratigraphic succession overlying the platform interior shelf lagoon facies begins with thin-bedded turbidites succeeded by conglomeratic debris base-of-slope apron deposits that in turn are overlain by slides and slumps. We propose that the lower member of the Devils Gate Limestone (platform interior shelf lagoon facies) was suddenly drowned by faulting and/or relative sea level changes related to Sequence #10 and the platform was forced to rapidly back-step to the east. Thus, we would interpret the contact between the lower member and upper member to be at or near the sequence boundary between Sequence #9 and #10 (Figure 2 and 3). Once a new platform margin was established it prograded seaward forming the highstand systems tract of Sequence 10. The deeper water Devils Gate Limestone of the upper member would represent a predicted upward progression from basinal turbidites to base-of-slope conglomeratic debris apron turbidites and debris flows to submarine slumps. In terms of carbonate depositional sequences the upper deeper water member would represent transgressive and highstand systems tract facies of Sequence #10.

It is significant to note how the Devils Gate platform margin was evolving in comparison to two other well-documented Upper Devonian reefs and bank margins. For example, in Alberta, Canada (Figures 41-43), Upper Devonian (Frasnian) Miette and Ancient Wall bank margins first went through a retrogradational phase (transgressive systems tract) that was followed by a progradational phase (highstand systems tract; Figure 41). In the Canning Basin of western Australia, the Upper Devonian reef complexes exhibit a complex evolution. They back-stepped several times during the Frasnian (transgressive systems tracts), and in the latest Frasnian and most of the Famennian, the reef margin prograded seaward (highstand systems tract; Figure 43). Then near the Famennian-Tournaisian boundary it appears a major transgressive event occurred (Figure 44).

Depositional Environments (Figure 45) – The base of the Devils Gate Limestone at this stop contains abundant hemispherical and bulbous stromatoporoids, and the dendroid stromatoporoids Amphipora and/or Stachyodes. This biota occurs in dark gray to black lime wackestones that contain an abundance of lime mud. Gastropods are also commonly associated with the stromatoporoids. Stromatoporoid-rich facies have been intensely studied in numerous Devonian carbonate provinces including the Upper Devonian of Canada (Figures, 46, 48) (for example, Klovan, 1964; Murray, 1966; Cook, 1972; Cook et al., 1972), Upper Devonian of Australia (Playford, 1980), Upper Devonian of Europe (LeCompte, 1956). These Upper Devonian studies suggest a paleoecological zonation of stromatoporoids from tabular forms in deeper, less-turbulent waters of the upper slope and massive (hemispherical) forms being adapted to shallow, turbulent environments at the platform margin. Within relatively quiet muddy shallow water shelf interior (back reef) settings bulbous stromatoporoids and Amphipora are common (Figures 47-50). Stachyodes was apparently more tolerant of high energy conditions and is commonly associated with massive and tabular-laminated stromatoporoids (Figures 47-48).

Power (1983) in her study of the Devils Gate Limestone in the northern Roberts Mountains concluded that the basal Devils Gate is a true stromatoporoid-coral boundstone that formed in a high-energy shoal water platform margin position and not on a carbonate ramp.

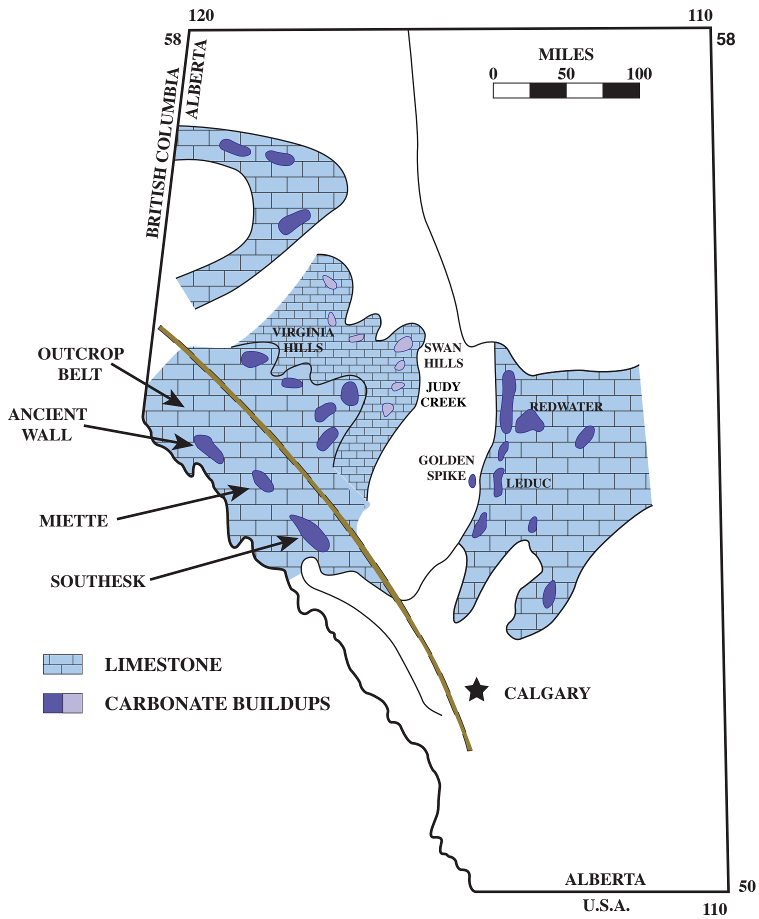

Figure 41. Distribution of Upper Devonian isolated carbonate buildups in Alberta, Canada. Isolated carbonate buildups evolved on top of broad carbonate platforms (Modifed from Cook and others, 1972).

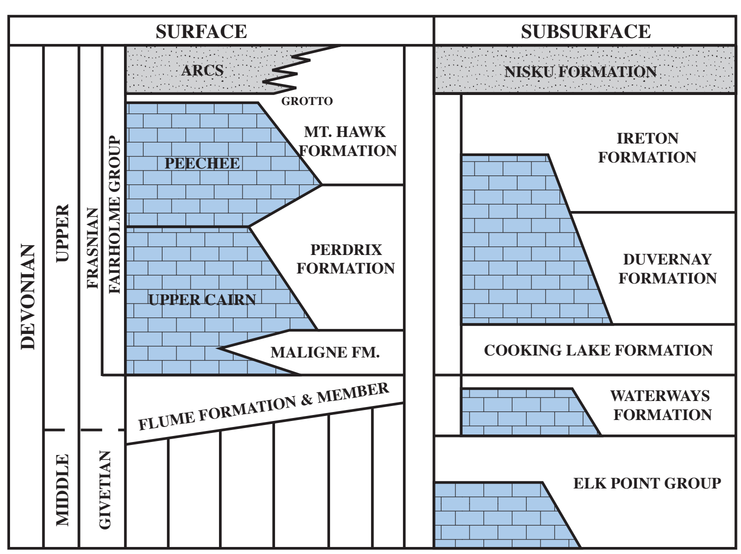

Figure 42. Correlation of formations exposed at Ancient Wall, Miette, and Southesk-Cairn with those of the subsurface (Figure 41 for location of buildups) (Modifed from Cook and others, 1972).

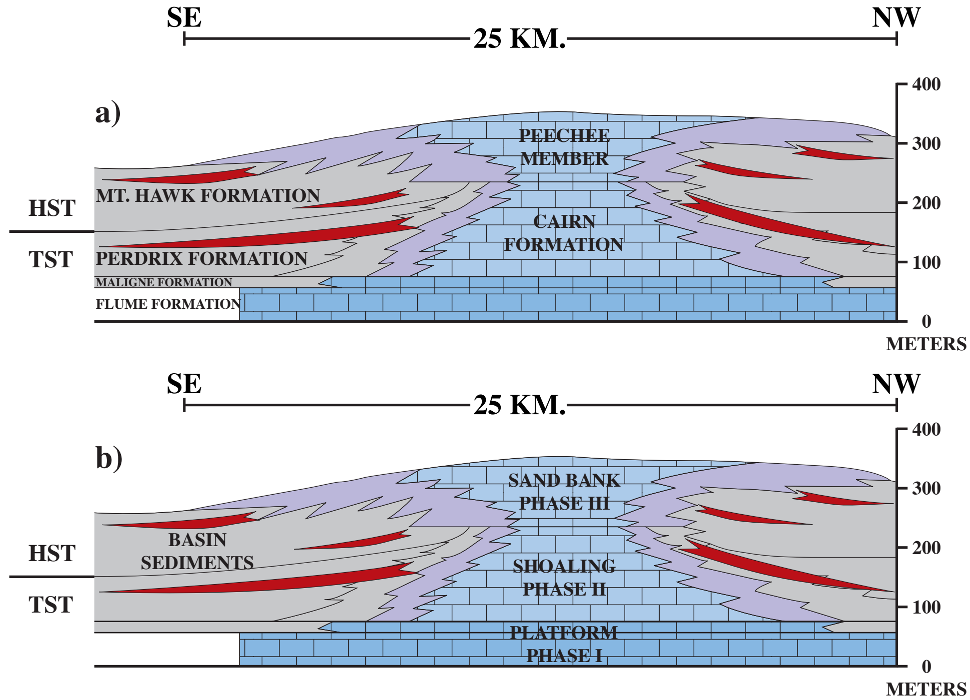

Figure 43a. Generalized stratigraphic cross-section showing the stratigraphic and facies relationships at the Upper Devonian Miette carbonate complex, Alberta, Canada (Modified from Cook and others, 1972).

Figure 43b. Generalized depositional phases of the Miette carbonate complex (Modified from Cook and others, 1972).

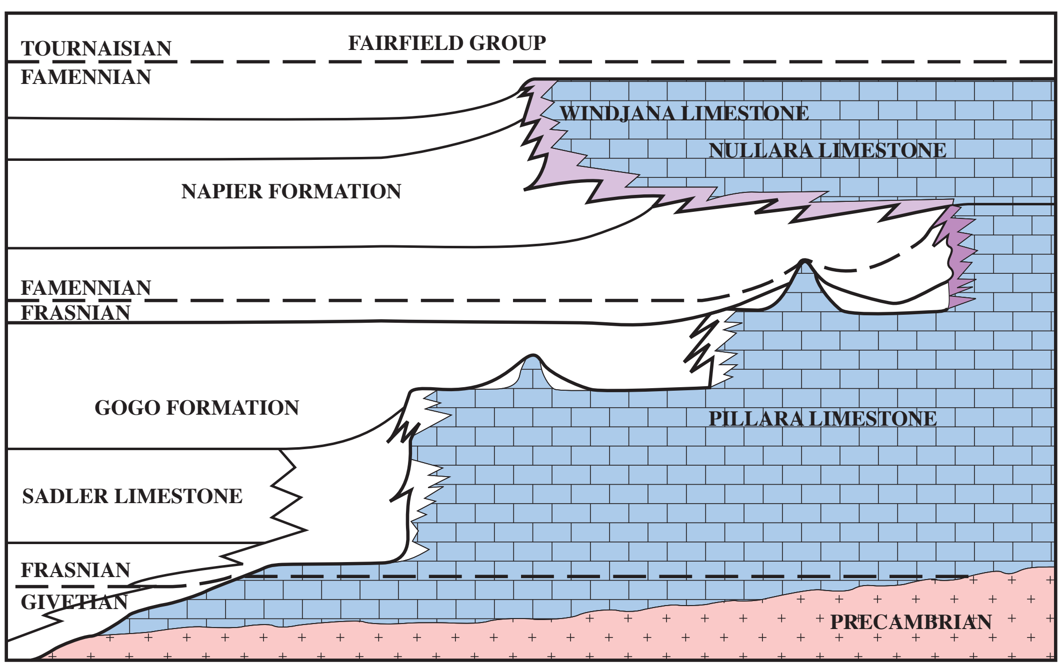

Figure 44. Correlation of formations exposed at Ancient Wall, Miette, and Southesk-Cairn with those of the subsurface (Figure 41 for location of buildups) (Modified from Playford, 1980).

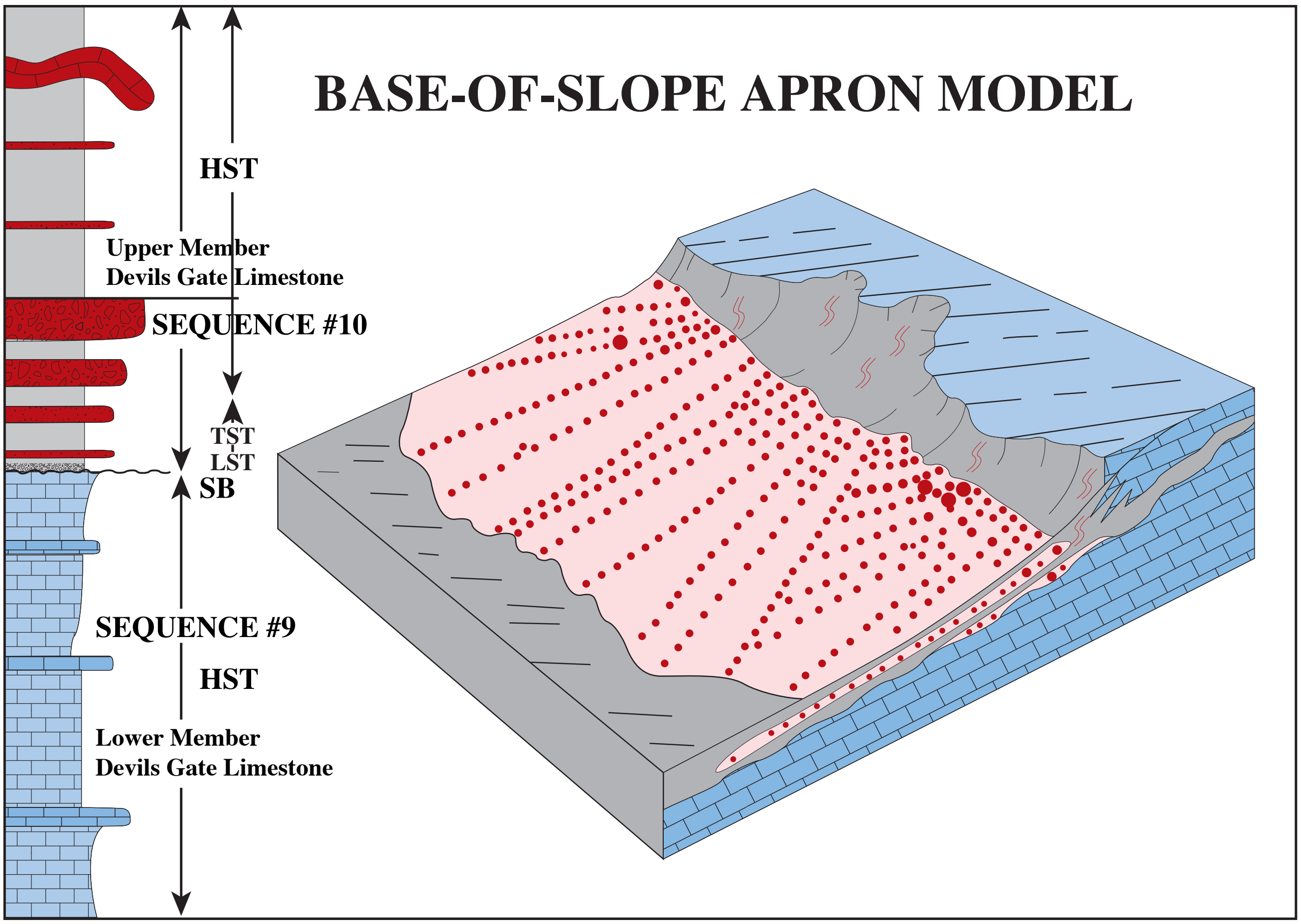

Figure 45. Interpreted depositional environments for retrogradational and back-stepping Devils Gate Limestone at Stop 2-1 and 2-2. Lower Member at Devils Gate is a middle shelf lagoon facies and the high energy platform margin grainstone facies is not exposed at Devils Gate. Lower Member is interpreted to be a highstand systems tract (HST). The lower part of the Upper Member is interpreted to be the transgressive systems tract (TST) with thick debris flows, turbidites and slumps that formed during the highstand system tracts (HST) (Modified from Cook and others, 1983). Carbonate base-of-slope apron model showing shoal water derived debris (highstand sytstems tract-HST) originating along line source. Mass-flow deposits originating at platform margin largely by-pass the slope with the bulk of debris deposited at the base-of-slope. Debris is transported as broad sheet flow (Compare to Figures 2, 30, 32, 33, 34, and 35; From Cook, 1982).

At Stop 2-2, we do not see the basal Devils Gate Limestone that Power (1983) describes in the Roberts Mountains to the north. Sandberg (personnel comm., 1983) states that near Stop 2-2, but lower in the section, stromatoporoid-coral boundstone are in-situ and represent shelf edge buildups. The lowest Devils Gate facies we will examine do not appear to have formed in a high-energy mud-free environment. Rather the association of bulbous and hemispherical stromatoporoids, Amphipora and gastropods encased in dark mud-rich matrix suggests quieter water setting in a middle shelf environment (Figure 47).

As one progresses upsection at Stop 2-2, into the upper member of the Devils Gate Limestone deeper water environments are encountered including basin-plain, base-of-slope, and slope. The abundance of thick carbonate debris flow deposits in association with slumps and slides support the interpretation of Power (1983) that the Devils Gate Limestone did not form on a low angle ramp. The high-energy facies described by Power (1983) and the significant amounts of submarine mass-transport deposits in the upper member of the Devils Gate Limestone suggests a rimmed carbonate shelf model and not a carbonate ramp or distally steepened ramp model for the Devils Gate Limestone at this locality.

Chief Features to be Observed –

<u>Devils Gate Limestone Formation</u>:

A. <u>Lower Member</u>-

1. Dark gray to black, bulbous, hemispherical, and dendroid (Amphipora and/or Stachyodes) stromatoporoid-gastropod wackestones and packstones (relatively low energy, subtidal, shelf edge or lagoon environments).

B. <u>Upper Member</u>-

1 Limestone turbidites (slope, base-of-slope, and basinal settings).
2. Limestone conglomeratic debris-flow deposits with clasts of bulbous and laminar stromatoporoids, Syringoporella colonial coral clasts and rugose corals (slope and base-of-slope settings).
3. Carbonate turbidite cap facies on top of debris flows with Bouma Tc rippled tops dipping to the west suggesting transport to the west.
4. Soft sediment deformation in in-situ slope sediments.

<u>Pilot Shale</u>:

1. Shale and calcareous shales (basin plain).

<u>Chainman Shale</u>:

1. Chert pebble turbidites, some of which contain Bouma T_c rippled tops with the ripples dipping to the west suggesting transport to the west.

Economic Considerations – The Devils Gate Limestone as observed here and in the Diamond Mountains, the next range to the east does not appear to represent potentially favorable petroleum reservoir facies. If the stromatoporoid-rich beds were dolomitized and/or leached as occurs in the Upper Devonian of Alberta and western Australia, for example, some Devils Gate Limestone facies could be attractive exploration targets. The carbonate turbidites could represent favorable reservoir (host) facies for petroleum and minerals. Sediment-hosted gold occurs at the contact between the Pilot Shale and Devils Gate Limestone at the Alligator Ridge deposit (Ilchik, 1991). Other sediment-hosted gold deposits have been discovered near the Devils Gate Limestone and Webb Formation at the Rain subdistrict (Thoreson, 1991), at the South Bullion deposit (Putman and Henriques, 1991), and the Trout Creek deposit (Jackson and Ruetz, 1991).

Relation to other areas – We will examine other deeper water slope and basinal sequences at Stop 3-2 (Silurian-Devonian), Stop 4-1 (Lower Devonian), Stop 5-4 (Upper Cambrian-Lower Ordovician), and Stop 5-6 (Lower-Middle Devonian).

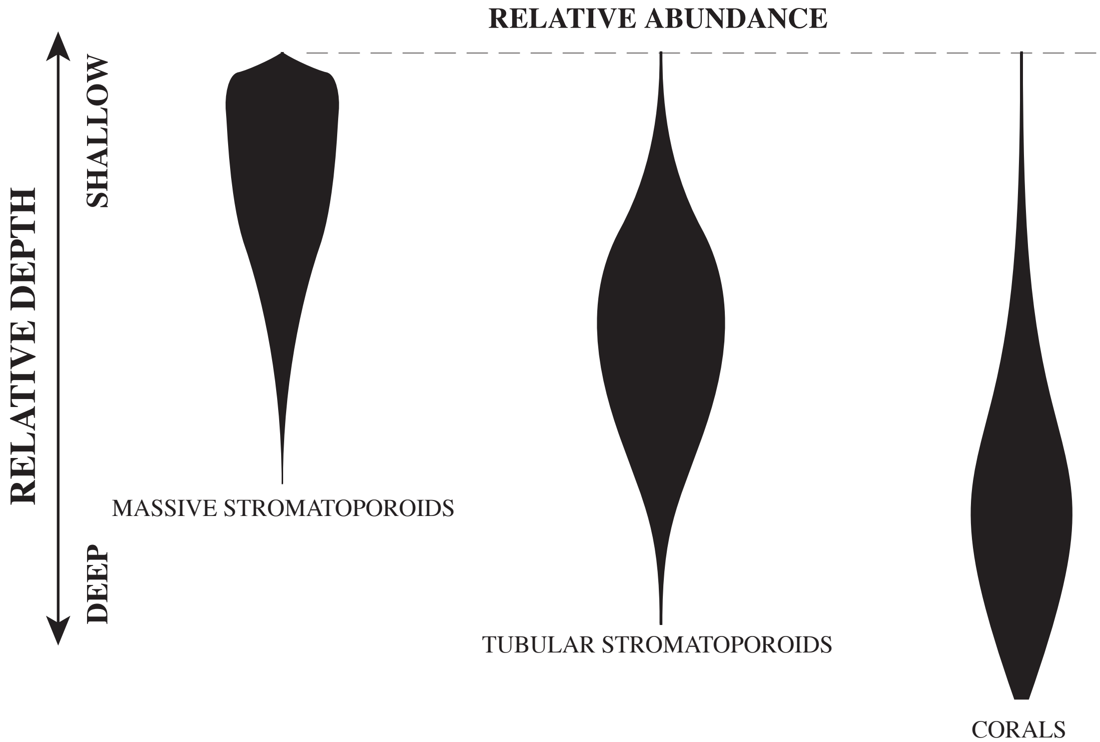

Figure 46. Depth Distribution of Upper Devonian reef-building organisms at Redwater Field, Alberta, Canada (Modified from Klovan, 1964).

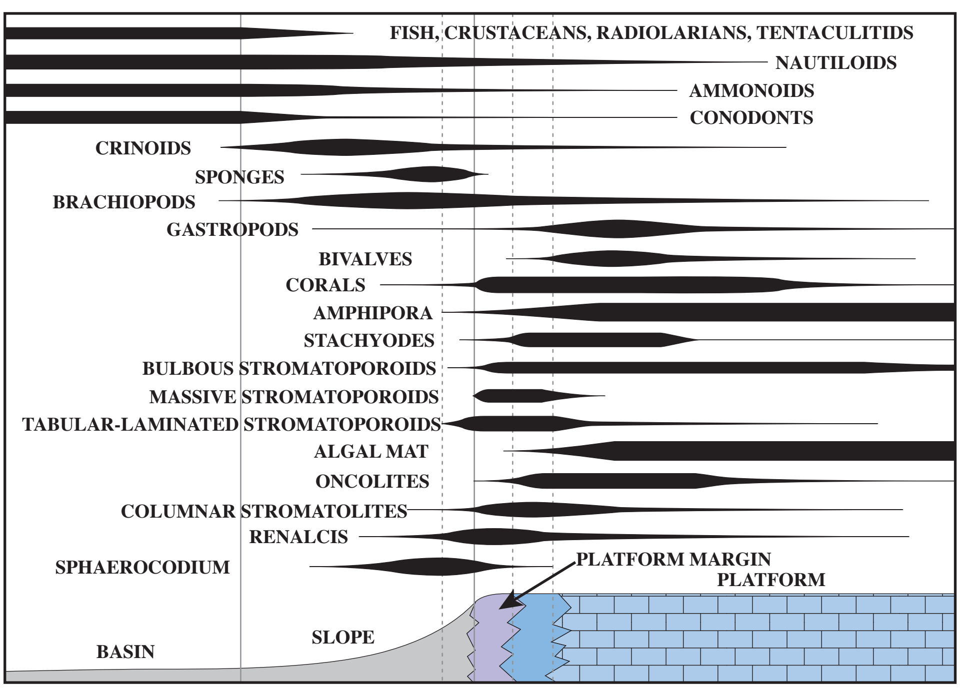

Figure 47. Biotic distribution in Upper Devonian (Frasnian) reef complexes, Canning Basin, western Australia (Modified from Playford, 1980).

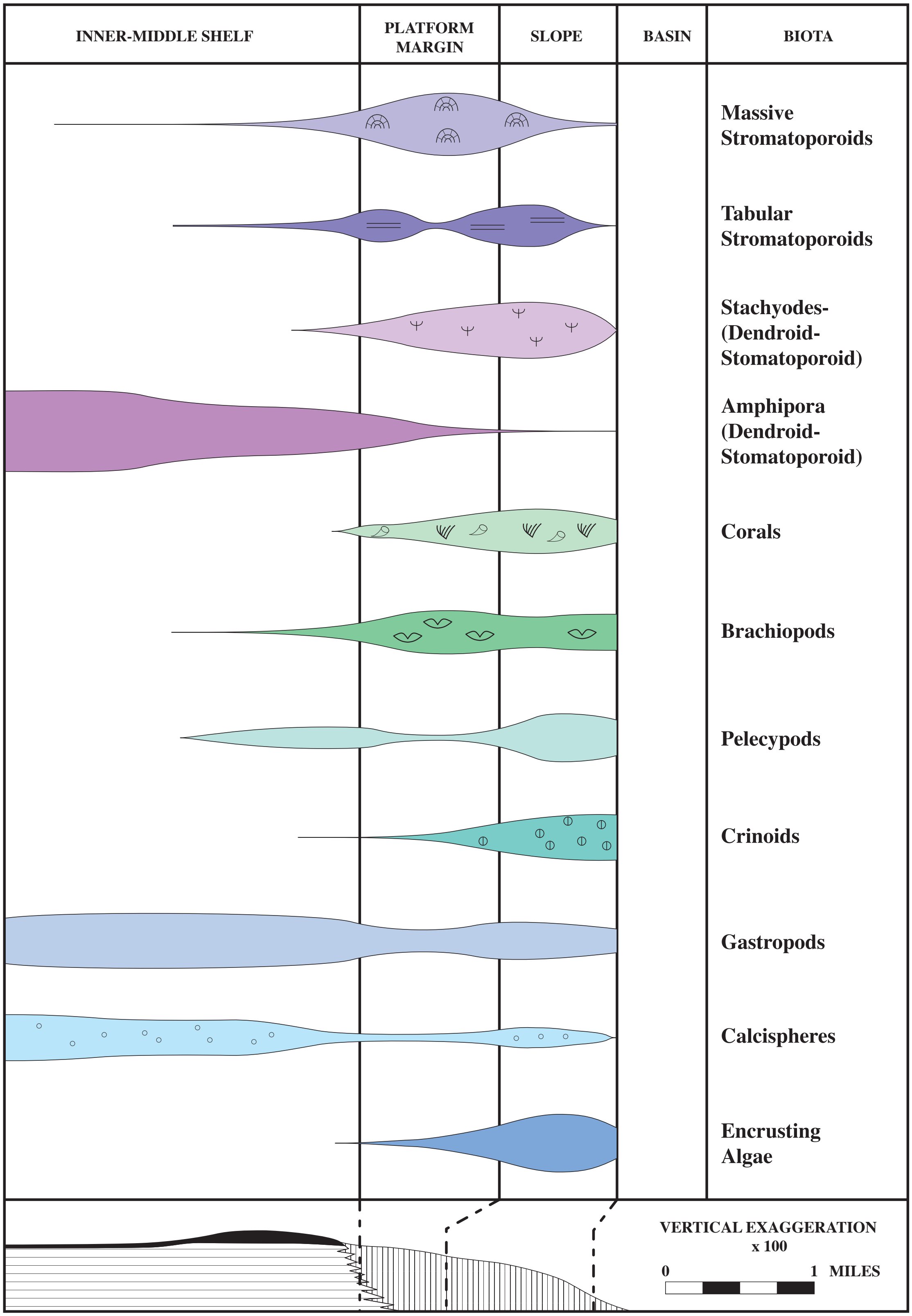

Figure 48. Distribution of organisms in Upper Devonian reefs and banks, Alberta, Canada (Modified from Klovan, 1964; Mountjoy, 1965, 1968; Playford and Lowry, 1966; Cook, 1972; Cook and others, 1972).

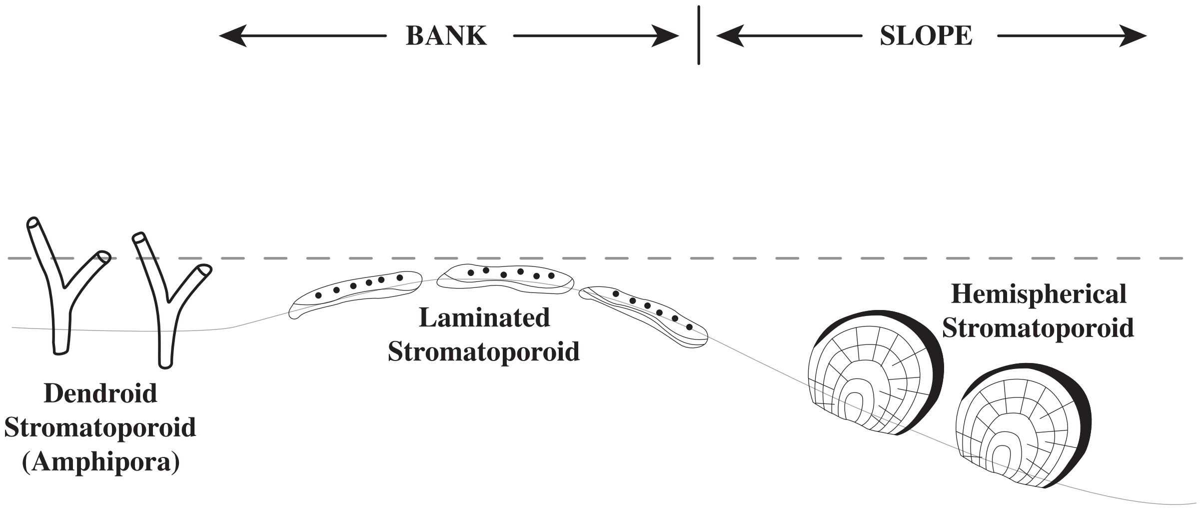

Figure 49. Schematic cross-section showing relationship of stromatoporoids to the environments in Lower Devonian Jeffersonville Limestone, Indiana (Modified from Perkins, 1963).

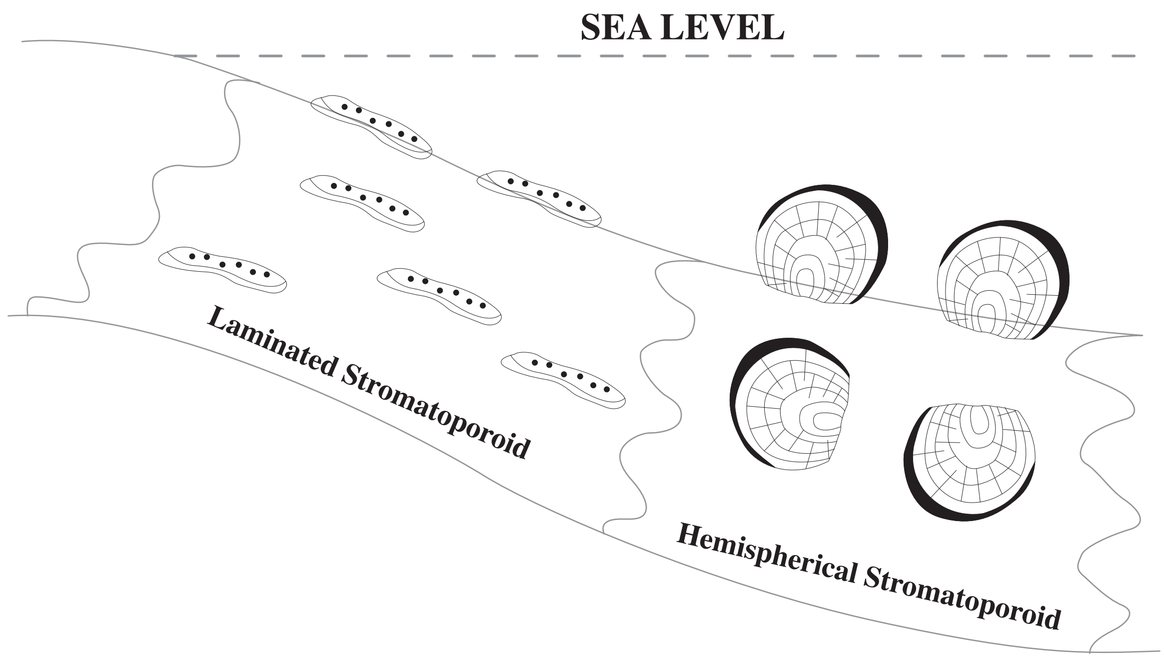

Figure 50. Schematic cross-section showing relationship of stromatoporoids to the environments in the Middle Devonian Manlius Formation, New York (Modifed from Laporte, 1967).

Photo 2-1a. Lower Member of Devils Gate Limestone is a shoal water middle platform facies and the overlying Upper Member is a deeper-water basinal to slope facies with abundant debris flows, turbidites, and slumps. Stops 2-1 and 2-2. Devils Gate, Whistler Mountain, Nevada.

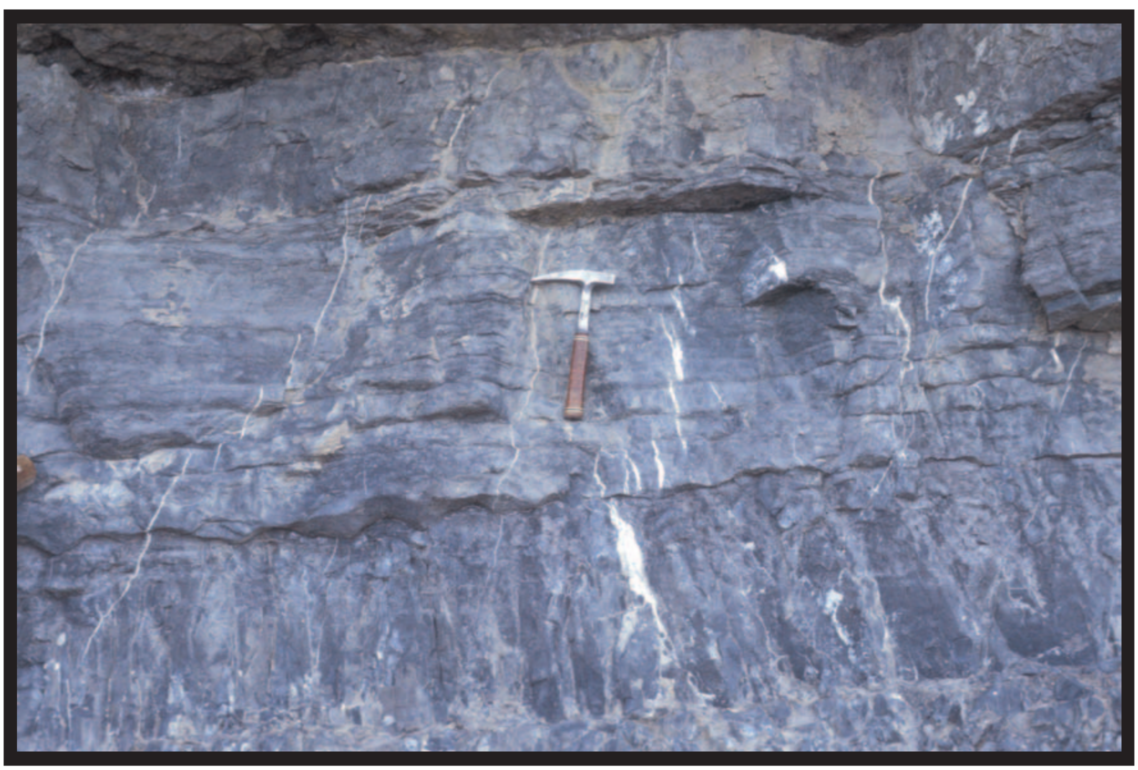

Photo 2-1b. Devils Gate Limestone, Lower Member. Middle platform. Stops 2-1 and 2-2. Devils Gate, Whistler Mountain, Nevada.

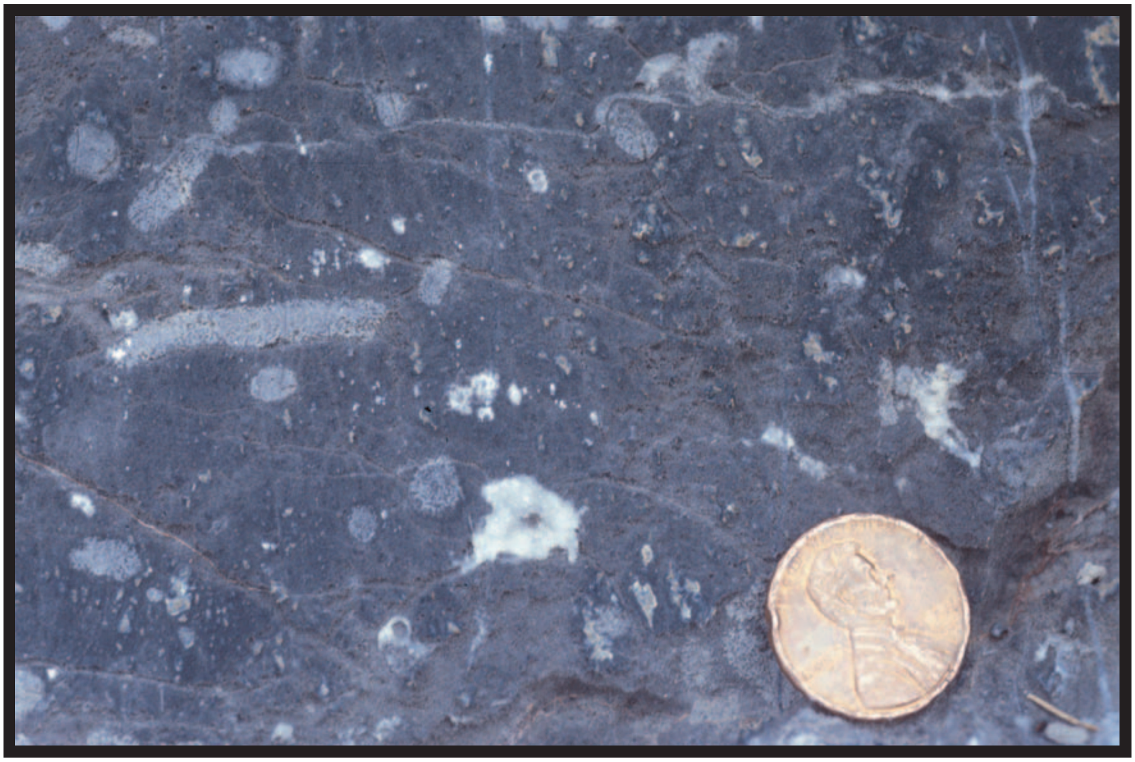

Photo 2-1c. Devils Gate Limestone, Lower Member. Amphipora rudstone and/or floatstone. Middle platform. Stops 2-1 and 2-2. Devils Gate, Whistler Mountain, Nevada.

Photo 2-1d. Devils Gate Limestone, Lower Member. Stromatoporoid-amphipora-gastropod rudstone. Middle platform. Stops 2-1 and 2-2. Devils Gate, Whistler Mountain, Nevada.

Photo 2-1e. Devils Gate Limestone, Upper Member. Massively bedded upward-thickening cycles of carbonate debris flow and turbidite deposits. Looking north. Slope and base-of-slope. Stops 2-1 and 2-2. Devils Gate, Whistler Mountain, Nevada.

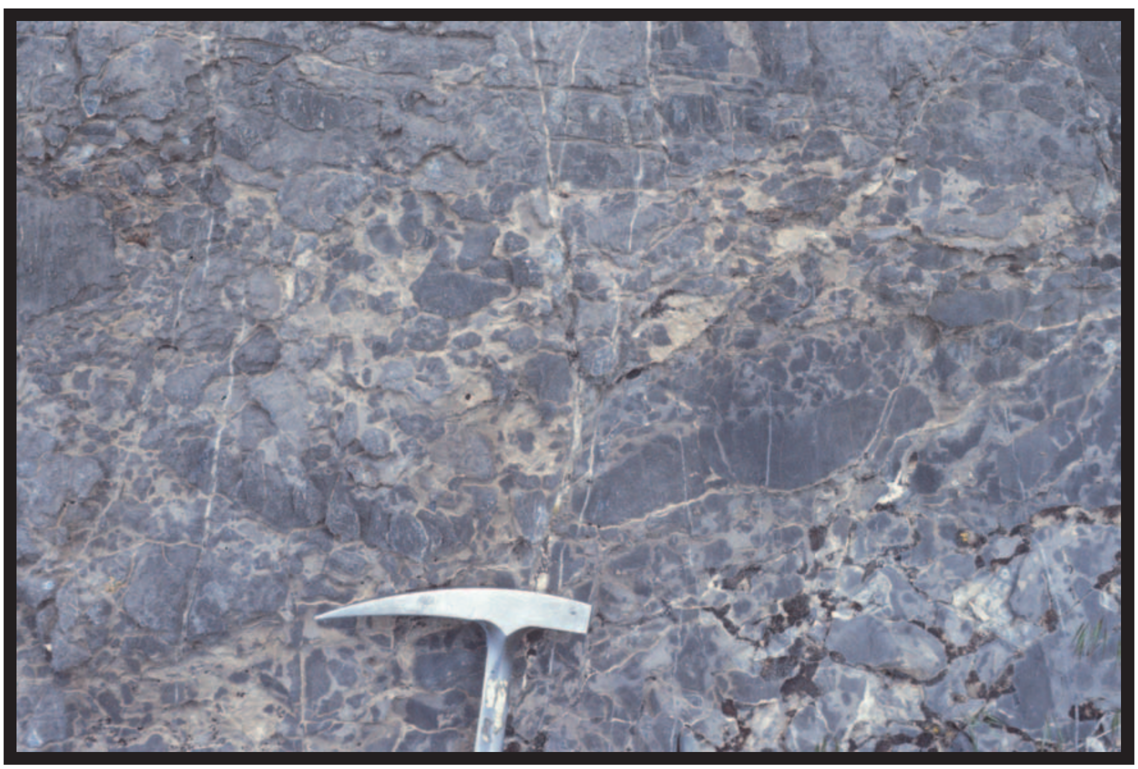

Photo 2-1f. Devils Gate Limestone, Upper Member. Debris flow conglomerate. Slope and base-of-slope. Stops 2-1 and 2-2. Devils Gate, Whistler Mountain, Nevada.

Photo 2-1g. Devils Gate Limestone, Upper Member. Top of a thick conglomeratic debris flow deposits showing cross-bedded turbidite cap facies. Cross-bedding Bouma C division indicates westerly (left) transport direction. Slope and base-of-slope. Stops 2-1 and 2-2. Devils Gate, Whistler Mountain, Nevada.

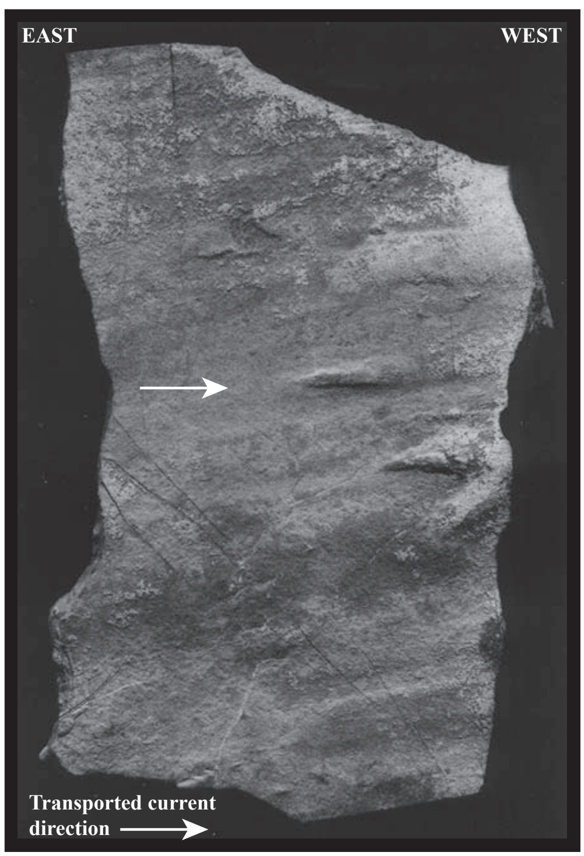

Photo 2-1h. Devils Gate Limestone, Upper Member. Base of thin-bedded turbidites with flute marks indicating turbidity currents were moving westerly. Slope and base-of-slope. Stops 2-1 and 2-2. Devils Gate, Whistler Mountain, Nevada.

Photo 2-1i. Devils Gate Limestone, Upper Member. Soft-sediment deformation. Upper slope. Stops 2-1 and 2-2. Devils Gate, Whistler Mountain, Nevada.

Photo 2-1j. Chainman Shale at Devils Gate. Siliciclastic turbidites with cross-bedded Bouma C division indicating transport to the west (left). Basinal setting. Stops 2-1 and 2-2. Devils Gate, Whistler Mountain, Nevada.

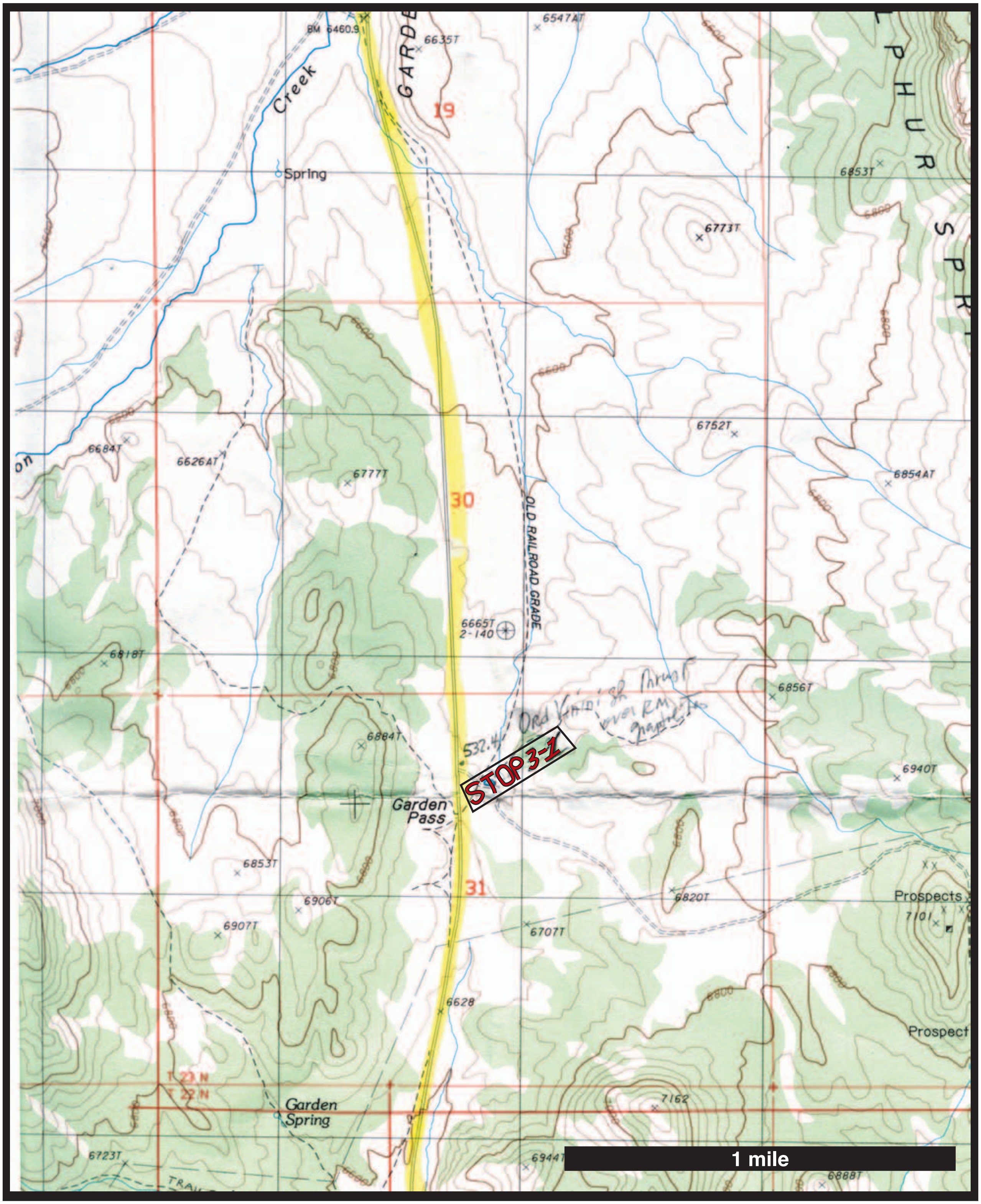

Map 6. Location of Stop 3-1 on the Garden Pass Quadrangle, Garden Pass, Nevada.

STOP 3-1 – GARDEN PASS, NEVADA

Age – Ordovician

Formations – Vinini Shale.

Carbonate Depositional Sequences – Vinini Shale is within Sequence #4 (Figure 2).

Depositional Environments – The Vinini Shale was deposited in a graptolitic-bearing deep basin plain setting.

Chief Features to be Observed –

Vinini Shale:

1. Black shale with graptolites.

Photo 3-1a. Vinini Shale. Graptolitic shales thrust eastward over platform margin. Stop 3-1. Garden Pass, Nevada.

Photo 3-1b. Vinini Shale. Graptolitic shales. Stop 3-1. Garden Pass, Nevada.

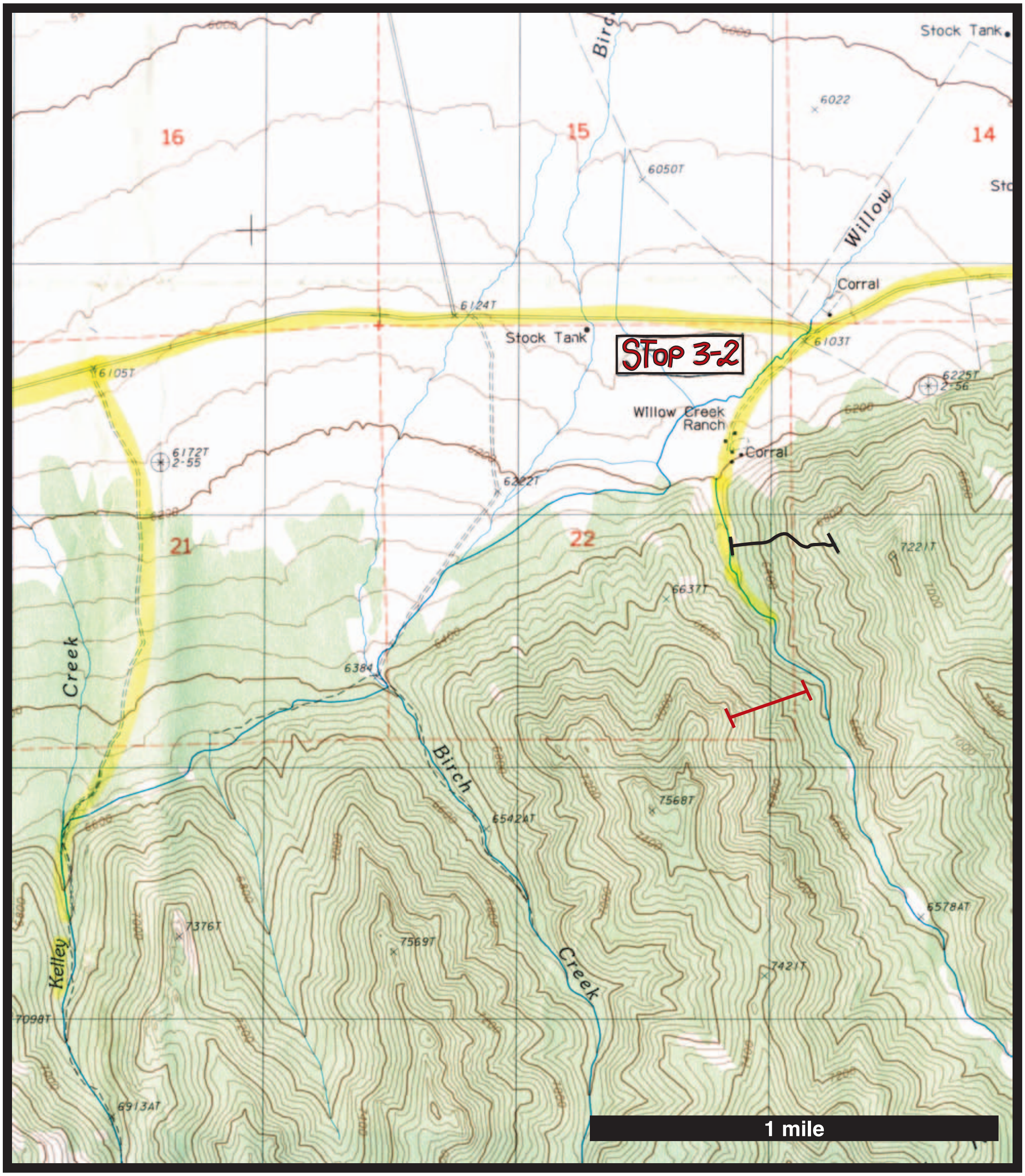

Map 7. Location of Stop 3-2 on the Cooper Peak Quadrangle, Willow Creek, Nevada. Photos 3-2c through 3-2h from line of section in black. Photos 3-2i and 3-2j from line of section in red.

STOP 3-2 – ROBERTS MOUNTAINS, NEVADA

Age – Late Silurian and Early Devonian.

Formations – Roberts Mountains Formation and the overlying Lone Mountain Dolomite.

Carbonate Depositional Sequences (Figure 2)– Sequence #5 and the lower part of Sequence #6 are represented at this locality Figure 2). Both a late transgressive systems tract (aggrading platform margin) and a highstand systems tract (prograding platform margin) of Sequence #5 can be seen and perhaps part of the lowstand systems tract of Sequence # 6 (i.e., erosional channels filled with platform margin clasts near the top of the Lone Mountain Dolomite on the west side of Willow Creek).

Depositional Environments (Figures 51-54) – Winterer and Murphy's classic paper (1960) was the first to interpret the dark gray Roberts Mountains Formation to be a basinal and slope facies. They considered the overlying light gray Lone Mountain Dolomite to be a true ecologic reef as defined by Lowenstam (1950). Matti and others (1975) and Matti and McKee (1977) modified the earlier interpretation of Winterer and Murphy (1960) by abandoning the reef hypothesis and proposing that the uppermost Roberts Mountains Formation was a skeletal bank margin facies that interfingered with the Lone Mountain Dolomite. Nichols and Silberling (1977) refuted several interpretive elements of Winterer and Murphy (1960), Matti and others (1975), and Matti and McKee (1977). Nichols and Silberling (1977) agreed with earlier interpretations in that the platform margin carbonates represent skeletal sands (bank) rather than skeletal boundstone facies (reef). However, Nichols and Silberling (1977) proposed that an unconformity exists between the dark-colored Roberts Mountains Formation and the light-colored Lone Mountain Dolomite. They state (p. 224) that "the abrupt change from outer-platform or off-platform crinoid grainstone of the upper Roberts Mountains Formation to inner-platform desiccated primary dolomite of the Willow Creek (Lone Mountain Dolomite) marks a pronounced progradation of the Lone Mountain Dolomite over the Roberts Mountain Formation. This suggests that the deposition of the two was interrupted by an episode of exposure and erosion of the Roberts Mountains carbonate ramp or platform before Lone Mountain Dolomite deposition". It should be noted at this point that apparently Nichols and Silberling failed to see that stratigraphically above the "crinoid grainstone" (discussed below) there occurs a coral-bearing horizon which marks the organic component of the platform margin facies. There is no "missing facies" as proposed by Nichols and Silberling (1977) which led them to propose an unconformity between the Roberts Mountains and Lone Mountain formations.

An alternative interpretation that is similar to that of Matti and others (1975) and Matti and McKee (1977) but differs in detail is offered here and in Cook and others (1983). First, our observations indicate that the mappable boundary between the Roberts Mountains and Lone Mountain Dolomite formations is a diagenetic contact, not a depositional event (Figures 51, 52). Thus, the formational boundary mapped has different facies at different locations along strike. This is a fundamental feature not reported and/or recognized for its importance by previous workers. The mapped formational boundary is defined as being dark gray limestone for the Roberts Mountains Formation and light gray dolostone of the Lone Mountain Dolomite. However, of major importance is that this color change does not always parallel bedding <u>planes</u> or depositional facies. Cook (1966) earlier pointed out that the mappable color boundary between these two formations is of a diagenetic origin and not a primary depositional feature. For example, in the Hot Creek Range at Field Stop 5-5 (north side of the lower Hot Creek Canyon) the color boundary between the Roberts Mountains Formation and Lone Mountain Dolomite is wavy and crosses bedding planes. Thus, where the beds are dark gray they are traditionally assigned to the Roberts Mountains Formation and where the beds are light gray they are referred to as the Lone Mountain Dolomite.

We have found no compelling evidence that supports the "missing facies" theory of Nichols and Silberling (1977). The mappable contact between the Roberts Mountains Formation and Lone Mountain Dolomite is herein interpreted to be a diagenetic feature, and we believe that the two formations are in depositional contact at this stop (Cook and others, 1983). When one ignores the color differences between formations and looks at the depositional facies themselves there appears to be a gradual stratigraphically upward transition in facies from lower slope turbidites to upper slope cross bedded crinoidal-oolite grainstone sand bars to coral-rich platform margin sediments to bedded and cross-bedded grainstones and conglomerates to tidal channel facies, to fenestral fabrics and oolite shoals. The dolomitizing fluids did not uniformly follow any one facies boundary but crossed facies boundaries. The resulting contact is considered to be a complex collage of interfingering limestone and dolostone facies (Figures 51-53).

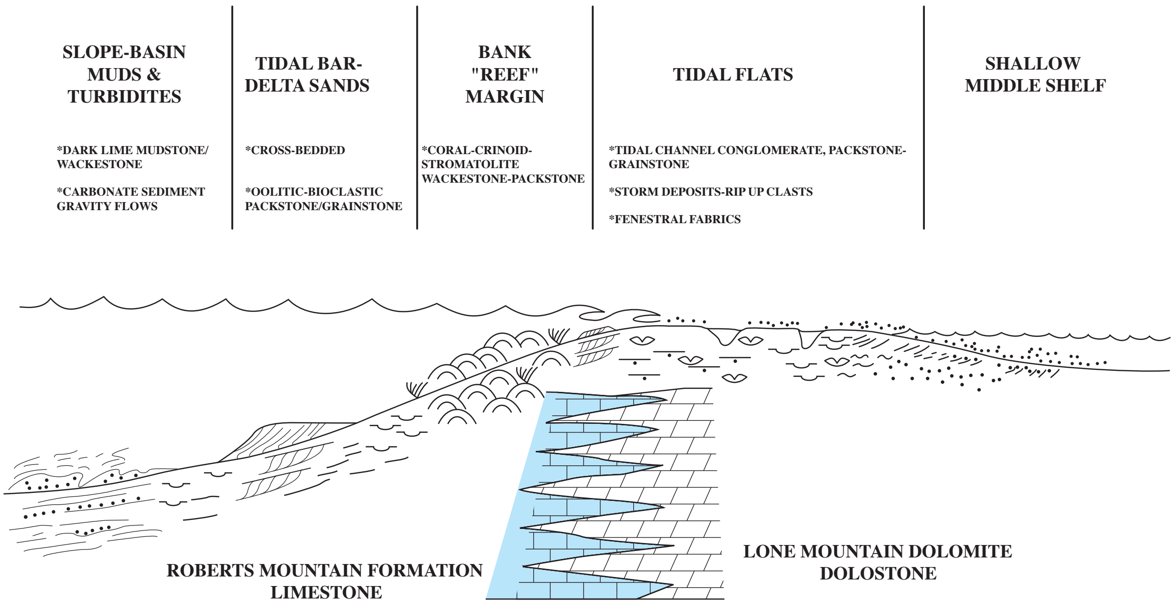

Figure 51. Interpretive depositional profile and environments for lower and upper Roberts Mountains Formation and lowermost Lone Mountain Dolomite at Stop 3-2, Willow Creek, Roberts Mountains, Nevada (From Cook and others, 1983).

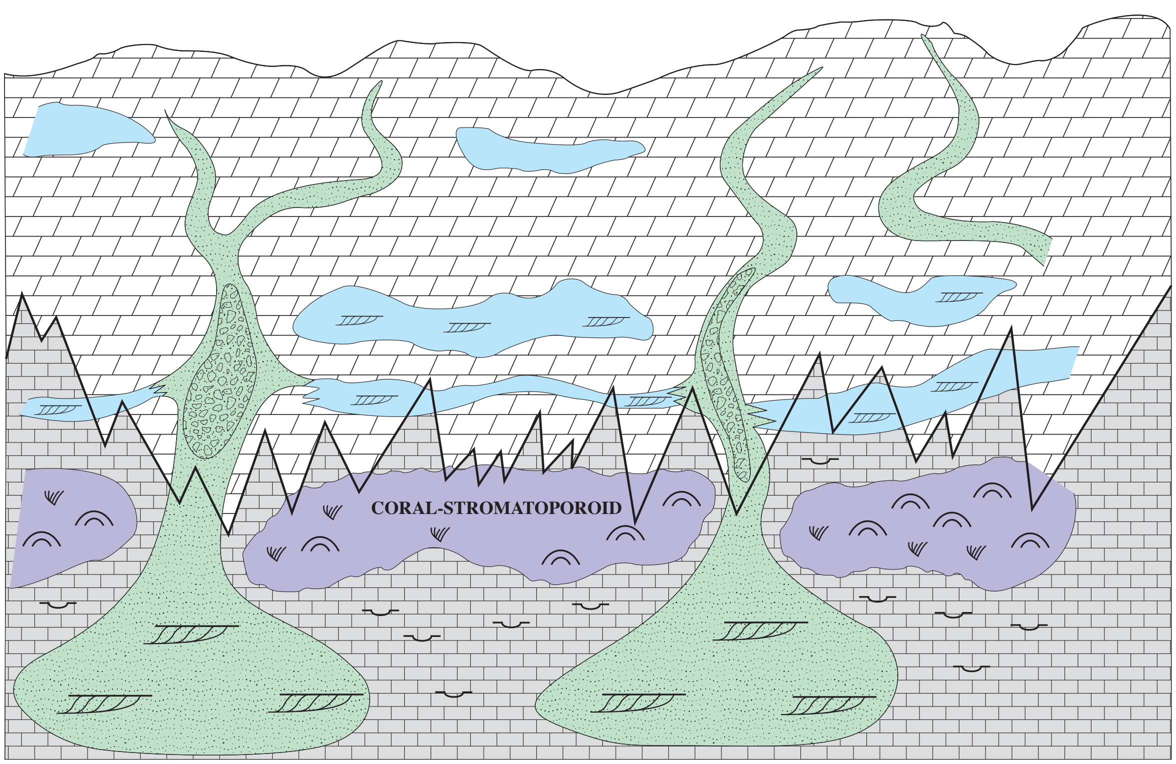

Figure 52. Map view of Figure 51 showing the interpreted diagenetic relationship between the Roberts Mountains limestones and the Lone Mountain Dolomite dolostones. Jagged wavy line schematically shows the diagenetic nature of the formational contact. Willow Creek, Roberts Mountains, Nevada (From Cook and others, 1983).

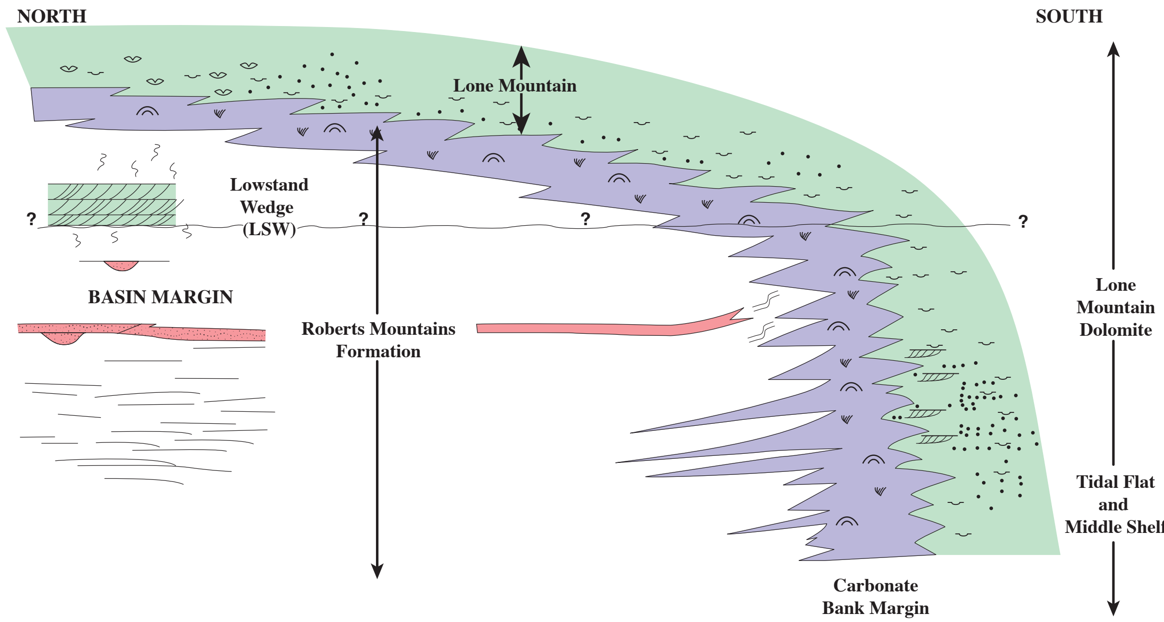

Figure 53. Interpretive geologic cross-section of Figure 51 showing aggrading phase in lower part of stratigraphic section and seaward prograding phase in upper part of section. Distance across figure is about 2500 feet. Willow Creek, Roberts Mountains, Nevada (From Cook and others, 1983).

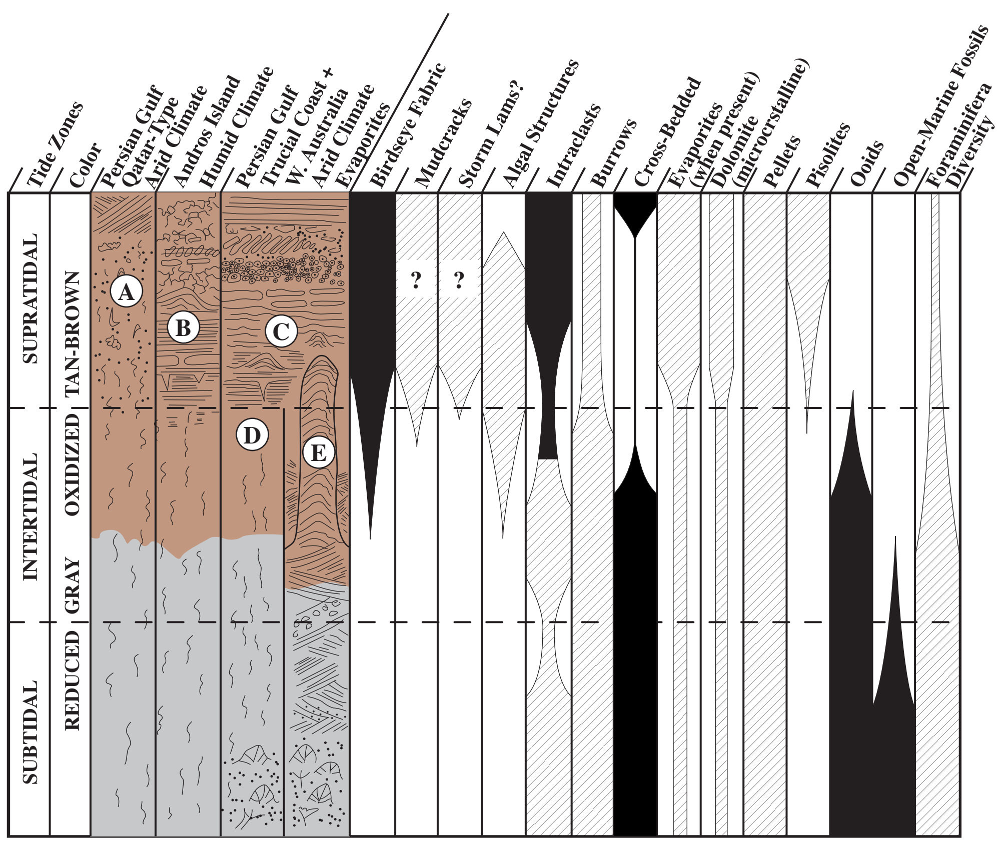

Figure 54. Solid black bars represent features present along the Roberts Mountains-Lone Mountain contact at Stop 3-2 (Modified from Shinn, 1983).

The above discussion refers to the area where the Lone Mountain Dolomite was prograding seaward over the Roberts Mountains Formation (Figure 53–left hand side). In the same canyon but stratigraphically lower this Silurian-Devonian bank margin was aggrading (Figure 53–right-hand side). In the aggrading area, the deeper water turbidites and in-situ slope and basinal beds in the Roberts Mountains Formation interfinger along strike into the platform margin Lone Mountain Dolomite sediments (Figure 53). There is no apparent "missing facies" evidence for an unconformity as proposed by Nichols and Silberling (1977). There may be an unconformity of unknown magnitude at or near the top of the Lone Mountain Dolomite (Figure 2) as at several localities erosional channels occur within the dolomitized Lone Mountain oolite and tidal flat facies. However, these channels could be normal tidal channels that are common on modern carbonate platform margins and tidal flats (for example, Scholle and others, 1983; Cook and others, 1983).

Chief Features to be Observed –

Roberts Mountains Formation:

1. Carbonate turbidites (slope).
2. Cross-bedded crinoid-ooid packstones and grainstones (subtidal marine tidal bars and/or deltas on gentle slopes just seaward of the bank margin). Lowstand systems tract (?).
3. Skeletal-rich (corals) platform margin limestone (subtidal, moderately high-energy platform margin).
4. Cross-bedded limestone conglomerates and grainstones (shallow, high-energy subtidal to supratidal).
5. Diagenetic nature of contact between Roberts Mountains Limestone and Lone Mountain Dolomite.

Lone Mountain Dolomite:

1. Dolomite breccia facies (tidal flat).
2. Dolomitized coral facies (possible storm deposits washed onto tidal flats from bank margin).
3. Dolomitized oolite grainstones (oolite tidal bars and /or tidal belts in tidal flat and shallow subtidal settings).

Economic Considerations – Four main depositional facies seaward and bankward of platform margin environments have the potential of forming important reservoirs for petroleum and minerals. These include 1) carbonate sediment gravity flow deposits in slope and base-of-slope settings. These facies can contain both primary and secondary porosity types. Two examples include the Cretaceous Poza Rica Field in Mexico (Enos, 1977, 1985; Magoon and others, 2001) and Permian Basin fields in the Delaware and Midland Basins of West Texas (Cook, 1983; Cook and others, 1983). 2) Tidal bar belts, tidal delta sands and marine sand belts composed of sand-sized organic grains as well as oolites and other coated grains. These carbonate sand bodies can occur on the seaward as well as landward side of the platform edge (Halley and others,1983). Bars and channels are plentiful along the Lower Cretaceous Stuart City Trend in Texas and in the Upper Jurassic Smackover oolite in Arkansas and Louisiana. These oolite bodies were deposited in tidal bars, deltas, channels, beaches, and islands. Carbonate sand bodies are particularly abundant in Mississippian, Permian, Jurassic, and Cretaceous ages although similar carbonate sands can be found virtually throughout the stratigraphic column. 3) Platform edge organic buildups including true boundstone reef facies and/or organic banks composed of skeletal grainstones are a common reservoir facies at platform margins. These reservoirs can contain both primary interparticle porosity secondary moldic porosity and intercrystalline porosity where the buildups have been dolomitized. A few examples include Devonian platform margin stromatoporoid facies in Canada and western Australia, Pennsylvanian coral-rich buildups in Texas, coral boundstone and rudist grainstone reservoirs in the Cretaceous of Texas and the Golden Lane of Mexico. 4) Skeletal packstones and wackestones on the inner side of the platform edge can have significant amounts of moldic porosity. These so-called "platform lagoon" facies form major reservoirs in the Devonian of Canada and the Canning Basin of western Australia. In these Devonian cases a major reservoir facies is an Amphipora wackestone and packstone. The matrix is dolomitized and the Amphipora are partially or wholly leached. The dominant porosity is moldic and intercrystalline. It is important to note that in the Diamond Mountains, a few miles east of Roberts Mountains, Devonian Amphipora-rich platform lagoon facies of the Middle Devonian Bay State Dolomite contain 4.0 % moldic porosity and 1100 millidarcys horizontal permeability similar to that forming reservoir facies in Canada and elsewhere (Cook, 1988). Other examples of platform margin and near platform margin reservoirs are reviewed by Wilson (1975, 1983), Halley and others (1983), and James (1983).

Most of the gold on the northern Carlin trend is hosted in the Lower Devonian (Lochkovian) part of the Roberts Mountains Fromation (oral comm., Poul Emsbo; Emsbo and others, 2003). The Rodeo deposit along the Carlin trend is hosted in upper mudstone member (informal) of the Middle Devonian (Eifelian) Popovich Formation (Emsbo and others, 2003). Sediment-hosted gold occurs at the Gold Acres deposit in the Roberts Mountains Formation near the contact with the overlying Roberts Mountains thrust (Hays and Foo, 1991). Possible mineral host facies in Roberts Mountains Formation could be carbonate turbidites and tidal bar-delta carbonate sands. These types of sediments were transported off the platform margin prior to early marine dolomitization of the platform margin. Post-depositional diagenesis of aragonite and magnesium calcite components in these facies could produce porosity.

Relation to other areas – At Stop 4-1, we will see Lower Devonian basin margin section that exhibits submarine slumping and sliding, carbonate turbidites, and possible carbonate contourites. At Stop 4-2, we will briefly discuss the Lower Devonian Tor Limestone and the role it plays in the interpretation that the Roberts Mountains Formation formed in a stagnant outer platform basin (Matti and McKee, 1977) rather than on the continental margin (Thomas and others, 1987).

Photo 3-2a. Looking east at shoaling upward section. Roberts Mountains Formation (slope and inner basin) in lower part of section overlain by Lone Mountain Dolomite (platform margin) at ridge top. Stop 3-2. Willow Creek, Roberts Mountains, Nevada.

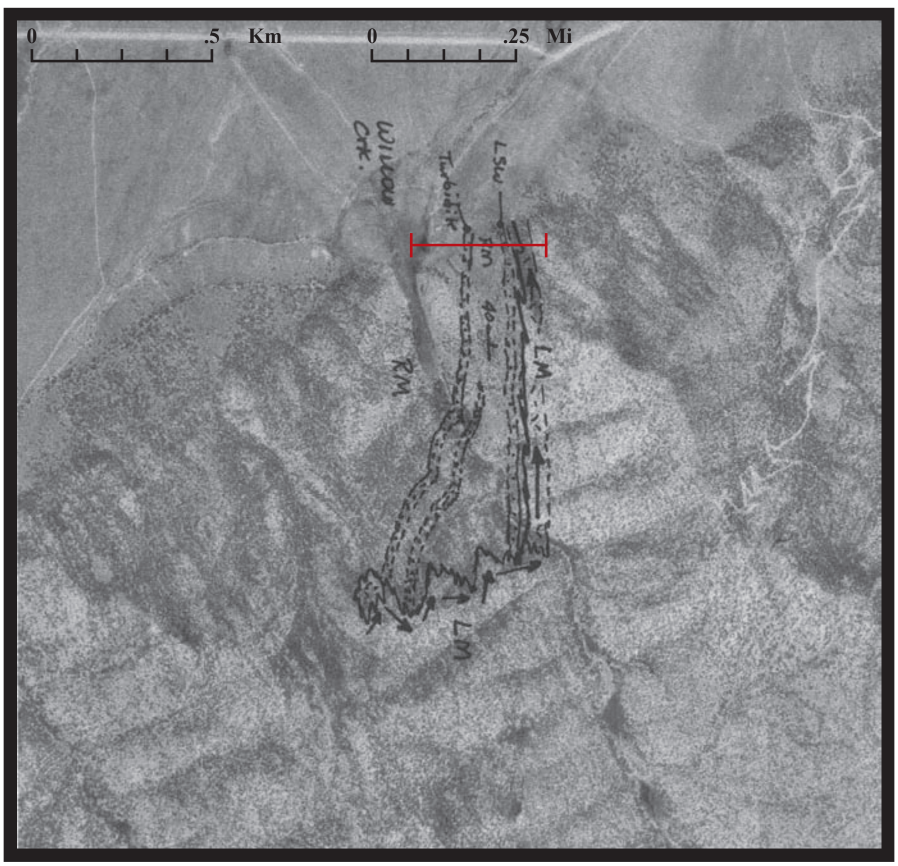

Photo 3-2b. Aerial photograph showing aggradation of Lone Mountain Dolomite and late phase progradation of Lone Mountain Dolomite over Roberts Mountains Formation. Line of section (in red) is the location shown in Photo 3-2a. Stop 3-2. Willow Creek, Roberts Mountains, Nevada.

Photo 3-2c. Roberts Mountains Formation. Normally graded bioclastic turbidite. Slope. Stop 3-2. Willow Creek, Roberts Mountains, Nevada.

Photo 3-2d. Roberts Mountains Formation. In-situ laminated lime mud slope facies. Slope. Stop 3-2. Willow Creek, Roberts Mountains, Nevada.

Photo 3-2e. Roberts Mountains Formation. Cross-bedded ooid-crinoid grainstones on upper slope. Ooids transported downslope prior to dolomitization of in-situ oolites shoals on platform margin. Stop 3-2. Willow Creek, Roberts Mountains, Nevada.

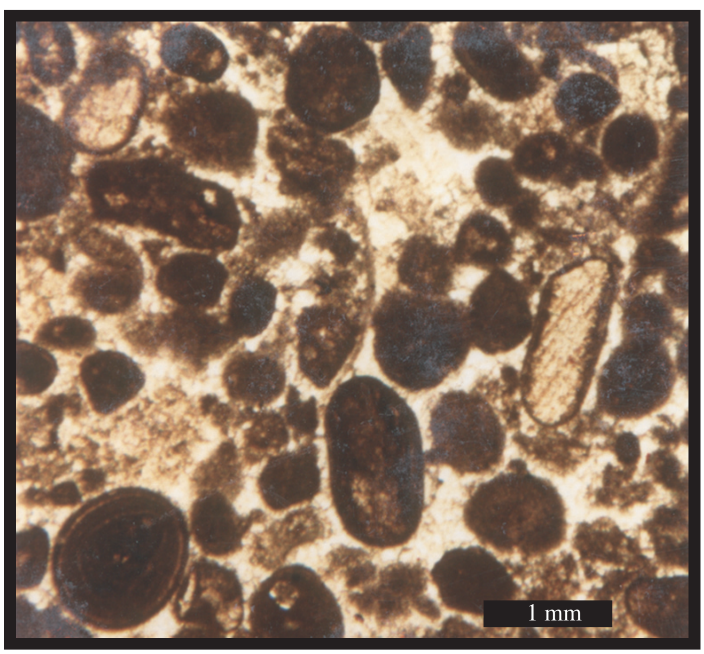

Photo 3-2f. Roberts Mountains Formation. Thin-section of cross-bedded ooid-crinoid grainstones on upper slope. Stop 3-2. Willow Creek, Roberts Mountains, Nevada.

Photo 3-2g. Roberts Mountains Formation. Stromatoporoid-coral biostromes forming along the uppermost slope setting. Stop 3-2. Willow Creek, Roberts Mountains, Nevada.

Photo 3-2h. Lone Mountain Dolomite. Platform margin with tidal channels filled with dolomitized limestones. Stop 3-2. Willow Creek, Roberts Mountains, Nevada.

Photo 3-2i. Lone Mountain Dolomite. Dolomitized ooid grainstone shoals at platform margin. Stop 3-2. Willow Creek, Roberts Mountains, Nevada.

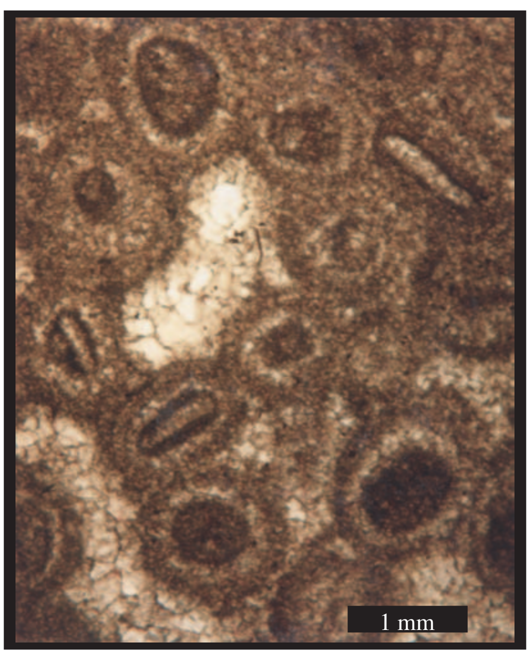

Photo 3-2j. Lone Mountain Dolomite. Thin-section of dolomitized ooid grainstone at platform margin. Stop 3-2. Willow Creek, Roberts Mountains, Nevada.

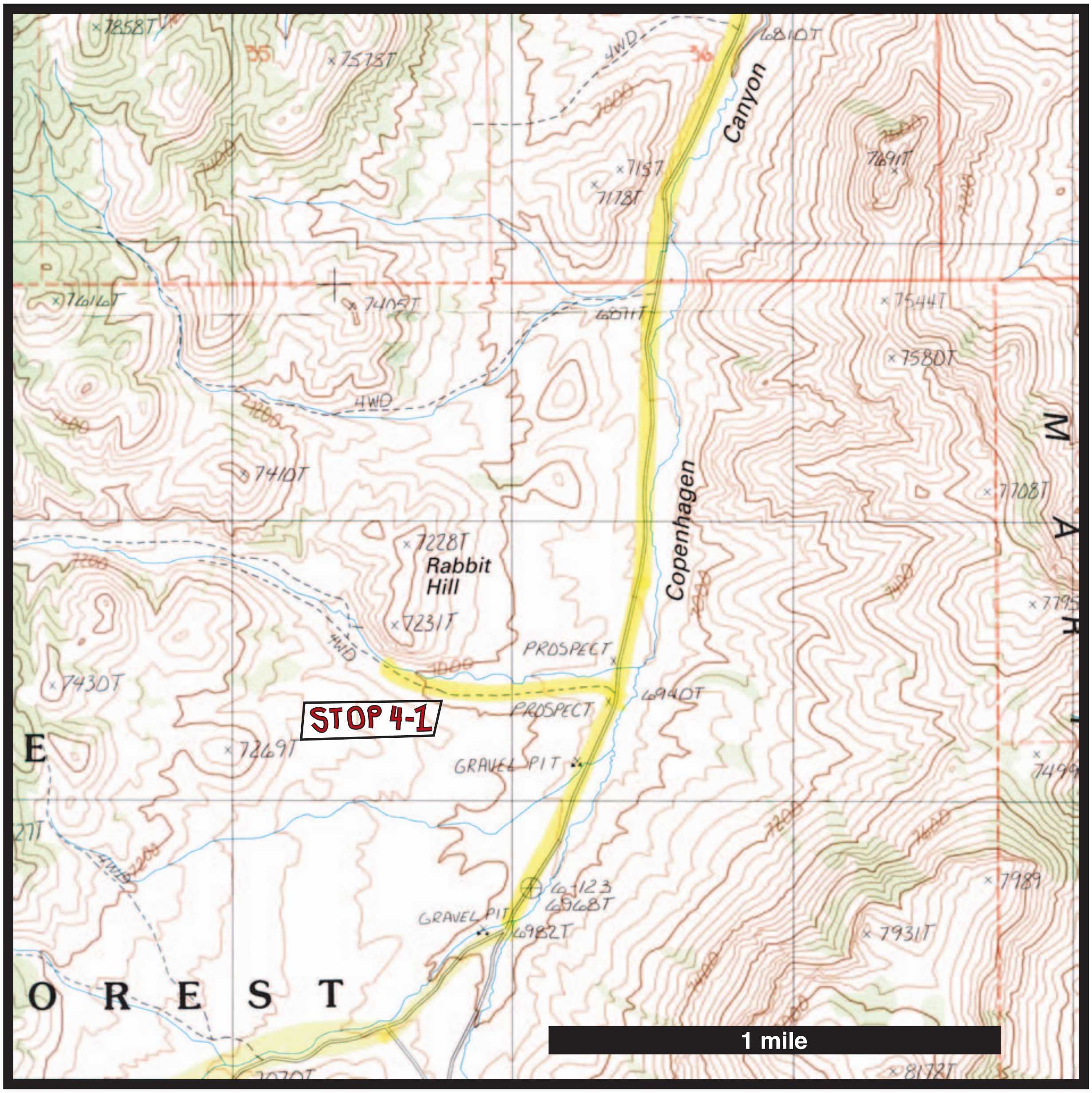

Map 8. Location of Stop 4-1 on the Horse Heaven Mountain Quadrangle, Copenhagen Canyon, Rabbit Hill, Nevada.

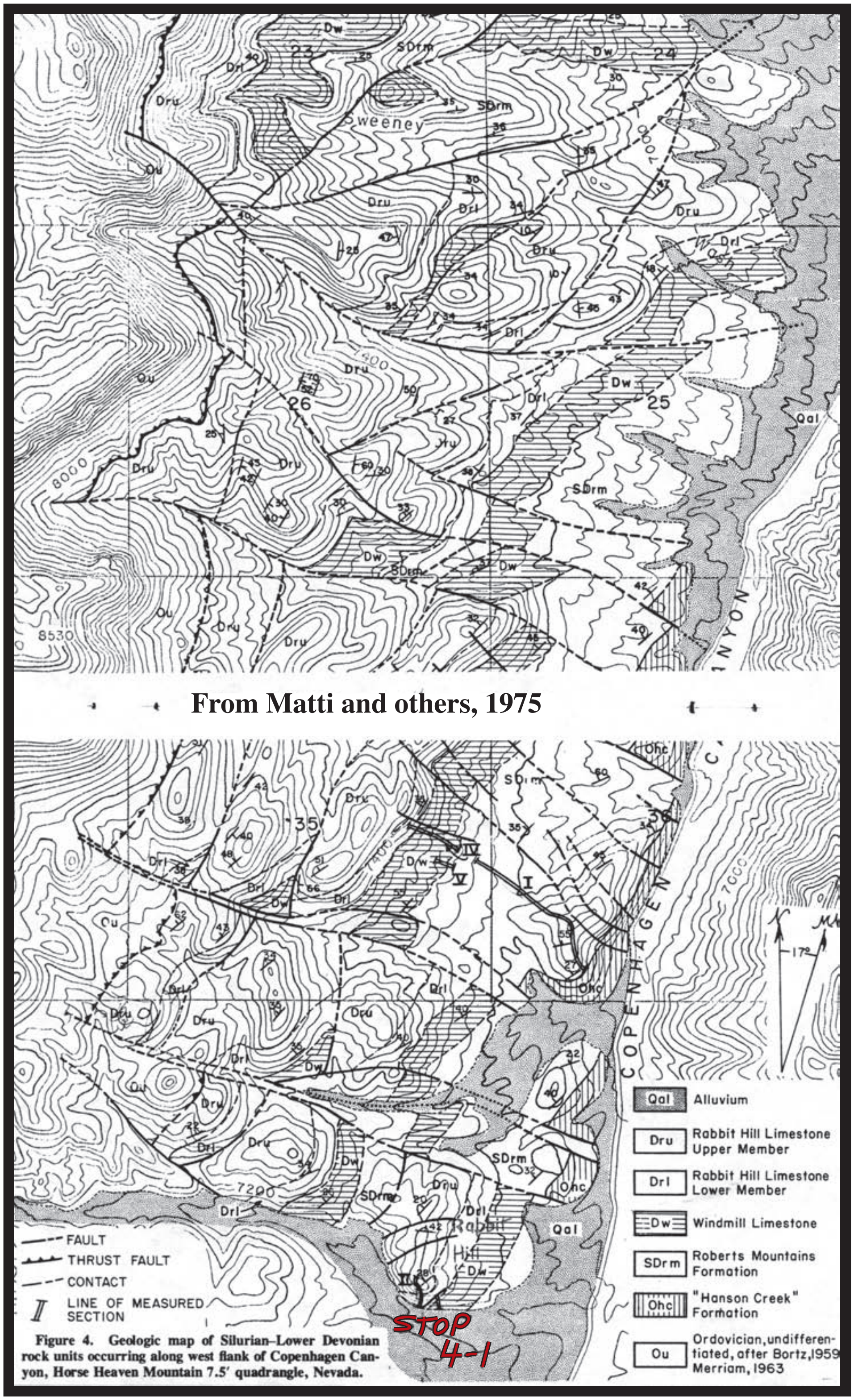

Map 9. Geologic map for Stop 4-1, Horse Heaven Mountain Quadrangle, Copenhagen Canyon, Rabbit Hill, Nevada.

STOP 4-1 – MONITOR RANGE, NEVADA

Age – Lower Devonian

Formation – Rabbit Hill Limestone.

Carbonate Depositional Sequences (Figure 2)– Its chronostratigraphic position suggests it is part of the lowstand and transgressive systems tracts of Sequence #6.

Depositional Environments – The Rabbit Hill Limestone has been interpreted by Matti and others (1975) and Matti and McKee (1977) as representing carbonate slope deposits. We agree with that interpretation. The presence of large-scale soft-sediment folds in dark gray lime mudstone, conglomeratic debris flow beds, possible contourites, and the regional position of Rabbit Hill Limestone support a slope setting. In terms of depositional models it appears to represent a location on Figure 31 someplace seaward of the platform margin on the upper slope but not seaward enough to be in a base-of-slope setting.

Chief Features to be Observed –

1. Carbonate turbidites with petroliferous odor.
2. Organic-rich lime mudstones.
3. Possible carlcarenite contourites.
4. Debris flow beds.
5. Large-scale soft-sediment folds.
6. Centimeter-scale rotational faults developed in semi-lithified lime muds (listric fault planes dip westerly).

Economic Considerations – As discussed at previous stops, the carbonate sediment gravity flow deposits under the right diagenetic conditions can serve as reservoirs for hydrocarbons and host facies for mineral deposits.

Relation to other areas – At Stops 5-4 and 5-6, we will have an opportunity to examine the similarities and differences between the slope facies in the Rabbit Hill Limestone and the well exposed slope, submarine fan, and apron facies in the Upper Cambrian-Lower Ordovician and the Lower-Middle Devonian of the Hot Creek Range, Nevada.

Photo 4-1a. Rabbit Hill Limestone. Arrow points to large soft-sediment slump overfolds. Slope. Stop 4-1. Rabbit Hill, Copenhagen Canyon, Nevada.

Photo 4-1b. Rabbit Hill Limestone. Close-up of soft-sediment slump overfold zone shown in Photo 4-1a. Slope. Stop 4-1. Rabbit Hill, Copenhagen Canyon, Nevada.

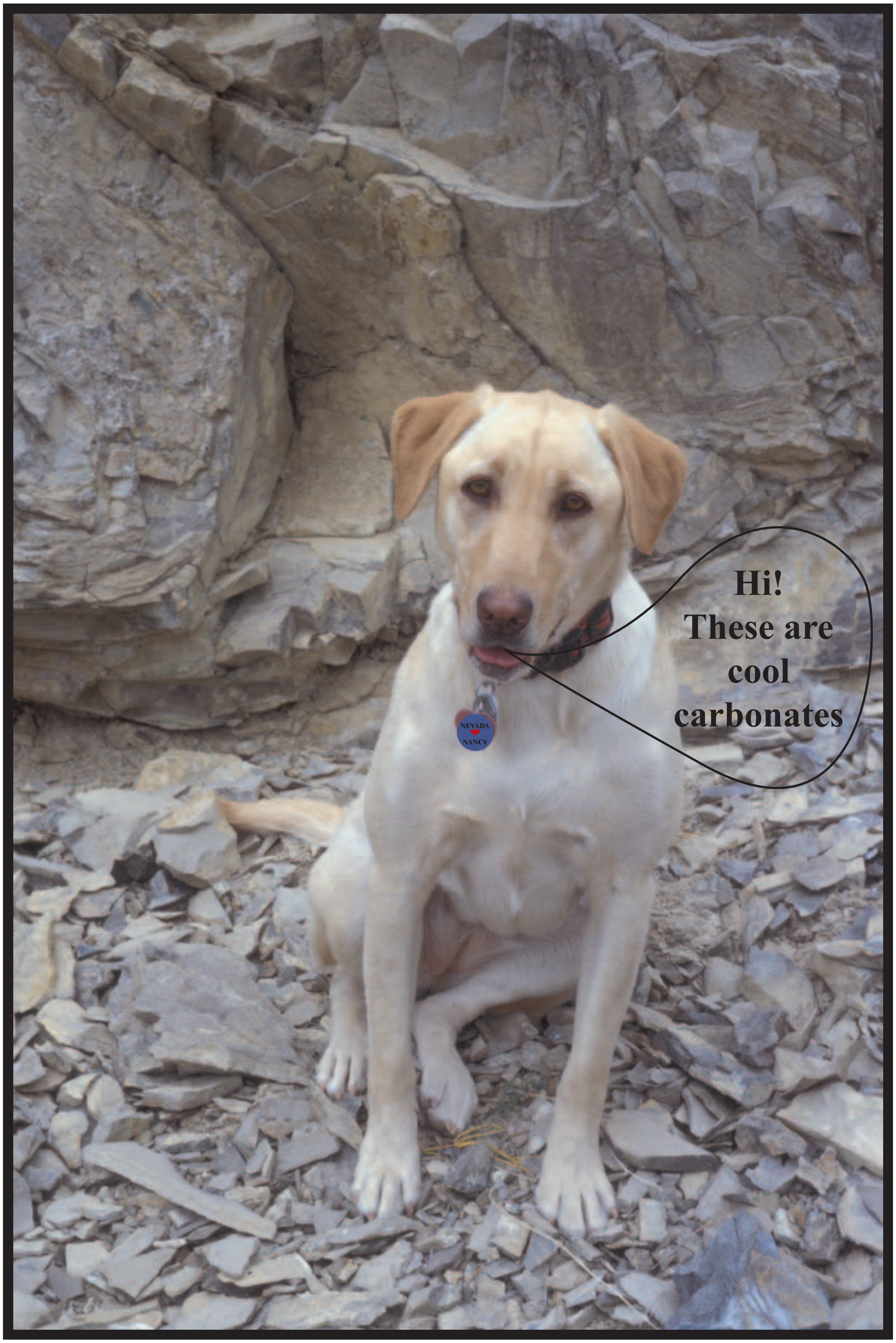

Photo 4-1c. Rabbit Hill Limestone. Right ear of "Nevada" shows trend of soft-sediment slump overfold axis. Slope. Stop 4-1. Rabbit Hill, Copenhagen Canyon, Nevada.

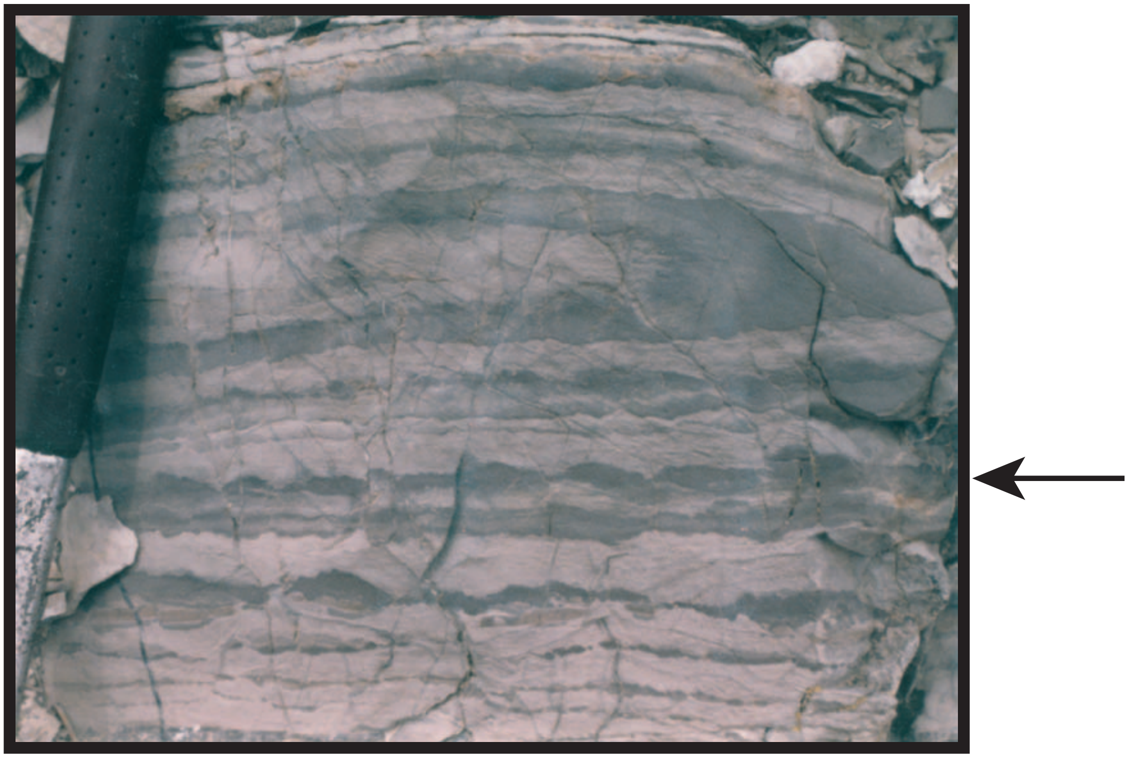

Photo 4-1d. Rabbit Hill Limestone. Soft-sediment slumping. Thin bed at arrow suggests rotation of some segments of the beds downslope (to the left). Slope. Stop 4-1. Rabbit Hill, Copenhagen Canyon, Nevada.

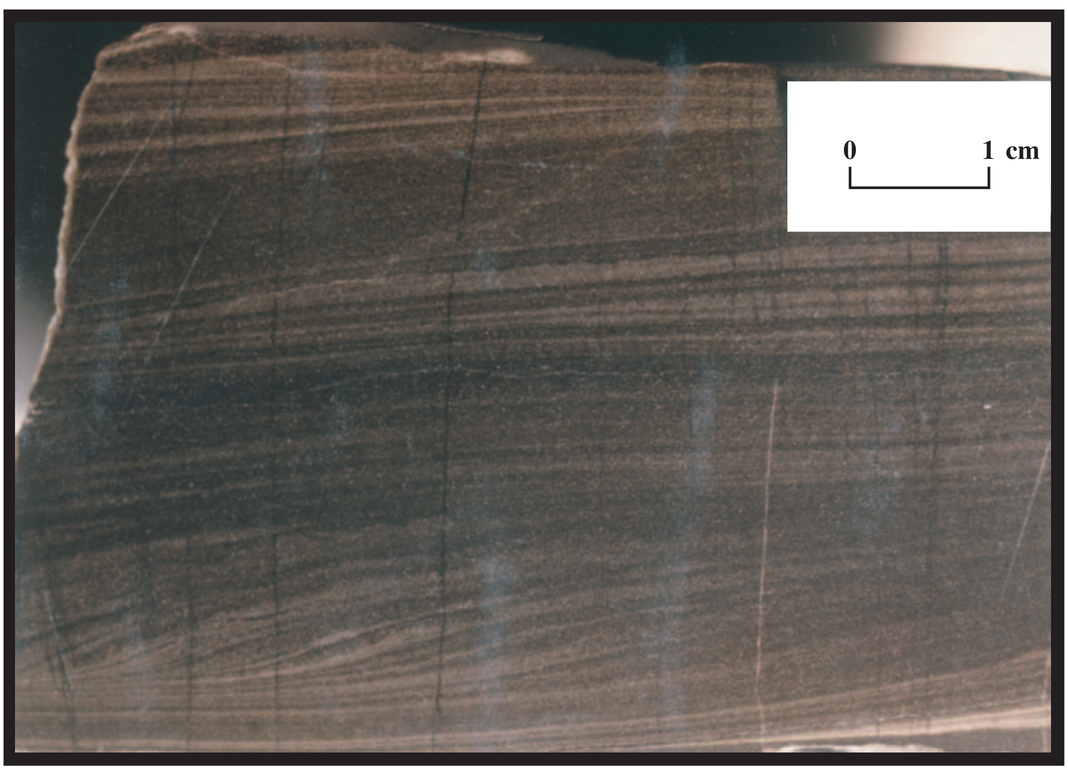

Photo 4-1e. Rabbit Hill Limestone. Turbidites and/or contourites. Slope. Stop 4-1. Rabbit Hill, Copenhagen Canyon, Nevada.

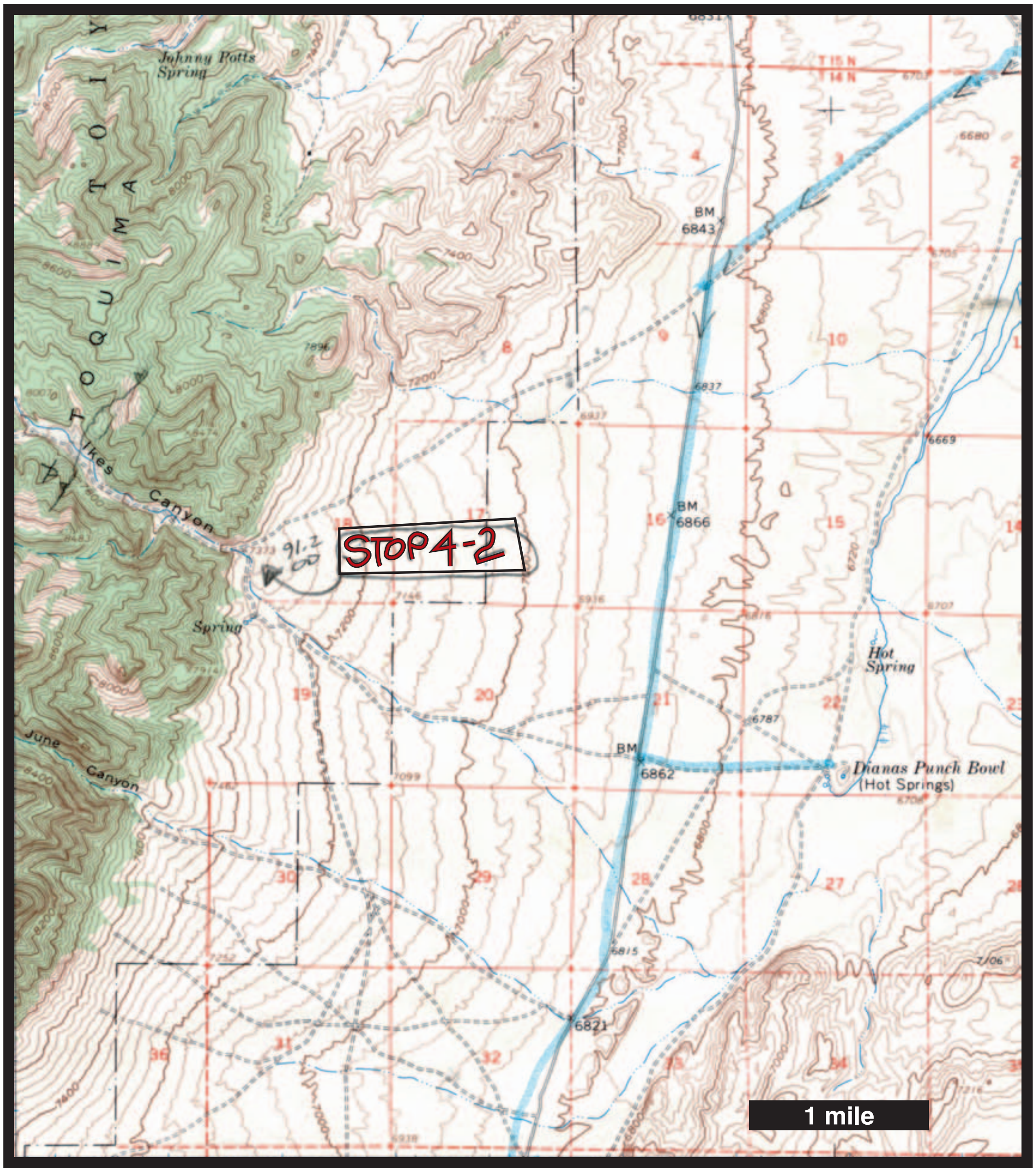

Map 10. Location of Stop 4-2 on the Dianas Punch Bowl Quadrangle, Ikes Canyon, Nevada.

STOP 4-2 – TOQUIMA RANGE, NEVADA
(Discussion Stop)

Age – Early Devonian.

Formation – Tor Limestone.

Carbonate Depositional Sequences (Figure 2) – The Tor Limestone is interpreted to represent submarine debris flow and turbidity current deposits that were derived from coeval shoal water Roberts Mountain and Lone Mountain platform margins to the east (Thomas and others, 1987). In this context the Tor Limestone is considered to represent the lowstand systems tract of Sequence #6. This interpretation contrasts with Kay and Crawford (1964) and Matti and McKee (1977) who in our opinion misinterpreted interpreted the Tor Limestone to be an in-situ shoal-water bank or reef.

Depositional Environments – The Lower Devonian Tor Limestone in the Toquima Range is the same age as the uppermost part of the Lone Mountain-Roberts Mountains platform margin (Figure 2). Kay and Crawford (1964) interpreted the Tor Limestone as an in-situ "reef or biostrome facies". Matti and McKee (1977) agree with that interpretation and also propose that the McMonnigal Limestone in the Toquima Range forms a circular band around the Tor Limestone and represents carbonate sediment gravity flow deposits derived from a shoal-water in-situ Tor Limestone bank.

The original interpretation of Kay and Crawford (1964) that the Tor Limestone is a shoal-water carbonate bank required the interpretation that the Tor was initiated on a shoal-water substrate. Out of this "shoal-water substrate" evolved the interpretation that the Tor developed on a north-south trending topographic ridge about 500 km in length (Matti and McKee (1977). This interpretation has important implications to the interpretative history of the continental margin during the Silurian-Devonian. The interpretation is the basis for Matti and McKee (1977) proposing that the Roberts Mountains Formation formed in an outer platform basin bounded on the landward side by the Lone Mountain platform margin and on the seaward side by the so-called "Toiyabe Ridge".

There are several things that should be pointed out about the internal makeup of the Tor Limestone (Thomas and others, 1987). All stratigraphic intervals within the Tor Limestone "bank" examined by Thomas and others (1987) and even its basal lower beds consist of carbonate conglomeratic debris flow and turbidity current deposits. For example, at the "Wall" in Ikes Canyon the basal most beds in the Tor at the unconformable contact with the Pogonip Formation consist of crinoid-rich turbidites and debris flow beds containing colonial Favosites coral heads up to 60 cm across. At another locality a single debris flow bed is up to 5 meters thick. In this debris flow sequence there are carbonate clasts up to about 25 x 75 centimeters across set within a crinoid wackestone matrix. Bear in mind these debris flow beds form the Tor Limestone "bank".

Sheehan and others (1993) also interpret large isolated carbonate bodies in the Lower Devonian Roberts Mountains Formation in Antelope Peak (near Wells Nevada in northeastern Nevada) to be a series of stacked debris flow and turbidity current deposits. These debris flows and turbidity current deposits, which are coeval with the Tor Limestone, were transported 50-100 km from the Roberts Mountains platform margin. The Roberts Mountains isolated debris bodies are up to about 50 m thick and 600 m wide.

Platform margin collapse during eustatic sea level lowstands are common and, for example, are interpreted to have occurred near the Cambro-Ordovician boundary in the Great Basin, Alaska, and in Southern Kazakhstan (Cook and Taylor, 1977; Cook, 1979; Cook and Taylor, 1991; Cook and others, 1991). Other platform margin collapse events are cited in the literature (Handford and Loucks, 1993). There are numerous cases in the literature where so-called "reefs" and "shoal-water banks" were originally misinterpreted. Later, these "reefs" and "shoal-water banks" were then shown to be shoal-water debris transported into deeper-water basinal setting (For example, Pray and Stehli, 1962; Cook and others, 1972; also see Cook and Mullins, 1983, text Figures 56, 57, and 60).

We believe that the origin of the Tor Limestone has been misinterpreted (i.e., an in-situ reef) and that the field evidence shows it is a series of carbonate debris flow and turbidity current deposits derived from the platform margin to the east as interpreted herein and by (Thomas and others, 1987). In this interpretation the Tor Limestone debris bodies represent a lowstand systems tract of Sequence 6 (Figure 2) that originated by massive collapse of the Lower Devonian platform margin during a relative sea level lowstand. Thus, the evidence and necessity for a “Toiyabe Ridge” vanishes and consequently the interpretation that a Silurian-Devonian outer platform basin (Matti and McKee, 1977) ever existed is suspect.

Photo 4-2a. Tor Limestone. Resistant light grey, cliff-forming limestone. Basin. Stop 4-2. Ikes Canyon, Toquima Range, Nevada.

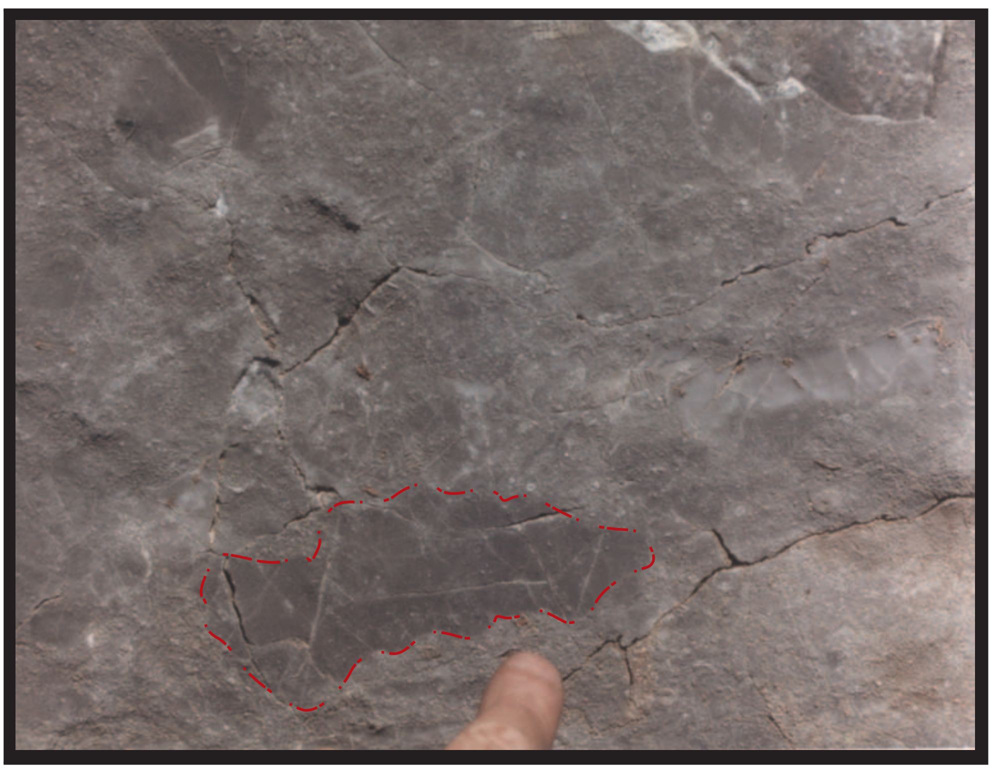

Photo 4-2b. Tor Limestone. Carbonate debris flow at base of Tor Limestone. Basin. Stop 4-2. Ikes Canyon, Toquima Range, Nevada.

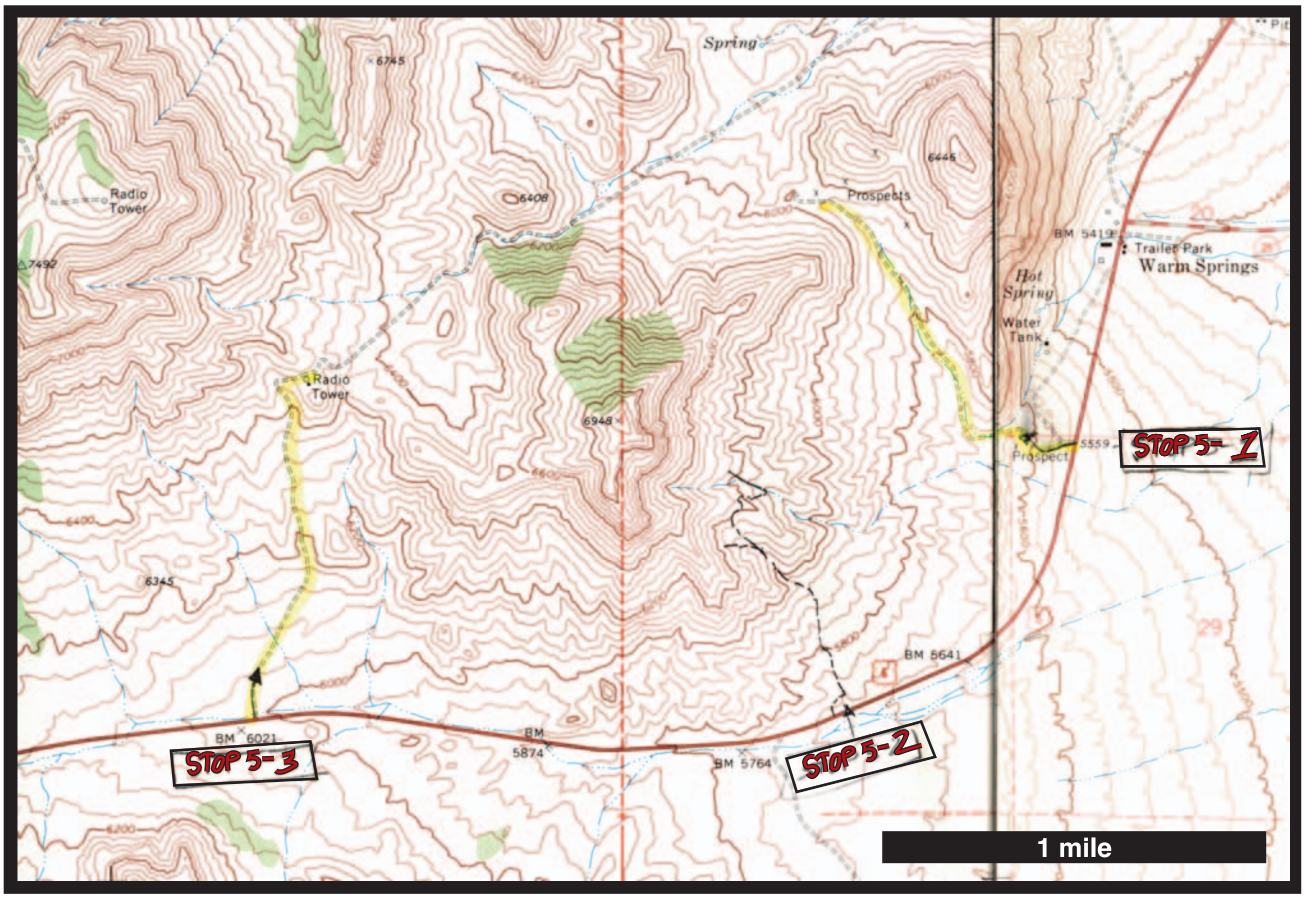

Map 11. Location of Stops 5-1, 5-2, and 5-3 on the Warm Springs NW Quadrangle, Hot Creek Range, Nevada.

STOP 5-1, 5-2, 5-3– WARM SPRINGS, HOT CREEK RANGE, NEVADA

Age – Late Devonian–Early Mississippian.

Formations – Late Devonian Denay, Pilot and Woodruff formations and Early Mississippian Webb, Tripon Pass, and Eleana formations.

Carbonate Depositional Sequences – These formations have not been studied in terms of carbonate sequence stratigraphy.

Depositional Environments (Figure 3) – These formations are interpreted to have been deposited in deeper water settings seaward of the Late Devonian Devils Gate platform margin and seaward of the Early Mississippian Joana Limestone carbonate bank (Poole and Sandberg, 1993; Sandberg and others, 2003; Poole, personnel communication, 2003).

Economic Considerations – Carlin-type gold deposits are found, for example, in the deeper water Lower Mississippian Webb Formation (e.g., South Bullion deposits, Putnam and Henriques, 1991; Trout Creek deposits, Jackson and Ruetz, 1991; Chert Cliff deposits, Vikre and Maher, 1995). An important exploration strategy is to determine the primary depositional facies types of the host facies for these mineral deposits. If the host facies are dominantly in the carbonate sediment-gravity flow deposits it would be important to know what part of a carbonate depositional sequence they represent and if these allochthonous facies are part of a slope section or base-of-slope apron or fan.

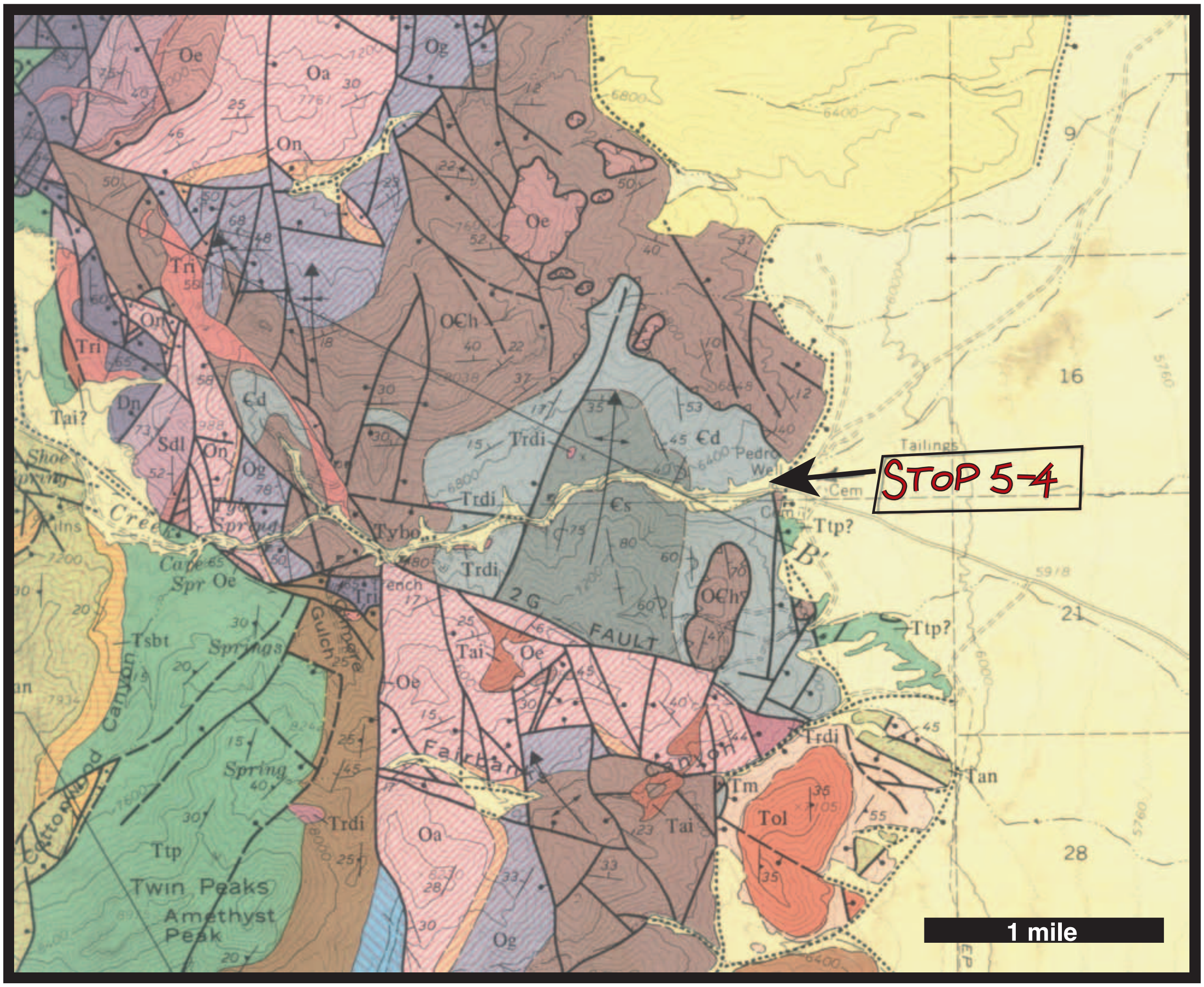

Map 12. Location of Stop 5-4 on the Geologic Map Tybo Quadrangle, Tybo Canyon, Nevada.

STOP 5-4– HOT CREEK RANGE, NEVADA

Age – Late Cambrian and Early Ordovician.

Formations – From base to top, the Swarbrick Formation, Dunderberg Shale, Hales Limestone, and Goodwin Limestone.

Carbonate Depositional Sequences (Figure 2) – Sequences #1 and #2 are interpreted to be represented at this stop. Two shoaling upward sequences from basin-plain to carbonate submarine fan to slope sediments (Cook and Taylor, 1975, 1977; Taylor and Cook, 1976; Cook, 1979; Cook and Egbert, 1981a, 1981b; Cook and Mullins, 1983; Cook and others, 1983) occur over an approximate 1,500 m-thick interval. These sequences represent a seaward progradation of a distally steepened ramp on the Late Cambrian-Early Ordovician continental margin.

Depositional Environments (Figures 55, 56) – These sequences are interpreted to have formed in ramp margin, slope, base-of-slope and basin-plain settings on the continental margin. The depositional facies consist of a basin-plain sequence of laminated hemipelagic lime mudstones, argillaceous limestones, thin-bedded cherts, and turbidites (Swarbick Formation and Dunderberg Shale). This is gradationally overlain by a wide variety of carbonate turbidite and debris-flow deposits whose facies collectively form a submarine fan (uppermost Dunderberg Shale and lower Hales Limestone) (Cook and Egbert, 1981a, Cook and others, 1983). The submarine fan facies, in turn, grade upward into submarine slide, slump, and contourite deposits that formed on the continental slope (upper Hales Limestone). The uppermost part of the sequence (uppermost Hales Limestone and lowermost Goodwin Limestone) appears to have been deposited on or near the outer distally steepened ramp margin.

During the latest Cambrian and earliest Ordovician relative sea level lowering has been recorded in North America, Kazakhstan, and China (Cook and others, 1989; Taylor and others, 1989). The thick sediment-gravity flow deposits and submarine slides at this stop are interpreted to represent a series of lowstand systems fan deposits that evolved during the latest Late Cambrian and the earliest Early Ordovician. These sea level lowstands are reflected to the east in the Egan Range by a change from shallow subtidal facies in the Whipple Cave Limestone to `tidal flat facies in the overlying House Limestone (Figure 2).

Chief Features to be Observed –

Swarbick Formation:

1. Thin bedded lime mudstone and reddish-brown partly silicified limestone with sponge spicules (basin-plain).

Dunderberg Shale:

1. Olive-green calcareous shale and calcarenite turbidites with T_b, T_{bc}, T_c, T_{cde}, bouma divisions (basin-plain and outer fan fringe).

Hales Limestone:

1. Outer fan lobe sheets (calcarenites), mid-fan distributary channels (conglomerates), interchannel facies (calcarenites), inner-fan feeder channels (conglomerates and megabreccias) (slope).
2. Submarine slides and slumps many of which exhibit various stages of remolding into debris flow deposits (slope).
3. Nuia quartz grainstone contourite (upper slope).

Economic Considerations – As discussed by Enos and Moore (1983), the best known example of petroleum production from carbonate slope and basin-margin settings is from the Cretaceous of Mexico (Figures 57, 58) (Enos, 1977, 1985; Magoon and others, 2001). These reservoirs are mainly in carbonate sedimentary gravity flow deposits. Similar, but less prolific petroleum reservoirs occur in Permian deep-water carbonate turbidites and debris flow base-of-slope deposits in the Delaware and Midland Basins, West Texas (Figures 59, 60) (; Cook and others, 1972; Cook, 1983; Cook and Mullins, 1983; Cook and others, 1983; Mazzullo, 1984; Hobson and others, 1985).

In the giant Cretaceous Poza Rica oil field of Mexico porosity includes some primary intergranular pores, but secondary molds of rudist skeletons are the most important type. Deep down dip circulation of fresh water from the exposed Golden Lane escarpment with its well-developed Cretaceous cave system is suggested as the process producing the extensive secondary porosity (Enos and Moore, 1983).

In the Permian Basin examples of west Texas and southeast New Mexico (Figures 59, 60), most of the reservoir porosity is of post-depositional origin, including solution interparticle, solution biomoldic, fracture, and solution fracture (Cook, 1983; Cook and Mullins, 1983; Cook and others, 1983).

In some deep-water slope and basin-margin settings lead-zinc sulfides occur in association with conglomeratic debris flows and submarine slides. For example, lead-zinc sulfides were deposited during the Devonian in the locality of the Jason prospect, Yukon Territory (Winn and others, 1981). Galena and sphalerite precipitated on the sea floor from exhalative fluids along the fault margin of a small graben. The geothermal systems are interpreted to have been driven by high heat flow associated with extensional tectonic regimes.

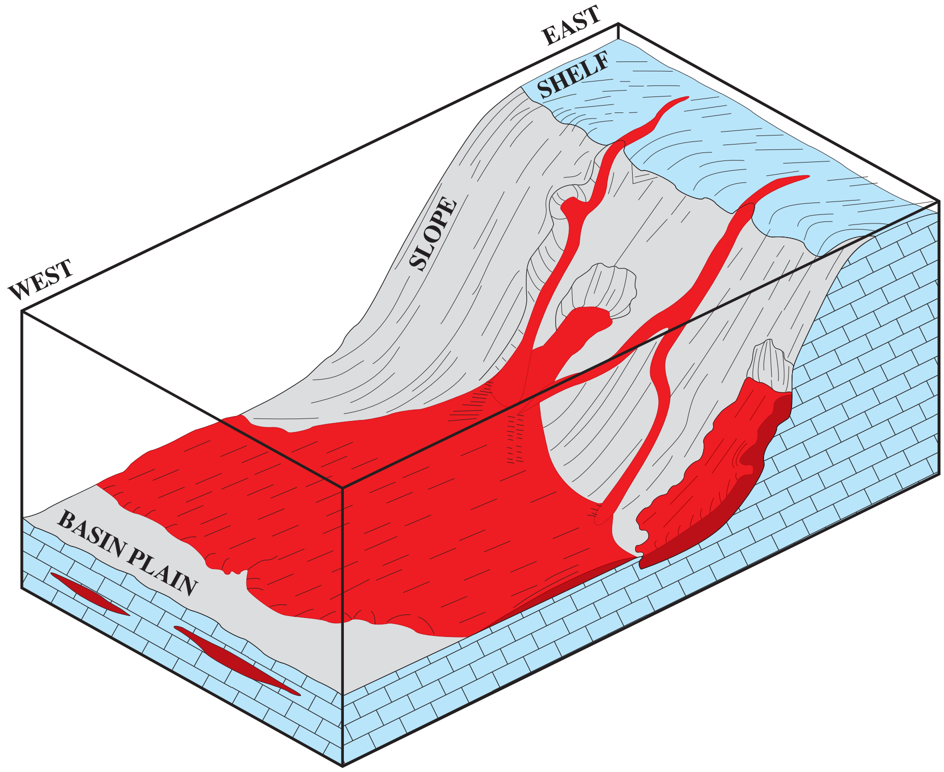

Figure 55. Model of interpreted shelf-slope basin plain transition in the Late Cambrian and Early Ordovician of Nevada. Model shows slope incised by numerous gullies but no major canyons; carbonate submarine fan develops at base of slope and basin plain; fan sediment is a mixture of shoal-water shelf carbonates and deeper water slide generated debris; contour currents flow northerly along upper slope (Cook and Egbert, 1981b).

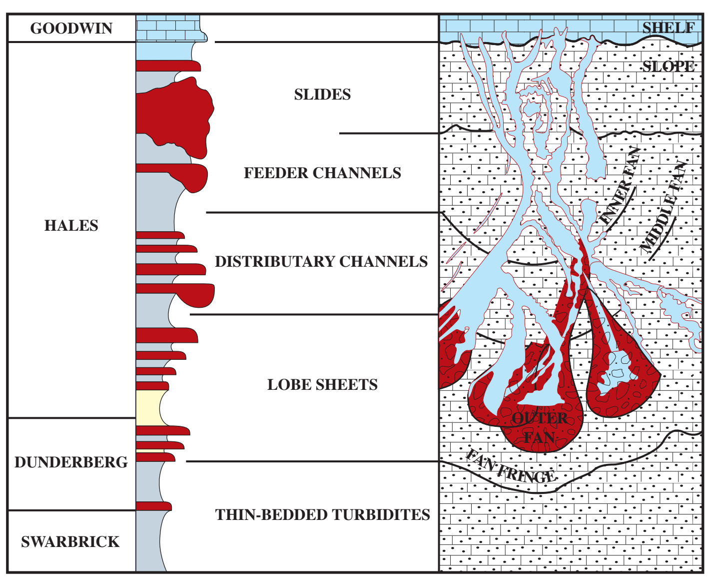

Figure 56. Carbonate submarine fan model showing that fan sediment is derived from both shoal-water shelf areas and by remolding of deeper water slides and slumps into mass-flows, large slides and channelized conglomerates that occur in outer fan region, calcarenites in non-channelized sheets in mid-fan sites, and thin-bedded silt-size to fine, sand-size bioclastic carbonate turbidites in fan fringe and basin plain. Slope and fan facies approximately 500 meters thick and basin plain facies approximately 1000 meters thick. Model based on studies in Cambrian and Ordovician strata in Nevada. (Modified from Cook and Egbert, 1981b).

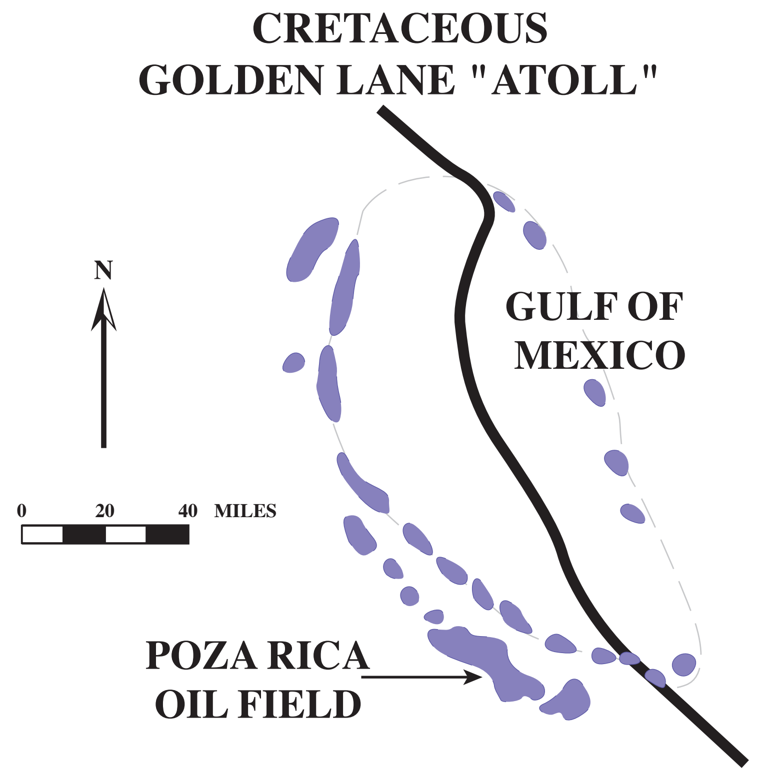

Figure 57. Location of the Cretaceous Poza Rica trend solid black and the adjacent Golden Lane fields, Veracruz, Mexico (Modified from Enos, 1977).

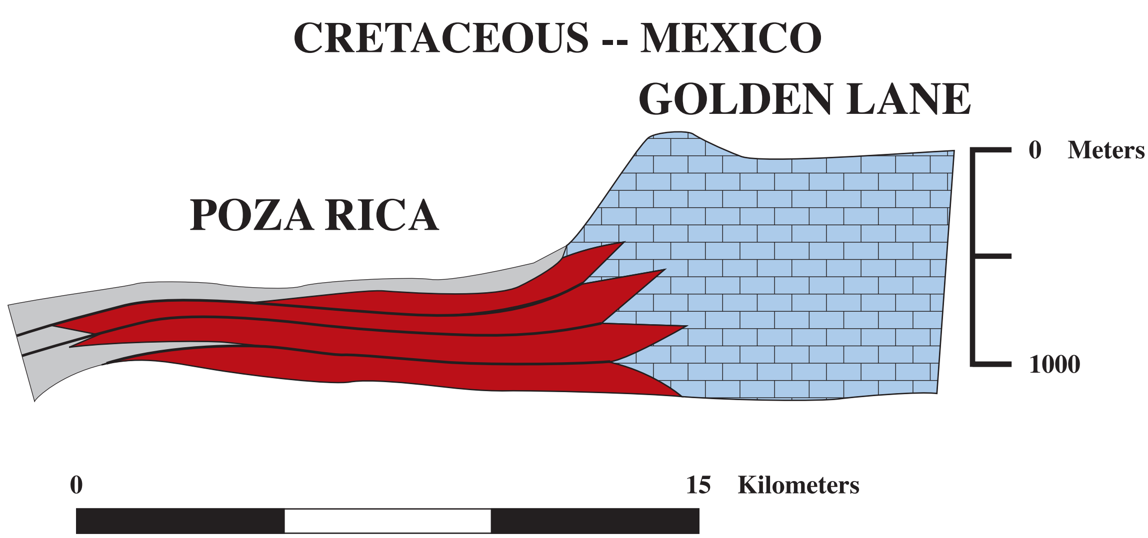

Figure 58. Interpretive cross-section from Cretaceous Poza Rica Field to Golden Lane, Veracruz, Mexico (Modified from Enos, 1977).

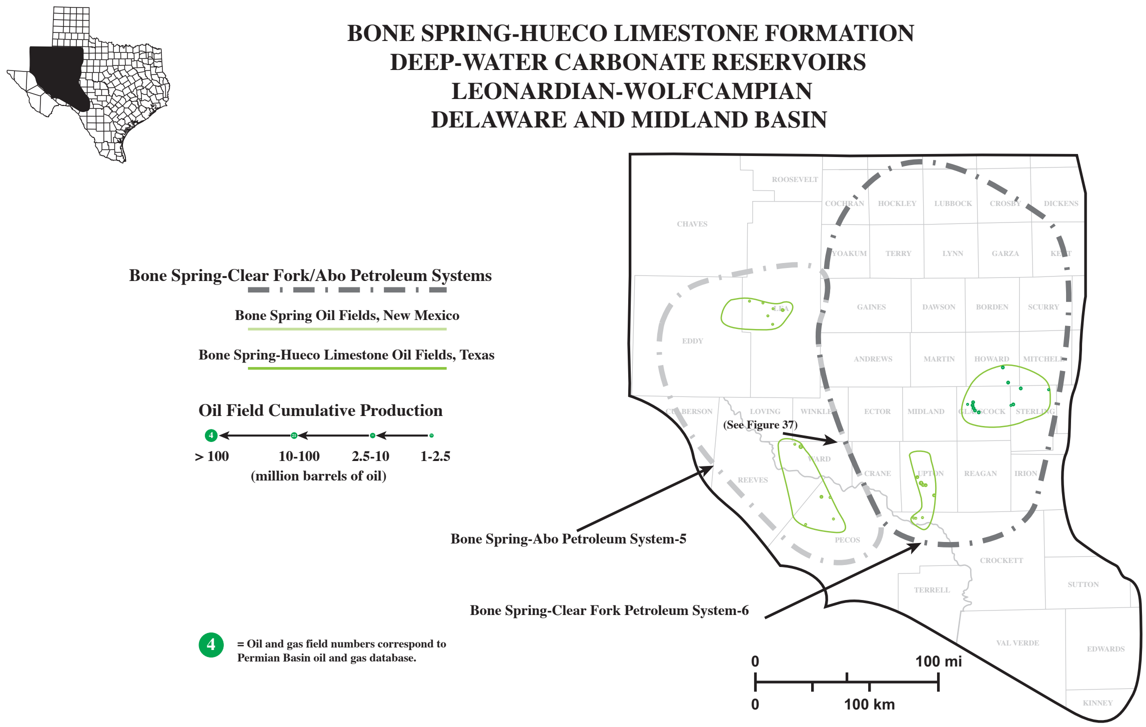

Figure 59. Location of Leonard-Wolfcamp (Lower Permian) basin margin petroleum fields, whose resevoir facies are in shoal-water derived carbonate turbidites (Modified from Cook, 1983; Dutton and others, 2001).

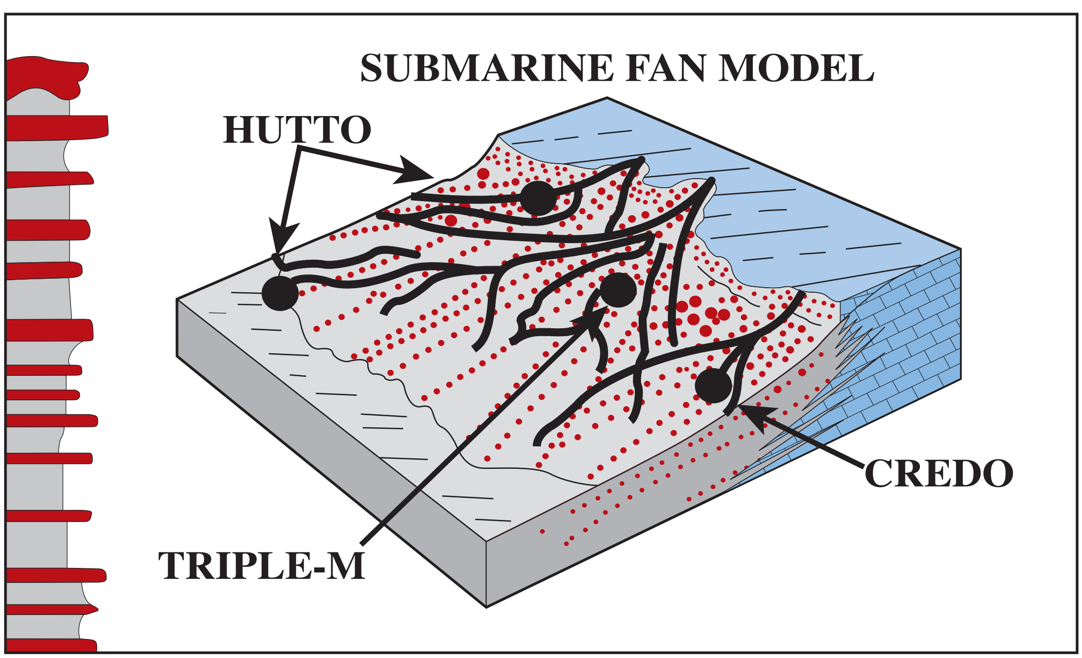

Figure 60. Interpretive of core and log data from Wolfcamp (Lower Permian) carbonate turbidite and debris flow deposits in Hutto, Triple M, and Credo oil fields in Midland Basin, west Texas (Modified from Cook, 1983).

Photo 5-4a. Hales Limestone. Upward-thickening outer fan turbidite lobe facies. Base-of-slope to inner basin. Stop 5-4. Tybo Canyon, Hot Creek Range, Nevada.

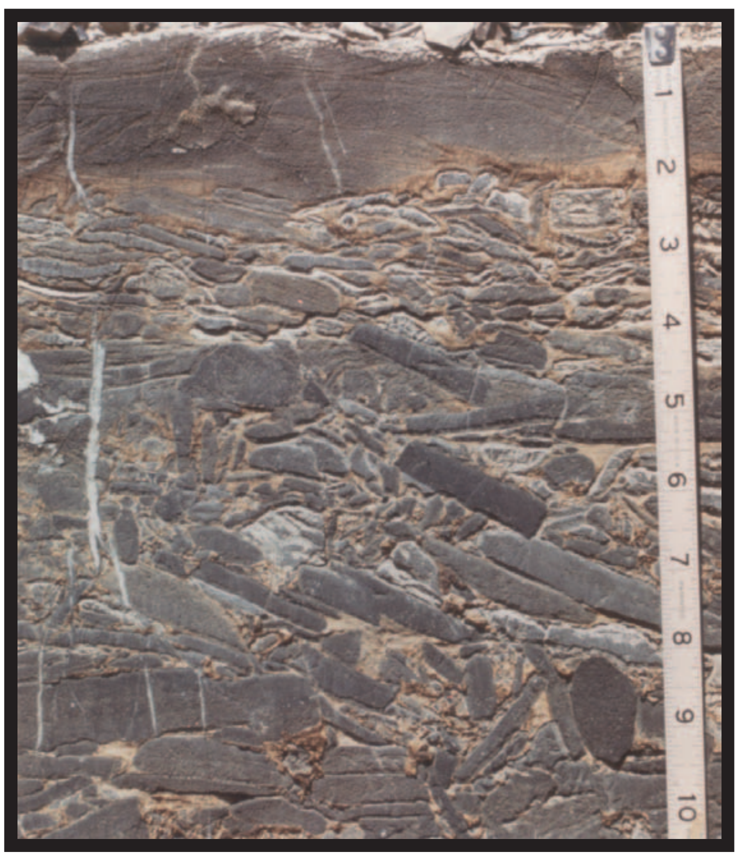

Photo 5-4b. Hales Limestone. Part of mid-fan distributary channel system. Clasts are normally graded, imbricated in an upslope direction. Rippled carbonate packstones and grainstones cap the bed. Base-of-slope to inner basin. Stop 5-4. Tybo Canyon, Hot Creek Range, Nevada.

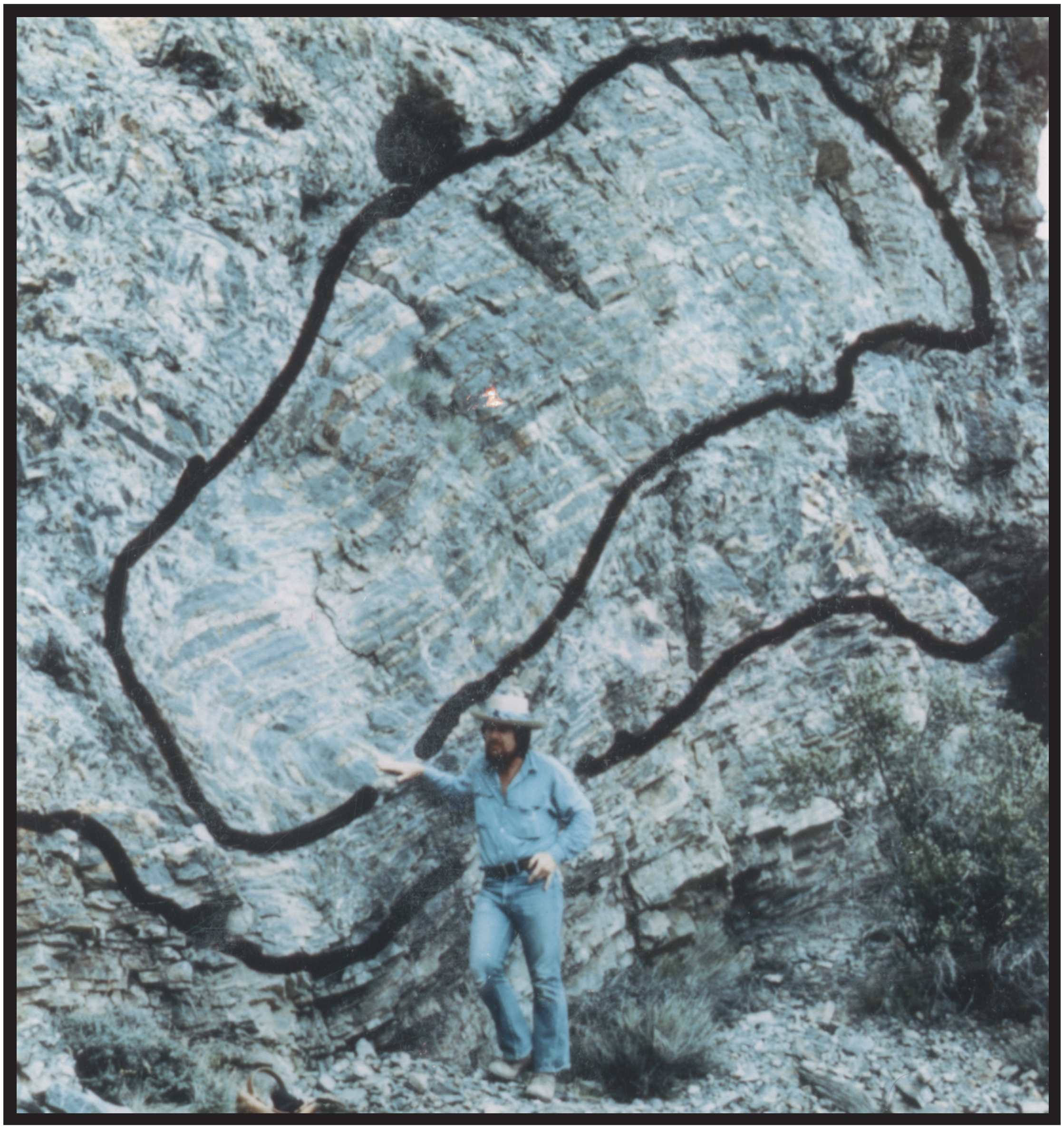

Photo 5-4c. Hales Limestone. Inner feeder fan channel. Large clast is 3 x 15 meters in cross-section. Channel is 15 meters deep and 400 meters wide. Base-of-slope. Stop 5-4. Tybo Canyon, Hot Creek Range, Nevada.

Photo 5-4d. Hales Limestone. Translational soft-sediment slide. Slide is 10 meters thick and 400 meters wide. Base-of-slope. Stop 5-4. Tybo Canyon, Hot Creek Range, Nevada.

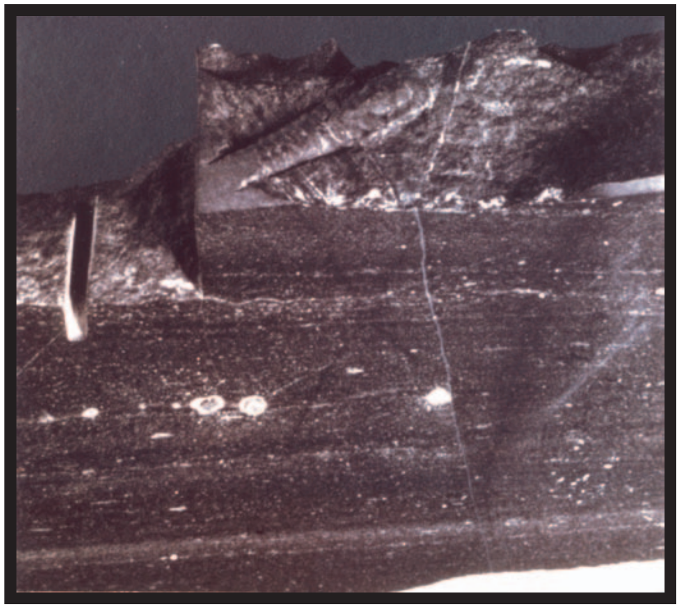

Photo 5-4e. Hales Limestone. In-situ slope lime mudstones with deep water *Hedanaspis* trilobite. Stop 5-4. Tybo Canyon, Hot Creek Range, Nevada.

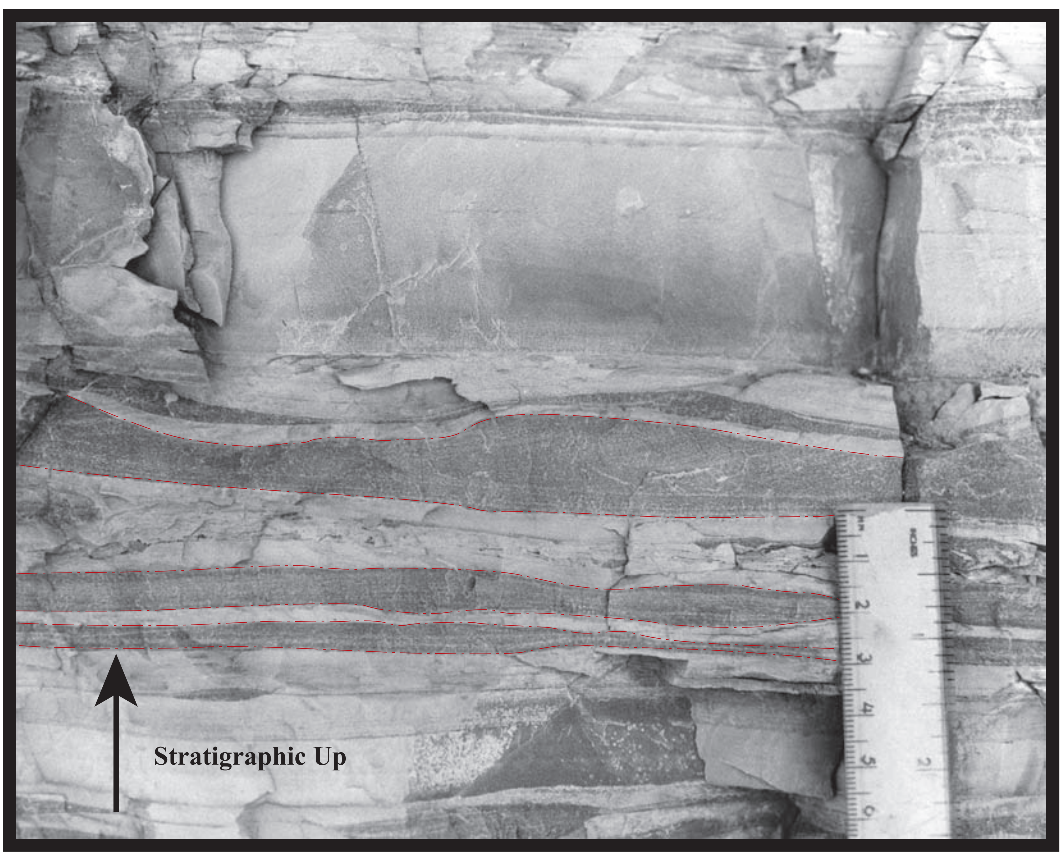

Photo 5-4f. Hales Limestone. Contourite grainstones (dark grey beds; enclosed in red). Composed of well-sorted, shallow-water derived alga *Nuia* grains. Flow direction to left (northwest), parallel to the strike of the Late Cambrian-Early Ordovician continental margin slope. Upper slope. Stop 5-4. Tybo Canyon, Hot Creek Range, Nevada.

Map 13. Location of Stop 5-5 on the Hobble Canyon Quadrangle, Hot Creek Canyon, Nevada.

STOP 5-5 – OVERVIEW OF HOT CREEK RANGE, NEVADA

Age – Lower Ordovician through Lower Devonian.

Formations – Antelope Valley Limestone (Pogonip Group), Copenhagen Formation, Eureka Quartzite, Hansen Creek Formation, Roberts Mountains Formation, and Lone Mountain Dolomite.

Carbonate Depositional Sequences (Figure 2) – Here we can see Sequences #2, #3, #4, and #5.

Depositional Environments – This well exposed canyon section records several fluctuations in sea level during the Paleozoic (Cook and others, 1983, Figure 5-32). The Antelope Valley and overlying Copenhagen (Sequence #2) probably formed in low energy, muddy, middle shelf environments. The overlying Upper Ordovician Eureka Quartzite (Sequence #3) formed during a relative sea level lowering that allowed quartz sands to prograde seaward over vast areas of the former carbonate continental margin. The upper surface of the Eureka Quartzite is eroded and represents the base of Sequence # 4. During the formation of the lowstand systems tract of Sequence #4, locally in the Hot Creek Range, parts of the Eureka Quartzite were totally removed such that the Hansen Creek formation rests directly on the Antelope Valley Formation (Cook, 1966). This was followed by a relative rise in sea level during which the Hansen Creek (Sequence #4) shoal-water carbonate banks became established on low angle ramps. A rapid rise in sea level inundated the Hansen Creek carbonate shoals thus causing the shelf edge to retrograde and establishing the deeper-water basinal to slope setting for the Roberts Mountains Formation. Here we can also see, as at Stop 5-1, the shoaling upward and seaward progradation of the Roberts Mountains Formation and the overlying Lone Mountain Dolomite (Sequence #5).

Economic Considerations –Hofstra and others (1999) describes disseminated gold deposits at Jerritt Canyon deposit that occur in the Hansen Creek-Roberts Mountains interval (Raines and others, 1991).

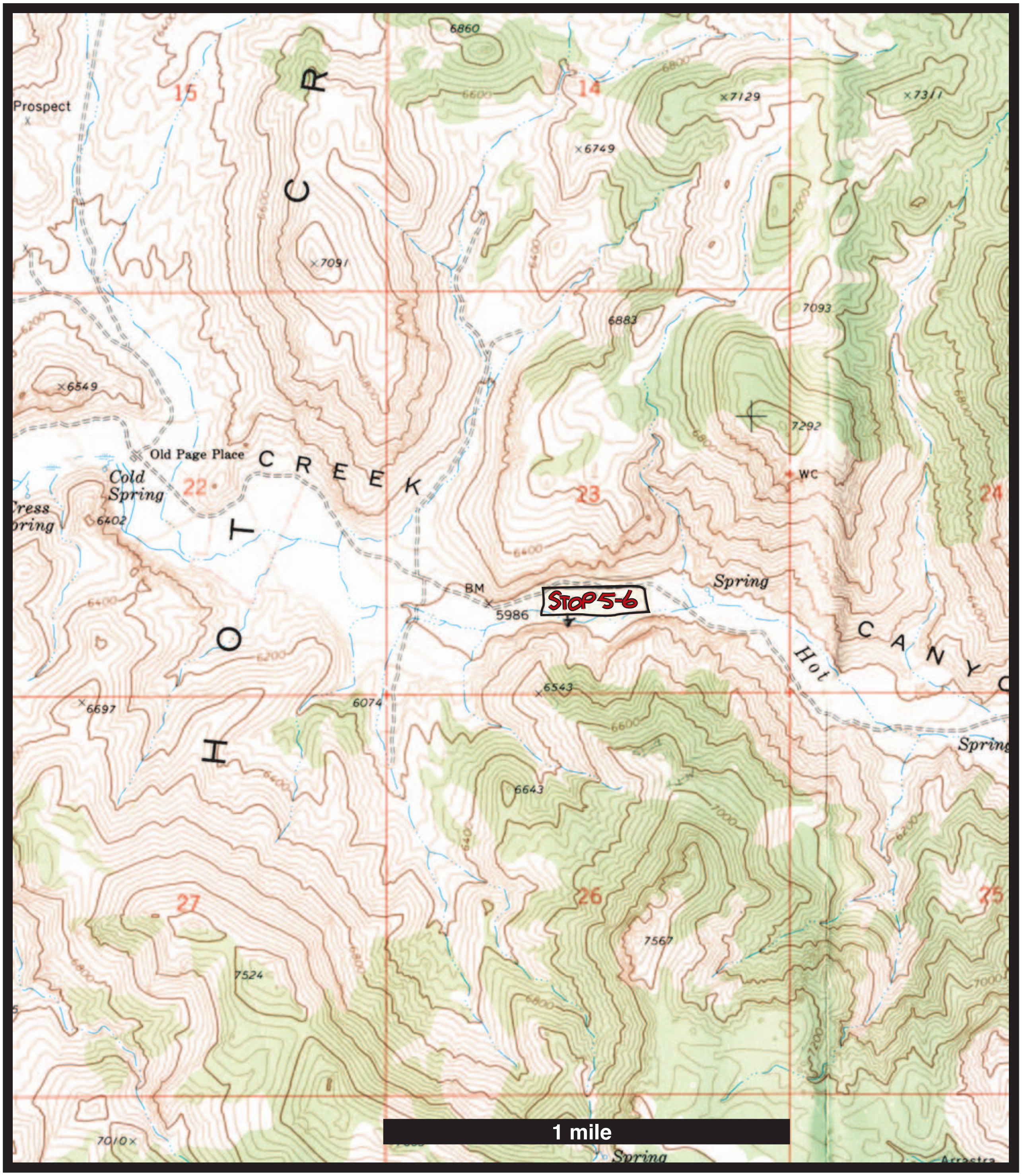

Map 14. Location of Stop 5-6 on the Little Fish Lake Quadrangle, Hot Creek Canyon, Nevada.

STOP 5-6 – HOT CREEK CANYON, HOT CREEK RANGE, NEVADA

Age – Lower-Middle Devonian.

Formations – Beacon Peak, Dolomite, McColley Canyon Limestone (Kobeh, Bartine and Coils Creek members), Denay Limestone, Bay State Dolomite, and Chainman Shale. The member names Kobeh, Bartine, and Coils Creek are provisionally used at this location, as is the name Bay State Dolomite. The assignment of these names is based on their stratigraphic position above the Lone Mountain dolomite, their probable age and their depositional facies characteristics to known occurrences of these stratigraphic units. The presence of abundant two-holed crinoids in Coils Creek (?) debris flows and turbidites suggests that these debris flows and turbidites were derived from the two-hole crinoid meadows of the Sadler Ranch Formation (Kendall and others, 1983, their figures 2 and 6).

Carbonate Depositional Sequences (Figure 2) – The following interpretations are provisional and are herein put forth as a working model. The Beacon Peak Dolomite and Kobeh Member of the McColley Canyon Limestone is interpreted to represent the highstand systems tract of Sequence #6. The Bartine represents the transgressive systems tract and highstand systems tract of Sequence #7. The lower part of the Coils Creek Member is interpreted to be a lowstand systems tract of Sequence # 8 and contains abundant carbonate turbidites and debris flow deposits, which are comprised of large amounts of two-hole crinoids. These two-hole crinoids were derived from the coeval upslope Sadler Ranch Member and transported downslope into base-of-slope settings. Denay Limestone is considered to represent a transgressive systems tract of Sequence # 9. The Bay State Dolomite is the highstand systems tract of Sequence # 9.

Depositional Environments (Figure 61) – The lower resistant ledge on the south side of Hot Creek Canyon is considered to be the Kobeh Member the McColley Canyon Limestone. It is interpreted by McGovney (1977) to have formed in a "subtidal, quiet water, dysaerobic environment in which sediment was strongly reworked by soft-body organisms". The sediments are dolomitized peloid wackestones and may have occupied a low energy shelf edge to middle shelf setting. Colonial coral heads can be found in this unit. A few hundred meters on the north side of Hot Creek Canyon the Beacon Peak Dolomite can be seen to lie stratigraphically beneath the Kobeh.

The contact between the Kobeh and the overlying Bartine is an abrupt sequence boundary and reflects a rapid relative rise in sea level that led to the drowning and back-stepping of the Kobeh (Figure 2). Basal Bartine rocks are organic rich, argillaceous lime mudstones and thin-bedded crinoid turbidites. Coils Creek beds are comprised of thick-bedded coral-crinoid turbidites, and debris flows arranged in thickening upward sequences (Cook and others, 1983; Figures 5-97, 5-98, 5-99). These thickening-upward debris flow deposits are interpreted to represent the base-of-slope carbonate aprons (Cook and others, 1983) of Sequence # 8 lowstand systems tract. The contact between the Coils Creek and overlying Denay is poorly defined at this time and requires further field work and dating. However, the Denay (Sequence # 9, Figure 2) contains debris flows, turbidites and occasional submarine slumps. Near the top of the section are dolomitized coral and hemispherical stromatoporoid wackestones and packstones, and dolomitized pelmatozoan and oolite (?) sands that represent a relatively high-energy platform margin bank facies of the Bay State Dolomite. These Bay State facies are coeval with parts of the Denay and formed as part of a highstand systems tract of Sequence # 9. These platform margin carbonates are in sharp contrast with the overlying Chainman Shale. The Bay State Dolomite at this locality is in erosional contact with the Chainman Shale. For diagrammatic purposes Figure 2 does not show the contact between the Bay State and Chainman.

The presence of a Bay State shoal-water platform margin facies establishes a paleogeographic position for the platform margin during the Middle Devonian in this part of the Great Basin.

Chief Features to be Observed –

<u>Kobeh Member of the McColley Canyon Limestone</u>:

1. Dolomitized peloid wackestones with colonial corals (shallow subtidal middle shelf).

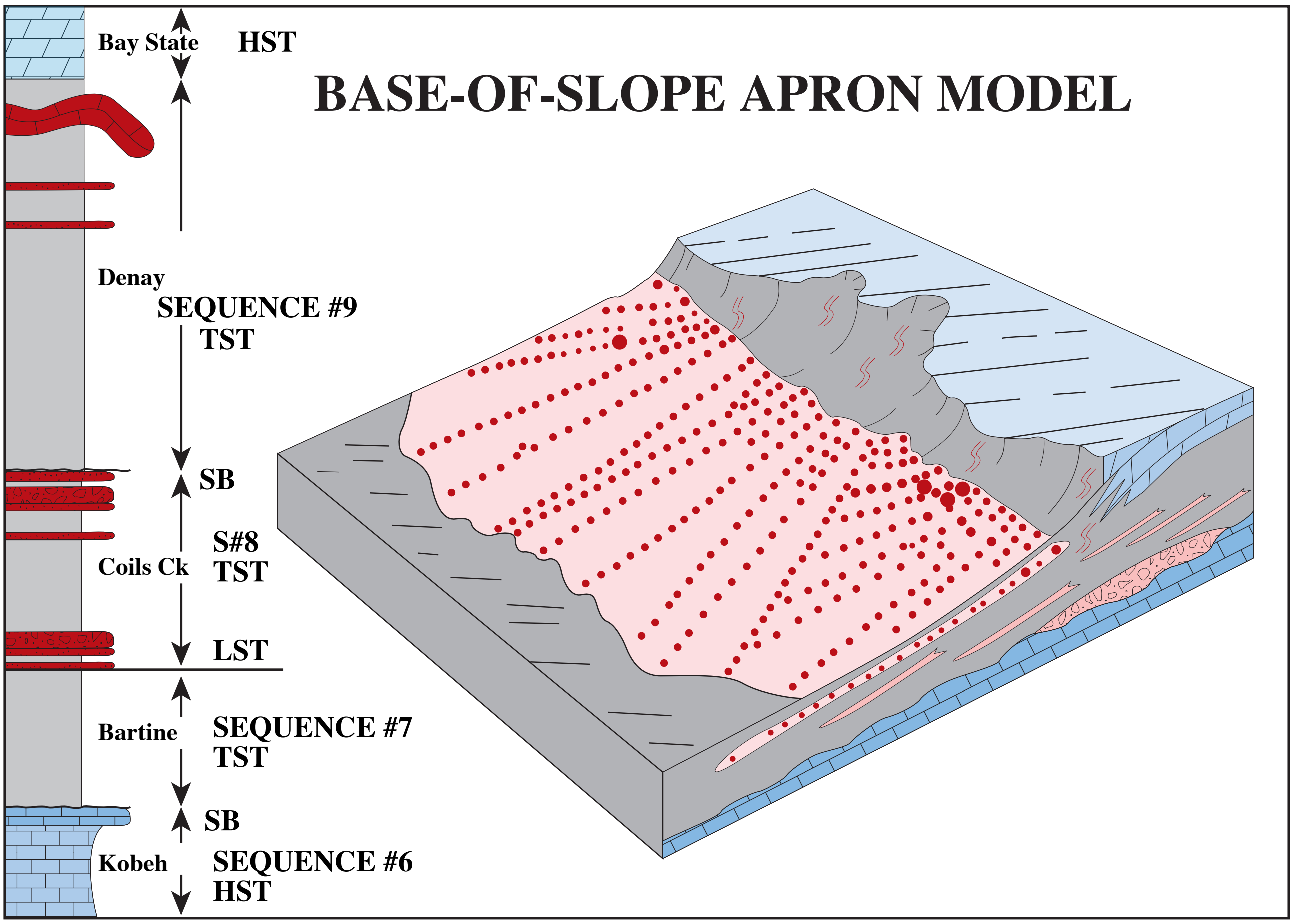

Figure 61. Provisional interpretation for stratigraphic section at Stop 5-6. Section illustrates the difficulty in placing sequence boundaries within basinal and slope settings such as the interpreted sequence boundaries between the proposed Bartine, Coils Creek, and the overlying Denay Limestone. These interpretations serve as a model to test and refine.

Bartine and Coils Creek members of the McColley Canyon Limestone and Denay Limestone:

1. Argillaceous lime mudstones with abundant Tentaculites; some black calcareous shales have up to about 2.0% total organic carbon; petroliferous odor on fresh surface (basin-plain setting).
2. Thickening upward sequence, about 10-15 meters thick, that consists of a variety of sediment gravity flow deposits some with shoal-water derived coral heads up to 50 cm across; abundant two-hole crinoids in mass-flow deposits; paleocurrents trend westerly.
3. Soft sediment slumping.
4. Thin-bedded channelized carbonate turbidites containing stromatoporoid clasts on upper slope settings near platform margin.

Bay State Dolomite:

1. Dolomitized colonial coral and stromatoporoid wackestones to packstone.
2. Dolomitized bioclastic grainstones; petroliferous odor on fresh surface.

Chainman Shale:

1. Argillaceous siltstone and siliciclastic facies.

Economic Considerations – The lowstand systems tract, base-of-slope debris apron facies in the Denay Limestone could offer petroleum and mineral exploration possibilities. If sufficient porosity is retained or enhanced these types of facies probably pinch out in an upslope direction thereby developing updip seals against lime mudstone slope facies. The source potential of these basin-plain and slope calcareous shales and argillaceous lime mudstones is not known but some of the potential source rock facies have total organic values of 1 to 2 percent. These types of redeposited shoal-water carbonates strongly resemble similar deep-water reservoir facies in the Permian Basin of west Texas (Cook, 1983; Cook and others, 1983; Mazzullo, 1984; Hobson and others, 1985) and elsewhere.

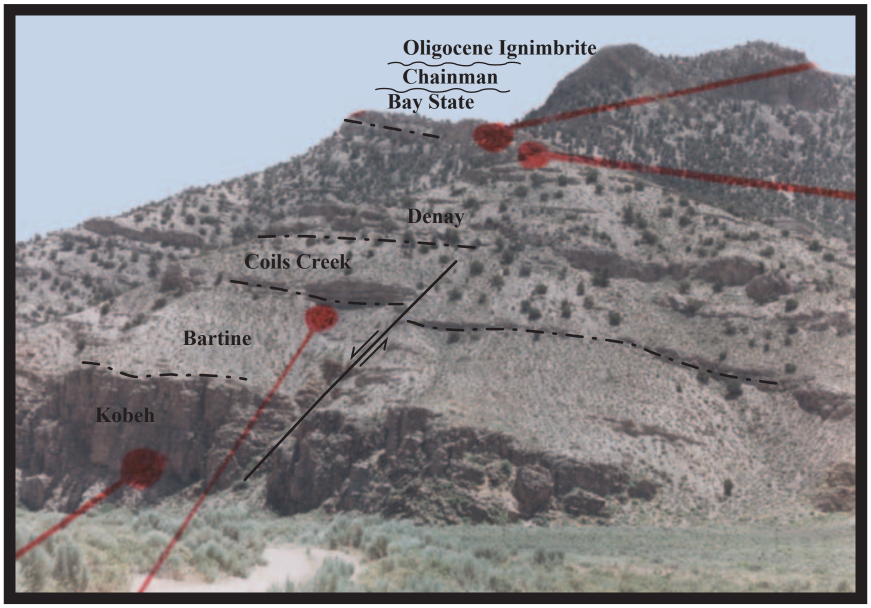

Photo 5-6a. The stratigraphic units labelled on this photo are provisional and subject to more fieldwork and age-dating. Stop 5-6. Hot Creek Canyon, Hot Creek Range, Nevada.

Photo 5-6b. Kobeh Member of the McColley Canyon Formation. Dolomitized middle platform facies. Stop 5-6. Hot Creek Canyon, Hot Creek Range, Nevada.

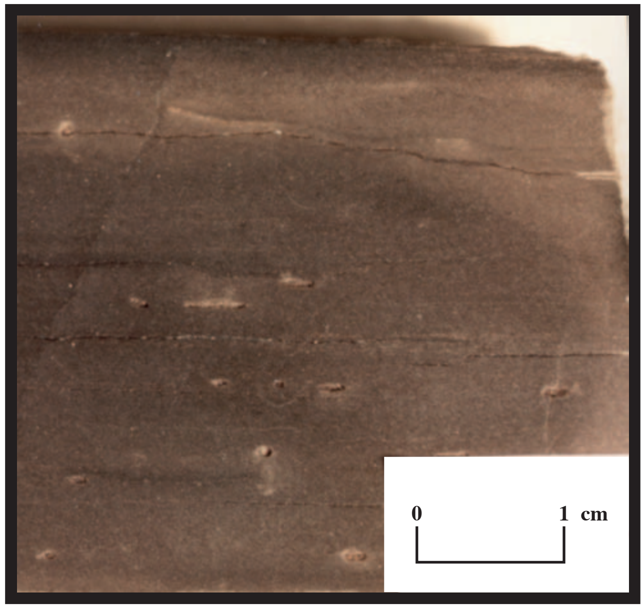

Photo 5-6c. Bartine Member of the McColley Canyon Formation. Laminated argillaceous organic-rich lime muds in basinal setting. Stop 5-6. Hot Creek Canyon, Hot Creek Range, Nevada.

Photo 5-6d. Coils Creek Member of the McColley Canyon Formation. Carbonate debris flow deposits with abundant two-hole crinoids and large colonial coral heads. Base-of-slope. Stop 5-6. Hot Creek Canyon, Hot Creek Range, Nevada.

Photo 5-6e. Coils Creek Member of the McColley Canyon Formation. Massive colonial coral head in debris flow bed in Photo 5-6d. Base-of-slope. Stop 5-6. Hot Creek Canyon, Hot Creek Range, Nevada.

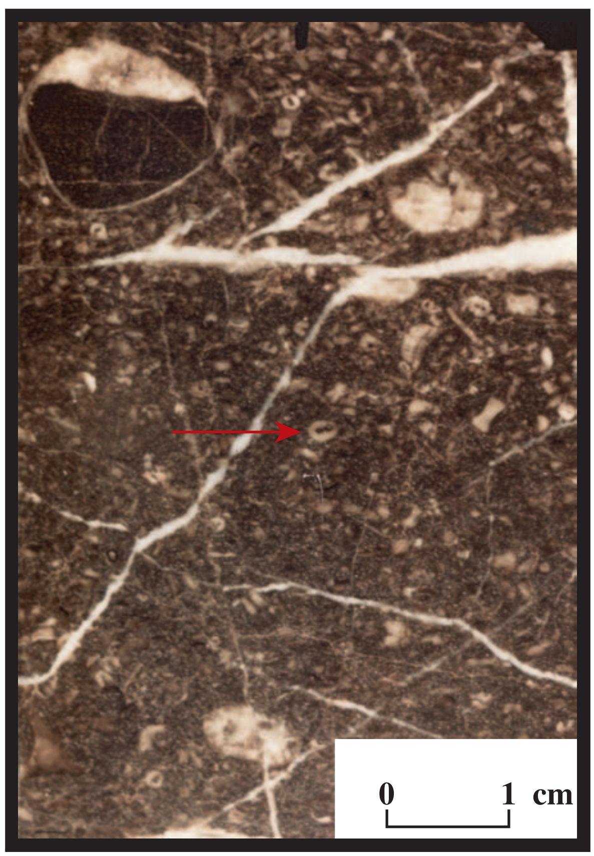

Photo 5-6f. Coils Creek Member of the McColley Canyon Formation. Matrix of debris flow shown in Photos 5-6d and 5-6e. Contains two-hole crinoids (see red arrow) which are common in the coeval platform margin, Sadler Ranch Formation (See Figure 2). Base-of-slope. Stop 5-6. Hot Creek Canyon, Hot Creek Range, Nevada.

Photo 5-6g. Denay Limestone. Soft-sediment folds on upper slope. Stop 5-6. Hot Creek Canyon, Hot Creek Range, Nevada.

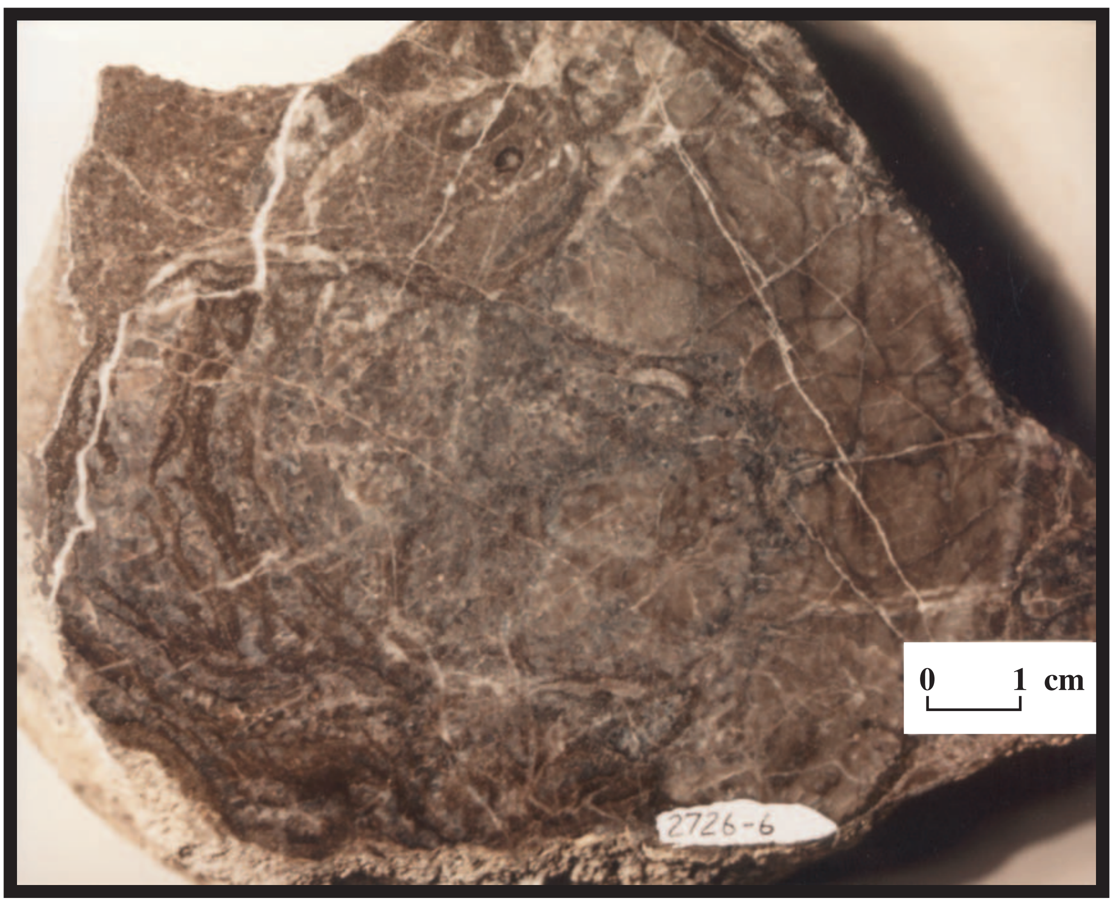

Photo 5-6h. Denay Limestone. Stomatoporoid clast from carbonate debris flow on upper slope near platform margin. Stop 5-6. Hot Creek Canyon, Hot Creek Range, Nevada.

Photo 5-6i. Bay State Dolomite. Dolomitized in-situ colonial coral (Syringoporella ?) in a packstone matrix. Platform margin. Stop 5-6. Hot Creek Canyon, Hot Creek Range, Nevada.

Photo 5-6j. Bay State Dolomite. Dolomitized ooid (?)-bioclastic grainstone shoal at platform margin. Stop 5-6. Hot Creek Canyon, Hot Creek Range, Nevada.

REFERENCES

Aalto, K. R., 1971, Glacial marine sedimentation and stratigraphy of the Toby Conglomerate (upper Proterozoic) southeastern British Columbia, northwestern Idaho, and northeastern Washington: Can. Jour. Earth Sci., v. 8, p. 753-787.

Ahr, W.M., Carbonate Ramp: alternative to Shelf Model: AAPG Bulletin vol.57, p. 1826.

Ainsworth, J.C., 1984, Stratigraphic controls on alteration at the Alligator Ridge gold mine near Ely, Nevada (abs.): GSA Abstracts, v. 16,p. 265.

Armstrong, A. K., Theodore, T.G., Oscarson, R.L, Kotlyar, B.B., Harris, A.G., Bettles, K.H., Lauha, E. A., Hipsley, R. A., Griffin, G. L., Abbott, E. W., and J. L. Cluer, 1998, Preliminary facies analysis of Silurian and Devonian autochthonous rocks that host gold along the Carlin Trend, Nevada: Open-File Report - U. S. Geological Survey, Report: OF 98-0338-B, pp.38-68.

Armstrong, R. L., 1968, Sevier orogenic belt in Nevada and Utah: GSA Bulletin v. 79, p. 429-458.

Atwater, T., and Molnar, P., 1973, Relative motion of the Pacific and North American plates deduced from sea-floor spreading in the Atlantic, Indian, and South Pacific Oceans, *in* R. L. Kovach and A. Nur, eds., Proceedings of the conference on tectonic problems of the San Andreas fault system: Stanford Univ. Pub. Geol. Sci., v. 13, p. 136-148.

Badham, J. P. N., 1978, Has there been an oceanic margin to western North America since Archean time?: Geology, v. 6, p. 621-625.

Blake, M. C., Jr., 1975, Nature and controls of Cordilleran orogenesis, western United States: Extensions of an earlier synthesis, *in* J. H. Ostrom, and P. M. Orville, eds., Tectonics and mountain ranges: Am. Jour. Sci. (Rogers Volume), v. 275-A, p. 363-396.

Blake, M. C., Jr., 1981, Mojave Desert and environs, in W. G. Ernst, ed., The geotectonic tectonic development of California: New Jersey, Prentice-Hall, Inc., p. 217-252.

Blake, M. C., Jr., Howell, D. G., and Jones, D. L., 1982, Preliminary tectono-stratigraphic terrane map of California: U.S. Geol. Survey Open-File Report 82-593, 10 p.

Brown, L. F. and Fisher, W. L., 1977, Seismic-stratigraphic interpretation of depositional systems: examples from Brazilian rift and pull-apart basins, *in* C. E. Payton, ed., Seismic Stratigraphy—applications to hydrocarbon exploration: AAPG Memoir 26, p. 213-248.

Browne, J. R., 1961, Mining Adventures, California and Nevada / 1863-1865: Pasano Press, Balboa Island, California, 207 p.

Burchfiel, B. C., and Davis, G. A., 1972, Structural framework and evolution of the southern part of the Cordilleran orogen, western United States: Am. Jour. Sci., v. 272, p. 97-118.

Burchfiel, B. C., Pelton, P. J., and Sutter, J., 1970, An early Mesozoic deformation belt in south-central Nevada—southeastern California: GSA Bulletin v. 81, p. 211-215.

Callahan, W. H., 1977, Some Thoughts Regarding Premises and Procedures for Prospecting for Base Metal Ores in Carbonate Rocks in the North American Cordillera: Econ. Geol., v. 72, p. 71-81.

Carden, J. R., 1991, The Discovery and Geology of the Nighthawk Ridge Deposit at Easy Junior, White Pine Country, Nevada, *in* G. L. Raines, R. E. Lisle, R. W. Shafer, and W. H. Wilkinson, eds., Geology and Ore Deposits of the Great Basin, Symposium Proceedings: Geological Society of Nevada, Reno, p. 665-676.

Choquette, P. W., and Pray, L. C., 1970, Geological nomenclature and classification of porosity in sedimentary carbonates: AAPG Bulletin v. 54, p. 207-250

Churkin, M., Jr., 1962, Facies across Paleozoic miogeosynclinal margin of central Idaho: AAPG Bulletin v. 46, p. 569-591.

Churkin, M., Jr., 1974, Paleozoic marginal ocean basin-volcanic arc systems in the Cordilleran foldbelt, *in* R. H. Dott, Jr., and R. H. Shaver (eds.), Ancient and modern geosynclinal sedimentation: SEPM Spec. Pub. 19, p. 174-192.

Coney, P. J., Jones, D. L., and Monger, J. W. H., 1980, Cordilleran suspect terranes: Nature, v. 288, p. 329-333.

Cook, E. F., 1960, Great Basin ignimbrites, in Intermountain Assoc. of Petrol. Geologists and Nev. Geol. Soc., Guidebook to the geology of east central Nevada, p. 134-140.

Cook, H. E., 1966, Geology of the southern part of the Hot Creek Range, Nevada: PhD Dissertation, University of California, Berkeley, 116 p.

Cook, H. E., 1968, Ignimbrite flows, plugs, and dikes in the southern part of the Hot Creek Range, Nye County, Nevada: in Studies In Volcanology: GSA Memoir 116, p. 107-152.

Cook, H. E., 1972, Miette platform evolution and relation to overlying bank ("reef") localization, Upper Devonian, Alberta: Can. Petrol. Geol. Bulletin v. 20, no. 3, p. 375-411.

Cook, H. E., 1977, Comparison of continental slope and shelf environments in the Upper Cambrian and lowest Ordovician of Nevada, *in* H.E. Cook, and P. Enos, eds., Deep-water Carbonate Environments: SEPM Spec. Pub. 25, p. 51-81.

Cook, H. E., 1979, Ancient continental slope sequences and their value in understanding modern slope development, *in* L. S. Doyle and O. H Pilkey, eds., Geology of continental slopes: SEPM Spec. Pub. 27, p. 287-305.

Cook, H. E., 1982, Carbonate submarine fans versus carbonate debris aprons: facies patterns, depositional processes, and models (abs.): GSA Bulletin v. 14, no. 7, p. 466-467.

Cook, H. E., 1983, Sedimentology of some allochthonous deep-water carbonate reservoirs, Lower Permian, west Texas: carbonate debris sheets, aprons, or submarine fans? (abs.): AAPG Bulletin v. 63, p. 442.

Cook, H. E., 1988, Overview: Geologic history and carbonate petroleum reservoirs of the Basin and Range Province, western United States, *in* S. M Goolsby and M. W. Longman, eds., Occurrence and petrophysical properties of carbonate reservoirs in the Rocky Mountain region: Rocky Mountain Association of Geologists Carbonate Symposium, p. 213-227.

Cook, H. E., 1993, Submarine carbonate breccia: Criteria for their recognition, depositional models, and their role in petroleum and hydrothermal mineral exploration, *in* C. L. William, ed., Northeastern Nevada breccia bodies: Geological Society of Nevada Symposium Proceedings, p. 1-7.

Cook, H.E., Alexeiev, D.V., Mikolaichuk, A.V., Dzhenchuraeva, A.V., Corboy, J.C., 2002a, Development of an isolated carbonate platform from an underlying attached platform: A newly discovered Devonian-Carboniferous carbonate platforms in the Tian Shan Mountains of Kyrgyzstan (abs.) 2002 AAPG Annual Convention, Official program, V. 11, p. A-34.

Cook, H. E., and Egbert, R. M., 1981a, Carbonate submarine fan facies along a Paleozoic prograding continental margin, western United States (abs.): AAPG Bulletin v. 65, p. 913.

Cook, H. E., and Egbert, R. M., 1981b, Late Cambrian-Early Ordovician continental margin sedimentation, *in* M. E. Taylor, Short papers for the Second International Symposium on the Cambrian System: U.S. Geological Survey Open-File Report 81-743, p. 50-56.

Cook, H. E., Hine, A. C., and Mullins, H. T., 1983, Platform margin and deep water carbonates: SEPM Short Course No. 12, 573 p.

Cook, H. E., McDaniel, P. N., Mountjoy, E. W., and Pray, L. C., 1972, Allochthonous carbonate debris flows at Devonian bank ("reef") margins, Alberta, Canada: Can. Petrol. Geol. Bulletin v. 20, p. 439-497.

Cook, H. E., and Mullins, H. T., 1983, Basin margin environment, *in* P. A. Scholle, D. G. Bebout, and C. H. Moore, eds., Carbonate Depositional Environments: AAPG Memoir 33, p. 540-617.

Cook, H. E., and Taylor, M. E., 1975, Early Paleozoic continental margin sedimentation, trilobite biofacies, and the thermocline western United States: Geology, v. 3, p. 559-562.

Cook, H. E., and Taylor, M. E., 1977, Comparison of continental slope and shelf environments in the Upper Cambrian and lowest Ordovician of Nevada, *in* Cook, H. E., and Enos, Paul, eds., Deep-water carbonate environments: SEPM Spec. Pub. 25, p. 51-81.

Cook H. E., Taylor, M. E., and Miller, J. F., 1989, Late Cambrian and Early Ordovician stratigraphy, biostratigraphy and depositional environments, Hot Creek Range, Nevada, *in* M. E. Taylor, ed., Cambrian and Early Ordovician stratigraphy and paleontology of the Basin and Range Province, western United States, Field Trip Guidebook T125 28th International Geological Congress, p. 28-36.

Cook, H. E., Zhemchuzhnikov, V. G., Zempolich, W. G., Lehmann, P. J., Buvtyshkin, V. M., Zhaimina, V. Ya., Kotova, E. A. Golub, L. Ya. , Zorin, A. Ye. , Alexeiev, D. V., Viaggi, M., Giovannelli, A., Lapointe, Ph. A., Fretwell, N., Bowman, M., De Coo, J. C. M., 2002b, Evolution of a Devonian and Carboniferous Carbonate Platform, Bolshoi Karatau, Southern Kazakhstan: Outcrop Analogs for Coeval Carbonate Reservoirs in the North Caspian Basin, *in* W. G. Zempolich and H. E. Cook (eds.), Carbonate Systems in the Commonwealth of Independent States (CIS): Comparative Studies of Outcrop and Subsurface Oil and Gas Reservoirs: SEPM Spec. Pub. 74, p. 83-124.

Crevello, P.D., Wilson, J.L., Sarg, J.F., and Read, J.F., 1989, Controls on Carbonate Platform and Basin Development, Based on a Symposium: SEPM Spec. Pub. 44, 405 p.

Dickinson, W. R., 1977, Paleozoic plate tectonics and the evolution of the Cordilleran continental margin, *in* J. H. Stewart, C. H. Stevens, and A. E. Fritsche, eds., Paleozoic Paleogeography the western United States, Pacific Coast Paleogeography Symposium 1: SEPM, Pacific Section, p. 137-155.

Dickinson, W. R., 1981, Plate tectonics and the continental margin of California, *in* W. G. Ernst, ed., The geotectonic development of California: New Jersey, Prentice-Hall, Inc., p. 1-28.

Dickinson, W. R., Beard, L. S., Brakenridge, G. R., Erjavec, J. L., Ferguson, R. C., Inman, K. F., Knepp, R. A., Lindberg, F. A., and Ryberg, P. T., 1983, Provenance of North American Phanerozoic sandstones in relation to tectonic setting: GSA Bulletin v. 94, p. 222-235.

Dietz, R. S., and Holden, J. C., 1966, Miogeoclines (miogeosynclines) in space and time: Jour. Geology, v. 74, p. 566-583.

Dorobek, S.L. and Ross, G.M., eds., 1995, Stratigraphic Evolution of Foreland Basins: SEPM Spec. Pub. 52, 310 p.

Dover, J. H., 1980, Status of the Antler orogeny in central Idaho-- Clarifications and constraints from the Pioneer Mountains, *in* T. D. Fouch, and E. R. Magathan, eds., Paleozoic paleogeography of the west-central United States Rocky Mountains Paleogeography Symposium 1: SEPM, Rocky Mountain Section, p. 371-386.

Dunham, J. B., 1977, Depositional environments and paleogeography of the Upper Ordovician, Lower Silurian carbonate platform of central Nevada, *in* J. H. Stewart, C. H. Stevens, and A. E. Fritsche, eds., Paleozoic Paleogeography of the Western United States, Pacific Coast Paleogeography Symposium 1: SEPM, Pacific Section, p. 157-180.

Dunham, R.J., 1962, Classification of carbonate rocks according to depositional texture, *in* W. E. Ham, ed., Classification of carbonate rocks, a symposium: AAPG Memoir 1, p. 108-121.

Eardley, A. J., 1947, Paleozoic Cordilleran geosyncline and related orogeny: Jour. Geology, v. 55, p. 309-342.

Eisbacher, G. H., 1983, Devonian-Mississippian sinistral transcurrent faulting along the cratonic margin of western North America: a hypothesis: Geology, v. 11, p. 7-10.

Elliot, R. R., 1966, Nevada's Twentieth-Century Mining Boom—Tonopah, Goldfield, and Ely: University of Nevada Press, Nevada, Reno, 344 p.

Emsbo, Poul, 2000, Gold in sedex deposits, SEG Reviews, v. 13, pp. 427-437.

Emsbo, Poul, 1999, Origin of the Meikle high-grade gold deposit from the superposition of Late Devonian sedex and mid-Tertiary carlin-type gold mineralization: PhD Dissertation, Colorado School of Mines, 379 p.

Emsbo, P., Hutchinson, R. W., Hofstra, A.H., Volk, J.A., Bettles, K.H., Baschuk, G.J., and Johnson, C.J., 1999, Syngenetic Au on the Carlin Trend: Implications for Carlin-type deposits: Geology, v. 27, p. 59-62.

Enos, P., 1977, Tamabra Limestone of the Poza Rica Trend, Cretaceous, Mexico, *in* H.E. Cook and P. Enos, eds., Deep-water carbonate environments: SEPM Spec. Pub. 25, p. 273-314.

Enos, P., 1983, Shelf environment, *in* P. A. Scholle, D. G. Bebout, and C. H. Moore, eds., Carbonate Depositional Environments: AAPG Memoir 33, p. 268-295.

Enos, P., and Moore, C. H., 1983, Fore-reef slope environment, in P. A. Scholle, D. G. Bebout, and C. H. Moore, eds., Carbonate Depositional Environments: AAPG Memoir 33, p. 508-537.

Esteban, M., and Klappa, C. F., 1983, Subaerial exposure environment, in P. A. Scholle, D. G. Bebout, and C. H. Moore, eds., Carbonate Depositional Environments: AAPG Memoir 33, p. 2-92.

Ferguson, H. G., 1924, Geology and ore deposits of the Manhattan District, Nevada: U.S. Geol. Survey Bulletin 723.

Ferguson, H. G., and Cathcart, S. H., 1924, Major structural features of some western Nevada ranges: Jour. Washington Acad. Sci., v. 14, p. 376-379.

Fischer, A. G., and Arthur, M. A., Secular variations in the pelagic realm, in H.E. Cook, and P. Enos, eds., Deep-water Carbonate Environments: SEPM Special Publication 25, p 19-50.

Giles, K. A. and Dickinson, W. R., 1995, The interplay of eustacy and lithospheric flexure in forming stratigraphic sequences in foreland settings: an example from the Antler foreland, Nevada and Utah, *in* S.L. Dorobek and G.M. Ross, eds., Stratigraphic Evolution of Foreland Basins: SEPM Spec. Pub. 52, p. 187-211.

Ginsburg, R. N., and James, N. P., 1974, Holocene carbonate sediments of continental shelves, *in* C. A. Burke and C. L. Drake, eds., The Geology of Continental Margins: New York, N.Y., Springer-Verlag, p. 137-155.

Gutschick, R. C., Sandberg, C. A, and Sando, W. J., 1980, Mississippian Shelf Margin and Carbonate Platform From Montana to Nevada, *in* T. D. Fouch, and E. Magathan, eds., Paleozoic Paleogeography of west central United States, Rocky Mountain Paleogeography Symposium 1: SEPM, Rocky Mountain Section, p. 111-128.

Hague, A., 1982, Geology of the Eureka District, Nevada: U.S. Geological Survey Mon. 20, 419 p.

Halley, R. B., Harris, P. M., and Hine, A. C., 1983, Bank Margin, in P. A. Scholle, D.G., Bebout, and C. H. Moore, eds., Carbonate Depositional Environments: AAPG Memoir 33, p. 464-506.

Handford, C. R., and Loucks, R. G., 1993, Carbonate depositional sequences and systems tracts—Responses of carbonate platforms to relative sea-level changes, *in* R.J. Loucks and J.F. Sarg, eds., Carbonate Sequence Stratigraphy, AAPG Memoir 57, p. 3-41.

Haq, B. U., and Eysinga, F. W. B. Van, 1998, Geologic time table, Elsevier Science B.V.
Harbaugh, D. W., and Dickinson, W. R., 1981, Depositional facies of Mississippian clastics, Antler foreland basin, Central Diamond Range, Nevada: Jour. of Sedimentary Petrology, v. 51, p. 1223-1234.
Harris, P. M., ed., 1983, Carbonate buildups: a core workshop: SEPM Core Workshop No. 4, 591 p.
Harris, P. M., Saller, A. H., and Simo, J. A. T., 1999, Advances in Carbonate Sequence Stratigraphy: Applications to Reservoirs, Outcrops, and Models: SEPM Spec. Pub. 63, p. 421.
Harrison, J. E., Griggs, A. B., and Wells, J. D., 1974, Tectonic features of the Precambrian Belt basin and their influence on post-Belt structures: U.S. Geol. Survey Prof. Paper 866, 15 p.
Hays, R.C. and Foo, S. T., 1991, Geology and Mineralization of the Gold Acres Deposit, Lander County, Nevada, *in* G. L. Raines, R. E. Lisle, R. W. Shafer, and W. H. Wilkinson, eds., Geology and Ore Deposits of the Great Basin, Symposium Proceedings: Geological Society of Nevada, Reno, p. 677-685.
Hobson, J. P., Caldwell, C. D., and Toomey, D. F., 1985, Early Permian deep-water allochthonous limestone facies and reservoir, West Texas: AAPG Bulletin v. 69, p. 2130-2147.
Hofstra, A. H., Snee, L. W., Rye, R. O., Folger, H. W., Phinisey, R. J., Loranger, R. J., Dahl, A. R., Naeser, C. W., Stein, H. J., and M. Lewchuk, 1999, Age Constraints on Jerritt Canyon and other Carlin-Type Gold Deposits in the Western United States--- Relationship to Mid-Tertiary Extension and Magmatism, Economic Geology Bulletin v. 94, p. 769-802.
Hofstra, A.H. and Cline, J.S., 2000, Characteristics and Models for Carlin-Type Gold Deposits, SEG Reviews, v. 13, p. 163-220.
Hose, R. K., 1966, Devonian stratigraphy of the Confusion Range, west central Utah: U.S. Geol. Survey Prof. Paper 550-B, p. B36-B41.
Ilchik, R.P., 1991, Geology of the Vantage Gold Deposits, Alligator Ridge, Nevada, *in* G. L. Raines, R. E. Lisle, R. W. Shafer, and W. H. Wilkinson, eds., Geology and Ore Deposits of the Great Basin, Symposium Proceedings: Geological Society of Nevada, Reno, p. 645-663.
Inden, R. F., and Moore, C. H., 1983, Beach environment, in P. A. Scholle, D. G. Bebout, and C. H. Moore, eds., Carbonate Depositional Environments: AAPG Memoir 33, p. 212-265.
Jacka, A. D., Beck, R. H., St. Germain, L., and Harrison, S. C., 1968, Permian deep-sea fans of the Delaware Mountain Group (Guadalupian) Delaware basin, in Guadalupian facies, Apache Mountain area, west Texas: SEPM/WTGS, Permian Basin Section Pub. 68-11, p. 49-90.
Jackson, P.R. and Ruetz, J.W., 1991, Geology of the Trout Creek Disseminated Gold Deposit, Elko County, Nevada, *in* G. L. Raines, R. E. Lisle, R. W. Shafer, and W. H. Wilkinson, eds., Geology and Ore Deposits of the Great Basin, Symposium Proceedings: Geological Society of Nevada, Reno, p. 729-734.
James, N. P., 1983, Reef environment, in P. A. Scholle, D. G. Bebout, and C. H. Moore, eds., Carbonate Depositional Environments: AAPG Memoir 33, p. 345-440.
Johnson, J. G., 1983, Comment on "Mid-Paleozoic age of the Roberts thrust unsettled by new data from northern Nevada": Geology, p. 60-61.
Johnson, J. G., and Pendergast, A., 1981, Timing and mode of emplacement of the Roberts Mountains allochthon, Antler orogeny: GSA Bulletin v. 92, p. 648-658.
Johnson, J. G., and Pendergast, A., 1983, Antler orogeny and foreland basin: A model: Discussion and reply (Discussion): GSA Bulletin v. 94, p. 684.
Johnson, J.G, Sandberg, C.A., and Poole, F.G., 1991, Devonian lithofacies of the western united States, *in* Cooper, J.D., and Stevens, C.H, eds, Paleozoic Paleogeography of the Western United States–II: SEPM, Pacific Section, v. 67, p. 83-105.
Johnson, J.G., and Bird, J.M., 1991, History of Lower Devonian basin-to-platform transects, in Nevada, in Cooper, J.D., and Stevens, C.H, eds, Paleozoic Paleogeography of the Western United States–II: Pacific Section SEPM, v. 67, p. 311-315.
Johnson, J.G., and Murphy, M.A., 1984, Time-rock model for Siluro-Devonian continental shelf, western United States, GSA Bulletin v. 95, p. 1349-1359.
Kay, M., and Crawford, J. P., 1964, Paleozoic facies from the miogeosynclinal to the eugeosynclinal belt in thrust slices, central Nevada, GSA Bulletin v. 75, p. 425-454.
Kellogg, H. E., 1963, Paleozoic stratigraphy of the southern Egan Range, Nevada: GSA Bulletin v. 74, p. 685-708.
Kendall, C. G. St. C., and Schlager, W., 1981, Carbonates and relative changes in sea level: Marine Geology, v. 44, p. 181-212.

Kendall, G.W., Johnson, J.G., Brown, J.O, and Klapper, G., 1983, Stratigraphy and facies across Lower Devonian–Middle Devonian boundary, Central Nevada, AAPG Bulletin v.67, p. 2199-2207.

Kerans, C. and Tinker, S.W., 1997, Sequence Stratigraphy and Characterization of Carbonate Reservoirs: SEPM Short Course Notes No. 40, 130 p.

Ketner, K.B., 1998, The Nature and Timing of Tectonism in the Western Facies Terrane of Nevada and California—An outline of Evidence and Interpretations Derived From Geologic Maps and Key Areas: U.S. Geol. Survey Prof. Paper 1592, p. 19.

Ketner, K. B., and Smith, J. F., Jr., 1982, Mid-Paleozoic age of the Roberts thrust unsettled by new data from northern Nevada: GSA Bulletin v. 10, p. 298-303.

King, P. B., 1959, The evolution of North America: Princeton, New Jersey, Princeton University Press, 189 p.

King, P. B., 1976, The evolution of North America (Revised edition): Princeton, New Jersey, Princeton University Press, 197 p.

Klovan, J. E., 1964, Facies analysis of the Redwater reef complex, Alberta, Canada: Can. Petrol. Geol. Bulletin v. 12, p. 1-100.

Langenheim, R. L., Jr., Carss, B. W., Kennerly, J. B., McCutcheon, V. A., and Waines, R. H., 1962, Paleozoic section in Arrow Canyon Range, Clark County, Nevada: AAPG Bull, v. 46, p. 592-609.

LaPorte, L. F., 1967, Carbonate deposition near mean sea level and resultant facies mosaic: Manlius Formation (Lower Devonian) of New York State: AAPG Bulletin v. 51, p. 73-101.

LeCompte, M., 1956, Stromatoporoidea, in Treatise on invertebrate paleontology, Part F (Coelenterata): Geological Society of America, p. F107-F144.

Lydon, J.W., 1996, Sedimentary exhalative sulphides (SEDEX), *in* O.R. Eckstrand, W.D. Sinclair, and R.I. Thorpe, eds., Geology of Canadian Mineral Deposit Types: Geological Survey of Canada, Geology of Canada, no. 8, p. 130-152.

Lowenstam, H.A., 1950, Niagaran reefs in the Great Lakes area: Jour. Geology, v. 58, p. 430-487.

Mackin, J. H., 1960, Structural significance of Tertiary volcanic rocks in southwestern Utah: Amer. Jour. Sci., v. 258, p. 81-151.

Magoon, L.B., Hudson, T.L., and Cook, H.E., 2001, Pimienta-Tamabra (!)—A Giant Supercharged Petroleum System in the Southern Gulf of Mexico, Onshore and Offshore Mexico: AAPG Memoir 75, p. 83-125.

Matti, J. C., and McKee, E. H., 1977, Silurian and Lower Devonian paleogeography of the outer continental shelf of the Cordilleran miogeocline, central Nevada, *in* J. H. Stewart, C. H. Stevens, and A. E. Fritsche, eds., Paleozoic Paleogeography the western United States, Pacific Coast Paleogeography Symposium 1: SEPM, Pacific Section, p. 181-216.

Matti, J. C., Murphy, M. A., and Finney, S. C., 1975, Silurian and Lower Devonian basin and basin-slope limestones, Copenhagen Canyon, Nevada: GSA Spec. Paper 159, 48 p.

Maxwell, J. C., 1974, Early western margin of the United States, *in* C. A. Burk and C. L. Drake, eds., The geology of continental margins: Springer-Verlag, New York, p. 831-852.

Mazzullo, S. J., 1981, Facies and burial diagenesis of a carbonate reservoir: Champman Deep (Atoka) field, Delaware Basin, Texas: AAPG Bulletin v. 65, p. 850-865.

Mazzullo, S. J., 1982, Types and controls of Permo-Pennsylvanian carbonate stratigraphic traps of shallow-marine origin in Permian basin: exploration models: Oil and Gas Journal, Oct. 4, 1982, p. 124-141.

Mazzullo, S. J., 1984, Foreshelf carbonate facies mosaics (abs.), SEPM Midyear Meeting, San Jose, CA, United States, Aug. 10-13, 1984, v.1, p. 52.

McGovney, J. E. E., 1977, The diagenesis and sedimentological history of a Silurian-to-Devonian bank-to-basin transition facies in the Hot Creek Range, Nevada: MS Thesis, Univ. of Calif., Riverside, 139 p.

McIlreath, I. A., and N. P. James, 1978, Facies models 12- carbonate slopes: Geoscience Canada, v. 5, p. 189-199.

McLean, H, 1995, Reconnaissance Study of Mississippian Siliciclastic Sandstones in Eastern Nevada: U.S. Geological Survey Bulletin 1988-I, p. 119.

Moore, C. H., 2001, Carbonate Reservoirs: Porosity Evolution and Diagenesis in a Sequence Stratigraphic Framework: Elsevier, Amstedam, 444 p.

Monger, J. W. H., Southes, J. G., and Gabrielse, H., 1972, Evolution of the Canadian Cordillera--A plate-tectonic model: Am. Jour. Sci., v. 272, p. 577-602.

Mountjoy, E. W., 1965, Stratigraphy of the Devonian Miette reef complex and associated strata, eastern Jasper National Park, Alberta: Geol. Survey of Canada Bulletin 110, 132 p.

Mountjoy, E. W., 1968, Factors governing the development of the Frasnian, Miette, and Ancient Wall reef complexes

(banks and biostromes), Alberta, *in* D. H. Oswald, ed., International Symposium on the Devonian System, v. 2: Calgary, Alberta Soc. Petrol. Geol., p. 387-408.
Muehlberger, W. R., 1980, The shape of North America during the Precambrian, *in* Continental tectonics: National Academy of Science, p. 175-183.
Mullins, H. T., and Cook, H. E., 1986, Carbonate apron models: alternatives to the submarine fan model for paleoenvironmental analysis and hydrocarbon exploration: Sedimentary Geology, v. 48, p. 37-80.
Murphy, M.A., and Anderson, M.E., 1991, Devonian formations in the Toquima Range, central Nevada, *in* J. D. Cooper and C. H. Stevens, eds, Paleozoic Paleogeography of the Western United States–II: SEPM, Pacific Section, v. 67, p. 299-310.
Murphy, M.A., and Gronberg, E.C., 1970, Stratigraphy and correlation of the Lower Nevada Group (Devonian) north and west of Eureka, Nevada: GSA Bulletin v. 81, p. 127-136.
Murray, J. W., 1966, An oil producing reef-fringed carbonate bank in the Upper Devonian Swan Hills Member, Judy Creek, Alberta: Bulletin Can. Petrol. Geol., v. 14, p. 1-103.
Mutti, E., and Ricci Lucchi, F., 1972, Le torbiditi dell 'Appennino settentrionale: introduzione all 'analisi di facies: Memoir Society Geology Italy, 11, p. 161-199. English translation in International Geology Review, 1978, v. 20, no. 2, p. 125-166.
Newman, G. W., 1979, Editor's comments, in G.W. Newman, and H.D. Goode, eds., 1979 Basin and Range Symposium, Rocky Mtn. Assoc. Petrol. Geol. and Utah Geol. Assoc., p. v.
Nicols, K. M., and Silberling, N. J., 1977, Depositional and tectonic significance of Silurian and Lower Devonian dolomites, Roberts Mountains and vicinity, east-central Nevada, *in* J. H. Stewart, C. H. Stevens, and A. E. Fritsche, eds., Paleozoic Paleogeography the western United States, Pacific Coast Paleogeography Symposium 1: SEPM, Pacific Section, p. 217-240.
Nilsen, T. H., 1977, Paleogeography of Mississippian turbidites in south-central Idaho, *in* J. H. Stewart, C. H. Stevens, and A. E. Fritsche, eds., Paleozoic Paleogeography the western United States, Pacific Coast Paleogeography Symposium 1: SEPM, Pacific Section, p. 275-299.
Nilsen, T. H., and Stewart, J. H., 1980, The Antler orogeny--Mid-Paleozoic tectonism in western North America: Geology, v. 8, p. 298-302.
Nolan, T. B., 1928, A late Paleozoic positive area in Nevada: Amer. Jour. Sci., 5th Ser., v. 16, p. 153-161.
North American Commission on Stratigraphic Nomenclature, 1983, Stratigraphic Code: AAPG Bulletin v. 67, p. 841-875.
Pelton, P. J., 1966, Mississippian rocks of the southeastern Great Basin, Nevada and California: PhD Dissertation, Rice University, Houston, Texas, 99 p.
Perkins, R. D., 1963, Petrology of the Jeffersonville Limestone (Middle Devonian) of southeastern Indiana: GSA Bulletin v. 74, p. 1335-1354.
Perry, A.J. and Abbott, E.W., 1997, The Roberts Mountains Thrust, Elko and Eureka County, Nevada: Nevada Petroleum Society 1997 Field Trip Guidebook, p. 766.
Playford, P. E., 1980, Devonian "Great Barrier Reef" of Canning Basin, western Australia: AAPG Bulletin v. 64, p. 814-840.
Poole, F. G., 1974, Flysch deposits of the Antler foreland basin, western United States, *in* W. R. Dickinson, ed., Tectonics and sedimentation: SEPM Spec. Pub. 22, p. 58-82.
Poole, F. G., Thorman, C., and Howard, E. L., 1979, Road log from Ely to Garden Pass via Ruth Pit, Moorman Ranch, and Eureka with extensions to Bruffey Seep and Devils Gate: *in* G.W. Newman, and H.D. Goode, eds., Basin and Range Symposium, Rocky. Mtn. Assoc. Geol. and Utah Geol. Assoc., p. 621-636.
Poole, F.G. and Claypool, G.E., 1984, Petroleum source-rock potential and crude-oil correlation in the Great Basin, *in* J. Woodword, F. F. Meissner, and J. L. Clayton, eds., Hydrocarbon source rocks of the Greater Rocky Mountain region: Rocky Mountain Association of Geologists, Denver, p. 179-229.
Poole, F. G., and Sandberg, C. A., 1977, Mississippian paleogeography and tectonics of the western United States, *in* J. H. Stewart, C. H. Stevens, and A. E. Fritsche, eds., Paleozoic Paleogeography the western United States, Pacific Coast Paleogeography Symposium 1: SEPM, Pacific Section, p. 67-85.
Poole, F. G., and Sandberg, C. A., 1991, Mississippian paleogeography and conodont biostratigraphy of the western United States, *in* J. D. Cooper and C. H. Stevens, eds., Paleozoic paleogeography of the Western United States—II: SEPM, Pacific Section, v. 67, p. 107-136.
Poole, F.G., Claypool, G.E., and Fouch, T.D., 1983, Major episodes of petroleum generation in part of the northern Great Basin: Geothermal Resources Council Special Report 13, p. 207-213.

Poole, F. G., Sandberg, C. A., and Boucot, A. J., 1977, Silurian and Devonian paleogeography of the western United States, *in* J. H. Stewart, C. H. Stevens, and A. E. Fritsche, eds., Paleozoic Paleogeography the western United States, Pacific Coast Paleogeography Symposium 1: SEPM, Pacific Section, p. 39-65.

Power, J. D., 1983, The Devils Gate Limestone of the Northern Roberts Mountains, central Nevada--reef or ramp? (abs.): GSA Bulletin v. 15, p. 305.

Powers, R. W. , 1962, Arabian upper Jurassic carbonate reservoir rocks: AAPG Memoir 1, p. 122-192.

Pray, L. C., Cook, H. E., Mountjoy, E. W., and McDaniel, P. N., 1967, Allochthonous carbonate debris flows at Devonian bank ("reef") margins, Alberta, Canada (abs.): Proceedings of the International Symposium on the Devonian System, p. 128-129.

Pray, L. C., Cook, H. E., Mountjoy, E. W., and McDaniel, P. N., 1968, Allochthonous carbonate debris flows at Devonian bank ("reef") margins, Alberta, Canada (abs.): AAPG Bulletin v. 52, p. 545-546.

Pray, L. C., and Stehli, F. G., 1962, Allochthonous origin, Bone Springs "patch reefs", west Texas (abs.): GSA Spec. Paper 73, p. 218-219.

Price, R. A., 1973, Large-scale gravitational flow of supracrustal rocks, southern Canadian Rockies, *in* K. A. DeJong, and R. Scholten, eds., Gravity and Tectonics: New York, Wiley, p. 491-502.

Putnam, B.R. and Henriques, E.Q.B., 1991, Geology and Mineralization at the South Bullion Deposit, Pinon Range, Elko County, Nevada---Implication for Western United States Cenozoic Tectonics, *in* G. L. Raines, R. E. Lisle, R. W. Shafer, and W. H. Wilkinson, eds., Geology and Ore Deposits of the Great Basin, Symposium Proceedings: Geological Society of Nevada, Reno, p. 729-734.

Raines, G.L., Lisle, R. E., Schafer, R. W., and Wilkinson, W.H., 1991, Geology and Ore Deposits of the Great Basin: Symposium Proceedings: Geological Society of Nevada, Reno, Nevada, 1257 p.

Read, J. F., 1982, Carbonate platforms of passive (extensional) continental margins: types, characteristics and evolution: Tectonophysics, v. 81, p. 195-212.

Read, J.F., Kerans, C., Weber, J.L., Sarg, J.F., and Wright, F. M., 1995, Milankovitch Sea Level Changes, Cycles, and Reservoirs on Carbonate Platforms in Greenhouse and Icehouse Worlds: SEPM Short Course Notes No. 35, 203 p.

Reso, A., 1963, Composite columnar section of exposed Paleozoic and Cenozoic rocks in the Pahranagat Range, Lincoln County, Nevada: GSA Bulletin v. 74, p. 901-918.

Rich, M., 1977, Pennsylvanian paleogeographic patterns in the western United States, *in* J. H. Stewart, C. H. Stevens, and A. E. Fritsche, eds., Paleozoic Paleogeography the western United States, Pacific Coast Paleogeography Symposium 1: SEPM, Pacific Section, p. 87-111.

Ridley, A. P., 1971, Devonian and Mississippian sedimentation and stratigraphy of the Mazourka Canyon area, Inyo Mountains, Inyo County, California: MS thesis, San Jose State Univ., San Jose, California, 78 p.

Roberts, R. J., 1949, Geology of the Antler Peak quadrangle, Nevada: U.S. Geol. Survey Open-File Report No. 37.

Roberts, R. J., 1964, Stratigraphy and structure of the Antler Peak quadrangle, Humbodt and Lander Counties, Nevada: U.S. Geol. Survey Prof. Paper 459-A, 93 p.

Roberts, R. J., Holtz, P. E., Gilluly, J., and Ferguson, H. G., 1958, Paleozoic rocks of north-central Nevada: AAPG Bulletin v. 42, p. 2813-2857.

Roberts, R. J., and Thomasson, M. R., 1964, Comparison of late Paleozoic depositional history of northern Nevada and central Idaho: U.S. Geol. Survey Prof. Paper 475-D, Article 122, p. D1-D-6.

Roehl, P. O., 1967, Carbonate facies, Williston Basin and Bahamas: AAPG Bulletin v. 51, p. 1979-2032.

Roehl, P.O. and Choquette, P.W., 1985, Carbonate Petroleum Reservoirs: Springer-Verlag, New York, 622 p.

Ross, R. T., Jr., 1977, Ordovician paleogeography of the western United States, *in* J. H. Stewart, C. H. Stevens, and A. E. Fritsche, eds., Paleozoic Paleogeography of the western United States, Pacific Coast Paleogeography Symposium 1: SEPM, Pacific Section, p. 19-38.

Ross, D. C., 1966, Stratigraphy of some Paleozoic formations in the Independence quadrangle, Inyo County, California: U.S. Geol. Survey Prof. Paper 396, 64 p.

Ruiz-Ortiz, P. A., 1983, A carbonate submarine fan in a fault-controlled basin of the Upper Jurassic, Betic Cordilleran, southern Spain: Sedimentology, v. 30, p. 33-48.

Sandberg, C. A., Poole, F. G., and Gutschick, R. C., 1980, Devonian and Mississippian stratigraphy and conodont zonation of Pilot and Chainman Shales, Confusion Range, Utah, *in* T. D. Fouch, and E. Magathan, eds., Paleozoic Paleogeography of west-central United States, Rocky Mountain Paleogeography Symposium 1: SEPM, Rocky Mountain Section, p. 71-79.

Sandberg, C. A., Morrow, J. R., Poole, F. G., and Ziegler, W., 2003, Middle Devonian to Early Carboniferous event

stratigraphy of Devils Gate and Northern Antelope Range sections, Nevada, USA: Cour. Forsch.-Inst. Senckenberg, v. 242, p. 187-207.
Schlager, W., 1981, The paradox of drowned reefs and carbonate platforms: GSA Bulletin v. 92, p. 197-211.
Scholle, P. A., 1978, A color illustrated guide to carbonate rock constituents, textures, cements, and porosities: AAPG Memoir 27, 241 p.
Scholle, P. A., Bebout, D. G., and Moore, C. H., eds., 1983, Carbonate depositional environments: AAPG Memoir 33, 708 p.
Sears, J. W., and Price, R. A., 1978, The Siberian connection: A case for Precambrian separation of the North American and Siberian cratons: Geology, v. 6, p. 267-270.
Shanmugam, G., and Moiola, R. J., 1982, Eustatic control of turbidites and winnowed turbidites: Geology, v. 10, p. 231-235.
Shaw, A. B., 1964, Time in Stratigraphy: McGraw-Hill Book Co., N. Y., 365 p.
Sheehan, P.M., Pandolfi, J.M., and Ketner, K.B., 1993, Isolated carbonate bodies composed of stacked debris-flow deposits on a fine-grained carbonate lower slope of Devonian age, Antelope Peak, Elk County, Nevada: USGS Bulletin 1988-E, p. E1-E12.
Shinn, E. A., 1983, Tidal flat environment, in P. A. Scholle, D. G. Bebout, and C. H. Moore, eds., Carbonate Depositional Environments: AAPG Memoir 33, p. 172-209.
Silberling, N. J., 1973, Geologic events during Permian-Triassic time along the Pacific margin of the United States, in A. Logan and L. V. Hills, eds., The Permian and Triassic systems and their mutual boundary: Alberta Soc. Petrol. Geol., Calgary, Canada, p. 345-362.
Silberling, N. J., 1975, Age relationships of the Golconda thrust fault, Sonoma Range, north-central Nevada: GSA Spec. Paper 163, 28 p.
Skipp, B., and Hall, W. E., 1980, Upper Paleozoic paleotectonics and paleogeography of Idaho, *in* T. D. Fouch and E. R. Magathan, eds., Paleozoic paleogeography of the west-central United States, Rocky Mountains Paleogeography Symposium 1: SEPM, Rocky Mountain Section, p. 387-422.
Sleep, N. H., 1971, Thermal effects of the formation of Atlantic continental margins by continental break up: Geophys. Jour. Royal Astron. Soc., v. 24, no. 4, p. 325-350.
Sleep, N. H., and Snell, N. S., 1976, Thermal contraction and flexure of mid-continent and Atlantic marginal basins: Geophys. Jour. Royal Astron. Soc., v. 45, p. 125-154.
Smith, J. F., Jr., and Ketner, K. B., 1968, Devonian and Mississippian rocks and the date of the Roberts Mountains thrust in the Carlin-Pinon Range, Nevada: U.S. Geol. Survey Bulletin1251-I, p. 1-18.
Smith, J. F., Jr., and Ketner, K. B., 1977, Tectonic events since early Paleozoic in the Carlin-Pinon Range area, Nevada: U.S. Geol. Survey Prof. Paper 867C, 18 p.
Speed, R. C., 1977, Island-arc and other paleogeographic terranes of late Paleozoic age in the western Great Basin, *in* J. H. Stewart, C. H. Stevens, and A. E. Fritsche, eds., Paleozoic Paleogeography of the western United States, Pacific Coast Paleogeography Symposium 1: SEPM, Pacific Section, p. 349-362.
Speed, R. C., 1983, Pre-Cenozoic Tectonics of northwestern Nevada, The role of heat in the development of energy and mineral resources in the northern Basin and Range Province (abs.), Geothermal Resources Council Program with Abstracts, Geothermal Resources Council, Davis, California, p. 5-6.
Speed, R. C., and Sleep, N. H., 1982, Antler orogeny and foreland basin: a model: GSA Bulletin v. 93, p. 815-828.
Speed, R. C., and Sleep, N. H., 1983, Antler orogeny and foreland basin: a model: discussion and reply (reply): GSA Bulletin v. 94, p. 685-686.
Stevens, C. H., 1977, Permian depositional provinces and tectonics, western United States, *in* J. H. Stewart, C. H. Stevens, and A. E. Fritsche, eds., Paleozoic Paleogeography of the western United States, Pacific Coast Paleogeography Symposium 1: SEPM, Pacific Section, p. 113-135.
Stevens, C. H., and Ridley, A. P., 1974, Middle Paleozoic off-shelf deposits in southeastern California: evidence for proximity of the Antler orogenic belt?: GSA Bulletin v. 85, p. 27-32.
Stewart, J. H., 1972, Initial deposits in the Cordilleran geosyncline: Evidence of a late Precambrian (<850 my.) continental separation: GSA Bulletin v. 83, p. 1345-1360.
Stewart, J. H., 1976, Late Precambrian evolution of North America: Plate tectonics implication: Geology, v. 4, p. 11-15.
Stewart, J. H., 1983, Spatial variation, style, and age of Cenozoic extensional tectonics in the Great Basin (abs.), GSA Abstracts with Programs, Rocky Mountain and Cordilleran Section, v. 15, no. 5, p. 286.
Stewart, J. H., and Poole, F. G., 1974, Lower Paleozoic and uppermost Precambrian Cordilleran miogeocline, Great

Basin, western United States, *in* W. R. Dickinson, ed., Tectonics and sedimentation: Soc. Econ. Paleontologists Mineralogists Spec. Pub. 22, 57 p.
Stewart, J. H., and Suczek, C. A., 1977, Cambrian and latest Precambrian paleogeography and tectonics in the western United States, *in* J. H. Stewart, C. H. Stevens, and A. E. Fritsche, eds., Paleozoic paleogeography of the western United States, Pacific Coast Paleogeography Symposium 1: SEPM, Pacific Section, p. 1-18.
Stewart, J. H., MacMillan, J. R., Nichols, K. M., and Stevens, C. H., 1977, Deep-water upper Paleozoic rocks in north-central Nevada--a study of the type area of the Havallah Formation, *in* J. H. Stewart, C. H. Stevens, and A. E. Fritsche, eds., Paleozoic paleogeography of the western United States, Pacific Coast Paleogeography Symposium 1: SEPM, Pacific Section, p. 337-347.
Suczek, C. A., 1977, Sedimentology and petrology of the Cambrian Harmony Formation of north-central Nevada (abs.): Geol. Soc. America Abs. With Prog., v. 9, p. 510.
Sverdrup, H. U., Johnson, Martin W., and Fleming, Richard H., 1942, The Oceans--their physics, chemistry, and general biology: New York, Prentice-Hall, Inc.
Taylor, M. E., 1976, Indigenous and redeposited trilobites from Late Cambrian basinal environments of central Nevada: Journal of Paleontology, v. 50 p. 668-700.
Taylor, M. E., and Cook, H. E., 1976, Continental shelf and slope facies in the Upper Cambrian and lowest Ordovician of Nevada, *in* R. A. Robinson and A. J. Rowell, eds., Cambrian paleontology and environments of western North America, a symposium: Brigham Young Univ. Geol. Studies, v. 23, pt. 2, p. 181-214.
Taylor, M. E., Cook, H. E., and Miller, J. F., 1989, Late Cambrian and Early Ordovician biostratigraphy and depositional environments of the Whipple Cave formation and House Limestone, Central Egan Range, Nevada, *in* M. E. Taylor, ed., Cambrian and Early Ordovician stratigraphy and paleontology of the Basin and Range Province, western United States, Field Trip Guidebook T125 28th International Geological Congress, p. 37-44.
Thomas, E. F., Cook, H. E., and Rees, M. N., 1987, Sediment-gravity in the Tor Limestone: A re-interpretation and its implications on the paleogeography of the western United States (abs.): GSA Annual Meeting Abs., v. 19, no. 7, p. 867.
Thoreson, R.F., 1991, Geology and Gold Deposits of the Rain Subdistrict, Elko County, Nevada, *in* G. L. Raines, R. E. Lisle, R. W. Shafer, and W. H. Wilkinson, eds., Geology and Ore Deposits of the Great Basin, Symposium Proceedings: Geological Society of Nevada, Reno, p. 635-643.
Vail, P. R., Mitchum, R. M., Jr., and Thompson, S., III, 1977, Seismic stratigraphy and global changes of sea level, Part 4: Global cycles of relative changes of sea level, *in* C.E. Payton, ed., Seismic Stratigraphy--Applications to Hydrocarbon Exploration, AAPG Memoir 26, p. 83-97.
Walker, R. G., 1966, Shale Grit and Grindslow Shales: transition from turbidite to shallow water sediments in the Upper Carboniferous of northern England. Jour. Sed. Petrol., v. 36, p. 90-114.
Whiteford, W. B., Little, T. A., Miller, E. L., and Holdsworth, B. K., 1983, The nature of the Antler orogeny view from north central Nevada (abs.), GSA Abstracts with Programs, Rocky Mountain and Cordilleran Section, v. 15, no. 5, p. 382.
Wilgus, C.K., Hastings, Kendall, C.G., Posamentier, H.W., Ross, C.A., and Von Wagoner, J.C., 1988, Sea-Level Changes: An Integrated Approach: SEPM Spec. Pub. 42, p. 407.
Wilson, B. R., and Laule, S. W., 1979, Tectonics and sedimentation along the Antler orogenic belt of central Nevada, in Newman, G. W., and Goode, H. D., eds., Basin and Range Symposium: Rocky Mountain Assoc. of Geologists, p. 81-92.
Wilson, J. L., 1975, Carbonate Facies in Geologic History: New York, N.Y., Springer-Verlag, 470 p.
Wilson, J. L., and Jordan, C., 1983, Middle shelf environment, in P. A. Scholle, D. G. Bebout, and C. H. Moore, eds., Carbonate Depositional Environments: AAPG Memoir 33, p. 298-343.
Wilson, W.L., 1986, Geology of the Eureka-Windfall and Rustler gold deposits, Eureka County, Nevada, *in* J. V. Tingley and H. F. Bonham, Jr., eds., Sediment-hosted precious-metal deposits of northern Nevada: Nevada Bureau of Mines and Geology, v. 40, p. 81-84.
Wilson, W.L., 1990, Discovery of the Windfall Mine, and Geology of the Eureka-Windfall Gold Deposit, *in* V. F. Hollister, ed., Discoveries of Valuable Minerals and Precious Metals Deposits Related to Intrusions and Faults: Case Histories of Mineral Discoveries, v. 2, p. 183-206.
Wilson, W.R., Cox, J.W., and Lance, D.L., 1991, Geology and Geochemistry of the Green Springs Gold Mine, White Pine County, Nevada, in G. L. Raines, R. E. Lisle, R. W. Shafer, and W. H. Wilkinson, eds., Geology and Ore Deposits of the Great Basin, Symposium Proceedings: Geological Society of Nevada, Reno, p. 687-700.
Winn, R. D., Jr., Bailes, R. J., and Lu, K. I., 1981, Debris flows, turbidites, and lead-zinc sulfides along a Devonian

submarine fault scarp, Jason Prospect, Yukon Territory, *in* C.T. Siemers, R.W. Tillman, and C.R. Williamson, eds., Deep-Water Clastic Sediments, A Core Workshop, Soc. Econ. Paleo. Min. Core Workshop No. 2, p. 396-416.
Winterer, E. L., and Murphy, M. A., 1960, Silurian reef complex and associated facies, central Nevada: Jour. Geol., v. 68, p. 117-139.
Zempolich, W. G. and Cook, H. E., eds., 2002, Paleozoic Carbonates of the Commonwealth of Independent States (CIS): Subsurface Reservoirs and Outcrop Analogs: SEPM Spec. Pub. 74, p. 250.